Investigation into Electrochemical Discharge Micro-Machining Process

Submitted by

BIJAN MALLICK

DOCTOR OF PHYLOSOPHY (ENGINEERING)

DEPARTMENT OF PRODUCTION ENGINEERING
FACULTY COUNCIL OF ENGINEERING & TECHNOLOGY
JADAVPUR UNIVERSITY
KOLKATA-700032, INDIA

2019

TITLE OF THE Ph.D.(Engg.) THESIS: Index N0.18/12/E

Investigation into Electrochemical Discharge Micro-Machining Process

NAME, DESIGNATION & INSTITUTION OF THE SUPERVISORS:

(i) Prof (Dr.) B. DOLOI
Professor, Production Engineering Department, Jadavpur University,
Kolkata – 700032, India

(ii) Dr. B. R. SARKAR
Associate Professor, Production Engineering Department, Jadavpur University,
Kolkata – 700032, India

LIST OF PUBLICATIONS

INTERNATIONAL JOURNAL

[1] B.Mallick, B.R.Sarkar, B.Doloi and B.Bhattacharyya, "Analysis on the effect of ECDM process parameters during micro-machining of glass using genetic algorithm". *Journal of Mechanical Engineering and Sciences*, 2018, Vol. 12, (3), 3942-3960.

[2] B.Mallick, B.R.Sarkar, B.Doloi and B.Bhattacharyya "Analysis on Electrochemical Discharge Machining during Micro-Channel Cutting on Glass". *International Journal of Precision Technology*, 2017, Vol.7, (1), 32-50.

[3] B.Mallick,B.R.Sarkar, B.Doloi and B.Bhattacharyya**.,** "Multi Criteria Optimization of Electrochemical Discharge Micro-Machining Process during Micro-Channel Generation on Glass", *Applied Mechanics and Materials*, 2014,Vol. 592-594, 525-529.

INTERNATIONAL CONFERENCE

[1]B. Mallick, R.M.Tayade, B. R. Sarkar, B. Doloi, B. Bhattacharyya, "Electrochemical Discharge Micro-Machining of Glass for Different Types of Micro-channel" Proceedings of 10th International Conference on, precision, meso, micro and nano engineering, (COPEN-10), held at IIT Madras, 2017, Vol.1, 631-635.

[2]B.Mallick, B.R.Sarkar,B.Doloi and B.Bhattacharyya, "Effects of process variables on ECDM performances during micro-channel cutting on Glass" 6th International and 27th All India Manufacturing, Technology, Design and Research conference, held at College of Engineering Pune, (AIMTDR 2016).

[3]B.Mallick, B.R.Sarkar,B.Doloi and B.Bhattacharyya, "Modeling and Optimization of Electrochemical Discharge Micro-Machining Process by Genetic Algorithm" 9th International Conference on, proceedings of precision, meso, micro and nano engineering, (COPEN-9), held at IIT BOMBAY, 2015, PAPER ID 237.

[4]Mallick, B.,M.N. Ali, Sarkar, B. R., Doloi, B. and Bhattacharyya, B "Parametric Analysis of Electrochemical Discharge micro-Machining Process during profile generation on glass." 5th International & 26th All India Manufacturing Technology, Design and Research Conference, (AIMTDR 2014), held at IIT Guwahati, Assam, India, 2014,Vol. 1, 540-1to 540-6.

[5]Mallick, B., Biswas, S.,Sarkar, B. R., Doloi, B. and Bhattacharyya, B. "Investigations into Performance Characteristics of Electrochemical Discharge Micro Machining Process" Proceedings of 8th International Conference on, precision, meso, micro and nano engineering, (COPEN8), held at NIT Calicut, 2013,Vol. 1, 386-391.

[6]Mallick, B., Biswas, S.,Sarkar, B. R., Doloi, B. and Bhattacharyya, B. "Experimental Investigation on ECDM during Micro Channel Cutting on Glass" Proceedings of 8th International Conference on, precision, meso, micro and nano engineering, (COPEN8), held at NIT Calicut, 2013,Vol. 1, 379-385.

PATENTS: NIL

BOOK CHAPTER:NIL

JADAVPUR UNIVERSITY
FACULTY OF ENGINEERING AND TECHNOLOGY
DEPARTMENT OF PRODUCTION ENGINEERING

CERTIFICATE FROM THE SUPERVISORS

This is to certify that the thesis entitled "INVESTIGATION INTO ELECTRO CHEMICAL DISCHARGE MICRO-MACHINING PROCESS" submitted by Mr. Bijan Mallick, who got his name registered on 7th June 2012 for the award of Ph.D. (Engg.) degree of Jadavpur University is absolutely based upon his own work under the supervision of Professor B.Doloi and Dr. B.R.Sarkar and that neither his thesis nor any part of the thesis has been submitted for any degree/diploma or any other academic award anywhere before.

…….	……
Prof.(Dr) B. Doloi	Dr. B. R. Sarkar
(Signature of the supervisor	(Signature of the supervisor
and date with official seal)	and date with official seal)

ACKNOWLEDGEMENT

I would like to express my warmest gratitude for the inspiration, encouragement and assistance that I received from my esteemed guides **Dr. Biswanath Doloi**, Professor, Department of Production Engineering, Jadavpur University and **Dr. Biplab Ranjan Sarkar**, Associate Professor, Production Engineering Department, Jadavpur University throughout the research work. It is because of their continuous guidance, encouragement and valuable advices at every steps from the embryonic to the developmental stage. I am very much indebted to them and express my sincere gratitude to them.

Also, I express my heartiest thanks to my respected teacher **Prof. Bijoy Bhattacharyya** for his useful advice and suggestions. I am grateful to **Prof. S. Chakraborty, Prof. D. Banerjee**, other respected faculty members, HOD of Production Engineering, librarian and other staffs of Production Engineering Department, Jadavpur University for their moral support, suggestion, immense help and co-operation during the course of this thesis work.

I gratefully acknowledge the financial support of the Centre of Advanced Study (CAS) – Phase IV Programme of Production Engg. Department under the University Grants Commission (UGC), New Delhi and Department of Production Engineering, Jadavpur University for providing the laboratory facilities. Thanks are also extended to FET office and Research section for their cordial assistance and administrative supports.

I acknowledge special thanks to Mr. Biswanath Das, Mr Biswajit Pathak and other technical staffs of Production Engineering Department, Jadavpur University and also to Mr. Prosun Mallick and Mr. Kumar Halder of Techno International Batanagar for their assistance and also Mr. Sibasish Chakraborty, B.Tech student of ME department, JISCE for support and encouragement during this research work.

I am highly thankful to Mr. Sumit Biswas, Engineer at Indian Railway & Md. M.N.Ali, Santosh Kumar, Mr. R.M.Tayade, Subhrajit Debnath, Kaushik Mishra, Premangshu Mukhopadhyay and all other Research scholars of Production Engineering Department, Jadavpur University for their support and encouragement during my research work. Author deeply extends thanks to Professor (Dr.) Ankur Ganguly, Principal and all the faculty & technical staffs of ME Department, Techno International Batanagar for their inspiration and support.

I gratefully acknowledge the support of all those people, not mentioned above but also have directly or indirectly rendered their help at different stages of this work.

I am very much thankful to my uncles Mr Keshab Lal Mallick, Mr Biplab Mallick, Mr Nitayananda Mallick and my father in law Mr Parimal Chandra Das and my mother in law Suniti Rani Das for their assistance, support and advice during my research work.

Last but not the least, thanks to my beloved parents Mr. Basudeb Mallick & Mrs. Rashmoni Mallick; sister Trisha Mallick, brother Rathin Mallick and my best friend, my wife Pronita Das (Mallick), as they always stood by me, caring about the prevalent situation. Finally I would like to mention from the deep of my soul to my lovely daughter, Aradhya Mallick who provides me new inspiration in my research work.

Bijan Mallick

PREFACE

Electrochemical discharge micro-machining (µ-ECDM) is a hybrid machining process used for machining of hard and brittle materials like glass, ceramics, quartz etc. 1n 1833 Michael Faraday discovered law of electrolysis as electro-deposition and dissolution. The discharge phenomenon in electrolyte was used first for machining of glass by Kurafuji and Suda in1968. Glass is one of the most popular materials preferred by industries due to high thermal resistance and high corrosion resistance properties. But machining of this material is very difficult by common conventional machining processes. Some other non-conventional machining processes such as AWJM, USM, and LBM can also be used to machine these materials. But these machining processes associated with inherent problems like high surface roughness, poor dimensional accuracy, large heat affected zone and low volume of material removal, high investment and skilled labour to operate machine. Therefore, there is an urgent need of special machining process, which can be used to machine electrically non-conducting materials such as glass and ceramics. Electrochemical discharge machining (ECDM) process is one such type process for machining of glass and ceramics.

Electro chemical discharge micro-machining process is a promising technology for micro-machining electrically non-conducting materials such as ceramics and glass. It is a hybrid technology that combines with the electrochemical machining (ECM) and electro-discharge machining (EDM) and can be employed irrespective of the electrical and mechanical properties of materials. In µ-ECDM process, the material removal takes place due to the combined effects of electrochemical (EC) reactions and electrical spark discharge (ESD) action. In µ-ECDM two electrodes, one is cathode where tool is generally connected and another is anode or auxiliary electrode are used to complete the electrolytic cell since the job specimen is electrically non-conducting material. The hydrogen gas bubbles are generated due to electrochemical reactions and accumulated at the surroundings of the tool and thereby form a gas bubble layer. If the applied voltage increases beyond the critical limit, the sparking is initiated between tool and electrolyte across the gas bubble layers due to electrical discharge and material is removed by melting and vaporization phenomena from the job specimen, which is placed just below the tool and immersed in an electrolyte solution in a machining chamber. The µ-ECDM process has various advantages such as low heat affected zone. The µ-ECDM process has potential to cut µ-channel, micro-profile, micro-groove, and µ-slot and also to generate complex shaped contours on advanced electrically non-conducting hard and brittle materials.

However, material removal mechanism of µ-ECDM process is not clear to the researchers. There are lot of aspects need to be investigated. Also fundamentals of µ-ECDM process depend on various process parameters. Therefore, there is an urgent need to control the machining parameters so that the desired machining rate with proper dimensional accuracy can be achieved. Keeping the above consideration in view, the objectives of the proposed research work are given as below.

(i) To design and develop of µ-ECDM set-up for carrying out micro-cutting operation on electrically non-conducting hard and brittle materials like glass.

(ii) To investigate the influences of various process parameters such as applied voltage, electrolyte concentration, inter-electrode gap, duty ratio and polarity on various machining performances such as material removal rate (MRR), overcut (OC), heat affected zone (HAZ), machining depth (MD) and surface roughness (R_a) etc during cutting of various micro-channels and profiles cutting on electrically non-conducting materials by micro-electrochemical discharge machining process.

(iii) To conduct comparative studies of performances of µ-ECDM process using different electrolytes and different shapes of tool.

(iv) To develop mathematical models to correlate different machining criteria such as material removal rate (MRR), overcut (OC), heat affected zone (HAZ), machining depth (MD) and surface roughness (R_a) with various process parameters during micro-channel cutting on glass.

(v) To perform the analysis for determining the optimal machining condition of µ-ECDM process during micro-cutting operation using optimization techniques like desirability function analysis and Genetic Algorithm.

(vi) To fabricate different shapes of micro-channels and micro-slots on glass as an application of µ-ECDM process.

The thesis work is documented in well-organized manner into six chapters. A brief summary of each chapter is given as follows:

CHAPTER-I outlines an overview of electro chemical discharge micro- machining process, concept of micro-machining, present needs, advantages and applications. This chapter includes the literature review and the research objectives those are outlined after identifying the existing knowledge gap.

Fundamentals of µ-ECDM, mechanisms of gas bubble generation spark generation, material removal and tool wear have been discussed in CHAPTER -II. The design and development of µ-ECDM set up have been included in CHAPTER-III in details. CHAPTER-IV presents the selection of process parameters for experimentation during micro-channel fabrication on glass. Influences of process parameters on machining criteria of electrochemical discharge micro-machining process using different types of cutting tools, electrolytes using counter weight feed mechanism during micro-channel cutting on glass by ECDM process. In this chapter influence of process parameters on responses during electrochemical discharge machining on glass for generation of micro-channel using counter weight feed mechanism based on desirability function analysis using response surface methodology (RSM) have been performed. The development of empirical modelling based on RSM and analysis of variance (ANOVA) test have been included and also genetic algorithm (GA) based single as well as multi-objective optimization have been analysed in this chapter. CHAPTER-V includes experimental investigations for analysis the effects of process parameters into performance characteristics of µ-ECDM process using cylindrical stainless steel tool, different mixed electrolytes, template guided spring feed mechanism and also comparative studies of various machining performances using direct and reverse polarity also have been analysed in this chapter. The development of empirical modelling based on RSM and analysis of variance (ANOVA) test have been also investigated in this chapter and for find out the optimal parametric combination for single and multi-objective optimization have been performed based on GA. Further the influences of process parameters based on SEM and XRD analyses have been demonstrated in this chapter during micro-channel cutting on glass. The different shapes of micro-channels, micro-slot and profile generation on glass by µ-ECDM process also included in this chapter.CHAPTER-VI includes the general conclusions of the research work and future scope of research.

The most significant and exceptional research findings have been observed in the present research includes the fabrication of micro-channel, micro-slot, profile, different shapes on glass using µ-ECDM process. It is evident that the existing research work on micro-channel cutting on glass by µ-ECDM process will provide useful information about the optimum process parameter settings to achieve the desired shapes of micro-channel and profile. The research work on µ-ECDM process for micro-machining on glass is expected to yield effective outcome, which will have immense utilization in the area of micro-fluidic devices, micro-machine tools, aerospace, automobile, computer, electrical and electronics engineering.

The research works on optimization analysis of the performance of the μ-ECDM provide technical guidelines for future applications in the field of micro-machining and opens up the challenges to the modern manufacturing industries to cope with the micro-machining of electrically non-conducting materials like glass.

VITA

The author, Bijan Mallick, son of Sri Basudeb Mallick and Smt. Rashmoni Mallick, was born on 15th February, 1985 in North 24 Parganas, West Bengal, India. He studied in Gangnapur high school and passed the Secondary Examination of WBBSE in 2000. Then he studied in Habra high school and passed Higher Secondary Examination of WBCHSE in 2002.The author graduated in Production Engineering in 2008 from Jadavpur University, Kolkata, West Bengal. Author completed his M. Prod.E. with specialisation of Production Technology in 2010 from Production Engineering Department, Jadavpur University, Kolkata-32.Then he joined Murshidabad College of Engineering as Assistant Professor in Mechanical Engineering Department in July, 2010. After that, he joined as Research Fellow under "UGC-BSR Research Fellowship in Science for Meritorious Students' in April, 2012. He has done his research work in the area of electrochemical discharge micro-machining during entire duration. Then he served as Assistant Professor in Mechanical Engineering Department, JISCE, Kalyani from May, 2013 –December, 2015. After that he worked as HOD of ME department of EIEM, Kolkata from January 2016 to July 2016. He has served in Ideal Institute of Technology from August 2016 to March 2017. After that he joined as an assistant professor in Mechanical Engineering Department of Techno International Batanagar (formerly Techno India Batanagar), Techno India Group, Kolkata on the 21st April, 2017 and working in the same department as HOD till date.

Author has published 3 research papers in international referred journals as well as presented more than 6 research papers in reputed national and international conferences related to advance machining processes.

The Thesis Dedicated to .....

My dada Thakurs, Late Brindaban Mallick, Nalini Ranjan Ojha and Sarat Chandra Das

For their LOVE, Bless, never ending encouragement and inspiration.....

TABLE OF CONTENTS

CHAPTER-I

CHAPTER-II

CHAPTER-III

CHAPTER-IV

CHAPTER-V

CHAPTER-VI

CHAPTER-I

1. INTRODUCTION

The production of miniature parts draws the most of attractions from industrial field to fabricate small or tiny products which have growing demands in modern society. To accomplish the demand, the scientists and technologists are facing more and more challenges and problems in the field of manufacturing industries. The difficulty in adopting the traditional manufacturing processes is caused by the three basic sources such as new materials with a low machinability, dimensional and accuracy requirements and a higher production rate with economy. The machining is referred as the removal of some material from the job specimen by direct contact or indirect contact with tool for development of a specific geometry at a definite degree of accuracy and surface quality. Parts manufactured by casting, forming and various shaping processes often require further operations before use or assembly. In many engineering applications parts have to be interchanged in order to function properly and reliably during their expected service lives.

There is a requirement of advanced machining processes in modern manufacturing industries to manufacture the products with advanced engineering materials such as ceramics, quartz, alumina and glass due to their some favorable characteristics. In Abrasive Water Jet Machining (AWJM) process has limited applications due to the transverse cutting speed, the quality of products is not so good due to poor surface quality and large space area required for installation, high investment as well as maintenance cost. Ultrasonic Machining (USM) has some inherent limitations such as tool wear, high capital cost and there is a chance of tool bending due to contraction and vibration. In case of Laser beam Machining (LBM) the formation of very large undesirable heat affected zone degrades the quality of the product and this process requires very high investment. ECM requires high capital investment, skilled worker to operate and large space for installation. Also the disposal of used electrolyte and effect of stray current are the major drawbacks of ECM process. Again electro-discharge machining (EDM) have some drawbacks like difficult to fabricate various shapes, long machining time required to produce micro-products and high cost of equipment. Further ECM and EDM are useful mainly for electrically conductive material. So the alternative machining process is tried to bring within the minimum investment for cutting non-conducting materials like glass and ceramics.

Hence, there is a need of special machining process, which will be helpful for fabricating products of electrically non-conductive materials and can cope up with the above adverse effects of above machining processes. Electrochemical Discharge Machining (ECDM) process has a great ability to machine electrically non-conductive materials like glass and ceramics. In comparison to above machining processes thermal effects i.e. formation of heat affected zone is small. There is no requirement of skilled worker to operate the ECDM machine and the process is independent of physical and chemical properties of the material. The investment cost is low, as simple construction of machine is required for ECDM process.

1.1 NEED OF MICRO-MACHINING

Micro- parts and devices used in modern industry are manufactured by utilizing micro-machining processes. The micro-machining technique has been used first time in the 1960s for the sake of miniaturized electronic components. Micro-machining deals with machining of miniature components or generating micro-features on macro or meso size components. In micro-machining material is removed as a form of micro-chips, ions or atoms. Literally the dimension range of micro-machining is 1μm- 999μm. According to CIRP the range of micro-machining is accepted up to 1- 500μm. It can be considered as micro-level unit removal of material. The most common use of micro machining is found in the medical, electrical and electronics industries. Micro-parts, which are fabricated by micro-machining, are typically so small that those must be inspected for quality control by using optical microscope, SEM analysis and X-RD analysis. Much more attention is required for maintaining dimensional accuracy during micro-machining operation. The identification and minimization of error generation are very important as micro-machining is one of the precision machining processes. Several error generations occurs during micro-machining due to machine tools, mechanical deformation, thermal deformation, surface integrity, gap between tool and job specimen, coordinate shift in tool handling etc.

There are various traditional micro-machining processes such as diamond micro-turning, micro-milling, micro-drilling etc, but selection of proper tools and materials are limited for generating micro-features on the job specimen. The applications of tradition micro-machining processes are limited due to problems of the development of harder micro-tools for machining of advanced ultra-hard job specimen materials with high accuracy. Some non-traditional or advance micro-machining processes have utilized micro-tools but the hardness

of the tool is lower than job specimen material. The mechanical, electrical, chemical and thermal energy and their combination are utilized to remove micro-level unit material from the job specimen.

The advanced micro-machining process is not limited to the mechanical properties of the job specimen material. There is a need of advanced micro-machining processes for micro-machining of ultra-hard and difficult to cut materials like glass, ceramics and composites etc.

1.1.1 Various Advanced Micro-Machining Processes

For performing different micro-machining operations such as micro-drilling, micro-cutting, micro-turning, micro-milling etc, on difficult to cut materials, various advanced micro-machining processes have been developed and some of those are discussed as follows:

1.1.1.1 Electro Discharge Micro-Machining (µ-EDM)

Electro Discharge Micro-Machining (µ-EDM) is electro-thermal non-traditional micro-machining process at which electrical energy is used for generation electrical spark and material is removed mainly due to the thermal energy of the spark.

It is difficult to machine complex geometrical shapes by µ-EDM in small batches or even on job-shop basis. Only electrically conductive material can be machined by µ-EDM. Potential difference is applied between the tool and job-specimen in µ-EDM during machining. The tools as well as the job specimen are to be conductors of electricity for this machining process. The micro-tool and the job material are immersed in a dielectric medium like hydrocarbon oil or deionized water in µ-EDM. A very small working gap is maintained between the tool electrode and the job specimen. An electric field is created depending upon the applied potential difference and the gap between the tool and job specimen. Generally the tool is connected to the negative terminal of the power supply and the job specimen to positive terminal in µ-EDM process. As the electric field is established between the micro-tool and job specimen, the free electrons in the form of spark from the tool are striking on the job specimen. A large number of electrons suddenly flow from the µ-tool to the job specimen and ions from the job specimen to the µ-tool. Such movement of electrons and ions are observed visually as sparking.

The kinetic energy of the electrons impact on the surface of job is converted into thermal energy or heat flux. This localized heat flux leads to extreme instantaneous confined rise of temperature, which is more than 10,000^{o}C and the extreme rise of temperature cause the material removal. Material is removed in the form of tiny particles leaving crater due to

instant vaporization of the material as well as due to melting. The molten metal is not removed completely but only partially. Thus the material removal from tool occurs in μ-EDM mainly due to formation of shock waves as the plasma channel collapse owing to discontinuation of applied potential difference. The positive ions impinge on the μ-tool and which lead to tool wear.

In μ-EDM, the electrical pulse generator with D.C. power source is used to apply voltage pulses between the micro-tool and the job specimen. A constant voltage is not applied since only sparking is desired in μ-EDM rather than arcing. Arcing leads to localized material removal at a particular point whereas sparks get distributed all over the job specimen surface, leading to uniformly distributed material removal under the tool.

The most important applications of μ-EDM include precision cutting of punch and dies, precision moulds, components for medical as well as engineering, sensors and optics, watch making /gears and holes/ or the production of tiny multi-components and electrodes etc. The μ-EDM process is applied for electrically and thermally conducting materials.

1.1.1.2 Electro Chemical Micro-Machining (μ-ECM)

Electrochemical Micro-Machining (μ-ECM) belongs to electro-chemical category of non-traditional machining (NTM) processes. μ-ECM is an opposite process of galvanic coating or deposition process. Thus μ-ECM can be thought of a controlled anodic dissolution at atomic level of the job specimen that is electrically conductive by a shaped tool due to flow of high current at relatively low potential difference through an electrolyte solution, which is quite often water based neutral salt solution.

During Micro-ECM, there will be electro-chemical reactions occurred at the electrodes *i.e.*one is the anodic reaction or reaction at job specimen and other is reaction at cathode or reaction at the micro-tool in the electrolyte.

For the machining of low carbon steel, this is primarily a ferrous alloy mainly containing iron. For electrochemical machining of steel, sodium chloride (NaCl) is taken as the electrolyte. The electrolyte and water undergo ionic dissociation when potential difference is applied and the reactions occurred are discussed briefly as below:

$NaCl \rightarrow Na^{+} + Cl^{-}$

$H_2O \rightarrow H^{+} + (OH)^{-}$

As the potential difference applied between the job specimen (anode) and the tool (cathode), the positive ions move towards the micro-tool and negative ions move towards the

job specimen. Thus the hydrogen ions will receive electrons from the cathode (micro-tool) and from hydrogen gas, as discussed below:

$2H^+ + 2e^- = H_2\uparrow$ at cathode

Similarly, the iron atoms will come out of the anode (job specimen) as:

$Fe = Fe^{++} + 2e^-$

Within the electrolyte iron, ions would combine with chloride ions to form ferrous chloride (if sodium chloride salt solution is used as electrolyte) and similarly sodium ions would combine with hydroxide ions to form sodium hydroxide.

$Na^+ + OH^- = NaOH$

Practically ferrous chloride and ferrous hydroxide would form and get precipitated in the form of sludge. It is notified that the job specimen gets gradually machined and gets precipitated as the sludge. Moreover there is no coating on the micro-tool, only hydrogen gas assembles at the tool or cathode. As the material is removed due to atomic level dissociation, the machined surface gets excellent surface finish and there is no stress.

The voltage is applied for the electrochemical reaction at a steady state. That voltage or potential difference is around 2 to 30 V for micro-machining.

The material removal rate or machining is not dependent on the mechanical or physical properties of the work material. It only depends on the atomic weight and valence of the work material and the condition that it should be electrically conductive. Thus micro-ECM can machine any type of electrically conductive materials irrespective of their hardness, strength or even thermal properties. Moreover, as μ-ECM leads to atomic level dissolution, the surface finish is excellent with almost stress free machined surface and without any thermal damage compared to other micro-machining processes. Micro-ECM can be used for micro-machining operations like micro-drilling, micro-channeling, micro-grooving etc.

1.1.1.3 Laser Beam Micro-Machining (μ-LBM)

Laser beam is highly coherent and monochromatic photons. Laser beam can be focused into a tiny spot of micron-level diameters and it produces a high power density, as 70 W/mm^2 required for micro-machining.

Nd: YAG laser, Excimer laser and Diode laser are effectively used for micro-machining applications as the spot diameter is in micron-range. Laser beam machining process is applied for various micro-machining operations such as drilling, cutting, turning, milling, cleaning

and marking etc, on varieties of materials from plastics to diamonds. As it is a thermal process, laser beam machining process has various disadvantages such as heat affected zone, taper surface, difficult to cut highly reflective and transparent materials, lower energy efficiency and higher investment cost.

The one of the major advantages of laser beam micro-machining is that it can machine electrically conducting and non-conducting material, with higher rate and accuracy compared to other micro-machining processes.

Laser beam can be applied for non-machining applications such as welding of similar and dissimilar materials in aircraft, automotive and ship building factories. Laser beam is applied in jewelry industry for welding of different micro-components and machinists use laser beam to repair corroded parts by fusing material to damaged areas. Laser beam is used for surgical purpose in the medical field for better accuracy and precision by controlling the energy of beam.

1.1.1.4 Abrasive Water Jet Micro-Machining (µ-AWJM)

In Abrasive Water Jet Micro-Machining (µ-AWJM), a high velocity focused stream of water and fine abrasive mixture is used for cutting almost any type of materials and also water pressure is observed during micro-abrasive water jet machining is 40,000 to 55,000 psi. Momentum of the water stream accelerates and entrains abrasive as it passes through the micro-hole of nozzle. In micro-abrasive water-air jet machining (µ-AWAJM), three phase mixture of air, water and fine abrasive particles are used. The high velocity abrasive particles impact on the kerf face and do the actual cutting. Kerf material is removed as a form of micro-chips from the job specimen, with negligible thermal effects on the material.

The quantity of abrasive depends on the cutting stream size, which is selected based on the material which is to be cut by µ-AWJM. Garnet is the most commonly used abrasive. It is a good abrasive due to its characteristics of clarity, contains no free silica and combines good cutting ability with reasonable wear on the consumables. Other abrasives which are rarely used in µ-AWJM are olivine sand and silica sand. Aluminum oxide has been used as abrasive for cutting of soft materials. Because of its high hardness, aluminum oxide rapidly wears out the nozzle and is expensive to operate in µ-AWJM. Advantages of µ-AWJM are to cut virtually any materials like pre hardened steel, mild steel, copper, brass, aluminum, brittle materials like glass, ceramic, quartz and stone and also cut thin stuff, or thick stuff. No heat is generated during µ-AWJM, so heat affected zone (HAZ) is neglected and generate smooth finish, thus no necessary of secondary operations and also clean cutting process without

gasses or oils or hydro carbons. Any dust or particles is produced during µ-AWJM is easily removed as waste after machining and pollution which is less than AJM process can be easily controlled.

1.1.1.5 Ultrasonic Micro-Machining (µ-USM)

Ultrasonic micro-machining (µ-USM) is one of the most efficient material removal processes from hard and brittle materials like bio-ceramics and glass. In µ-USM ultrasonic vibration frequency varies from 19-25 KHz and amplitude may vary from 1-50µm [1]. Aluminum oxide or bron carbide fine abrasive slurry is used on the top of the job specimen. Rotating tool strikes on abrasive particles into slurry and material is removed by the mechanical action of the micro-tool to fine abrasive. During micro-machining operations by USM process, higher rotational speed with abrasive particle size 0-5, abrasive concentration 0.5-3%, medium of the slurry water/oil and tool diameter is chosen with in micro-range and also vibration amplitude has been taken very less.

Some major advantages of ultrasonic micro-machining are as it generates burr-less and electric, thermal and chemical defects free surface. As no chemical action takes place during machining, so no change of micro-structures of job specimen found. Micro-hole, production of machinery parts, round, square and contour shape can be produced on electrically non-conductive materials like glass and ceramics but for this machining high investment is and skilled operator is highly required.

1.1.1.6 Electrochemical Discharge Micro-Machining (µ-ECDM)

Electrochemical discharge micro-machining is a hybrid non-traditional machining (HNTM) process that combines the two machining processes such as electrochemical machining (ECM) and electro discharge machining (EDM) [2]. Two electrodes are used in µ-ECDM: one is a cathode (the µ-tool) and the other is an anode or an auxiliary electrode. The job specimen is placed just below the micro-tool and along with the auxiliary electrode, is immersed in an electrolytic or alkaline solution in a machining chamber. In the µ-ECDM process the thermal erosive effects of electrical discharge (ED) action is followed by an electrochemical (EC) reaction. This electrochemical reaction helps in the generation of the positively charged ions and gas bubbles. These gas bubbles accumulate across the interface of the micro-tool and the job specimen. The electrical discharge action takes place between the micro-tool and the electrolyte across the gas bubble layers. If the applied voltage is greater than the break down voltage of the insulating layer of the gas bubbles, sparking is started.

The intensity of sparking and energy of the spark increases with the increase of the applied voltage between two electrodes. If a non-conducting job specimen is placed in the closed vicinity of the electrical discharge, the material of the job specimen is melted, vaporized and eroded due to the transmission of a fraction of spark energy to the job specimen. This raises the temperature of the region dramatically and a part of the molten portion of the job specimen is removed due to the mechanical shock resulting from the sudden phase change and the electrical spark discharge. Additional material is removed due to thermal spalling on the job specimen.

1.2 ADVANTAGES OF μ –ECDM

μ-ECDM process is a compound hybrid process consists of electrochemical reaction and electric discharge helps in machining electrically hard and brittle materials such as aluminum oxide, silicon nitride, zirconia and glass etc. Also there are other advantages of μ-ECDM process as stated below:

(i) There is no direct contact between tool and job specimen for better machining. No external forces are required to remove material during μ-ECDM process.

(ii) The machining process requires softer but electrically conducting tool materials.

(iii) Using ECDM heat treatment of the surface of job specimen improves the hardness of the job specimen.

(iv) No isolated chamber is required for the μ-ECDM set up. It can be set up in the laboratory with other machining system in particular shop floor.

(v) No skilled worker is required for micro-machining operations. It is easy to handle as well as maintenance cost is very small.

(vi) Less Heat Affected Zone (HAZ) is found during micro-machining by ECDM process.

(vii) ECDM process can be applied for varieties of micro-machining operation such as drilling, cutting, milling, dressing, grinding etc.

1.3 APPLICATIONS OF μ–ECDM

Electrochemical discharge micro-machining is applicable in various modern industrial field like aerospace engineering, medical science and instruments, automobile industries, glass industries and electrical and electronics industry etc. For fabrication of micro-fluidic device μ -ECDM process has the ability to generate micro-channel and micro-slots on electrically non-conducting materials like ceramics, glass quartz and composites etc. Sometimes it can be used for drilling, cutting micro-hole on non-conducting materials. There also other

applications such as welding and surface hardening can be done by μ-ECDM process. Micro-holes, micro-complex profile, micro-slot cut, round, square or taper marking, contour machining, micro-structure of glass wafers preparation and micro-reactor applications and also micro fluidic channel generation can be performed by μ-ECDM process.

1.4 REVIEW OF PAST RESEARCH

1n 1833 Michael Faraday discovered the law of electrolysis as electro-deposition and dissolution and ECDM process was utilized first for machining operation by Kurafuji and Suda in 1968. After that many researchers, scientists and manufacturing engineers are trying to overcome the problematic areas by their research and invention, so that μ-ECDM process can be utilized successfully in modern manufacturing industrial field. But the material removal mechanism and the effect of various process parameters of μ-ECDM process are not cleared properly. Therefore, to exploit full potential of ECDM in micro-machining domain, research is still needed to improve the accuracy and compactness. The survey of past research investigations from different engineers, scientists and researchers have been documented as follows:

Tandon *et al.* [3] proposed new approach using electrochemical spark machining (ECSM) for drilling hole in composites. Kevlar-fiber-epoxy and Glass-fiber-epoxy materials were used as job materials and copper was used as tool electrode. The parametric study of process parameters was performed using a design of experiment (DOE) as well as a "one variable at a time" approach. Material Removal Rate (MRR), Tool Wear Rate (TWR), Overcut (OC) were found to increase but relative tool wear was found to decrease with the increase of applied voltage during micro-drilling operation. In case of drilling of holes MRR, TWR and OC was increased with the increase of electrolyte conductivity and decreased with increase of tool diameter during the machining of non-conducting fiber rein forced plastics (FRP).

Raghuram *et al.* [4] propounded the effects of external circuit parameters on performance of the electrochemical discharge (ECD) process and performed experimental investigations using NaOH and KOH electrolytes. The best circuit configuration for the machining of non-conductive material was analyzed. The external circuit parameters had a definite influence on the discharge characteristics. The authors showed the voltage current behavior during ECD process and also the effects of internal inductance and capacitance in electrochemical discharge machining process. The rectified and smooth D.C. voltage with the internal

inductance and capacitance were applied during experimentation. By using external inductor into the circuit and constant power supply the through holes were fabricated successfully in quartz glass by electrochemical discharge machining process.

Basak and Ghosh [5] described electro-chemical discharge phenomenon in ECDM process. If a beyond-critical voltage was applied to an electrochemical cell, discharge would be taken place between one tool of the electrodes and the surrounding electrolyte, which was termed here as 'electro-chemical discharge'. The authors developed a simplified model to predict the performance characteristics of the material removal rate (MRR) for varying input parameters with the objective of finding the possibility of enhancing the capability of the process. The ECD phenomenon was analyzed as a switching process between the tool and the electrolyte. The theoretical and experimental results indicated that a substantial increase in the material removal rate could be achieved due to the additionally introduction of inductance to circuit.

Basak and Ghosh [6] revealed that the process of electro-chemical discharge was a very complex phenomenon involving a number of processes taking place simultaneously. The authors also presented a simplified model based on an idealistic mechanism, which suggested a number of interesting characteristics, which were supported by the experimental observations. The authors showed the discharge phenomenon as switch on and off action. The current distribution over the length of the tool was investigated. Hence, the idealized mechanism of ECD represented the actual physical phenomenon with reasonable accuracy.

Xiaowei *et al.* [7] proposed a combined machining process of electrical discharge machining (EDM) and pulse electrochemical machining (PECM). The authors performed experiments on electrical discharge machining (EDM) with orbital motion of the job specimen as a result the arc shape of the subtle neck was performed without deformation. Electrical discharge machining (EDM) caused more heat affected zone (HAZ) and stress affected into the layers of the subtle neck during machining. The authors revealed that the machine holes were fabricated with high dimensional accuracy and mirror like surfaces by the pulse electrochemical machining (PECM). By this hybrid machining process the authors fabricated better quality of holes with higher accuracy and precision.

Bhattacharyya *et al.* [8] analyzed the basic material removal mechanism in the ECDM process for the effective machining of non-conducting ceramic materials with enhanced machining rate and higher machining accuracy. The major influencing parameters in the

ECDM process were found as applied voltage, the inter-electrode gap, concentration and type of electrolyte, the shape, size and material of the electrodes and the nature of the power supply etc. A well designed and developed machining set-up for conducting experimental investigations was documented. Experimental investigations were conducted by the authors for the machining of aluminum oxide ceramic job specimen under varying process parametric conditions such as applied voltage (70-90 V) and electrolyte concentration (20-30%). A pulsed D.C. electric supply was utilized for the drilling operation on ceramic work-samples with varying NaOH electrolyte concentration. In addition, an attempt was made to explore the influence of a suitable and effective tool tip geometrical shape for greater machining rate and accuracy. The most suitable tool geometry which can enhance better result for further machining process, was suggested after performing some experiments with different tool tip geometries. Detailed analysis of various test results was conducted to provide further insight into the fundamental mechanism of process by a large number of micro-graphs of the machined work samples.

Kozak *et al.* [9] explored some of fundamental processes, which occurred during abrasive electrochemical machining (AECM) and abrasive electrical discharge machining (AEDM).Actually advanced manufacturing processes were hybridized with other traditional and non-traditional machining processes to create entirely various new techniques with superior manufacturing capabilities for machining of advanced conducting as well as non-conducting engineering materials. The authors reported about the fundamental of various advanced processes such as abrasive electrochemical machining (AECM), abrasive electro chemical grinding (AECG) and electro chemical honing (ECH) and abrasive electrical discharge machining (AEDM) and abrasive electrical discharge grinding (AEDG).These were used as advanced hybrid machining processes to cut advanced engineering materials. Actually by combination of two or more processes, a new technique would come and the new process could be utilized with superior manufacturing and control capabilities.

Jain *et al.* [10] proposed that the electrochemical spark machining (ECSM) process was a potential process for machining of alumina and glass. However, ECSM had its own inherent limitations. The authors also conducted electrochemical spark abrasive drilling experiments by using abrasive cutting tools, with a view to enhance the capabilities of the process. Authors used the abrasive tool electrode of diameter 1.5 mm and applied rotary motion to drilling hole on Al_2O_3. The author also observed that at 70 V crack was formed on ceramic

job specimen and volume of material removed were not more than 20 mg. The use of an abrasive cutting tool, compared to a conventional cutting tool, improved the process performances.

Kulkarni *et al.* [11] proposed the basic mechanism of material removal of ECDM process based on experimental observations of time-varying current in the circuit. When an isolating film of hydrogen gas bubbles covered the cathode tip portion in the electrolyte, a large dynamic resistance was presented and the current through the circuit became almost zero. A high electric field was generated across the cathode tip and isolated electrolyte causing discharge within the gas bubble layers covering the tip. The electrons flow towards the job specimen was kept near the cathode tip. The bombardment of electrons raised the temperature of the job specimen momentarily and then the temperature decreased due to quenching. The authors suggested that the discharge on job specimen under an optical microscope showed the evidence of separate discharge striking the surface, and their distribution over the surface. The discharge-affected region was found as a circular zone.

Mediliyegedara *et al.* [12] performed a preliminary study on electrical pulse classification to develop a control strategy for electro-chemical discharge machining (ECDM) process. Pulses were classified into five groups by observing the voltage and current waveforms. The authors applied the theory of artificial neural network. A feed-forward neural network was trained to classify pulses with various activation functions. Classification accuracy was utilized to measure the performance of a pulse classification system and the neural networks with five different activation functions. The simulation results showed that an ANN with the SATLINS and SATLIN functions take longer time to train, but their classification accuracy was comparable with that of other activation functions. ACA of the neural network with SATLINS activation function was higher than the neural network with SATLIN activation function.

Skrabalak *et al.* [13] proposed a model that was built of rules based on fuzzy-logic control of ECDM process. Investigations were carried out on ECDM process in 6% water solution of sodium nitride as electrolyte. Electrode feed and current were considered as the important process parameters and the electrolyte temperature was fixed at a constant value during machining. Fuzzy-logic and adaptive fuzzy-logic control systems helped to reduce the number of micro-cracks and surface roughness. The way of process control was found

beneficial to increase of metal removal rate for this process and current estimation, micro crack formation and reduced surface roughness using fuzzy logic. But practical application of the fuzzy-logic controller at the real machine was very difficult, as it was very hard to measure quickly. Although MRR and quality of machining surface were also improved.

Peng and Liao [14] observed that in Travelling Wire Electrochemical Discharge Machining (TWECDM), the spark discharge occurred across the gas bubbles around the wire while the applied voltage was higher than the transition voltage. Traveling wire electrochemical discharge machining was done to slice the small size (10–30mm diameter) optical glass and quartz bars. The electrical–thermal etching effect and its feasibility were investigated. The pulsed DC power source was proved better for spark stability and more spark energy than constant DC power source. The ion translation rate, the electrolyte immersing depth and the concentration of the alkali electrolyte were found as the dominant factors for bubbles formation during TWECDM process.

Wüthrich *et al.* [15] documented that machining with electrochemical discharges was able to machine electrically non-conductive materials like glass or some ceramics. The machining mechanism was combination of thermal and chemical machining, where the thermal effect clearly dominated the machining process. The researcher studied the effect of different parameters on the material removal rate, which was depended on a large number of parameters like electrolyte type, material to be machined, applied voltage and temperature. Various types of materials (glass, quartz, various ceramics and others) could be machined. Not only simple structure such as holes but very complex structures like thread could be machined. The authors suggested that the reproducibility should be at least a few microns for micro-machining application. One of the major challenges in reaching this goal was certainly the control of gas film built around the tool-electrode where the discharge took place. The authors concluded that not only thin gas film was necessary for machining to occurs, but also the stability of the film conditions are important for the machining.

Kim *et al.* [16] investigated into the micro-drilling of glass wafers using electro-chemical discharge machining (ECDM) process. In this study a series of rectangular voltage pulses, were applied instead of the rectified or full-wave DC voltages in order to reduce heat affected zone (HAZ) on the micro-drilled hole surface. An experimental investigation was done to check the effect of the frequency and duty ratio of the voltage pulse during ECDM of Pyrex

glass. The experimental results showed that the heat affected zone thickness surrounding the micro-drilled hole decreased with increase in frequency and decrease in duty ratio and also the clearance increased as the tool diameter decreased. The results also showed that as the duty ratio increased, the removal rate also increased but the drilled surface became rougher. A series of voltage pulses in place of full wave DC voltage was recommended because at this condition of machining the micro drilled surface quality was improved.

Yang *et al.* [17] investigated into the possibility of using wire electrochemical discharge machining (WECDM) of difficult to cut materials with high hardness, brittleness, strength and showed the effectiveness of process as independent of the mechanical characteristics of job specimen materials. The experimental results revealed that adding abrasive the slit expansion was reduced because it increased the critical voltage. The particles disrupted the bubbles' accumulation to form an isolating layer around the wire, increasing the critical voltage and reducing the discharge energy. The surface roughness was improved as the abrasives helped to refine the micro-cracks and melted zone. Meanwhile, smaller grit produced lower roughness. The quality of the slit could be controlled. The expansion and roughness of the slit were found 0.024 mm and 0.84 μm respectively. Increasing the power frequency and reducing the duty factor improved the expansion because less energy was released during the discharge at this condition. Less discharge energy was released during machining, so the area of machining was less using KOH electrolyte. Increasing the feeding rate of the wire suppressed the accumulation of the brass chips because of the contact between wire and glass. Preventing the secondary discharge improved the expansion. The surface topography was improved with the increase in power frequency to reduce the energy during discharge.

Sarkar *et al.* [18] utilized the electrochemical discharge machining (ECDM) process for micro- machining of silicon nitride ceramics. A second order, non-linear mathematical model for establishing the relationship among machining parameters, such as applied voltage, electrolyte concentration and inter-electrode gap, with the dominant machining process criteria, namely material removal rate (MRR), radial overcut (ROC) and heat affected zone (HAZ), was developed based on response surface methodology (RSM) using the relevant experimental data. The authors also focused on the analysis of variance (ANOVA) and a confirmation test to verify the adequacy of the developed mathematical models. The authors observed that applied voltage had more significant effects on MRR. The authors reported that

MRR in micro-ECDM processes increased initially with an increase of electrolyte concentration and then it decreased after reaching its maximum value. The nature of variation of MRR with respect to electrolyte concentration was similar for different applied voltages. The radial overcut during micro-ECDM operations increases with an increase of applied voltage because of the fact that at high voltage a large number of gas bubbles were generated at the tool sidewall. The thickness of HAZ was increased with an increase in applied voltage and with the electrolyte concentration.

Bhondwe *et al*. [19] discussed on the material removal mechanism of electro-chemical spark machining (ECSM), which combined the features of the electrochemical machining (ECM) and electro-discharge machining (EDM). An attempt was made to develop a thermal model for the calculation of material removal rate (MRR) during ECSM operation. The temperature distribution within zone of influence of single spark was obtained with the application of finite element method (FEM). The nodal temperatures were further post processed for estimating MRR. The developed FEM based thermal model was found to be in the range of accuracy with the experimental results under the same machining conditions within the acceptable range. Further the parametric studies were carried out for different parameters like electrolyte concentration, duty factor and energy partition. The change in the value of MRR for soda lime glass with concentration was found to be more than that of alumina. MRR was found to increase with increase in duty factor and energy partition for both soda lime glass and alumina job specimen material.

Han *et al.* [20] reported a new method for improvement of the surface integrity in electro-chemical discharge machining (ECDM) process by use of conductive particles in the electrolyte. In this study fine graphite powder, which has good thermal and electrical conductivity, mixed with electrolyte was applied in ECDM process. Borosilicate glass was used as a job specimen. The experiment was conducted using cylindrical tungsten carbide (WC) electrode of diameter of 0.2 mm, 30% NaOH as electrolyte and 35V DC as the applied voltage. At 0.5 and 1.0 wt% powder concentration, the machined surface became fine and smooth. However, when the concentration was above 2.0 wt%, micro-cracks were developed. The experimental results demonstrated that the breakdown voltage was reduced and the peak current during the process was decreased by 10%. Discharging pattern was modified such that a single discharge pulse was branched into two or three. The number of micro-cracks was

significantly reduced and the surface roughness was improved from 4.86 to 1.44 μm by using 1.0 wt. % graphite powder concentration in 30% NaOH electrolyte solution.

Chak and Rao [21]investigated the possibility of drilling large size holes by comparatively smaller electrodes efficiently and economically in electro-chemical discharge machining (ECDM) process on electrically non-conductive high-strength, high temperature-resistant ceramics such as aluminum oxide (Al_2O_3) by trepanning method (i.e. orbital motion of tool). However, by the use of conventional electrode configurations the machining performance were gradually deteriorated with increase in tool depth and finally caused micro-cracks were found on the machined surface due to thermal shocks at high voltage. To overcome this problem and to enhance the machining performance during trepanning operation of Al_2O_3, a spring fed cylindrical abrasive electrode of 1.5 mm diameter was used under the effects of three most influencing parameters, pulsed DC supply voltage, duty factor and electrolyte conductivity, each at five different levels to assess the volume of material removed, machined depth and diametric overcut. The authors concluded that pulsed DC reduced the tendency of cracking at high supply voltage compared to smooth DC and the machining ability of the abrasive electrode was better than copper electrode as it would enhance the cutting ability due to the presence of abrasive grains during machining.

Furutani and Maeda [22] analyzed the performance of electro-chemical discharge machining (ECDM) of a revolving glass rod. In conventional ECDM, an insulating job specimen was dipped in an electrolyte and a tool electrode was pressed on the surface with a small load. In the investigations, a job specimen was revolved to provide fresh electrolyte into a positive gap between the tool electrode and job specimen. A soda lime glass rod was machined the tool of tungsten rod in NaCl solution. The applied voltage was increased up to 40 V. The rotational speed was set to 0, 0.3, 3 and 30 rpm. Discharge was observed over an applied voltage of 30 V. The width and depth of machined grooves and the surface roughness at the bottom of grooves were increased with increase of the applied voltage. Although the depth of machining at 3 rpm was the same as that at 30 rpm, the width and roughness at 30 rpm were smaller than those at 3 rpm. Vaporization around the tool electrode was decreased with increase of the rotation speed and the width of the machined groove became smaller.

Jain and Adhikari [23] investigated on electro-chemical spark machining (ECSM) process during cutting of quartz using a controlled feed and a wedge edged tool. The authors used

cathode and anode as a tool, i.e. ECSM with reverse polarity (ECSMWRP) as well as ECSM with direct polarity (ECSWDP) to machine quartz plates. In ECSMWRP, deep crater on the anode (as a tool) and job specimen interface was formed because of chemical reaction. In reverse polarity quartz plate was cut at a faster rate as compared to the direct polarity. But in direct polarity overcut, tool wear and surface roughness were found low as compared to the reverse polarity machining. Magnified views of the machined surface also showed a difference in the mode of material removal in ECSMWDP and ECSMWRP. The cutting was possible even if an auxiliary electrode of small size was used. The authors revealed that cutting could be performed simultaneously at both the electrodes (anode and cathode) during ECSM.

Wuthrich *et al.* [24] proposed that 'micro fabrication of Pyrex glass was one of the key processes in MEMS. Several applications needed glass because of its unique properties like its chemical resistance, transparency, low electrical and thermal conductivity or biocompatibility. The authors focused on experimentation of the machining of various materials and investigated on the effect of different parameters on the material removal rate. It was shown that various types of materials (glass, quartz, various ceramics and others) could be machined. Holes as well as complex structures like threads could be machined on non-conducting materials. A material removal rate was influenced by a large number of process parameters like type of electrolyte, applied voltage and temperature. Gas film is necessary for machining of non-conducting materials and at around 25 V the cathode reaction starts and at around 30 V the sparking clearly visible and this discharge took place for material removal.

Liu *et al.* [25]investigated into the discharge mechanism in wire electrochemical discharge machining (WECDM) of a particulate reinforced metal matrix composite and also developed a model to reveal the electric field acting on a hydrogen bubble in ECDM process. A high applied voltage or long pulse duration reduced the material removal rate. High machining current led to increase MRR. During ECM, an enlargement of the machining gap was introduced to improve the condition for the ceramic reinforcement to be washed away from the gap. The simulation of current density showed that when an emulsion electrolyte instead of deionized water was used, high current densities appeared around the ceramic particles. From the orthogonal analysis it was observed that during machining of 10% Al_2O_3 reinforced material, MRR was influenced by the machining parameters in the order of, current, pulse duration and then electrolyte concentration. But for the 20% Al_2O_3 reinforced material, the

order of importance was found as current, electrolyte concentration and then pulse duration. The experimental results also showed that an increase in current, duty cycle, pulse duration or electrolyte concentration would promote the occurrence of arcing action in WECDM.

Cao *et al.* [26] studied micro-electrochemical discharge machining (micro-ECDM) to improve the machining of 3D micro-structures of glass. To obtain good surface microstructures and to minimize structures, the effects of the electrolyte, the pulse on/off-time ratio, the voltage, the feed rate, the rotational speed and the electrolyte concentration in the drilling and milling processes were analyzed. The authors documented that in ECDM, voltage was applied to generate a gas film and sparks on a tool electrode, although, high voltage produced poor machining resolution. To obtain a stable gas film over the whole surface of the tool at a low voltage, a new mechanical contact detector, based on a load cell, was used. The immersion depth of tool electrode in the electrolyte was reduced as much as possible. Various micro-structures less than 100μm in size, such as Ø60μm micro-holes, a 10μm thin wall and a 3D micro-structure were fabricated to demonstrate the potential for micro-machining of glass by ECDM. The use of pulse voltage reduced the hole size and improved surface quality. Micro-hole with a 60 μm diameter and a 150 μm depth was obtained at 30V pulse voltage and a 1 ms/1ms pulse on/off-time ratio. In ECDM milling, 0.099 μm R_a was obtained with a 23V pulse voltage. Also the author observed that KOH electrolyte gave a smaller machining gap than NaOH solution. The smallest machining gap, 15μm, was achieved in KOH 30 wt%. In micro-milling, the depth of the machined layer should be small to avoid tool breakages and job specimen cracks. A feed rate that was too slow produced a rougher surface; one that was too fast broke both the tool and job specimen due to mechanical contact. The machining feed rate was 3μm/s and the depth of the machining layer was 25μm.

Liu *et al.* [27] discussed about the analysis of the discharge mechanism in electro-chemical discharge machining (ECDM) of a particulate reinforced metal matrix composite. A model, which was found capable of predicting the position of the maximum field strength on the bubble surface as well as the critical break down voltage for spark initiation and for a given processing condition was established to reveal the electric field acting on a hydrogen bubble in ECDM process. The authors reported that the maximum field strength acting at the surface of hydrogen bubble occurred at an angle of 90^0 perpendiculars to the vertical line drawn between the two electrodes. The model was found to be capable of predicting the breakdown

voltage of a discharge, which in the present study was between 26.2 and 34.2V. The model showed that the breakdown voltage did not have a relationship to the presence of the reinforcement phase. The experimental breakdown voltage was found to lie between 26 to 30V.After performing the set of experiments to verify the model, the results showed that an increase in current, pulse duration, duty cycle, or electrolyte concentration would promote the occurrence of arcing action in ECDM. Also, by studying the wave form of ECDM and surface craters, the authors concluded that the spark action was in the form of an arc. The volume of an arc eroded crater in ECDM was less than that of EDM. An XRD analysis of the phases of EDMed and ECDMed specimens showed that the Al_4C_3 phase was detected on the job specimen after machining by EDM but not to machining by ECDM.

Yang *et al.* [28] stated that electro-chemical discharge machining (ECDM) was a non-conventional machining process that involved high-temperature melting assisted by accelerated chemical etching. The authors fabricated the tool electrode of 200 mm by wire electrical discharge grinding (WEDG). The surface roughness of tool electrode materials like stainless steel, tungsten carbide and tungsten were investigated and find different results due to their different physical properties. The author observed that tungsten carbide electrode was the best electrode and its surface roughness would less effect during machining due to its high melting point. The authors also explored the wettability and machining characteristics of different tool electrode materials and their impact on the gas film formation.

Khas and Manna [29] designed and fabricated a micro-electrochemical discharge machining (μ-ECDM) setup for the purpose of machining non-conductive materials like aluminum oxide (Al_2O_3) ceramics. The authors reported that at higher setting value of DC supply voltage e.g. 90 V and at moderate setting values of gap between electrodes e.g. 200mm the material removal rate (MRR) was found as the highest. The mathematical model for MRR was developed to predict the setting value of micro-ECDM parameters in advance. Based on the experimental results during drilling on Al_2O_3 ceramics the authors concluded that the most influential parameters on micro-hole depth were electrolyte concentration and DC supply voltage. Parametric combination of 90V DC supply voltage, 110 g/l electrolytic concentration and 100 mm gap between anode and cathode was recommended for maximum material removal rate (MRR). It was observed that at the initial stage of drilling the shape of generated micro hole was conical during drilling. Even after 5 minutes of continuous machining the shape of micro hole still was conical in shape.

Cheng *et al.* [30] showed an idea about transition voltage. Electrochemical discharge machining (ECDM) was demonstrated to be an alternative spark-based micro-machining method for producing micro-holes and micro-channels in non-conductive hard and brittle materials. In this process, the gas film on the electrode surface was used as the dielectric medium required for producing discharge. Quality of gas film was an important and dominant factor that determined the machining qualities such as geometric accuracy, surface roughness and repeatability. In this study, current signals and machined contours were taken as indexes of gas film quality. A stable and dense gas film could be obtained when the applied voltage exceeded the critical voltage and reached a specific level, which was called the ‘‘transition voltage’’. At the transition voltage, a stable electrochemical discharge activity could be generated, thus producing the smallest deviation of contour dimensions.

Wei *et al.* [31] reported an idea about electro-chemical discharge dressing (ECDD). ECDD was based on electro chemical discharge effect of ECDM process. Experiments were conducted to evaluate the dressing performance of ECDD in terms of surface morphology of the tool, grinding force and surface roughness of the job specimen. A dull micro-end grinding bit and an auxiliary electrode were connected to the negative and positive terminals of a power supply respectively while the auxiliary electrode was immersed in an electrolyte and the grinding face of the tool was in contact with the electrolyte surface. During dressing operation, the metal bond on the tool–electrolyte interface was progressively removed by electro chemical discharge effect. Creation of grain protrusion took place. The experimental results showed that abrasive grains on the tool protruded without observable damage. The normal grinding force and the surface roughness of the job specimen were reduced by 50% after dressing. ECDD was integrated to a micro-grinding machine to avoid error induced by tool re-clamping. ECDD might be a truing process when a high power was used for faster material removal.

Yang *et al.* [32] documented electrochemical discharge machining (ECDM) as a non-conventional processing technique involving high-temperature melting and accelerated chemical etching under the high electrical energy discharged. The hole entrance diameter and machining time were found to increase with increasing machining depth. Both the high efficiency and accuracy in drilling a through hole in hard and brittle materials by ECDM process were improved using a tool electrode with a spherical end whose diameter was larger than that of its cylindrical portion. The authors reported that the curve surface of the spherical

tool electrode reduced the contact area between the electrode (tool) and the job specimen hence, the availability of electrolyte at the electrode end and enabled rapid formation of gas bubbles. As a result deeper micro-hole was produced by drilling. Moreover, the curve surface reduced the concentration of current density and the growth of bubbles took place at a more uniform speed. Thus the discharge frequency increased. A comparison was made between the machining depth of 500 μm achieved by conventional cylindrical tool electrode and that obtained by the proposed spherical tool electrode. The authors exhibited that the machining time was reduced by 83% and hole diameter was also decreased by 65%, due to application of spherical tool electrode.

Mochimaru *et al.* [33] demonstrated feedback circuit for machining-stop system and two-step machining, which were developed to reduce the diameter of micro hole. The diameter of micro hole was obtained as 12 μm and with the following process parameters such as depth of electrolyte 0.5mm, Voltage 30-35V, Pulse frequency 15- 25Hz, Duty factor 10-80%. The authors also documented that at the first step, ECDM process was stopped in the middle depth of the job specimen, and the penetration was completed at the second step. The shape of micro hole was improved by using the micro tool electrode which had high accuracy straightness. The diameter and length of this tool electrode which was formed by ECM process from tungsten rod were 20 μm and 1.6 mm, respectively. The smallest diameter and the exit diameter were reduced by integrating this system into ECDM device. From this research work it was concluded that the smallest diameter of micro hole was reduced by two-step processing and achieved as 12 μm.

Jawalkar *et al.* [34] observed that the applied voltage was found as the most influencing parameter in both machining rate (MR) and tool wear (TW) during investigations by electrochemical discharge machining (ECDM). The authors documented that the presence of micro-cracks on micro-channel, which was observed by using field emission scanning electron microscopy (FESEM). Chemical etching was also observed along the edges. The energy dispersive spectroscopy (EDS) results were used to detect the elements present in the debris and specimens. The applied voltage was found to be the most influencing parameter. The length of micro channels were varied from 10 to 15 mm. Width of channels were0.8 to 1mm and machining depth was 0.1 to 0.2 mm during channel cutting by ECDM process. **Jana *et al.* [35]** showed that the electrolyte viscosity was found to be the most significant factor influencing the channel texture among other factors including tool job specimen gap,

machining voltage and tool travel speed. Pulsed voltage was applied to control the local temperature at the machining spot, also proved to influence the surface texture. The surface texture obtained was depended on the concentration of NaOH electrolyte and its viscosity. It was demonstrated that for low electrolyte concentration the channels machined at low speed (5 mm/s) had a uniform surface texture and flat walls as compared to channels machined at higher speed (10 mm/s and 20 mm/s). It was also shown that the tool-job specimen gap affected the depth of micro-channels. The tool speed also influenced the machining depth and the depth was decreased when the speed was increased.

Jawalkar *et al.* [36] reported the application of ECDM on soda-lime glass for making shallow holes. In the current study, Taguchi's standard orthogonal array L_9 was used to examine the influence of process parameters, mainly the electrolyte concentration, applied voltage, distance between electrodes and time of current flow on material removal (MR) as response parameter. The authors also discussed that all the parameters were significant and the applied voltage was found to be the most influencing parameter (70.14%). Field Emission Scanning Electron Microscopy (FESEM) results showed the predominant presence of thermal cracks and some etching marks on the machined area. Micrographs obtained using Scanning Electron Microscope (SEM), revealed the evidence of the side sparking effect on tool edges.

Paul *et al.* [37] investigated on the effect of processes parameters on material removal rate (MRR) on silicon wafers and NaOH was used as electrolyte solution. The machining of micro-holes was done on silicon wafer and musical string steel wire was used as tool and graphite plate as anode with pulsed DC power supply during micro-hole fabrication by electrochemical discharge machining (ECDM) process. Designs of experiments (DOE) were utilized to plan the experiments and the optimized process parameters were found using Taguchi method. The mathematical model for material removal rate was developed using Response Surface Modeling (RSM) and the process parameters were optimized for finding out the best optimal parametric combination during micro-hole generation on silicon wafers by ECDM process. The statistical model of RSM was developed and validated with analysis of variances (ANOVA) to predict adequacy of the model which were validated with experimental results.

Chak *et al.* [38] reported that the volume of material removed from the job specimen was increased with increase of supply voltage, duty factor and electrolyte conductivity. Pulsating nature of power supply improved the machining performance and reduced the tendency of cracking at high supply voltage while the use of abrasive electrode had partially relaxed the

inherent limitations of the machining process. Material removal rate was increased with increase of duty ratio and electrolyte conductivity and abrasive electrode. Abrasive electrode gave better results compare to other electrode which was used in electro chemical discharge machining process (ECDM). The authors also mentioned that the orbital motion of abrasive electrode showed the maximum volume of material removed compared to rotary abrasive electrode while rotary abrasive electrode showed the increased volume of material removed compared to stationary brass electrode.

Kulkarni *et al.* [39] fabricated micro-channels on glass using electrochemical spark micro-machining (ECSMM) process with the square pulsating waveform as machining power source to investigate the effect of the duty cycle on the micro-machining performances. The waveform was programmable with pulse on time (T_{on}) and pulse off time (T_{OFF}) and the peak voltage amplitude. The authors also reported that micro-channels were formed on glass with 17%NaOH concentration electrolyte, platinum tool wire of 100 μm diameter and tool work piece gap (TWG) of 20 μm at different duty cycle and amplitude of the pulsating power source. The authors finally revealed that the square pulse power supply source with the combination of tool material as platinum and job specimen as glass, the shape of the heat source was high energy at edges and low energy in the Centre of the heat source. The machined area resulted was comparatively less in size than that of the tool. According to the authors it could be commented that with the pulsed power source, the machining was qualitatively better.

Biswas *et al.* [40] presented an optimization technique to optimize experimental data by utilizing multi-objective optimization by ratio analysis (MOORA). Also a multi choice decision analysis i.e. analytic hierarchy process (AHP) was applied for optimization. Silicon nitride ceramics was successfully machined with the ECDM experimental set-up. The authors also documented that MOORA method could be used effectively for parametric optimization of μ-ECDM of Silicon Nitride ceramics during drilling operation. This method was computationally very simple, easily comprehendible and robust, simultaneously consider any number of quantitative and qualitative selections attributes, while offering a more objective and logical selection approach. The authors revealed the optimal condition for maximum material removal rate (MRR) and machining depth rate (MDR), and minimum radial overcut (ROC) and heat affected zone (HAZ) were obtained at 70V, 20wt% of NaOH electrolyte and 30mm inter electrode gap using counter weight feed mechanism.

Liu *et al.* [41] developed a grinding-aided electrochemical discharge machining (GECDM) process to improve the performance in machining particulate reinforced metal matrix composites (MMCs). A comparative study on quality of the G-ECDM and ECDM machined surfaces of the 10ALO composite was studied. The surface roughness (R_a) measured for the G-ECDM specimen (0.26 μm) was significantly smaller than that of the ECDM specimen (2.5 μm). The authors also reported the material removal rate (MRR) in G-ECDM was a function of pulse current, with the experimental controlled factors such as electrolyte concentration, applied voltage, pulse duration, duty cycle, and spindle speed. The authors showed that MRR in two processes for both the 10ALO and 20ALO composites were increased with an increase of current. During machining both the 10ALO and 20ALO materials, MRR was influenced by the machining parameters in the order of duty cycle, current and then electrolyte concentration.

Cao *et al.* [42] investigated into a hybrid process of ECDM and micro-grinding using polycrystalline diamond (PCD) tools to reduce the machining time and improve the surface quality that obtained by ECDM process. The authors showed that 3D micro structures with high surface quality in glass could be machined efficiently by combining ECDM and PCD grinding. A comparison of machining time was between the conventional grinding and the hybrid process revealed that the machining time in the hybrid process was considerably low compared to that under the grinding action. The hybrid micromachining process could be applicable in the fabrication of complicated structures with high quality in glass material. The effect of machining feed rate was also studied in order to the material removal rate (MRR). The researchers proposed that surface roughness 0.05 μm could be achieved by grinding using PCD tools of 10 μm grit sizes by WEDG under the conditions of a capacitance of 400 pF and 100V.

Jiang *et al.* [43] presented an experiment-based stochastic model for spark energy estimation in electrochemical discharge machining process. Tungsten tool was used with 250 μm diameter and the electrolyte was 30 wt% NaOH. Tapered tool electrodes were used to improve the consistency of spark generation. The authors showed that using tapered tool the consistency of spark generation was improved and suppressed the generation of minor discharges. The authors also presented a finite element based model to correlate spark energy and the rate of removed material and stated that material removal was due to thermal melting and chemical etching. In this study, gas film formation was explained with the help of current output of DC power supply. It was suggested that material removal can be simulated by

solving heat transfer problems as electrical energy transfer, converted into heat source acting on the job specimen in machining process.

Huang *et al.* [44] applied ECDM process for drilling micro-holes with 304 grade stainless steel. Tungsten carbide with from diameters 250 μm to 400 μm was used as micro-tool electrodes with high-speed rotating. Tool wear of the tool was observed before and after marching operation. The authors observed the shape and surface characteristics of the drilled micro-holes by scanning electron microscopy (SEM) and showed that in holes edge there was hardly burrs and stray current corrosion. Finally the authors concluded that the machining voltage was a significant influence on the tool electrode wear and by increasing of the rotating speed and the diameter of tool electrode and the machining voltage, tool electrode wear was found decreased.

Chak *et al.* [45] reported electrochemical discharge machining process as the combination characteristic of electro-chemical machining and electric-discharge machining. The author used pulsed DC power supply considering, applied voltage, duty factor and electrolyte conductivity as process parameters during machining of SiC with different electrode configurations. The volume of material removed from the job specimen was increased with increased of supply voltage, duty factor and electrolyte conductivity. Pulsating nature of power supply had improved the machining performance characteristics and reduced the tendency of cracking at high applied voltage using orbital motion of abrasive electrode. The author also showed that orbital motion of abrasive electrode provided the maximum volume of material removed and rotary abrasive electrode gave the increased volume of material removed compared to non-rotating brass electrode.

Paul *et al.* [46] introduced electro chemical discharge machining (ECDM) process as innovative non-conventional hybrid process. The authors investigated into the effect of process parameters on material removal rate (MRR) and heat affected zone (HAZ) during machining a silicon wafer by ECDM process. The author also observed that material removal rate (MRR) was found to be non-linear behaviour due to many process parameters such as voltage, electrolyte concentration and duty factor etc. Those parameters had a greater effectiveness on MRR as well as HAZ. Applied voltage had a dominating power in the field of HAZ area. The authors used response surface modelling (RSM) for studying the effect of parameters on MRR as well as HAZ and the desirability function was used for optimization.

Jawlkar *et al.* [47] illustrated electro chemical discharge machining (ECDM) process as proven process for micro machining. The experimental results analysed on material removal (MR) and tool wear (TW)] during fabrication of hallow holes on soda lime glass using ECDM process. The author used two types of electrolytes such as NaOH and $NaNO_3$ for micromachining on soda lime glass. The author used L_9 orthogonal array for analysis. The researchers also tried to execute the effect of process parameters, such as electrolyte concentration, applied voltage, distance between electrodes and time of current flow. The authors showed that NaOH was more efficient as compared to $NaNO_3$ and found that applied voltage was the most influencing parameter which could play a role of 70.14% and also debris analysis were investigated using field emission scanning electron microscopy (FESEM).

Baoyang *et al*. [48] used tapered tool electrodes to improve the consistency of spark and generated an analytical model of the gas film.The authors presented analytical modeling of the gas film, involving bubble growth and departure on electrode, gas film evolution, and electrolysis characteristics. Gas film is essential for the improvement of machining quality and efficiency of electro chemical discharge machining. The authors compared models based on experimental results to the actual discharging phenomenon. High speed camera was used for imaging the formation of a gas film on the tool electrode during electrochemical discharge micro-machining process (μ-ECDM). The range of thickness of gas film indicated good consistency with the range of film thickness which provided higher machining rate, which estimated from analytical models.

Gupta *et al*. [49] illustrated that the pulse duration has a great effect to achieve better control on quality characteristics and aspect ratio of glass material machined by ECDM process and investigated into the effect of pulse duration on aspect ratio of glass material machined by ECDM. Also the effective range of pulse duration was found to achieve better control over the quality characteristics. The machining characteristics were machining depth; surface damage, aspect ratio, and tool wear which were affected by a wide range of pulse duration and duty factor. It was observed that the increased of duty factor increased aspect ratio in case of both NaCl as well as NaOH electrolytes. For NaOH electrolyte, longer pulse duration was required for sparking.

Hajian *et al*. [50] observed that the machined surface was smoother for the lower concentration of electrolyte and higher machining voltage and the machining depth was

increased using magnetic field. The authors showed that the Lorenz force of magnetic field was active at the direction of bubble's motion. The authors also studied that the electrochemical discharge behavior of electrolyte during micro-channel cutting on glass. Magnetic field caused magneto hydrodynamic (MHD) convection, by which hydrogen bubbles turned and accelerated with the repulsion from the cathode surface. The direction of bubble movement depended upon the magnetic field orientation. It was found that when the magnetic field was applied, the machined surface became smoother if lower concentration of electrolyte was used at higher machining voltage. Applied voltage and magnetic field increased the machining depth (MD) during micro-channel cutting on glass with the lower value of electrolyte concentration.

Goud *et al.*[51] presented the concepts of material removal mechanism of ECDM and the possibility of future scope to enhance the material removal rate of ECDM, used for machining of electrically non-conducting materials like glass, ceramics, quartz, etc. The authors reported that the phenomena involved in the material removal were to be investigated well in order to improve the process. The machining criteria of the process depended on many parameters like tool-electrode material, electrode size and shape, wettability characteristic of tool-electrode, feed-rate, job specimen material, applied voltage, current, duty cycle, pulse duration, type of electrolyte and concentration and temperature, gap between tool-electrode and job specimen, distance between cathode and anode etc. The authors revealed that the most of the researcher frequently used NaOH and KOH as electrolyte and tungsten carbide tools were commonly used due to high wear resistance and high temperature resistance.

Saranya *et al*.[52]explored the electrical and 2D machining characteristics of ECDM process using a dynamic cylindrical tool electrode.The influence of various process parameters like electrolyte type, electrolytic concentration, tool travel rate (TTR) and applied voltage on the process characteristics have been reported. Two different electrolytes, i.e., KOH and NaOH with concentrations varying from 10 to 50 % had been used to study the effect on critical voltage (Vc) and critical current (Ic).When NaOH was used as electrolyte critical current was more at any concentration than KOH but the author observed that KOH required a higher critical voltage than NaOH solution during micro-channel cutting on glass by electrochemical discharge machining process. For any electrolyte, critical voltage decreased and critical current increased when electrolytic concentration was increased using the developed ECDM set up.

Behroozfar *et al*. [53] discussed about the tool wear of the different materials and tool surface temperature in high voltage.Machining of the refractory materials such as ceramics required high voltages to produce the required thermal energy. In this condition, the tool wear would be increased significantly. For the study of tool wear, the different tool materials were used and observed that the tool wear started at about 46, 48, and 53 V for brass, steel and WC, respectively. It was noted that tool wear in brass was more severe compared to the other materials due to its low melting temperature. Steel and tungsten carbide were used because of their high melting temperature and better resistance in higher voltages. The tungsten carbide played to the best performance because of higher melting point. The surface temperature of the tool during ECDM process at 50 V, increased to approximately 2800^0C,as results the tool material converted to plastic deformation and accelerated of tool wear. Pulsed DC voltage was used to reduce the tool wear.

Bindu *et al.* [54] conducted the experiments to machine holes and channels with a developed ECDM setup. The authors explained the effects of voltage, duty factor and electrolyte concentration on material removal rate (MRR), tool wear rate (TWR) and radial overcut (ROC) and cut micro holes of 0.92 mm diameter and micro channels of length 14 mm and width of cut 0.34 mm and 0.63 mm on borosilicate and soda lime glass using tungsten carbide and tungsten copper alloy tool of 0.3mm diameter. At 60 V, 25 wt% of electrolyte concentration and duty factor of 70 % provided stable hydrogen bubble layer formation. Micro cracks were formed at 70 V and electrolyte concentration of 30 wt%. The author observed that maximum MRR was found at 60 V, 25 wt% and 70 % and minimum TWR was found at 50 V, 25 wt% and 70 % and also minimum ROC was observed at 50 V, 30 wt% and 60 %.

Elhami *et al.* [55] performed the analysis on the effects of ultrasonic vibration and single discharge on material removal and tool wear. Ultrasonic vibration, as a technical augmentation, was added to electrochemical discharge machining process to study the related effects. Special configuration and equipment were used to apply ultrasonic vibration and generate only single discharge. Material removal rate and tool wear were considered as two important machining criteria for drilling process to determine the machining efficiency. The current signal was applied to find out the current variation and discharge condition during ECDM process. The authors showed that the ultrasonic vibration changed the current signal pattern to increase the material removal up to 35% and also tool wear was reduced up to 14%.

Singh *et al.* [56] analyzed that the crystal size was increased with an increase of electrolyte temperature.It was found that with ultrasonic vibration, electrolyte temperature may be reduced. The authors showed that the average crystal size of CuO particles could be attained in the range of 17-23 nm under magnetic stirrer condition and 11-18 nm under ultrasonic condition for reducing the electrolyte temperature which caused the tool wear. The crystal size was increased with an increase of electrolyte temperature under both the conditions and led to the creation of bigger-size nano particles. Moreover, morphological analysis had been performed by the authors. The authors declared that size of the CuO nano particles were also influenced by synthesis conditions during micro-machining by electrochemical discharge machining.

Elhami *et al.* [57] represented the effect of ultrasonic vibration on the thickness of gas film and small discharges that increased the material removal rate (MRR) and hole accuracy. An analytical model was presented for both electro-chemical discharge machining (ECDM) and ultrasonic assisted electro-chemical dis-charge machining (UAECDM) to study the effect of ultrasonic vibration on the thickness of gas film. Actual gas film thickness, machining speed, entrance overcut and tapering zone were studied for both ECDM and UAECDM to understand the effect of integration of ultrasonic vibration into the traditional ECDM process. The gas film in different condition confirmed that ultrasonic vibration had reduced the thickness of gas film. Applied ultrasonic vibration, gas film become smaller, then the duration of discharge was increased.

Singh *et al.* [58] used pressurized feeding system with abrasive coated micro-tool to control on working gap to stable gas films just below the tool. In pressurized feeding system, the exerted pressure maintained constant working gap which was considered almost zero during micro-machining, and that was provided by the development of a job specimen holding fixture. The existence of micro cavities between abrasive coated tool and job material generated thin and stable gas films below the tool electrode. The developed pressurized feeding system provided 207.4% improvement in machining depth (MD) while compared to the other feeding systems.The parametric combination during drilling by ECDM process on borosilicate glass for achieving higher machining depth using developed pressurized feeding system was applied voltage 55 volt, exerted pressure 3 N/m^2, electrolyte concentration 20% wt. /vol., pulse on time 3 µs, and pulse off time 1 µs.

Wang *et al.* [59] showed that MRR and surface roughness initially increased and then decreased with the increasing DC voltage. The high temperature generated during electro chemical discharge machining on ceramics by the moving diamond wire. The authors reported that the material removal rate (MRR) of the new cutting method increased compared with the conventional diamond wire cutting process. Electrochemical discharge machining had limited influence on the surface roughness and wear of diamond wire. The combination of electrochemical discharge (ECD) and diamond wire cutting processes (DWC) increased material removal rate and surface roughness. The author found stable sparking when the voltage was between 47 and 55 V during electro chemical discharge machining (ECDM) process. MRR increased with the increase of wire speed but the surface roughness varied very little. When the counter weight was increased MRR was improved but the machined surface got rougher.

Hajian *et al.* [60] applied the bending force on tool electrode in the presence of magnetic field and showed that the bending force was decreased when the electrolyte concentration and applied voltage were increased. During the ECDM milling operation, the tool was penetrated into the job specimen, which might lead to a breakage in the tool. In order to avoid the tool breakage, machining parameters such as feed rate should be selected properly. The bending force applied on the tool was evaluated as a function of tool diameter, electrolyte concentration, presence of the magnetic field, and tool feed rate. The optimum feed rate could be approached by assessing the horizontal tool force. When the electrolyte concentration was elevated, the optimum feed rate could be increased. As a result material removal rate was increased. Using magnetic field at15wt% of NaOH electrolyte concentration in the ECDM process, the optimum feed rate was raised more than that of the NaOH electrolyte of 25 wt% was used.

Tang *et al.* [61] used the side insulated tool with proper diamond coating to prevent the side wall discharge and achieved better surface integrity. The gas film formed and electrical discharge appeared generally at both the tool end and the tool sidewall during ECDM process. The undesirable sidewall discharge enlarged the hole entrance diameter and destroyed the hole surface integrity. For preventing the sidewall discharge, a side-insulated tool electrode with a 4 μm-thick diamond coating layer was used in ECDM during micro-hole drilling. The gas film formation and electrical discharge mostly happened on the tool end due to the insulation layer on the tool sidewall. The authors achieved smaller hole diameter and

better surface integrity without an obvious heat affected zone at the hole entrance using the side-insulated tool electrode. The machining depth was increased from 50 μm to 500 μm. The side-insulated electrode had an advantage in enhancing shape accuracy by reducing the taper angle of the micro hole. When the machining depth was 600 μm, the side-insulated electrode achieved a much smaller hole taper angle of 3.3^0 whereas the taper angle for traditional tool electrode was 6.4^0.

Han *et al.* [62] produced micro-grooves with high aspect ratio of 1:4 and improved the step milling depth during electrochemical discharge milling process (ECDMP). The authors created high-aspect-ratio microgrooves on hard and brittle materials using an electrochemical discharge machining (ECDM) process by introducing micro textured machining tool. The authors revealed that the morphology of the tool side surface was treated via micro-electrical discharge machining (μ-EDM) to produce fine micro protrusive patterns on job specimen. Using the finite elements (FEM) analysis, the evaluation of the field enhancement factor was also addressed by the authors. The authors fabricated microgrooves with aspect ratio of 1:4, with high geometric accuracy and precision and also crack-free surfaces were generated using one-step electrochemical discharge machining (ECDM) process.

Sarkar *et al.* [63] fabricated micro-hole at first on the electrically semi-conductor type silicon carbide (SiC) material by electrochemical discharge micro-machining process based on L_9 array of Taguchi method for designing the experimentation (DOE) with stainless steel μ-tool of 300μm diameter and NaOH electrolyte and studied the influences of applied voltage, electrolyte concentration and inter-electrode gap on material removal rate (MRR) and radial overcut (ROC). The authors also found out the single as well as multi-objective optimal parametric combinations for maximum MRR and minimum ROC. The single-objective parametric combinations was found as 45V/20wt%/20mm and 25V/20wt%/40mm for maximum MRR and minimum ROC respectively and multi-objective optimal parametric combinations was found as 25V/20wt%/40mm and using grey relation analysis (GRA) mathematical models was developed and verified during micro-drilling of silicon carbide by micro-ECDM process.

Nasim and Razfar [64] announced that the micro channels played a vital role in micro electro mechanical systems (MEMS), micro fluidic and lab-on-a-chip devices. The electrolyte was a dominant and vital parameter that effect on the accuracy of performances of electrochemical discharge machining (ECDM). The authors observed that 15 and 25 wt% concentrations provided more electrical conductivity using mixed electrolyte of NaOH and

KOH in the 1: 1 ratio than KOH and NaOH separately at the same concentrations and produced deeper micro-channel with better sharper sidewalls compared to KOH and NaOH. Also, using 25, 30, and 35 wt% mixed electrolyte with higher viscosity compared to KOH, produced better quality of micro-channel. The authors showed with help of scanning electron microscopy (SEM) and energy-dispersive X-ray (EDX)that the tungsten carbide tools used in NaOH and $NaNO_3$ had more severe wear compared to KOH and mixed electrolyte. Also, tool erosion was more serious at the applied voltages of 50 V to tool erosion at 35 V.

Yadav [65] reviewed and documented about the research trends and opportunities of electrochemical spark machining process (ECSM). ECSM process presented by the researchers and scientist in different names such as drilling ECSM, TW ECSM, milling ECSM, sinking ECSM, grinding ECSM and turning ECSM positively created complex profiles with better surface quality during machining. ECSM turning process had been recently developed. Saw-cut ECSM was a new configuration of ECSM which was used to disk cutting on non-conductive materials. Ultrasonic vibration–assisted ECSM enhanced the flow of electrolyte into the gap resulting in reduction in arcing phenomenon. The mixing of abrasive particles in electrolyte such as silicon carbide (SiC) effectively reduced the formation of micro-crack, and heat-affected zone which was formed during ECDM process and as a results surface quality was improved. Abrasive-aided grinding ECSM represented their potential to remove micro-cracks and recast layer formed due to spark energy at the job specimen surface. By dressing on micro-tools or wheels, surface quality could be enhanced. Also the magnetic field in ECSM was applied to fabricate deep hole with better quality because effective circulation of electrolyte could be facilitated at the machining zone.

Oza *et al.* [66] used zinc coated brass wire as tool for reducing the wire breakage and improved the efficiency of travelling wire electrochemical discharge machining process (TWECDM) during machining of quartz. The authors also considered applied voltage, electrolyte concentration and wire speed as process parameters and Taguchi robust design and L9 orthogonal array was used to find out the optimal parametric conditions and analysed signal to noise (S/N) ratio and analysis of variances (ANOVA) for finding out the relative contribution of the input parameters. The authors also analysed the surface finish and kerf width characteristics by scanning electron microscope (SEM). The authors used coated wire with diameter of 0.15 mm during travelling wire electrochemical discharge machining process (TW-ECDM) process.

Tang *et al.* [67] employed a high-speed imaging technology for investigation into the evolution process of the gas film around the tool electrode. The authors also analysed the effect of current pulses on the gas film and showed that a large bubble was generated around the electrode owing to the gas production and bubble coalescence before the formation of a complete gas film. Current pulses on the gas film indicated that the current pulses with peak values was found larger than 1 A during the sparking stage. If the applied voltage was turned off, the gas film broke. Gas bubble was generated around the tool electrode due to electrolysis. The author observed that the current pulses with peak values larger than 1 A during the spark discharge. Gas bubbles were generated and reformed during current pulse-on time. In the pulse-off stage, the gas film moved upwards due to surface tension. The mean speed of the upward-moving gas film was observed by the researcher as 1.03 m/s.

Madhavi *et al.* [68] fabricated micro-channel using μ-ECDM on 4 mm thick quartz glass with 370 μm diameter stainless steel (SS) tool considering various levels of voltage (V), electrolyte concentration (wt% C) and duty factor (% DF). The authors performed the optimization of process parameters using signal to noise (S/N) ratio and grey relational analysis (GRA) to enhance responses separately. The authors obtained the maximum material removal rate (MRR)as 753 μg/min at 60 V, 30 wt%C, 60 %DF and minimum tool wear rate (TWR) as 2.99 μg/min at 40 V, 20 wt%C, 50 %DF and also minimum overcut as 130 μm at 40 V, 20 wt%C, 60 %DF. By using GRA optimized parameter, the authors generated textures of 45° hatch, square hatch and 45° criss-cross hatch on quartz glass by micro-ECDM process.

After the proper study of the previous research articles and research gap has been identified and with respect to that, the objectives of the present research have been drawn out.

1.5 OBJECTIVES OF THE PRESENT RESEARCH

From the analysis of previous research work, several of research gaps have been clearly identified on electrochemical discharge micro-machining process. Keeping these considerations in view the objectives of the present research work have been presented as follows:

(i) To design and develop the μ-ECDM set-up for carrying out micro-cutting operation on electrically non-conducting hard and brittle materials like glass.

(ii) To investigate the influences of various process parameters such as applied voltage, electrolyte concentration, inter-electrode gap, duty ratio, pulse frequency and polarity on various machining performances such as material removal rate (MRR), overcut (OC), heat affected zone (HAZ), machining depth (MD) and surface roughness (Ra) etc during various micro-channels and profiles cutting on electrically non-conducting materials by micro-electrochemical discharge machining process.

(iii) To perform comparative studies on machining performances of μ-ECDM process using different electrolytes and different shapes of tool.

(iv) To develop a mathematical model to correlate different machining criteria such as material removal rate (MRR), overcut (OC), heat affected zone (HAZ), machining depth (MD) and surface roughness (R_a) with various process parameters during micro-channel cutting on glass.

(v) To perform the analysis for determining the optimal machining condition of μ-ECDM process during micro-cutting operation using optimization techniques like desirability function analysis and Genetic Algorithm.

(vi) To fabricate different shapes of micro-channels and micro-slots on glass as an application of μ-ECDM process.

This research work on μ-ECDM process for micro-machining of glass is expected to yield effective outcome, which immense for applications in the area of micro-fluidic devices, micro-machine tools, aerospace, automobile, computer, electrical and electronics engineering. The research work on optimization analysis of the performance of the micro-ECDM provides technical guidelines for future applications in the field of micro-machining.

This research work is useful for effective utilization and it opens up the challenges to the modern manufacturing industries to cope with the micro-machining of electrically non-conducting materials such as glass, composites and ceramics etc.

CHAPTER-II

2. FUNDAMENTALS OF µ-ECDM PROCESS

After exhaustive review on previous research works in previous chapter it is cleared that electrochemical discharge micro- machining (µ-ECDM) is hybridized with the combination of electro-chemical machining and electro-discharge machining. The material removal mechanism in µ-ECDM process is similar with that of conventional ECDM process. Material is removed due to the combined effects of electrochemical (EC) reactions and electrical spark discharge (ESD) action. The spark discharge is initiated if the applied voltage is more than the critical voltage and the material is removed from the job specimen due to the melting and vaporization when an electrically non-conducting material is kept at the closed vicinity of spark between micro-tool and electrolyte across the gas bubble layer. An arrangement of the electrolyte cell in the µ-ECDM process is shown in the Fig. 2.1. From the analysis of the electrochemical machining (ECM), it is identified that there are two types of reactions usually occur in the process. These are as below:

i. Electrochemical reactions at the electrode, gas evolution, plating, electrode dissolution and oxidation etc.

ii. Chemical reactions in the bulk of the electrolyte, chemical combinations, the complex formation or precipitation reactions for precipitates and sludge etc.

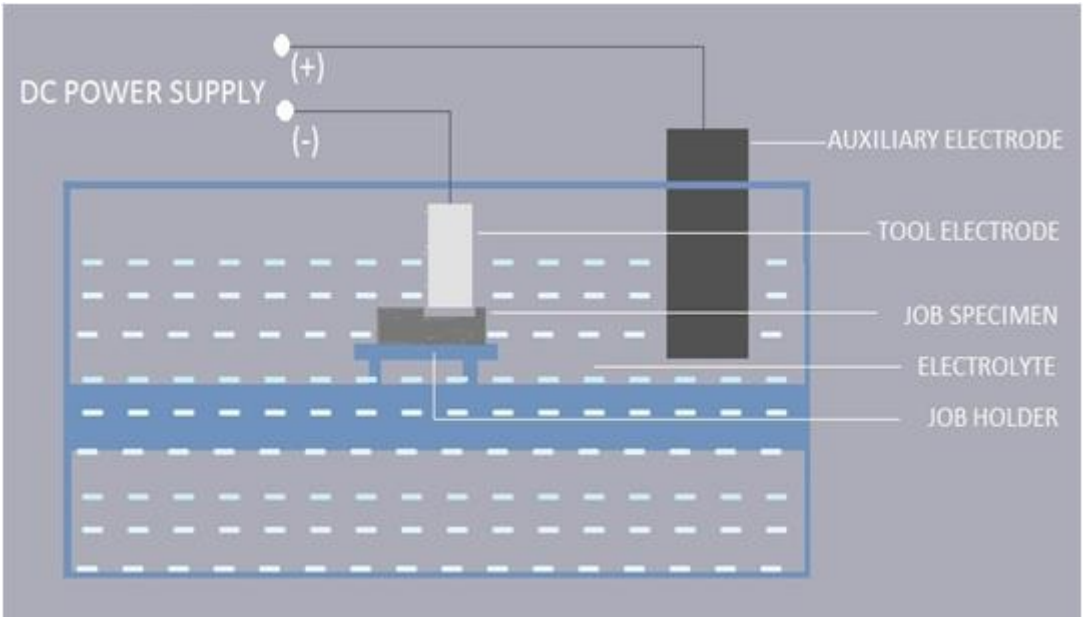

Fig. 2.1 Electrochemical cell of the µ-ECDM process

The electrochemical reaction happens at the metal-electrolyte interface and the transfer of ions in the electrolytic solution takes place by migration in an electrical field.

The cathode and anode reactions take place when the potential in the inter-electrode gap of the machining zone is reached to a threshold value.

2.1 MECHANISM OF GAS BUBBLE GENERATION

In micro-ECDM process gas bubbles generated due to electrochemical reactions at cathode and anode are discussed as below:

2.1.1 Reactions at Cathode (or Tool-Electrode)

The types of reaction at the cathode are: (i) plating of metal ions; and (ii) evolution of hydrogen gas.

The reactions for metal plating is:

$A^+ + e^- \rightarrow A$, where A represents any anode material.

The reactions for hydrogen evolution are:

$2H^+ + 2e^- \rightarrow H_2\uparrow$ (in acidic electrolytic solution.)

$2H_2O + 2e^- \rightarrow 2(OH)^- + H_2\uparrow$ (in alkaline solution.)

2.1.2 Reactions at Anode (Auxiliary Electrode)

There will be two types of anodic reaction: (i) metal ions dissolution in the electrolytic solution and (ii) oxygen gas evolution at the auxiliary electrode surface.

The anodic dissolution reaction is: $A \rightarrow A^+ + e^-$ (in acidic electrolyte solution)

The oxygen evolution reaction is given as below:

$2H_2O \rightarrow O_2\uparrow + 4H^+ + 4e^-$ (in acidic electrolyte solution)

$4(OH)^- \rightarrow 2H_2O + O_2\uparrow + 4e^-$ (in alkaline electrolyte solution)

The inter-electrode gap in the electrochemical discharge machining (ECDM) process is very large compared to the process of electrochemical machining (ECM).The material removal rate from the auxiliary electrode is very small because the very low current passes through a large inter-electrode gap.

2.1.3 Mechanism of Spark Generation

In µ-ECDM process the tool is immersed into electrolyte about 2-3 mm below the upper level of the electrolyte solution. Actually the narrow gap between micro-tool and job specimen is kept in the order of few microns. Pulsed DC power supply is applied between the micro-tool and the auxiliary electrode. Micro-tool acts as cathode or tool electrode and auxiliary electrode acts as an anode. A large number of hydrogen bubbles formed at the vicinity of the micro-tool. Vapor bubbles are formed due to high heat produced by Joule heating in the machining zone and some electrolyte is evaporated. It has been observed that the H_2 gas bubbles generated due to electrochemical actions and water vapor produced by heating of electrolyte at the tool-electrode interface cover the maximum area of the tool electrode. If the high voltage is applied across the electrodes, the rate of bubble generation at the electrodes is also increased. Under the normal conditions of bubble formation, with increase of the voltage supply, a critical or threshold voltage is attained. When the threshold value of the voltage is reached, the sparking is started at the smaller electrode. This sparking is not between electrodes, but from the tool to the electrolyte across the gas bubble layer. The voltage, at which the sparking starts mainly, depends upon the types, concentration and conductivity of the electrolyte and the tool geometrical shape and size. The smaller the diameter of the tool, the smaller will be the sparking initiation voltage. Violent sparking is observed to take place if the voltage is increased further. The pattern of change at the r.m.s, value of the current with the r.m.s, value of the voltage applied during machining is shown in Fig. 2.2

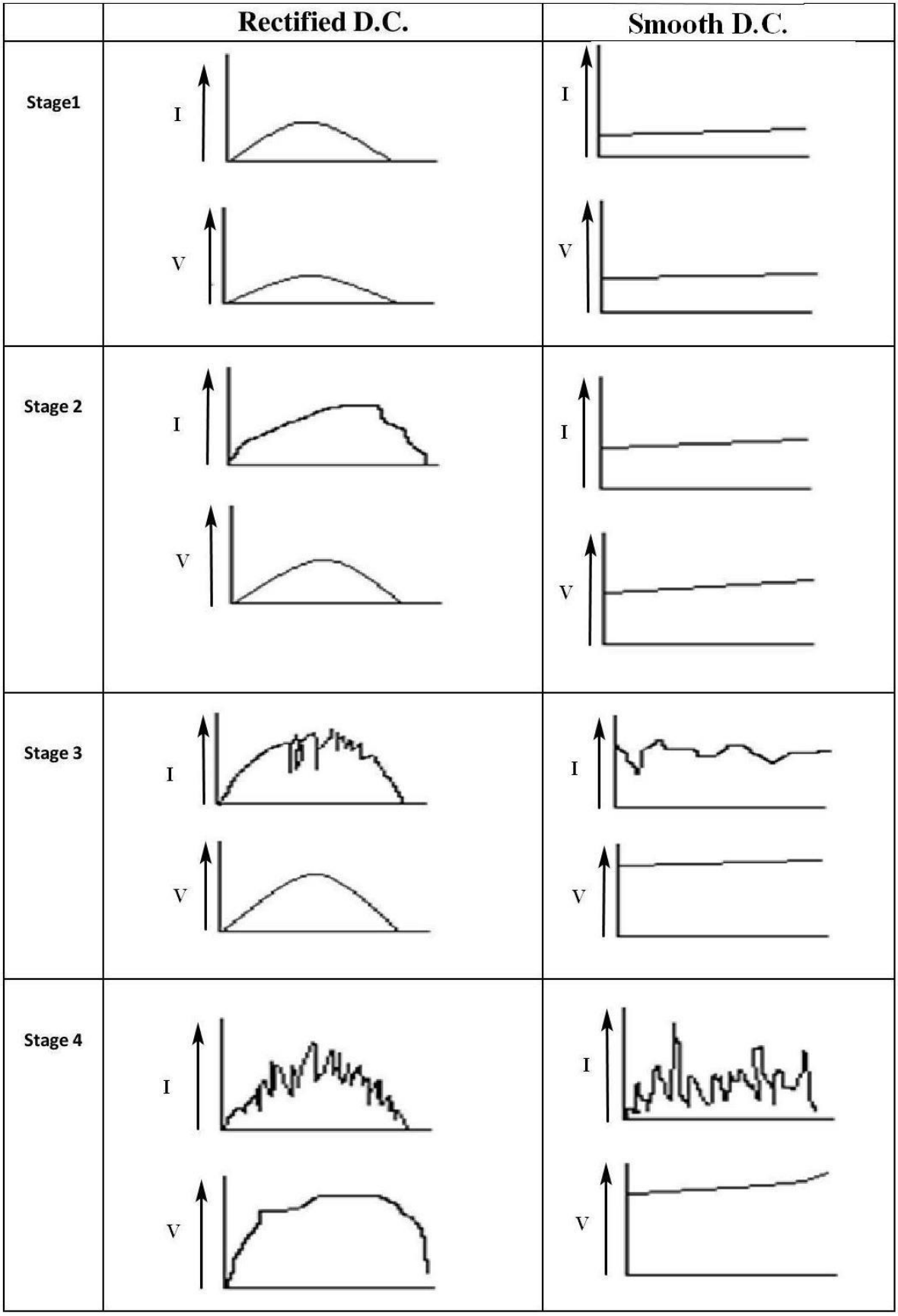

Fig. 2.2 Traces of voltage and current for different values of applied potential

The sparking start at critical voltage (V_C) and the corresponding current is critical current (I_c). The bubble distribution on the tool electrode surface for different values of applied voltage is shown in Fig. 2.3. At the 1st stage hydrogen bubble formation is initiated at 5V and after that more hydrogen bubble is accumulated at 25V and after that at 35V it reach at critical voltage and sparking is started and also from 35V sparking rate is increased and machining is started. But at 50V continuous sparking is happened.

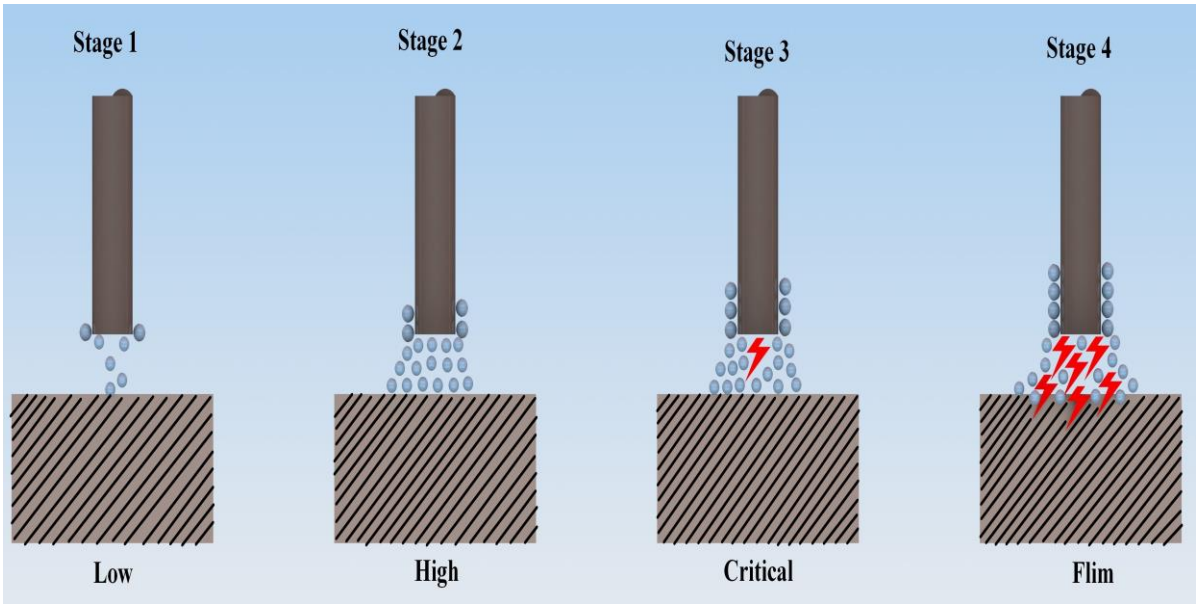

Fig. 2.3 Distribution of bubbles on the tool electrode for different applied voltages

It is clear that at the critical condition the electrode surface is fully covered with bubbles fully in a closed-packed form.

The isolation between the electrode and the electrolyte leads to discharge due to switching effect. A switching e.m.f is generated and is given as: $E = -L\frac{dI}{dt}$; where, L is the inductance and I is the instantaneous current. The equivalent circuit of electrochemical discharge (ECD) can be represented as shown in the Fig. 2.4 and the idealized equivalent circuit at discharge is shown in the Fig. 2.5

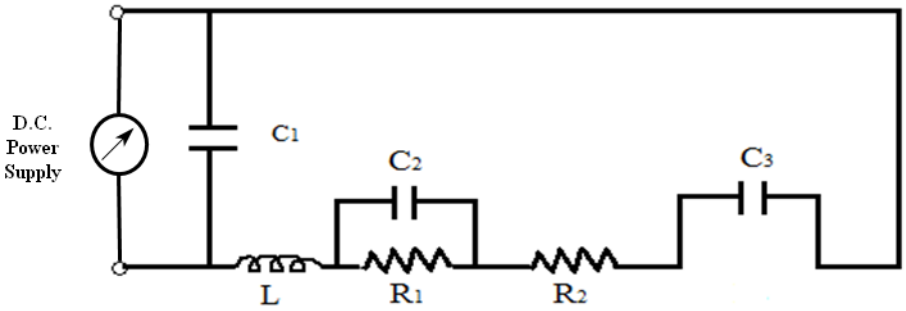

Fig. 2.4 Schematic diagram of idealized equivalent circuit at discharge

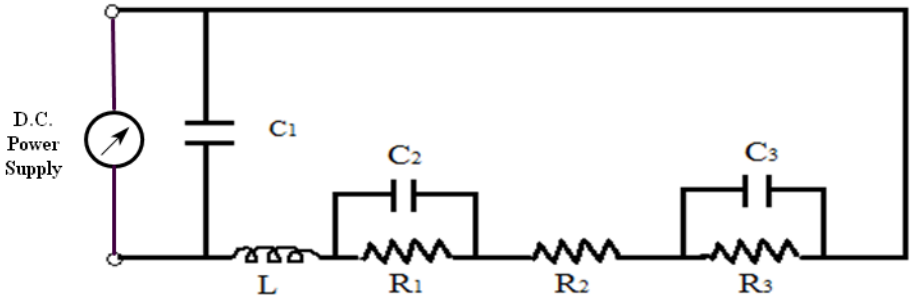

Fig. 2.5 Schematic representation of equivalent circuit of ECDM set up

Where R_1 is resistance at the larger electrode-electrolyte interface, R_2 is resistance at the electrolyte path and the tool electrode-electrolyte interface, R_3 is resistance at the electrolyte path and the tool electrode-electrolyte interface. C_1 is capacitance of the circuit, C_2 is capacitance of the larger electrode-electrolyte interface, C_3 is capacitance of the tool electrode- electrolyte interface, L is Inductance of the circuit. R_1 is negligible for a very sparse distribution of bubbles owing to the large size of the electrode. R_2 is constant for any particular composition of electrolyte, electrolyte concentration and system configuration. It is also independent of the applied voltage. R_3 increases with the applied voltage and attains a maximum value R_{3c} at the critical value of the applied voltage, V_c. The magnitude of R_3 depends on the constriction effect due to the accumulated bubbles on the tool electrode surface.

2.2 MECHANISM OF MATERIAL REMOVAL

There are micro-gaps between the micro-tool and the job specimen due to the surface irregularities present on both the surfaces of micro-tool and job specimen. The H_2 gas bubbles and vapor bubbles are evolved due to the presence of electrolyte in that micro gap and these develop a low ionic bubble layer at the surrounding of tool surface. When the voltage gradient is sufficient to breakdown the gas bubble layer between the micro-tool and job specimen, an electrically conducting path is developed for spark discharge owing to the ionization of gas bubble. It thereby causes a flow of high amount of current. Each electrical discharge causes a focused stream of electrons to move with a very high velocity and acceleration from the cathode (or micro-tool) towards the job specimen and ultimately creates compressive shock waves on the job specimen surfaces. The phenomenon is accomplished within a few microseconds and the temperature of the spot hit by electrons may rise to a very high value. As this high temperature is above the melting point of job specimen material, it melts and evaporates the material. The high pressure of compressive shock waves creates a blast, causing metallic vapor to form wear products in the shape of metallic globules, leaving craters in the job specimen surface. The material is removed from the job specimen surface during electrical spark discharge is proportional to the pulse energy of spark, which is released as a form of heat energy during micro-machining. If low pressure compressive shock waves are developed on the tool, tool wear becomes very less and the positive ions strike the tool surface with less momentum. Mechanism of material removal of µ-ECDM process is shown in Fig. 2.6 and Fig. 2.7 shows the spark generation and reactions during µ-ECDM process.

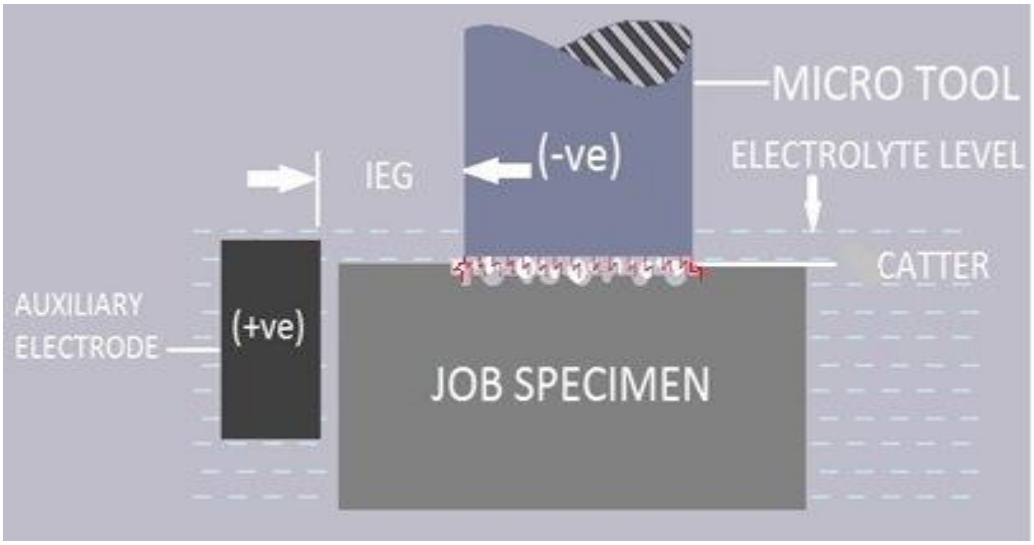

Fig. 2.6 Mechanism of material removal in µ-ECDM process

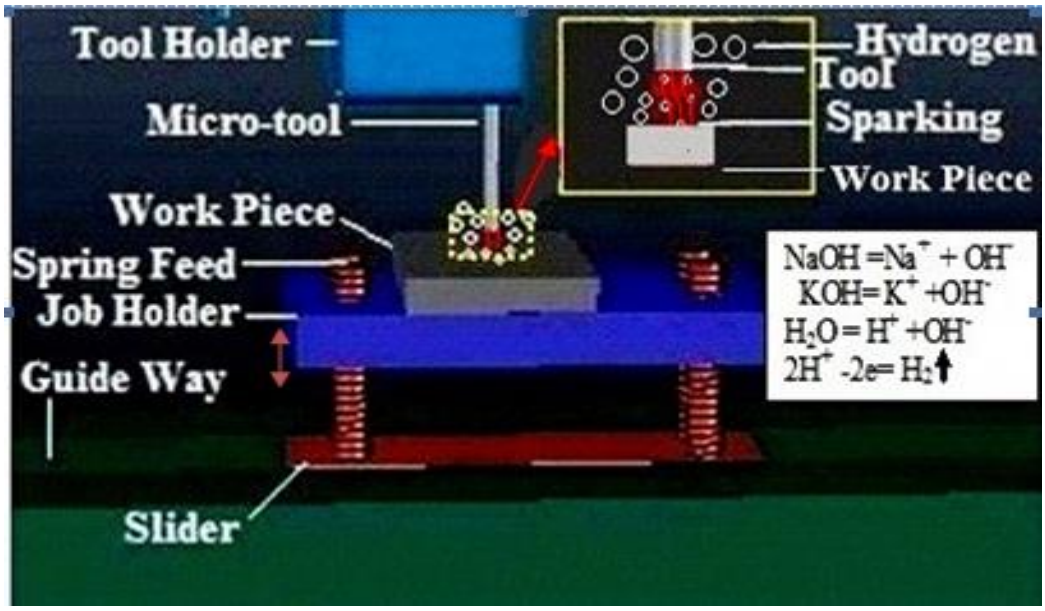

Fig. 2.7 Spark generation and reactions during µ-ECDM process

Scientist and researchers have pointed out that rather than melting of the job specimen, the heat generated by the electrical sparking may cause the job specimen materials to spall. This phenomenon is known as thermal spalling, where the material removal takes place due to mechanical failure without melting. A temperature gradient is developed due to the sudden temperature change in the machining area of job specimen and this creates the internal stresses that may be sufficient to overcome the bonding strength in job specimen grains, resulting in mechanical failure. In order to achieve effective and controlled material machining, various predominant input variables of µ-ECDM process are to be properly and optimally controlled during micro-machining operation by µ-ECDM process.

2.3 MECHANISM OF TOOL WEAR

The material from the micro-tool is removed in the same way as the removal of job specimen is occurred. In µ-ECDM tool metal plating also take place due to electrolyte reactions but major portion of tool material is removed due to thermal effect of electro discharge action. When the area of micro-tool electrode is about 100 times smaller than the auxiliary electrode, the bubbles which are evolved due to electrochemical reactions, more at the surroundings of the micro-tool and forms a gas bubble layer. As the voltage is increased at the critical level *i.e.* the breakdown voltage of gas layer spark is initiated from the tip of the micro-tool with emission of light and releases high heat energy. A fraction of this energy is absorbed by the electrode (micro-tool) as conduction mode of heat transfer, which raises the temperature of micro-tool. When the temperature of that portion tool-electrode exceeds the melting temperature the fusion of tool material takes place *i.e.* the tool starts to melt and sometimes it also vaporizes. This material removal from tool mainly depends on the size of the micro-tool. The positive ions strike on the tool tip as well as on the tool side wall, as a result material is also removed from micro-tool. If the dimension of the tool is small then the wear will be more as the current density is more. The erosion of tool material is also varied due to the variation of applied voltage and electrolyte condition. Applied voltage has predominant effects on tool electrode wear rate (TEWR).

After studying the material removal mechanism of ECDM process, for carrying out micro-machining operation, the experimental set up of µ-ECDM has been developed.

CHAPTER-III

3. DESIGN AND DEVELOPMENT OF μ-ECDM SET UP

To accomplish the objective of the present research work on electrochemical discharge micro-machining (μ-ECDM) an experimental μ-ECDM set-up was indigenously designed and developed in house to carry out the experiment of micro- machining on glass, which is electrically non-conducting in nature.

3.1 DETAILS OF μ-ECDM SET-UP

To reach the goal of the present research work and to control the process parameters such as machining voltage, machining current, the feeding movement of job specimen and inter electrode gap, pulse frequency, duty ratio, pulse on-time, pulse off-time and rate of tool movement etc. The μ-ECDM experimental set up consists of mainly three sub systems as follows:

a) Mechanical hardware system
b) Electrolyte supply system
c) Electrical power supply unit

3.2 MECHANICAL HARDWARE SYSTEM OF DEVELOPPED μ-ECDM SYSTEM

The mechanical hardware system is the vital part of micro-ECDM set-up. The development of this mechanical hardware system is a challenging task for achieving the goal of the present research work. It has six main units, which are as below:

i) Main machine chamber,
ii) Job holding unit,
iii) Tool holding unit,
iv) Inter-electrode gap control device,
v) Auxiliary electrode unit and
vi) Job feeding arrangement.

I. The specification of mechanical hardware module of the developed micro-ECDM set up is as follows:

Maximum dimension of job that can be machined is;

(i) For square job: 50 mm X 50 mm X 5mm.
(ii) For circular type job: φ25 mm X 5 mm.

(iii) Inter electrode gap (IEG): 40 mm (fixed).

(iv) Dimensions of main machining chamber: 200 mm X 150 mm X 150 mm.

(v) Maximum movement in horizontal direction through the guide way: 180 mm.

(vi) Auxiliary electrode material: Graphite plate of 100 mm X 100 mm X 10 mm.

(vii) Capacity of reservoir tank: 4 lit

(viii) Job specimen feeding arrangement: Automated Spring feed mechanism.

The schematic diagram of µ-ECDM set-up is shown in Figs. 3.1. The 3D CAD model and photographic view of the developed µ-ECDM set-up is shown in Fig. 3.2-3.3 respectively.

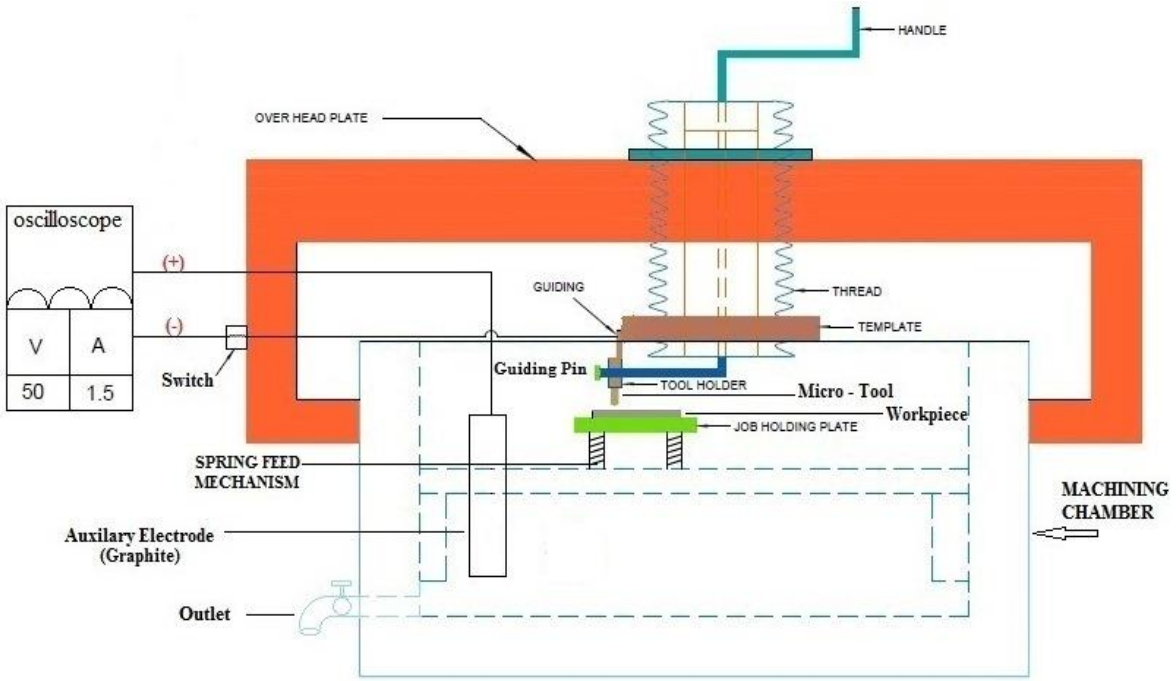

Fig. 3.1 2D Schematic Diagram of new µ-ECDM set-up

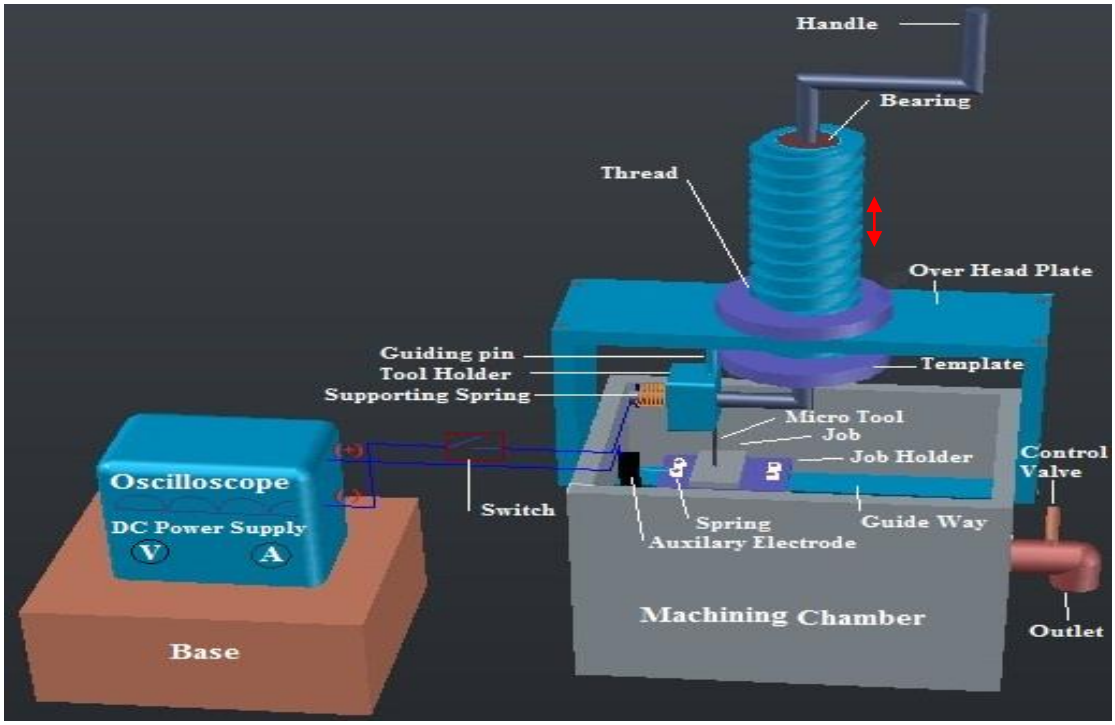

Fig.3.2 3D CAD Model of µ-ECDM Set up

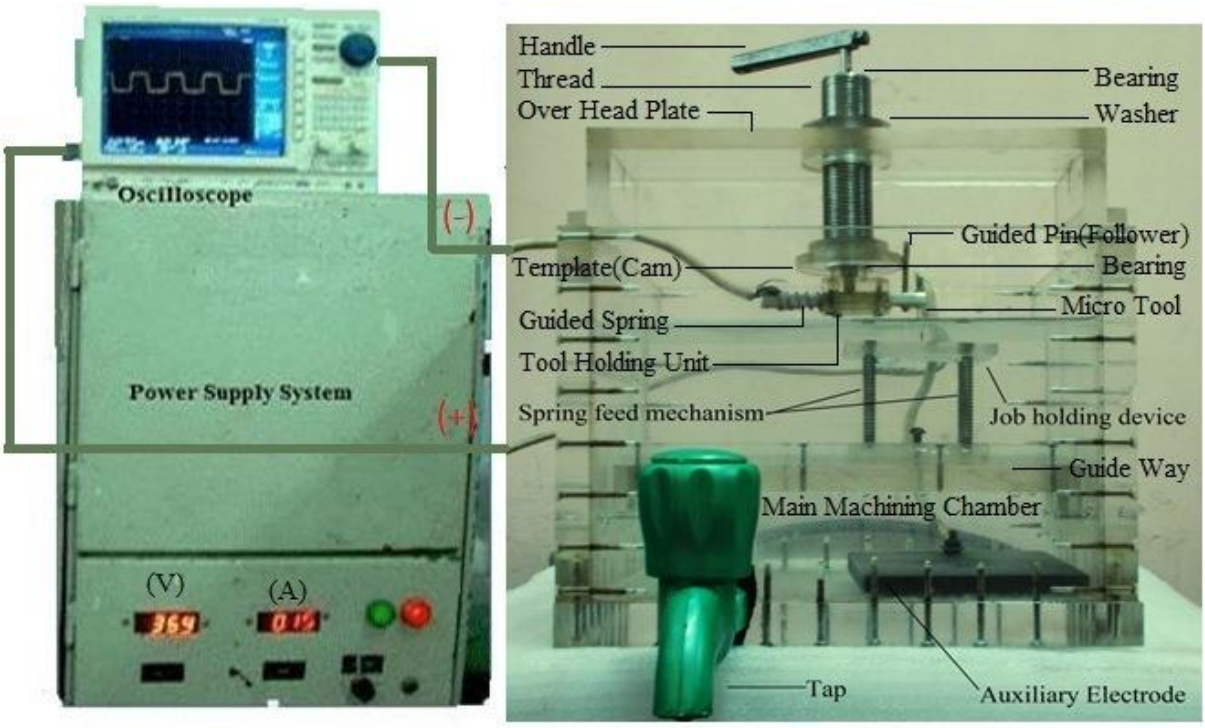

Fig.3.3 Developed µ-ECDM Set up

3.2.1 Main Machine Chamber

The machining chamber is made of Perspex as it is a transparent material and also possessing the shock resistance property. This is a rectangular box having dimensions 220 x 150 x 150 mm with wall thickness of 10 mm. The proper material selection is one of the vital tasks where manufacturing can be done. This material is selected to build up the main machining chamber because it does not chemically react with the electrolytic solution and also its transparent property helps the researcher to observe the sparking phenomena during the experiment clearly. Easy handling feature makes it suitable for fabricating the machining chamber. Fig. 3.4 shows the 3D CAD diagram of machining chamber, used for µ-channel cutting in ECDM process.

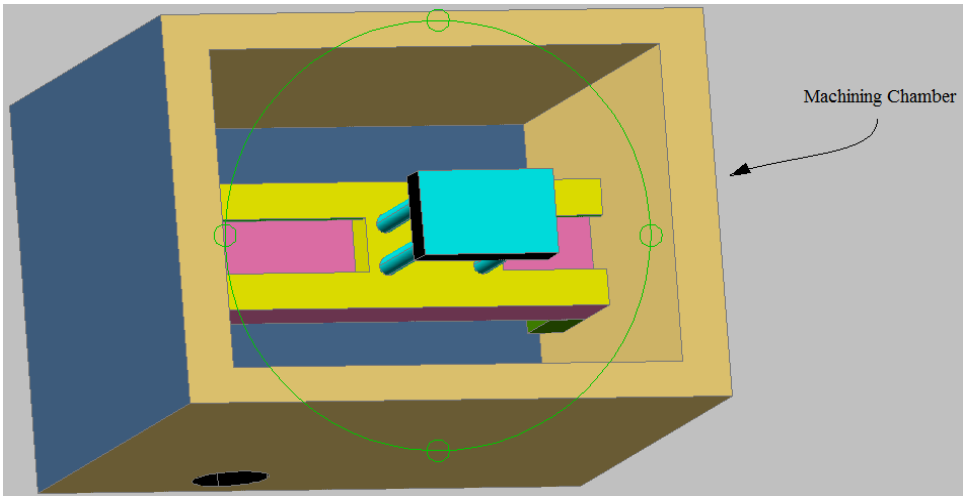

Fig. 3.4 3D CAD drawing of the machining chamber.

3.2.2 Job Holding Unit

The job specimen should be kept fixed tightly for getting desired machining performance and better quality of micro-channel, machined on glass. In this system the job is placed on a Perspex plate of size 50 x 50 x 5 mm, which itself rests on four stainless steel rod of diameter 5 mm each, located at four different corners of the plate. The whole system of the job holding unit is fixed with a slider, which can slide along a dovetail path to keep the job in an appropriate position. Fig. 3.5 shows the 3D CAD model of the job holding unit and guide way for fixing the position. The job specimen is fixed to the job holding plate with clamping unit.

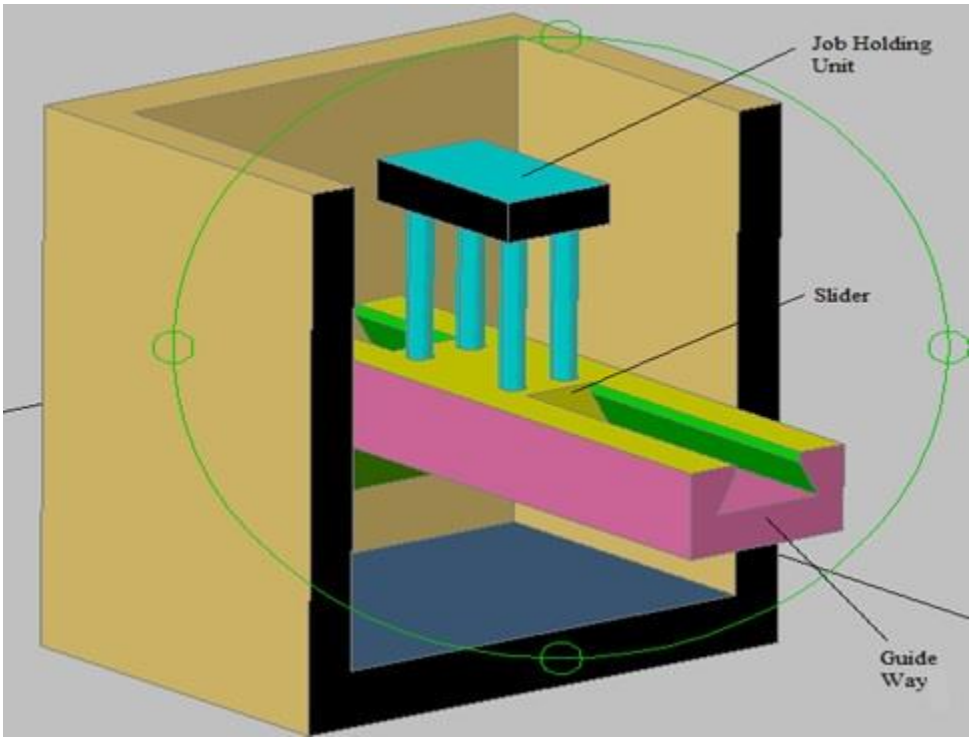

Fig. 3.5 3D CAD model of the job holding unit and guide way of the machining chamber.

3.2.3 Tool Holding Unit

The tool holder is made of stainless steel. It was made to serve the purpose for holding the circular tool, which is used to generate micro-channel on the job specimen. With the help of newly developed set-up and using cylindrical micro-tool, the micro-channel of different nature is possible to generate on glass, quartz and ceramics. A template with a curved profile on its outer edge is made and fitted with the tool holding unit so that the tool can move in the same profile guided by the template. The tool holder along with micro-tool can be rotated by a handle. The tool holding unit is fitted with the cover plate by means of screw-nut mechanism so that the position of the tool can be adjusted according to the requirement. This mechanism will help in upward and downward motion of the tool holding unit. Fig. 3.6 and 3.7 shows the schematic diagram and 3D CAD model of the tool holding unit respectively. Fig. 3.8 shows the photographic view of tool holding unit with guiding pin and rotating component.

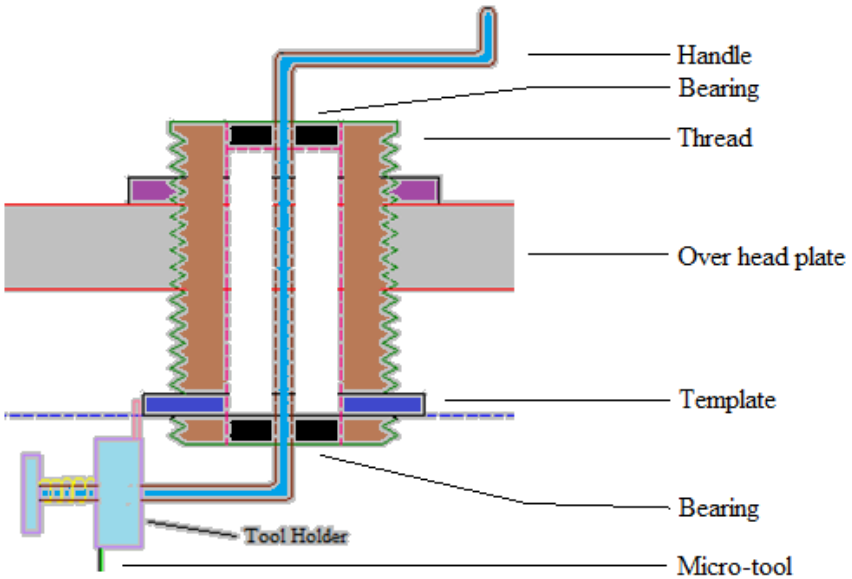

Fig. 3.6 Drawing of the tool holding unit.

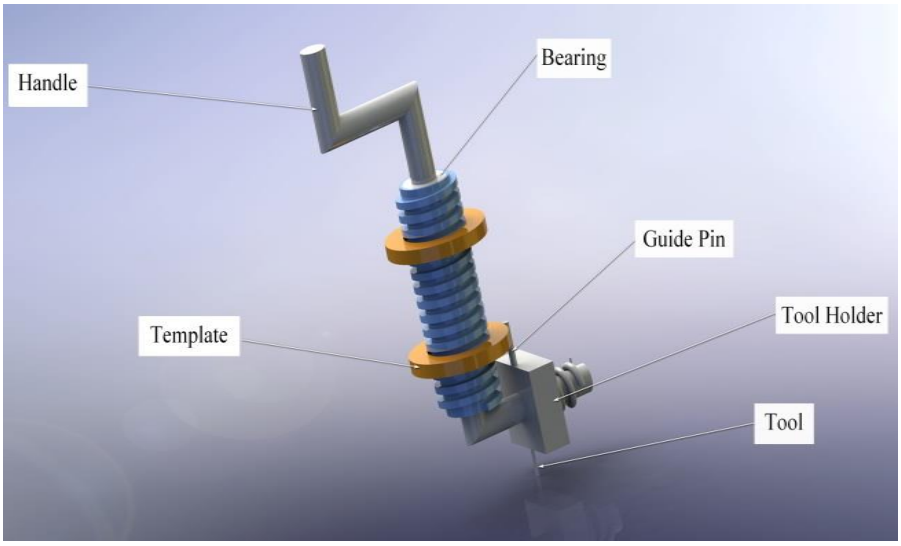

Fig. 3.7 CAD model of the tool holding unit.

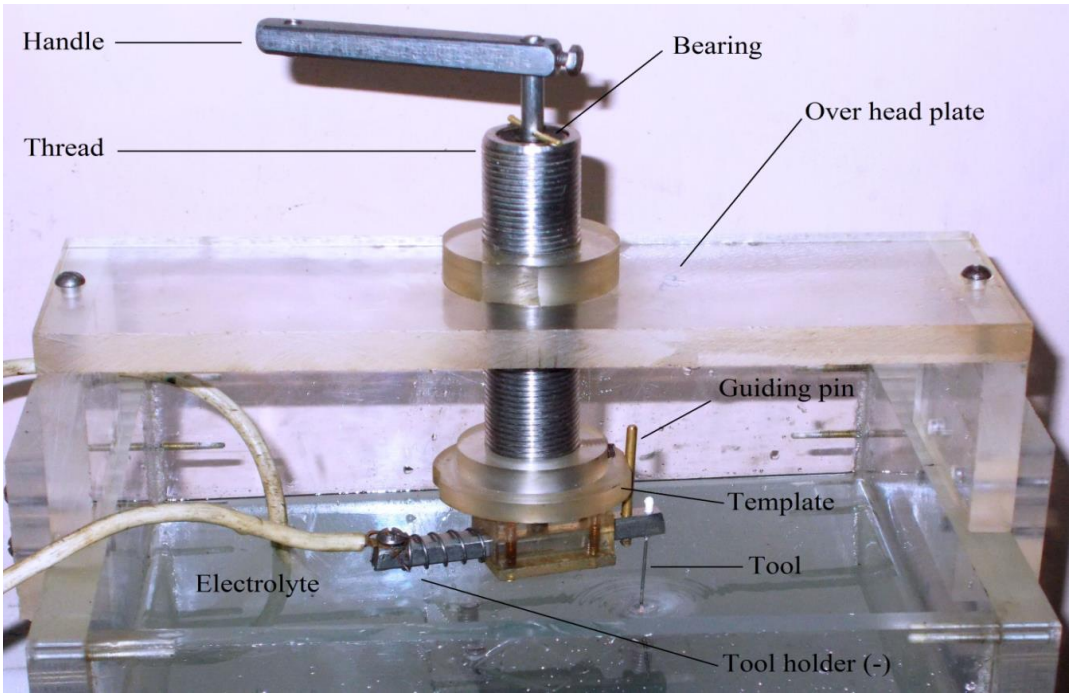

Fig. 3.8 Photographic view of tool holding unit with guiding pin and rotating component.

3.2.4 Inter-Electrode Gap Control Unit

The inter-electrode gap (IEG) is referred as the distance between the micro-tool (stainless steel) and the auxiliary electrode (Graphite plate). IEG has a significant role on performance characteristics of µ-ECDM process. The Inter electrode gap (IEG) was adjusted with the aid of linear scale. However the gap between micro-tool and auxiliary electrode remains constant during experimentation.

3.2.5 Auxiliary Electrode Unit

In µ-ECDM process, the auxiliary electrode is a flat rectangular graphite plate of 100 x 100 x 10 mm, which is placed parallel to holding plate.

3.2.6 Job Feeding Unit

The stainless steel rods guide the spring in such a way that the job holding plate can move up and down along the axis of the rods i.e. only vertical motion is possible for the job holding plate as well as the job specimen. Fig.3.9 shows 3D CAD model of the job feeding unit.

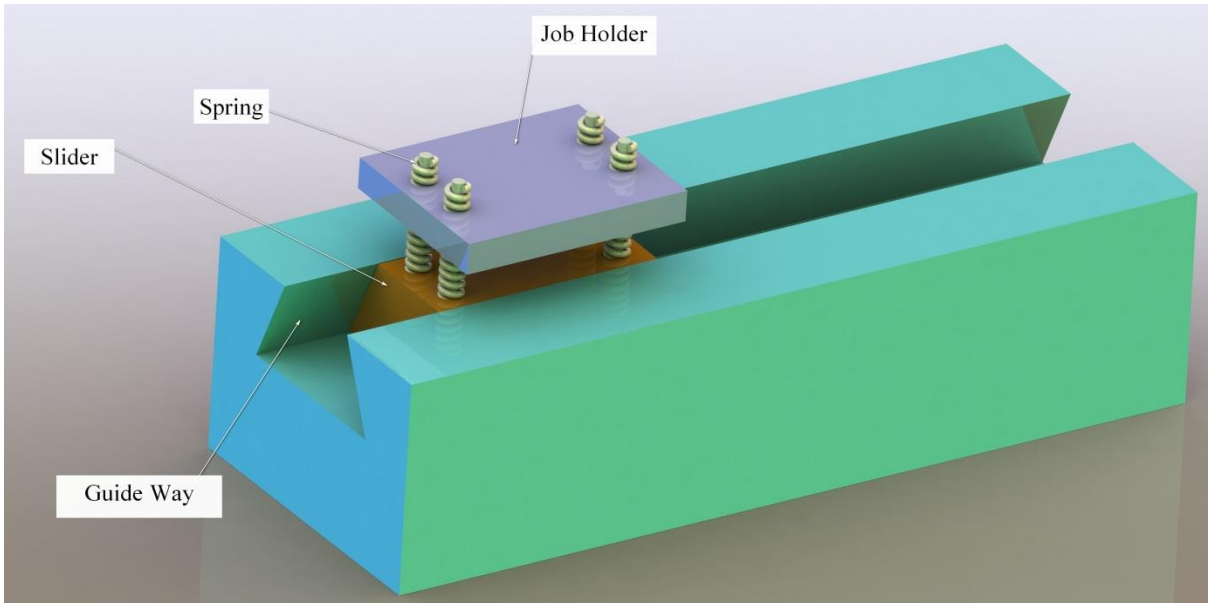

Fig.3.9 3D CAD model of the job feeding unit

3.2.7 Orthographic Views of Various Units of µ-ECDM set up

The orthographic views of different major parts of indigenously designed and developed experimental µ-ECDM set up have been exhibited in Figs 3.10-3.14 and all the dimensions are taken in mm.

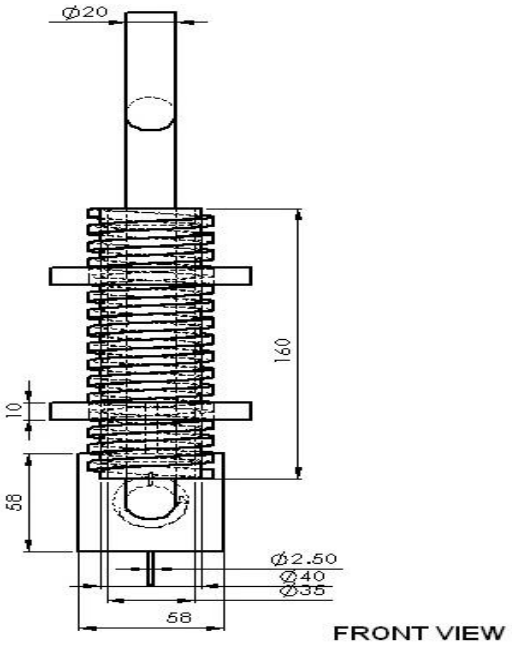

(a) Front view of tool holding unit

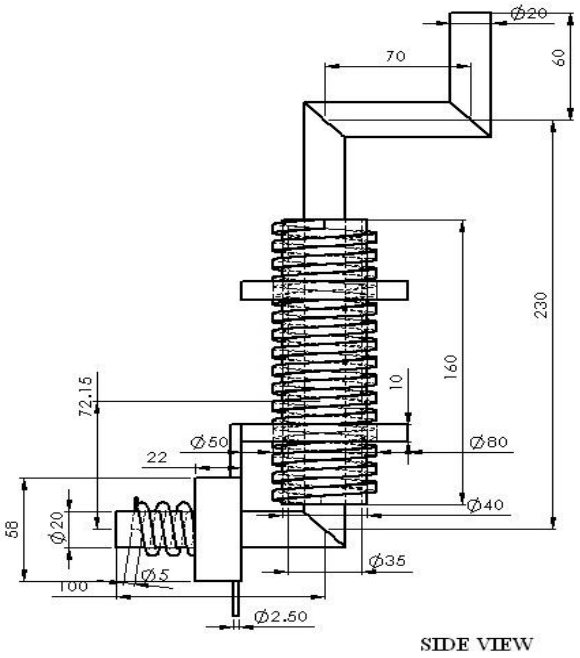

(b) Side view of tool holding unit

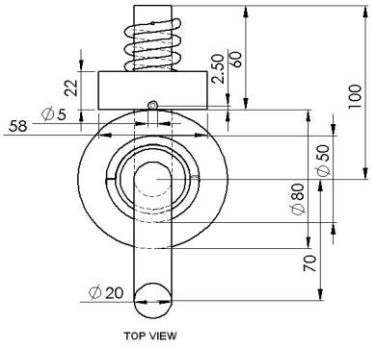

(c) Top view of tool holding unit

Fig.3.10 Orthographic view of tool holding unit

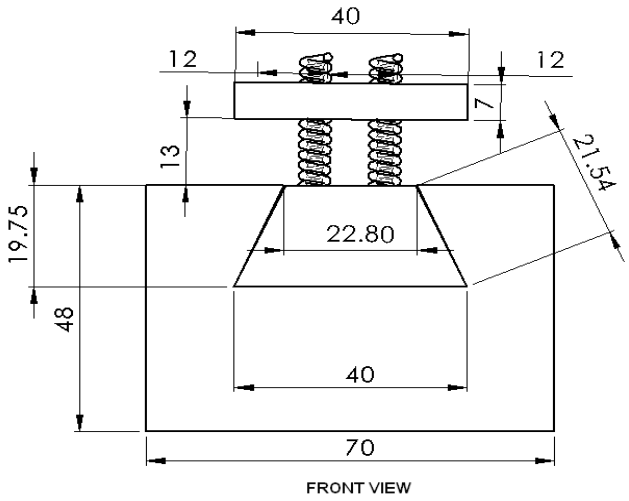

(a) Front view of job feeding unit

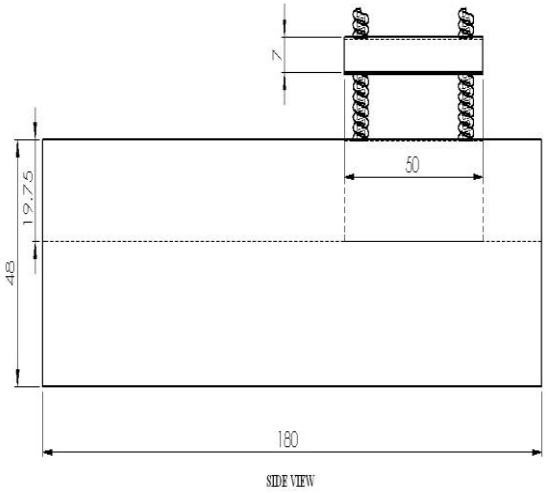

(b) Side view of job feeding unit

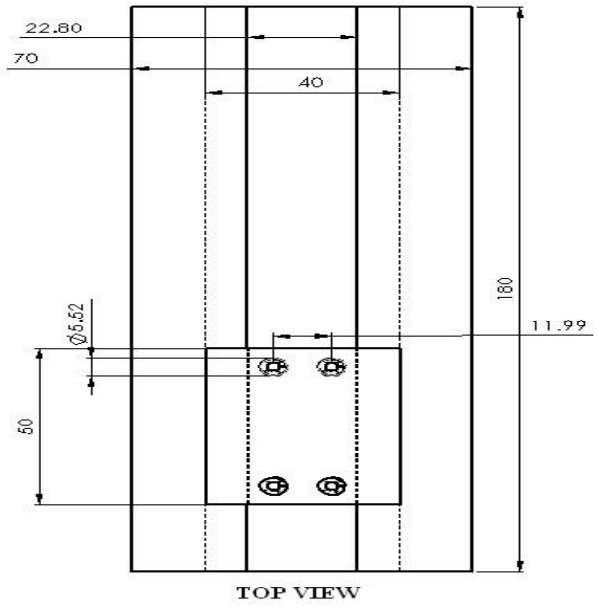

(c)Top view of job feeding unit

Fig.3.11 Orthographic view of job feeding unit

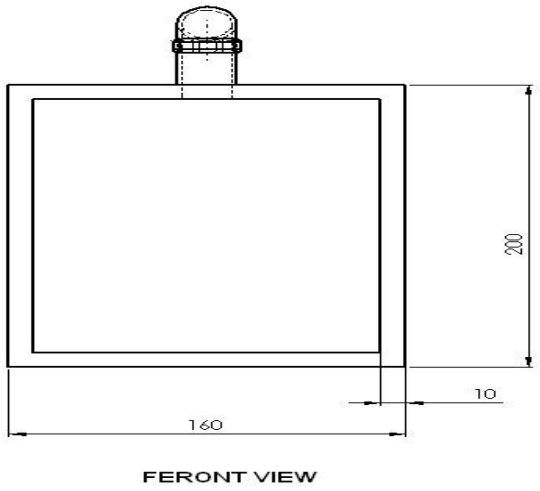

(a) Front view of main machine chamber

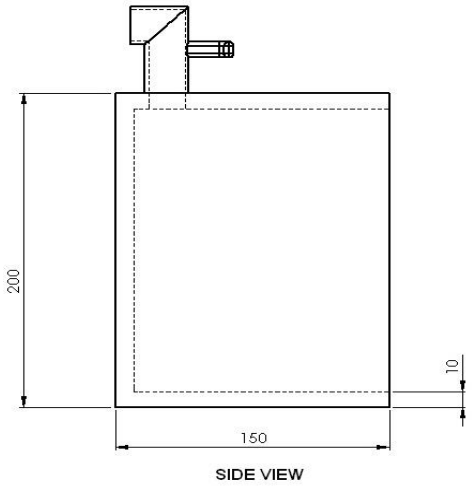

(b)Side view of main machine chamber

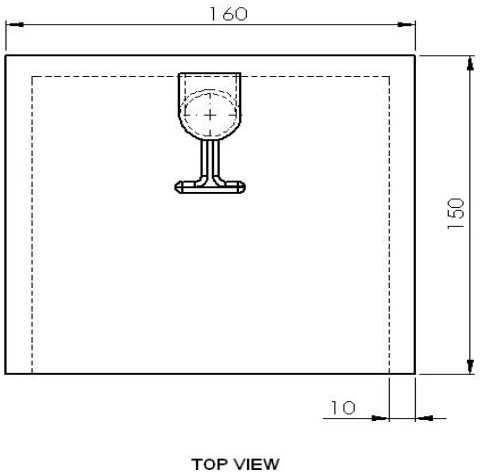

(c)Top view of main machine chamber

Fig.3.12 Orthographic view of main machine chamber

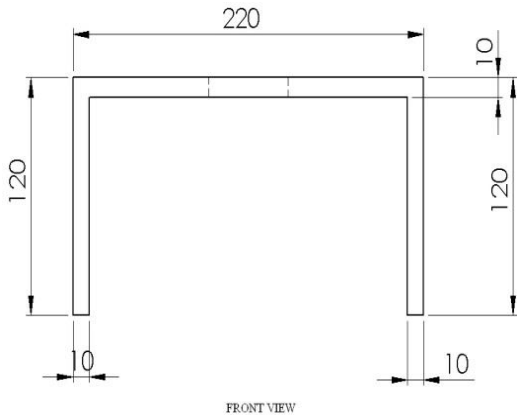

(a) Front view of over head plate

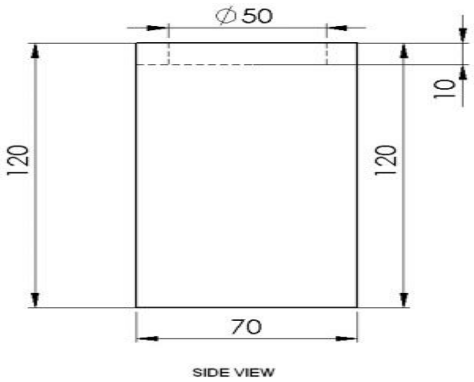

(b) Side view of over head plate

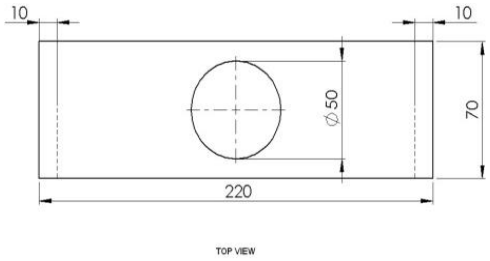

(c) Top view of over head plate

Fig.3.13 Orthographic view of over head plate

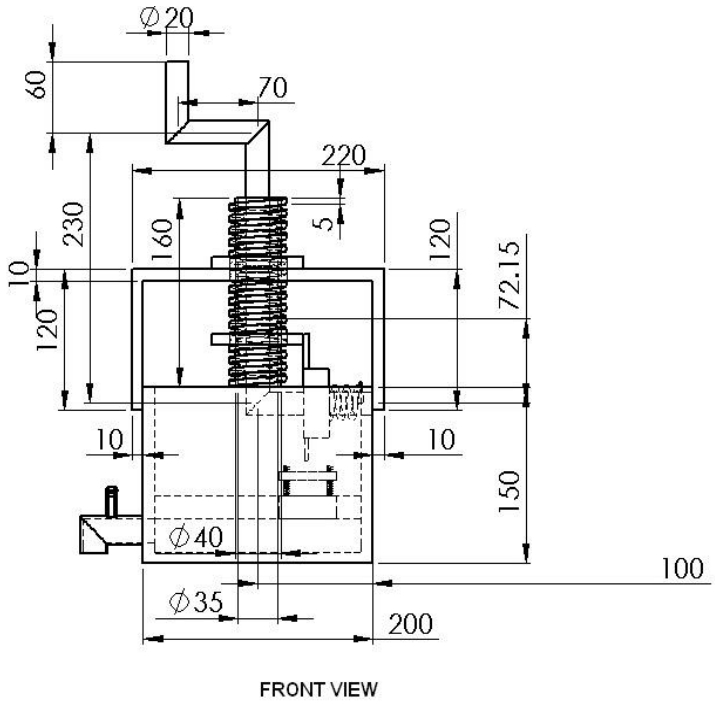

(a) front view of µ-ECDM Set up

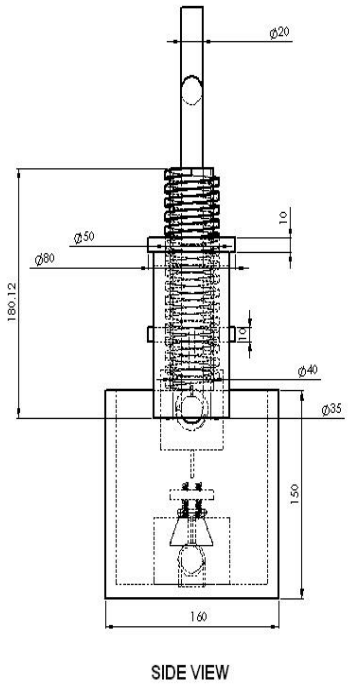

(b) side view of µ-ECDM Set up

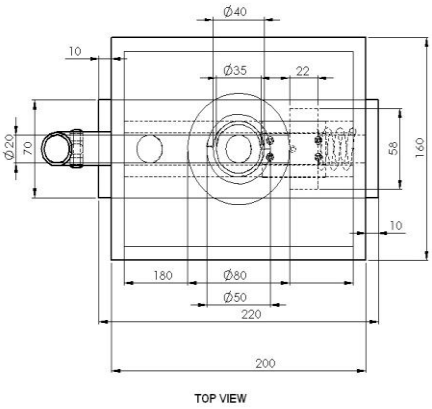

(c) Top view of µ-ECDM Set up

Fig.3.14 Orthographic View of developed µ-ECDM Set up

3.3 ELECTRICAL POWER SUPPLY SYSTEM

The electrical power supply system can control voltage, pulse frequency and duty ratio during µ-ECDM process. The schematic diagram of the power circuit of the µ-ECDM set-up is shown in Fig. 3.15.The photographic view of electrical power supply unit is shown in Fig. 3.16 for micro-channel cutting operation in which the applied voltage can be varied from 0 to 100 V.

Specification details of electrical power supply unit are given as follows:

(i) Main input power supply: 3 phase 440 V A.C.

(ii) Power supply: Pulsed D.C.

(iii) Voltage range: 0 to 100 V

(iv) Range of current: 0 to 5 amps.

(v) Range of pulse frequency: 60Hz to1.2kHz

(vi) Range of duty ratio: 35% to 70%

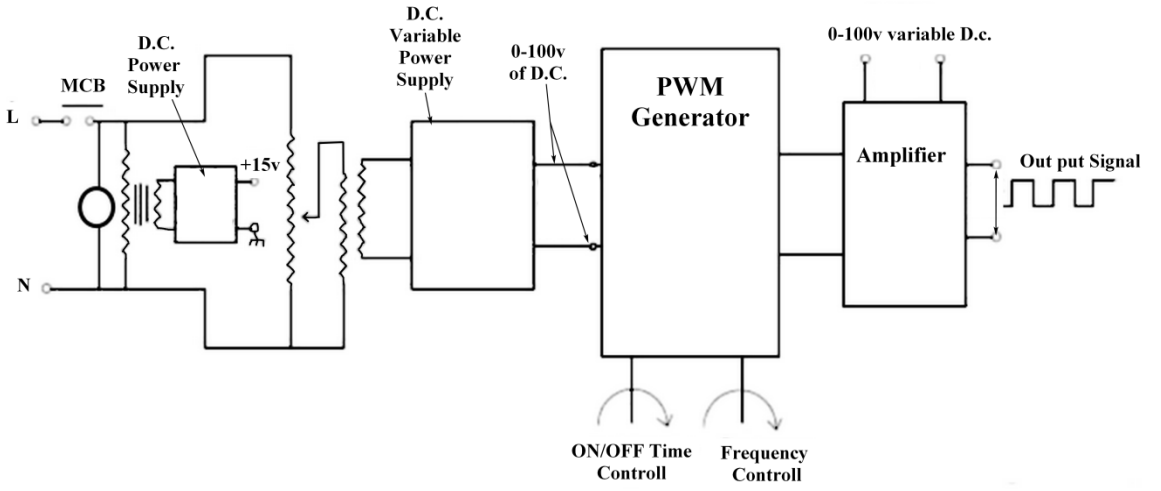

Fig.3.15 Schematic diagram of electrical power circuit of power supply unit

Fig. 3.16 The electrical power supply system

4. INVESTIGATIONS INTO µ-ECDM PROCESS FOR MICRO-CHANNEL CUTTING ON GLASS USING DIFFERENT TYPE OF ELECTROLYTES WITH FORM TOOL AND GRAVITY FEED MECHANISM

4.1 EXPERIMENTAL PLAN

The experimental plan has been designed in such a way that the objectives of the investigation can be fulfilled satisfactorily. In this work the fundamental studies were carried out to identify the influences of process variables such as applied voltage, type and concentration of electrolyte and tool shape during micro-channel cutting on glass by electrochemical discharge phenomena. Experimental conditions are shown in the Table 4.1. Materials of the job and the tool are removed due to the thermal effect of electrochemical discharge phenomenon. During the basic experimental investigation it is observed that hydrogen bubbles are formed at 5V and sparking is initiated at 35V but continuous discharge takes place at 50V and up to 60V during electrochemical discharge machining. The length of the tool is limited and if it increases, internal resistance increase, so tool length is kept at 8mm.Therefore, to investigate on ECDM process material removal rate (MRR), overcut (OC), surface roughness (R_a) and also heat affected zone (HAZ) were considered as performance criteria in this research work.

The experiments were conducted using counter weight feed mechanism in µ-ECDM set up. Fig. 4.1 shows the 3D CAD model of µ-ECDM set-up with counter weight feed mechanism and Fig. 4.2 shows the photographic view of different shapes of forming tool used in µ-ECDM during micro-channel cutting operation.

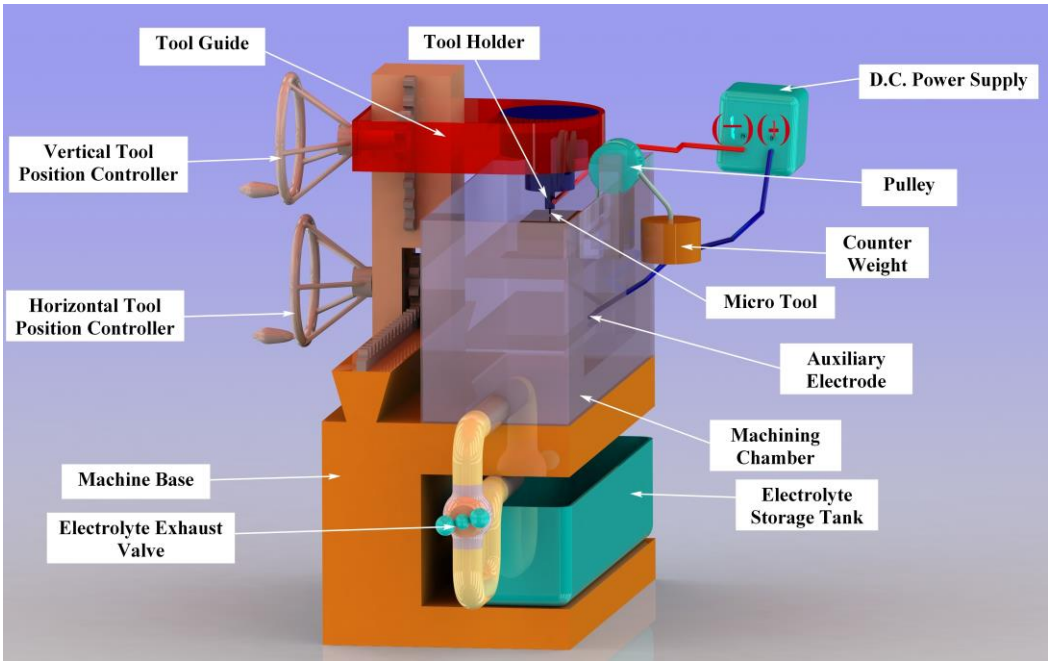

Fig. 4.1 3D diagram of µ-ECDM set-up with counter weight gravity feed

The detailed specifications of the µ-ECDM set-up are as follows:

II. The specification of some vital mechanical hardware module of µ-ECDM set up is:

(i) Maximum dimension of job specimen that can be machined by the µ-ECDM set up

For square type job: 20 mm X 20 mm X 5mm

For circular type job: 30 mm X 5 mm

(ii) Maximum inter electrode gap (IEG) that can be set: 30-50 mm

(iii) Dimensions of machining chamber: 250 mm X 250 mm X 150 mm

(iv) Maximum movement to horizontal direction with the help of vice: 50 mm

(v) Auxiliary electrode material(secondary electrode): stainless steel of 80 mm X 50 mm X 1 mm

(vi) Volume of the reservoir tank: 5000 cm^3

(vii) Job specimen feeding arrangement: Gravity feed with counter weight.

The experimental procedures for performing the experiments are described as follows:

a) Firstly the machining chamber was cleaned properly with distilled water.
b) The electrolyte solution was prepared for a particular concentration by mixing the required electrolyte with distilled water.
c) The job specimen was clamped just below the tool tip and the tool tip was immersed 1mm below the upper level of the electrolyte.
d) The desired inter-electrode gap was maintained by means of lowering or lifting the auxiliary electrode to the proper position using a screw-nut mechanism.
e) The feed motion was applied to the job specimen by gravity feeding unit with an adjustable counter weight.
f) The voltage was applied by rotating the variac. The readings of applied voltage and current were observed with the help of voltmeter and ammeter. Both readings were recorded for analyses.
g) The level of electrolyte was changed due to the boiling and evaporation. It was adjusted by means of regulating the flow of electrolyte in the machining chamber.
h) Each machining operation was performed for 20 minutes.
i) After the machining operation, the machine was switched off and the job specimen was removed and dried. The weight of the job was measured with METTELER TOLLEDO weighing machine (LC of 1 x 10^{-5} g).
j) The Width of Cut (WOC), Machining Depth (MD), Heat Affected Zone (HAZ) area were measured at magnifications of 5X, 10X and 20X respectively with LEICA microscope and the surface roughness (R_a) was estimated in terms of R_a using tally surf of 5 µm stylus tip diameter. The 3D diagram of the cross section of micro-channel is shown in Fig.4.3 with machining depth, width of cut and heat affected zone.
k) The Material Removal Rate (MRR) of the micro-channel was calculated by using the following formula:

$$MRR = \frac{\text{Wt.of job before machining} - \text{Wt of job after machining}}{\text{Machining time}} \quad \text{.....Eq.(4.1)}$$

Table 4.1 The µ-ECDM experimental conditions

Job specimen	Material	Glass (silica)
	Size	20x10x1.5 mm^3
Tool	Material	Stainless steel
	Profile	Rectangular
	Thickness	100 µm
	Length	8 mm
Fixed Process Parameters	Electrolyte flow	Stagnant
	Inter electrode gap	40 mm
	Pulse frequency	50 Hz
	Duty ratio	0.5
	Machining time	20 min.
Variable Process Parameters	Applied Voltage (V)	50 - 65 V
	Electrolyte Concentration.	10-30wt%
	Electrolyte	NaOH & KOH solution
	Tool shape	Straight and curve

In this present research work micro-channel cutting operation was done on silica glass slide. Glass has high refractive index, low density, significant strength and high insulation properties etc. Glass is generally three types namely Silica Glass, Soda Lime Glass and Borosilicate Glass. The silica glass was used for experimentation. The physical properties of silica glass are listed in the Table 4.2

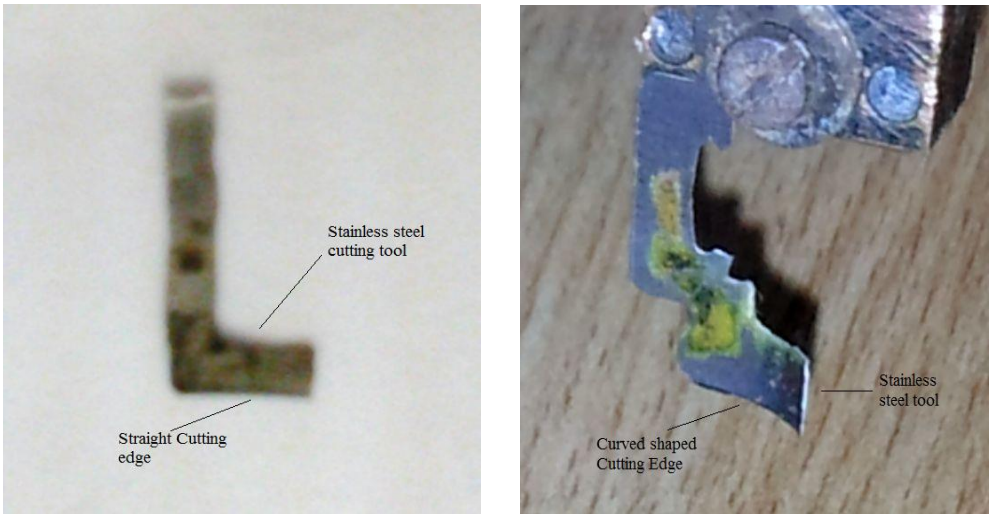

(a) Straight tool (b) curved tool

Fig. 4.2 Photographic view of different forming tool used in µ-ECDM

Table 4.2 Properties of Silica Glass

Properties	**Silica Glass**
Density (Kg/m^3)	2.52×10^3
Thermal Conductivity (W/m-k)	1.2
Thermal Expansion (K^{-1})	0.54×10^{-6}
Young's Modulus (N/m^2)	72×10^9
Tensile Strength (N/m^2)	50×10^6
Refractive index	1.518
Melting temperature (ºC)	1040

Silica glass is very widely used for biomedical instruments, optical products such as camera, microscope and binocular and also as micro-fluidic channel. It can also be used for manufacturing optical fibre for IT industries, wind screen of vehicle, traffic signals, utensils for house hold purpose etc. Glass can be used for making micro-fluidic devices for laboratory and research purpose etc.

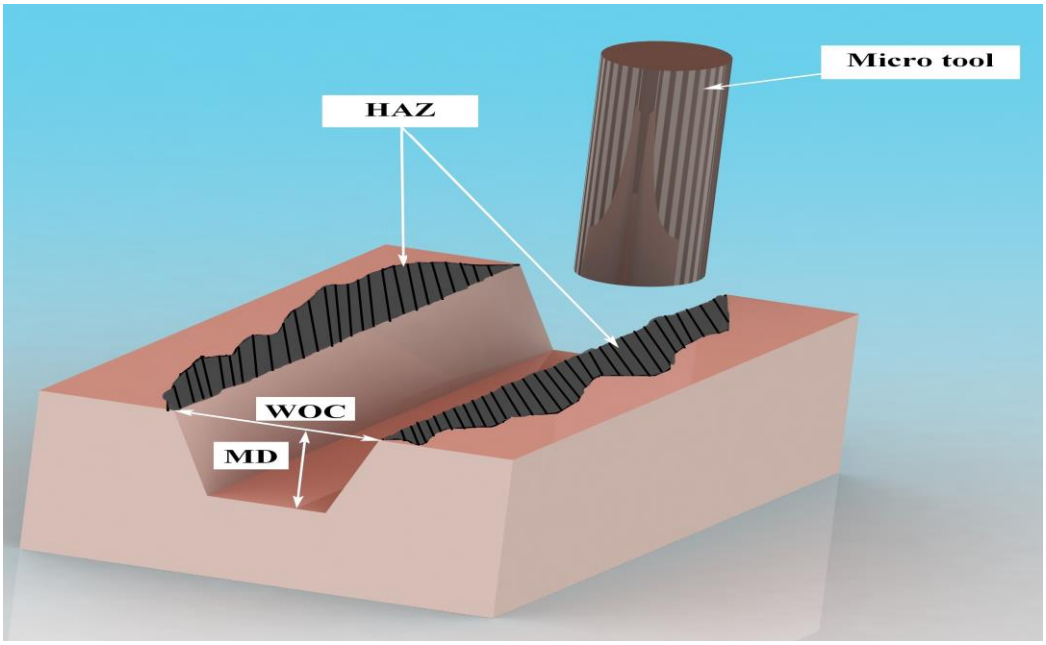

Fig. 4.3 Cross-section of µ-channel with machining depth (MD) Width of Cut (WOC) & Heat Affected Zone (HAZ)

4.2 EXPERIMENTAL RESULTS AND DISCUSSION

The influences of process parameters such as applied voltage (V), electrolyte concentration and tool shape on MRR, OC, HAZ area and surface roughness (R_a) in µ-ECDM are analyzed based on the results of experiments conducted using two different electrolytes such as NaOH and KOH alkaline solution and tool of different shape. At every process parametric condition experiments were conducted three times and the average experimental results were used for analyses. Total 120 (40x3) experiments were conducted in this research work. Experimental test results are shown in the Table 4.3. Though the thickness of the curved and straight shape of tool is same but the surface area is different. The current density is different. The hydrogen bubble generation rate and resistance are also different, so machining performances are different for straight and curved tool.

Table 4.3 Experimental condition and test results

	Experimental Conditions			Responses							
Expt. No.	Elect. Conc.	Voltage (V)	Tool Shape	MRR (mg/hr)		OC(µm)		R_a (µm)		HAZ (mm^2)	
				Using NaOH	Using KOH	Using NaOH	Using KOH	Using NaOH	Using KOH	Using NaOH	Using KOH
1	10	50	Straight	7.104	7.614	188.093	131.565	1.309	1.899	1.034	0.622
2	10	55	Straight	9.963	8.463	183.154	176.798	1.276	1.476	1.138	0.851
3	10	60	Straight	10.368	11.433	219.949	190.589	1.394	1.494	1.414	0.963
4	10	65	Straight	12.251	12.624	323.964	197.891	1.804	2.204	2.397	1.142
5	10	50	Curved	2.085	9.017	153.392	89.266	2.096	2.085	0.724	0.264
6	10	55	Curved	6.327	15.739	309.018	252.365	2.104	2.044	1.099	0.356
7	10	60	Curved	8.445	27.637	324.883	318.362	1.87	1.882	1.490	0.796
8	10	65	Curved	11.467	34.245	543.905	497.365	2.464	2.313	1.789	1.025
9	15	50	Straight	8.163	8.392	164.139	20.676	1.344	2.044	0.722	0.725
10	15	55	Straight	12.247	16.628	172.287	98.472	1.29	1.334	1.294	0.789
11	15	60	Straight	15.637	17.261	308.335	136.199	1.727	1.537	1.236	0.967
12	15	65	Straight	16.816	28.217	374.387	196.444	2.214	2.313	2.196	1.210
13	15	50	Curved	3.509	10.325	90.489	246.985	1.892	2.143	0.761	0.696
14	15	55	Curved	7.203	16.342	132.172	305.321	2.165	2.095	0.935	0.726
15	15	60	Curved	9.342	21.648	293.66	365.258	1.899	1.979	1.102	1.195
16	15	65	Curved	13.257	33.364	361.005	393.164	2.687	2.687	1.549	1.245
17	20	50	Straight	8.315	17.654	43.329	53.249	1.356	1.356	0.572	0.966
18	20	55	Straight	14.214	23.159	110.216	221.877	1.217	1.297	1.009	1.191
19	20	60	Straight	20.407	25.364	234.886	245.364	1.612	1.288	1.354	1.217
20	20	65	Straight	27.257	36.214	419.526	275.315	2.042	2.582	2.752	1.600
21	20	50	Curved	4.295	15.28	163.823	280.879	2.164	2.564	1.254	0.684
22	20	55	Curved	8.981	27.227	173.823	375.445	2.543	2.243	1.351	0.930

23	20	60	Curved	9.714	29.615	182.704	428.782	2.335	2.145	1.402	1.266
24	20	65	Curved	13.574	30.636	341.791	443.761	2.889	2.882	1.894	1.521
25	25	50	Straight	8.491	19.224	252.894	88.365	1.534	1.482	0.745	1.256
	Experimental Conditions			**Responses**							
Expt. No.	**Elect. Conc.**	**Voltage (V)**	**Tool Shape**	**MRR (mg/hr)**		**OC(µm)**		**R_a (µm)**		**HAZ (mm^2)**	
				Using NaOH	**Using KOH**	**Using NaOH**	**Using KOH**	**Using NaOH**	**Using KOH**	**Using NaOH**	**Using KOH**
26	25	55	Straight	15.412	22.361	250.856	265.914	1.384	1.394	1.519	1.285
27	25	60	Straight	21.583	27.614	291.746	275.321	1.832	1.399	1.551	1.425
28	25	65	Straight	28.418	39.868	478.831	366.287	2.464	2.712	2.834	1.856
29	25	50	Curved	12.843	17.638	156.103	316.288	2.195	2.425	0.834	0.795
30	25	55	Curved	18.138	27.483	197.649	337.393	2.664	2.364	1.413	1.442
31	25	60	Curved	23.407	30.41	231.979	401.477	2.456	2.256	1.667	1.483
32	25	65	Curved	24.743	36.709	467.193	536.28	3.16	3.06	2.194	1.761
33	30	50	Straight	12.669	27.326	224.019	305.346	1.494	1.534	0.935	1.261
34	30	55	Straight	18.863	29.361	296.853	428.913	1.485	1.475	1.623	1.563
35	30	60	Straight	26.814	30.524	357.428	437.642	1.994	1.487	1.864	1.686
36	30	65	Straight	34.656	42.394	510.416	589.369	2.782	2.987	2.967	2.012
37	30	50	Curved	19.261	24.362	275.489	353.651	2.329	2.71	1.594	1.594
38	30	55	Curved	32.819	29.321	353.276	410.745	2.689	2.52	1.856	1.680
39	30	60	Curved	41.527	33.127	396.463	497.658	2.534	2.614	1.965	2.019
40	30	65	Curved	56.387	45.354	596.487	568.157	3.419	3.199	2.925	2.316

4.2.1 Influences of Process Parameters on Material Removal Rate (MRR)

The influences of applied voltage and concentration of electrolyte on material removal rate (MRR) have been analysed during electrochemical discharge micro-machining process. Micro-channels on glass have been produced by straight and curved tools using NaOH and KOH solutions as electrolyte. The Fig. 4.4 shows the effects of applied voltage on material removal rate at different electrolyte concentration (i) using NaOH and (ii) using KOH for (a) straight tool and (b) curved tool for both NaOH as well as KOH electrolyte solutions. Material removal rate enhances with the increment of applied voltage and electrolyte

concentration for fixed length of straight and curved tools. The generation of vapour bubbles and hydrogen gas is more with the increase of voltage on account of joule heating of electrolyte and electro-chemical reactions, which is promoted due to increase of electrolyte concentration. All hydrogen bubbles and vapour bubbles are accumulated at the periphery of tool electrode and there is a rapid growth of bubbles' layer or insulating gas film around the tool. As a result spark discharge density between tool and electrolyte across the bubbles increases. Since the discharges are responsible for formation of focused stream of electrons, which hit the job sample with high velocity and acceleration and kinetic energy is converted into thermal energy. It increases the temperature of job specimen to very high level at the sparking zone. Large quantity of material is melted and vaporised even thermally spelled from the job specimen due to increased discharge energy per spark and high heat generation. Fig. 4.4 (i) shows that MRR is found large for curved tool as compared to straight tool. From the Fig. 4.4(ii) it is cleared that MRR increases with increase of voltage and concentration for fixed length of straight and curved tools when KOH electrolyte solution is used as electrolyte. The reason behind it has already been discussed as above. Further by analysing Fig. 4.4(ii) it is cleared that average MRR is obtained higher for curved tool than that of straight tool.

A comparison on MRR for two different electrolytes (NaOH & KOH) with varying concentrations and applied voltage can be carried out quantitatively based on the Figs. 4.4(i) and (ii). The Fig.4.4 indicates that MRR is found to be more by using KOH than NaOH electrolyte since KOH electrolyte has higher specific conductance than that of NaOH electrolyte at the 10-25wt% of electrolyte concentration but at 30wt% of electrolyte concentration of NaOH provides higher machining rate at higher voltage than KOH. MRR reaches the maximum value at higher concentration and applied voltage of 65V for both electrolytes and tools but NaOH is better than KOH at higher voltage and concentration. The highly energised sparking is occurred at higher level of concentration and applied voltage, which speed up the electrolysis process. It causes the faster rate of material removal. Also the higher applied voltage and concentration aggravate the thermal etching of material at higher rate.

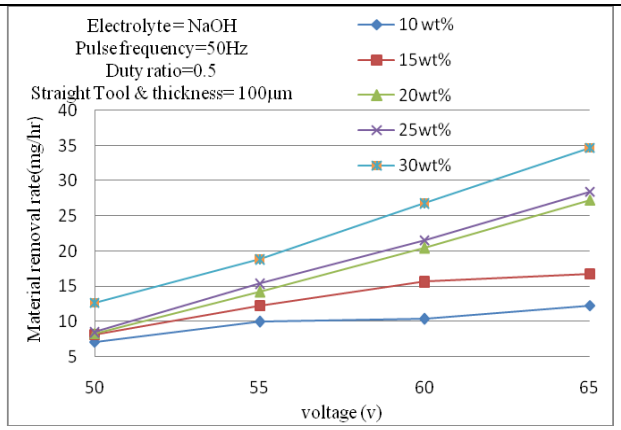

(a) straight tool

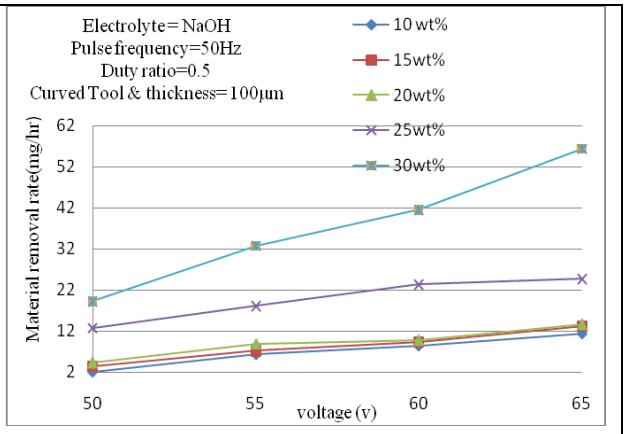

(b) curved tool

(i) Using NaOH electrolyte

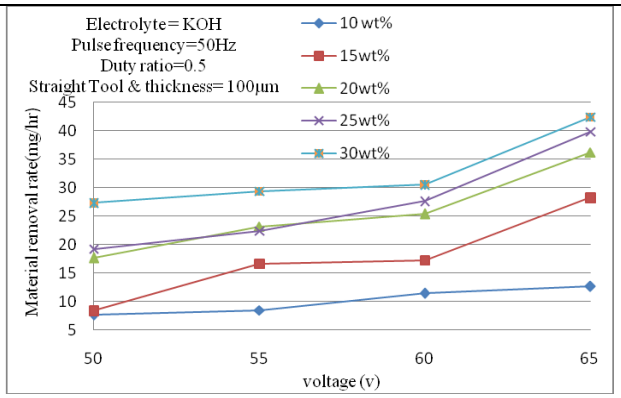

(a) straight tool

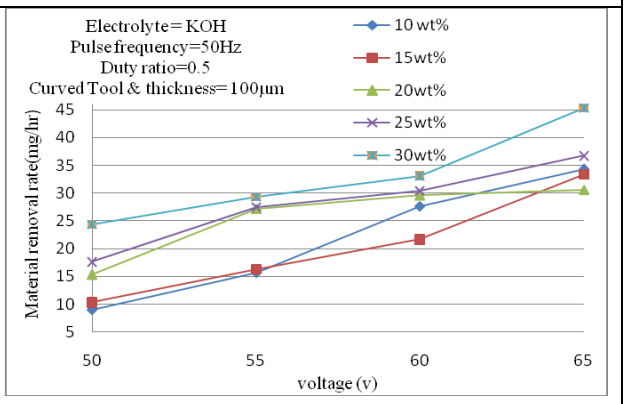

(b) curved tool

(ii) Using KOH electrolyte

Fig. 4.4 Effects of applied voltage and electrolyte concentration on MRR (i) using NaOH and (ii) using KOH for (a) straight tool and (b) curved tool.

4.2.2 Influences of Process Parameters on Overcut (OC)

Fig. 4.5(i) exhibits the influences of electrolyte concentration and applied voltage on overcut (OC) in case of NaOH electrolyte for straight and curved tools. Generally, the rate of

sparking from bottom surface of tool as well as side surface of tool enhances with the rise of bubble formation and accumulation. The overcut depends mainly on the tool's side sparking. The nucleation site of bubbles' generation is influenced by applied voltage, electrolyte concentration and some extent wet ability and roughness of the tool. Therefore, sparking density at the side of tool changes with the change in concentration and applied voltage. This enriches not only MRR but also enlarges overcut of micro-channels. The overcut (OC) increases with increase of electrolyte concentration and lower OC is found at 15 wt% electrolyte concentrations whereas it reaches to the higher level at 30 wt% NaOH as well as KOH electrolyte concentration with applied voltage above 60V for both tools. Narrower micro-channel is obtained for 15 wt% KOH electrolyte concentration while straight cutting tool is used. This observation is almost similar to other observations when KOH is used as electrolyte.

From the Fig. 4.5(ii), (a) it is found that the OC is lower at applied voltage of 50 V, 15 wt% of KOH electrolyte concentrations using straight tool but it enters to the higher level at 30 wt% KOH electrolyte concentration with applied voltage above 55V. The width of cut is smaller for intermediate KOH electrolyte concentrations due to the fact that an intense sparking occurs at the bottom face of both types of tool.

From the Fig. 4.5(i), (a) it is understandable that the overcut can be attained with the lowest value by using NaOH electrolyte for straight tool at the parametric setting of 50 V and 20 wt% concentration. Also, from the Fig. 4.5(i), (b), OC is found lower with curved tool for NaOH electrolyte at 15 wt% electrolyte concentration and applied voltage of 50 V. The width of cut (WOC) becomes more than 500µm during machining of 65V at higher concentration for both tools and electrolytes. The Figs. 4.5(i) and (ii) also indicate average OC is lower when µ-channelling is performed with straight tool by using KOH electrolyte. As the number of bubbles' generation and their growth rate are more for curved tool owing to the surface tension and these enhance the sparking density, thereby OC increases for curve tool.

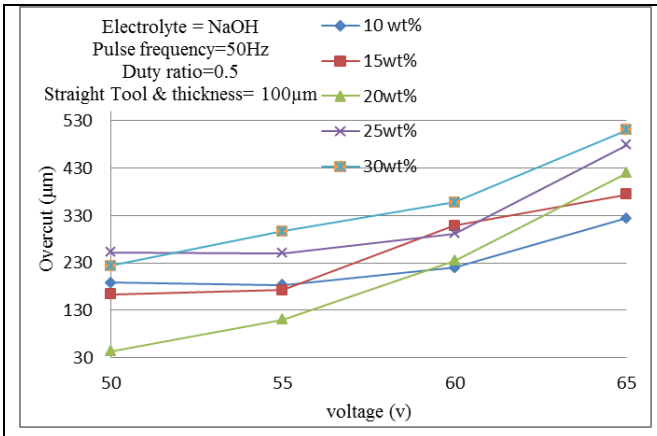

(a) Straight tool

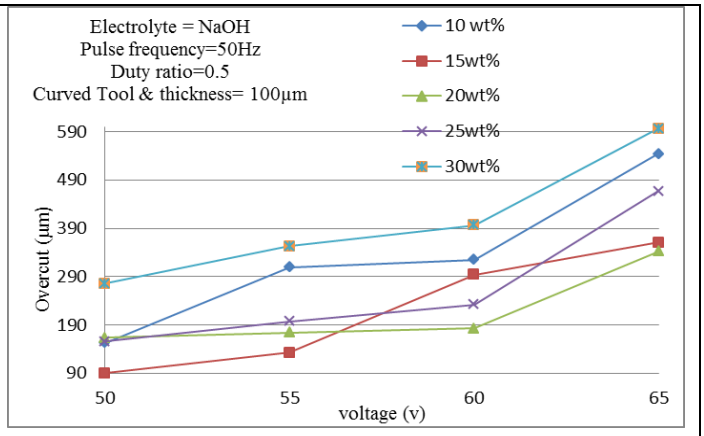

(b) Curved tool

(i) Using NaOH electrolyte

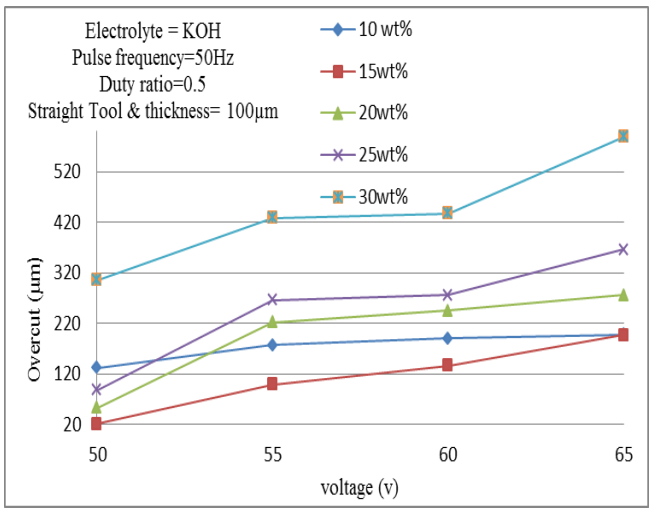

(a) Straight tool

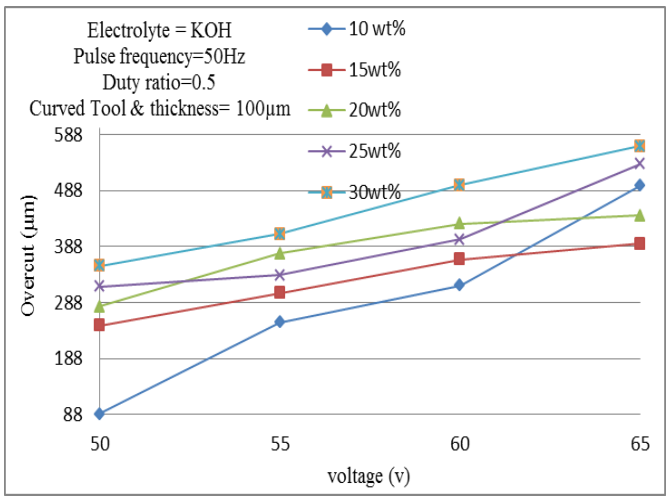

(b) Curved tool

(ii) Using KOH electrolyte

Fig.4. 5 Effects of applied voltage and electrolyte concentration on OC (i) using NaOH and (ii) using KOH for (a) straight tool and (b) curved tool.

4.2.3 Influences of Process Parameters on Heat Affected Zone (HAZ) Area

A large amount of thermal energy is generated during the machining of a glass by electrical spark discharge (ESD) phenomenon in μ-ECDM process. A portion of this energy goes to electrolyte and atmosphere by convection and radiation modes of heat transfer respectively and rest is conducted to the job sample. This energy is also responsible for development of heat-affected zone in the region of the machined profile. So, HAZ area depends on the amount of thermal energy i.e. heat conducted to the material. The higher heat energy conduction to the job produces higher HAZ area at the machining zone. The effects of voltage and electrolyte concentration on HAZ area is exhibited in Fig. 4.6(i) and (ii), which show that HAZ area increases with the rise of applied voltage for straight tool and curved tool. Under these conditions, a great amount of thermal energy is fed to the job specimen in the region of micro-channel through spark discharge. But the thermal energy evolved at low concentration is not sufficient to vaporise the job material completely and at same time the molten material gets solidified due to cooling effect of electrolyte. HAZ area also differs with electrolyte concentration. Initially, HAZ area reduces with an increase in electrolyte concentration because high density of concentrated electrochemical spark discharge takes place at the bottom side of the tool rather than side surface. Thereafter, HAZ area enlarges with electrolyte concentration. The area of HAZ not only depends on the process parameters but it may depend upon the distribution of sparking. Spark discharge in μ-ECDM process plays a key role during micro-channel cutting on glass material. Therefore, there is an urgent need for controlling the discharge phenomenon to improve HAZ area in micro-machining domain. The Fig. 4.6 show the effects of applied voltage and electrolyte concentration on HAZ area (i) using NaOH and (ii) using KOH for (a) straight tool and (b) curved tool. It is found from the Fig. 4.6 (i) and (ii) that HAZ is higher for 30 wt% of both electrolytes at 65 V but it attains more while NaOH is used at that concentration with straight as well as curved tool. From the Fig. 4.6 (i), (a) and (b) it is clear that HAZ area is lower at 20wt% of NaOH/50V/straight tool but for curved tool HAZ is lower at 15wt% of electrolyte. From the Fig. 4.6 (ii), (a) it is observed that for straight tool at 50 V, 10 wt% of KOH electrolyte provides lower HAZ area but after 50V, 15wt% of concentration is more effective for micro-machining operation while KOH is used as electrolyte but from Fig. 4.6 (ii), (b) it is obvious that 10wt% of KOH provides lower HAZ area when curved tool is used at 50-65 V. From

Fig.4.6, after details observation it is concluded that lowest HAZ area is found at 50V while 10wt% of KOH is used with curved tool.

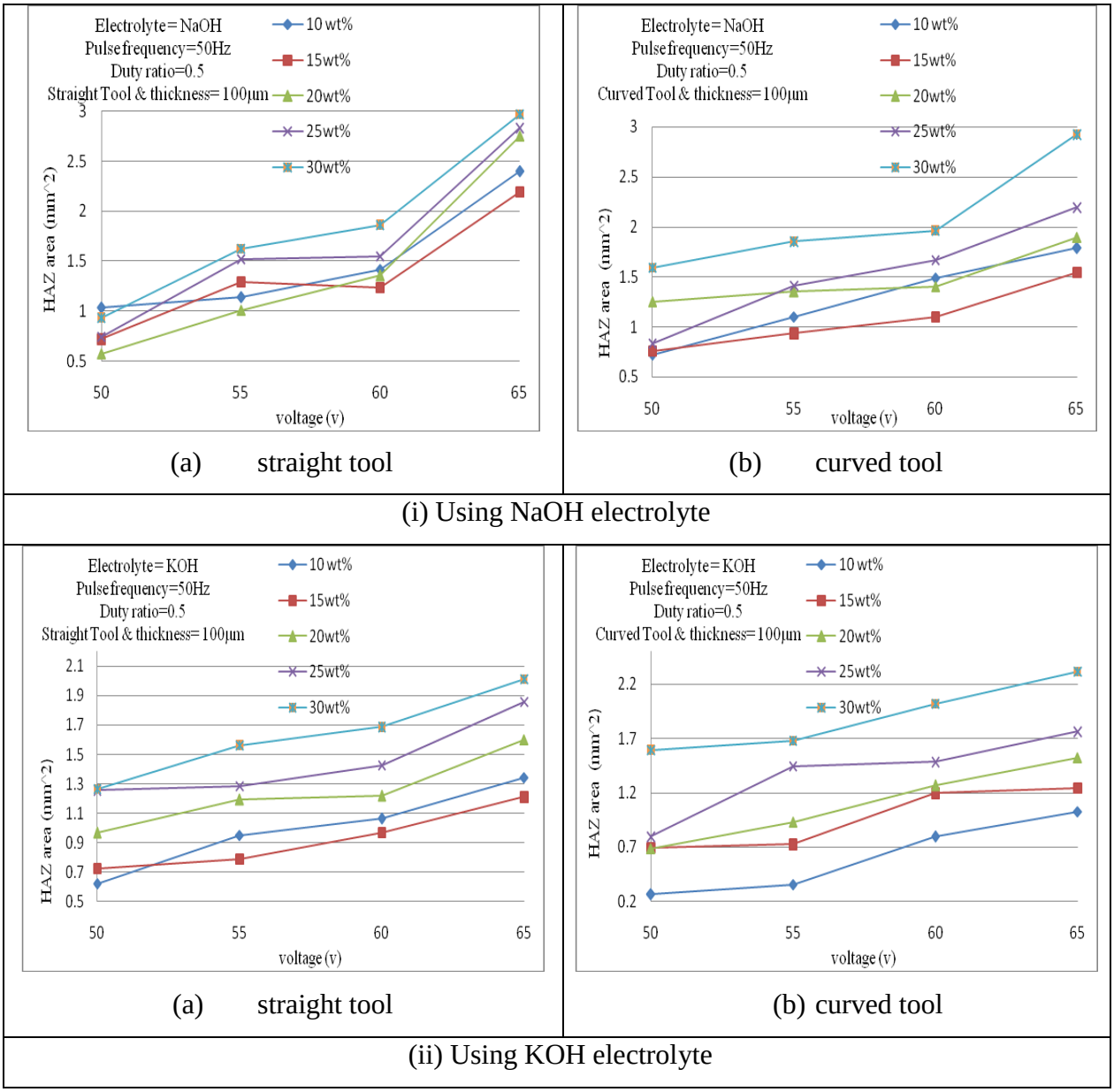

(a) straight tool (b) curved tool

(i) Using NaOH electrolyte

(a) straight tool (b) curved tool

(ii) Using KOH electrolyte

Fig. 4.6 Effects of applied voltage and electrolyte concentration on HAZ area (i) using NaOH and (ii) using KOH for (a) straight tool and (b) curved tool.

4.2.4 Influences of Process Parameters on Surface Roughness (R_a)

The effects of voltage and concentration on the surface roughness (R_a) for fixed inter-electrode gap of 40 mm using NaOH electrolyte and straight and curved stainless steel tool are depicted in Fig. 4.7(i). From the Fig. 4.7(i) it is found that surface roughness is increased slightly with a boost of applied voltage as a result of continuous sparking up to 60 V for different electrolyte concentrations when straight tool is used but after that by increasing voltage the surface is found rougher. In μ-ECDM process, material is removed from the machining region in the shape of crater since the glass material is brittle in nature. With the increase of applied voltage a consistent rate of sparking takes place at the 60 V due to uniform bubble generation and evenly dispersed in the machining zone. So, surface obtained is comparatively smooth. But further increase of applied voltage after 60 V the size of craters becomes bigger due to high heat generation and abnormal sparking. As a result machined surface becomes rougher. The surface roughness is higher at higher voltage as well as stronger electrolyte concentration on account of high rate of bubble generation. Further same results are found when KOH is used as electrolyte and these are exhibited in Fig. 4.7(ii).

From the Figs. 4.7(i) and 4.7(ii) it can be said that the surface roughness is higher when curved tool is used. In case of straight tool the rate of continuous sparking is more than stray sparking so surface is found smooth. But in case of curved tool side sparking is more predominant due to more bubble accumulations at the bent of tool. Fig. 4.8 represents various surface profiles obtained using different electrolytes and tool shapes at different parametric conditions. Also, these figures reveal that R_a is measured almost same for both electrolytes and the observations corroborate the variations of MRR and OC for both electrolytes.

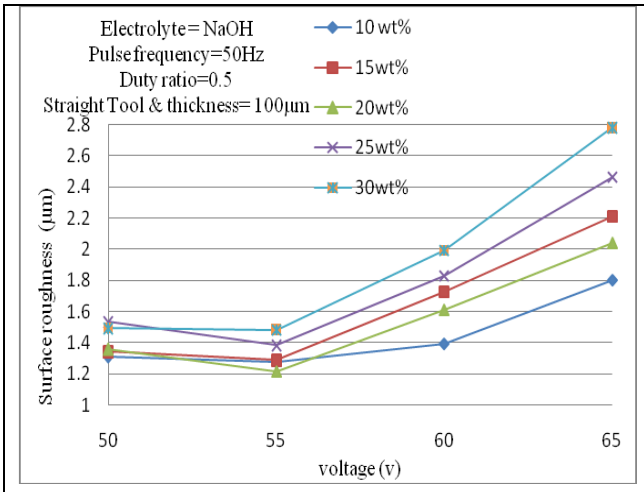

(a) straight tool

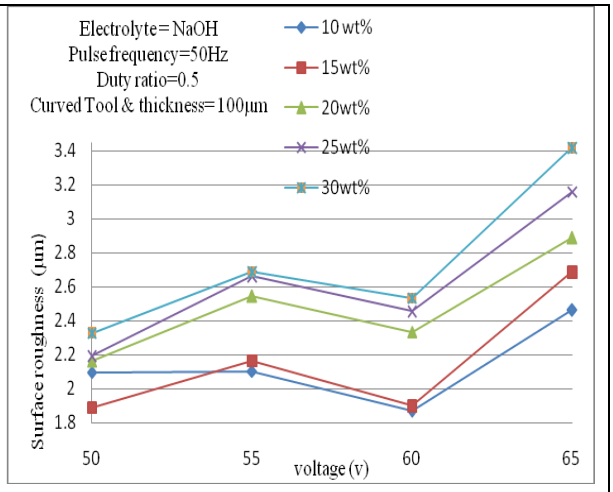

(b) curved tool

(i) Using NaOH electrolyte

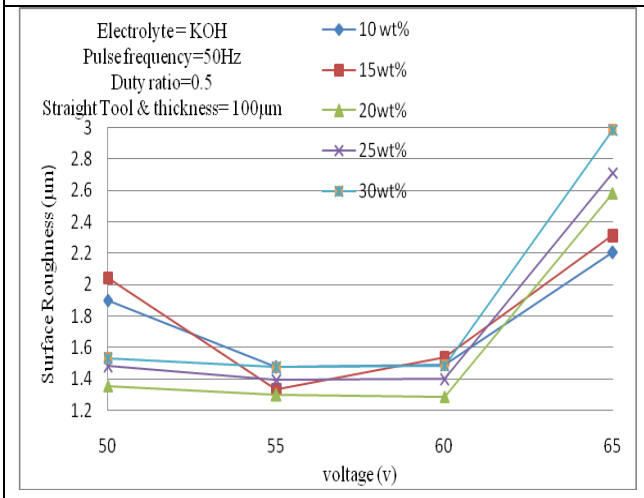

(a) straight tool

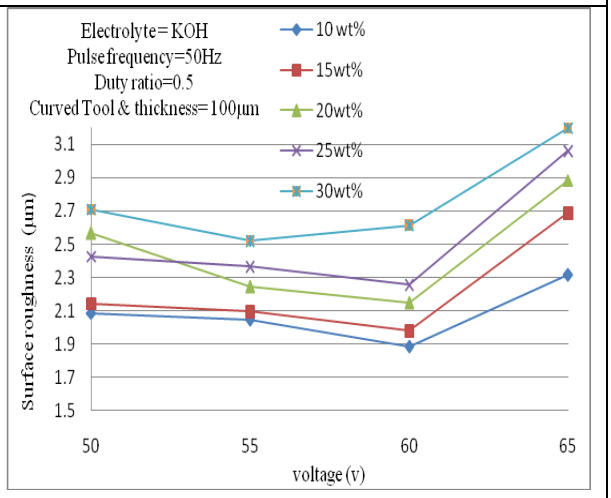

(b) curved tool

(ii) Using KOH electrolyte

Fig.4.7 Effects of applied voltage and electrolyte concentration on Surface roughness (i) using NaOH and (ii) using KOH for (a) straight tool and (b) curved tool.

NaOH electrolyte	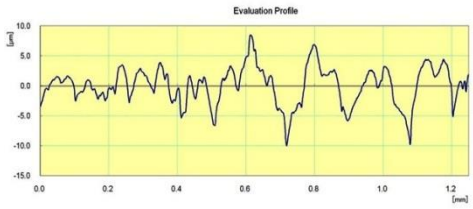 50V/10wt%/IEG 40mm/ straight tool	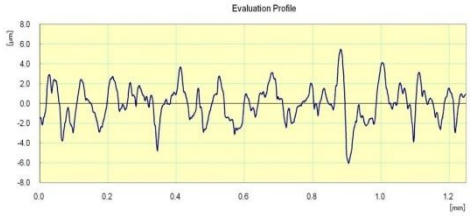 50V/30wt%/IEG 40mm/ straight tool
	 55V/25wt%/IEG 40mm/straight tool	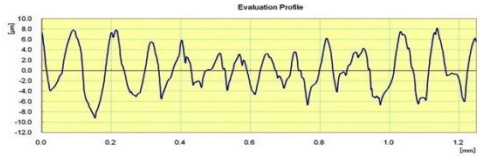 55V/25wt%IEG 40mm/curved tool
	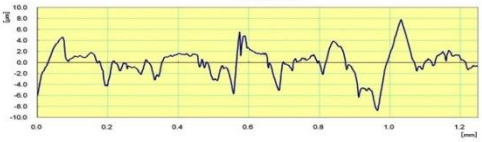 60V/15wt%/IEG 40mm/straight tool	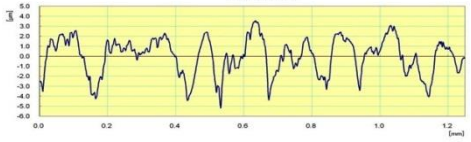 65V/30wt%/IEG 40mm/ curved tool
KOH electrolyte	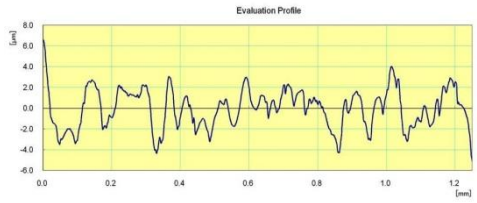 50V/30wt%/IEG 40mm/ straight tool	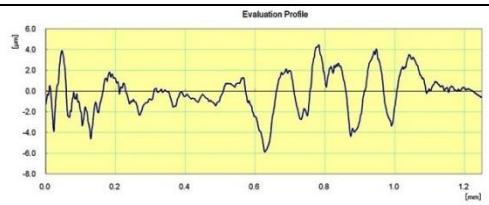 50V/30wt%/IEG 40mm/curved tool
	 50V/25wt%/IEG 40mm/ straight tool	 55V/20wt%/IEG 40mm/curved tool
	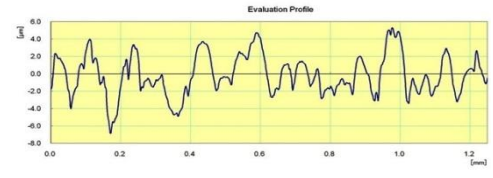 60V/15wt%/IEG 40mm/straight tool	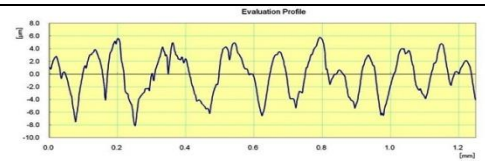 60V/30wt%/IEG 40mm/straight tool

Fig. 4.8 Surface roughness (R_a) obtained using different electrolytes and tool shapes at different parametric conditions.

4.2.5 Comparative Studies on Performances of µ-ECDM Process Using Different Electrolyte and Different Shaped Micro-Tool

In this section, a detailed comparison of various machining performance characteristics has been performed for the investigation of the influence of NaOH and KOH electrolyte solution for micro-channelling on glass. The results of comparison of machining performances such as material removal rate (MRR), overcut (OC), heat affected zone (HAZ) area and surface roughness (R_a) with respect to process parameters *i.e.* applied voltage and electrolyte concentration and tool shapes have been presented and analysed.

4.2.5.1 Comparative study on Material Removal Rate (MRR)

Fig. 4.9 shows the influences of different tool shapes (straight and curved) on MRR for NaOH and KOH electrolyte solution at different concentration. From the Fig.4.9 it is clear that MRR is found higher by using straight tool than curved tool at10wt% as well as 15 wt% of NaOH electrolyte but in case of 10wt% and 15 wt% of KOH alkaline with curved tool MRR is found higher. It is also found that using straight tool with KOH and NaOH as electrolyte at 20 wt% of concentration; MRR is obtained higher than curved tool. It is observed that using 25wt% and 30wt% NaOH with curved tool, MRR is higher but using 25wt% and 30wt% of KOH with straight tool, MRR is higher when other parameters like duty ratio and pulse frequency are kept constant at 50% and 50Hz respectively.

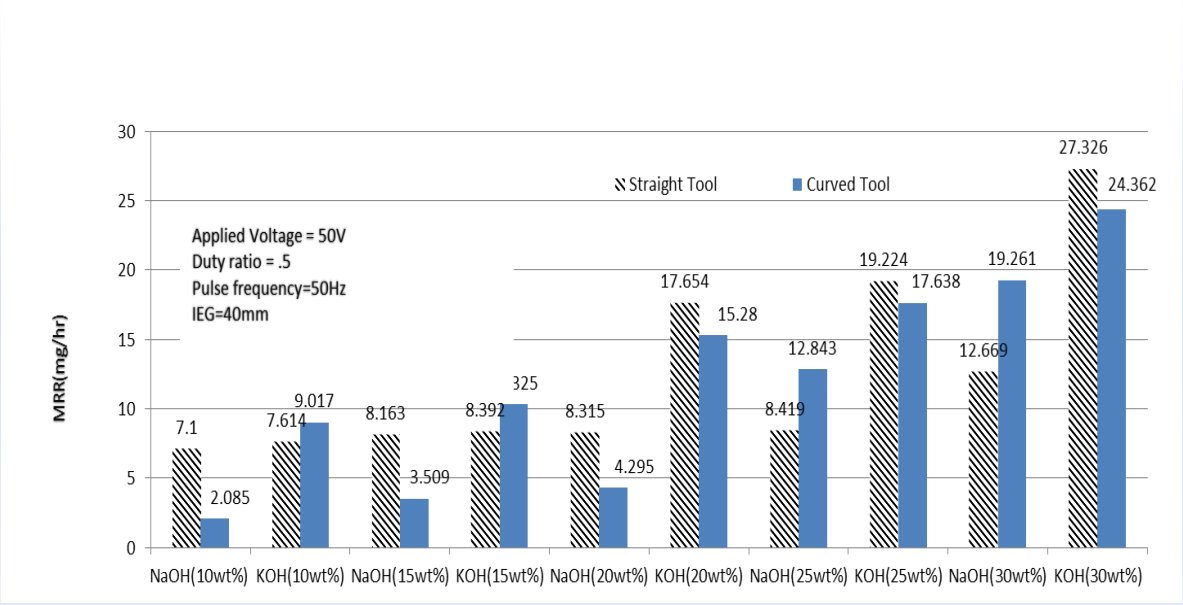

Fig. 4.9 Effects of different tool shapes on MRR using NaOH & KOH at different electrolyte concentrations

4.2.5.2 Comparative study on Overcut (OC)

The influences of different tool shapes on overcut (OC) using NaOH & KOH alkaline solution at different concentration are exhibited in Figs. 4.10. The Fig.4.10 depicts that at 10wt% of NaOH and KOH electrolyte, using straight tool more overcut is occurred due to higher rate of side sparking. It is also found that at 15wt% of KOH, using curved tool higher overcut is found but at 15 wt% of NaOH electrolyte, OC is lower when curved tool is utilized. From Fig.4.10 it is clear that by using KOH electrolyte with 20wt% concentration with curved tool OC is higher than that of same concentration of NaOH. OC is lower at 50V/.5 duty ratio/pulse frequency 50Hz when 20wt% NaOH electrolyte solution and straight tool is used. It is also obvious that lower overcut is achieved by using straight tool at 25wt% KOH than that of same concentration of NaOH but at 30wt% of KOH with curved tool provokes to create higher overcut and at this concentration NaOH with straight tool creates lower overcut.

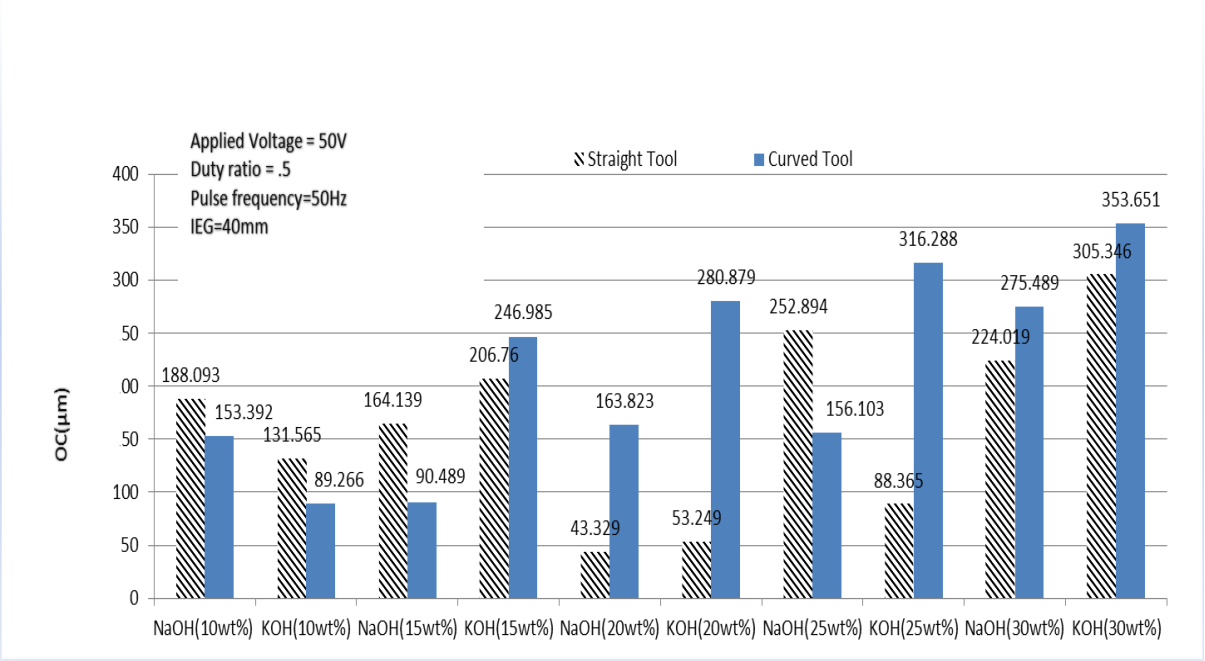

Fig. 4.10 Effects of different tool shapes on OC using NaOH & KOH at different electrolyte concentration

4.2.5.3 Comparative study on Heat Affected Zone (HAZ) Area

Fig. 4.11 shows the influences of different tool shapes on HAZ area using NaOH and KOH alkaline solutions at different concentrations. From the Fig. 4.11 it is obvious that using 10wt% of NaOH and KOH electrolyte with straight tool higher HAZ area creates during micro-ECDM process as compared to that obtained by using curved tool and at 10 wt% of KOH provides least heat affected zone when curved tool is used. From the Fig. 4.11 it is propounded that by using 15wt% of NaOH and KOH electrolyte with straight tool as well as curved tool both case uniform sparking occurs and creates near about same HAZ area. It is clear that by using straight tool & 20 wt% NaOH provides lower HAZ but curved tool at that conditions attains higher HAZ. From the Fig. 4.11 it is clear that HAZ is lower when straight tool with 25 wt% of NaOH electrolyte solution is used, HAZ is higher when 25wt% KOH with straight tool is used. From the Fig. 4.11 it is observed that straight tool at higher concentration for both electrolytes creates less HAZ area than that of curved tool and 30wt% of NaOH and 30 wt% of KOH electrolytes with curved shapes micro-tool produce maximum HAZ area.

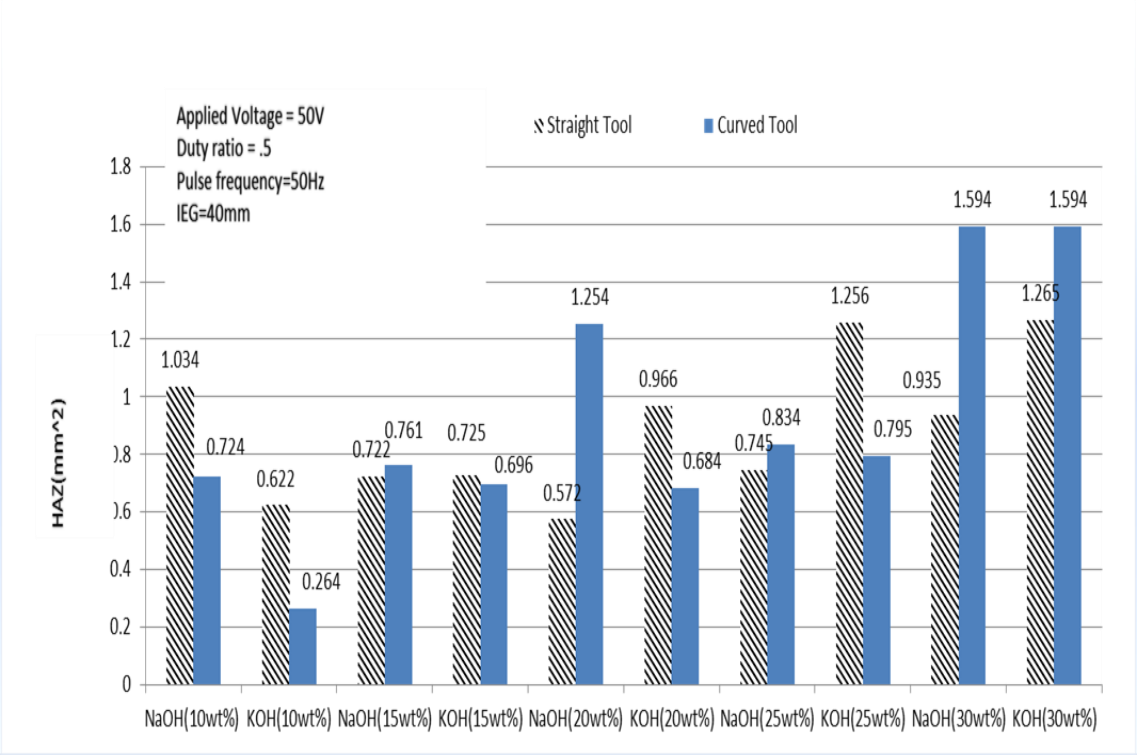

Fig. 4.11 Effects of different tool shapes on HAZ using NaOH & KOH at different electrolyte concentrations

4.2.5.4 Comparative study on Surface Roughness (R_a)

The influences of different tool shapes on surface roughness using NaOH & KOH electrolyte solutions at different concentrations are shown in Fig. 4.12. From the Fig. 4.12 it is observed that better surface finish can be achieved when straight tool and NaOH is used at 50 V at any concentration level but10 wt% of NaOH provides least value of surface roughness (R_a) when straight tool is used. From the Fig. 4.12 it is clear that surface roughness (R_a) is near about same at 50 V with 15wt% to 20 wt% of NaOH with straight tool with curved tool and 15 wt% to 20 wt% of KOH solution attains higher HAZ than that of NaOH with straight tool at the same concentration. From the Fig. 4.12 it is finally observed that straight tool with NaOH is better than KOH with curved tool and surface roughness becomes higher when KOH at 30wt% with curved tool is applied during micro-channel cutting on glass.

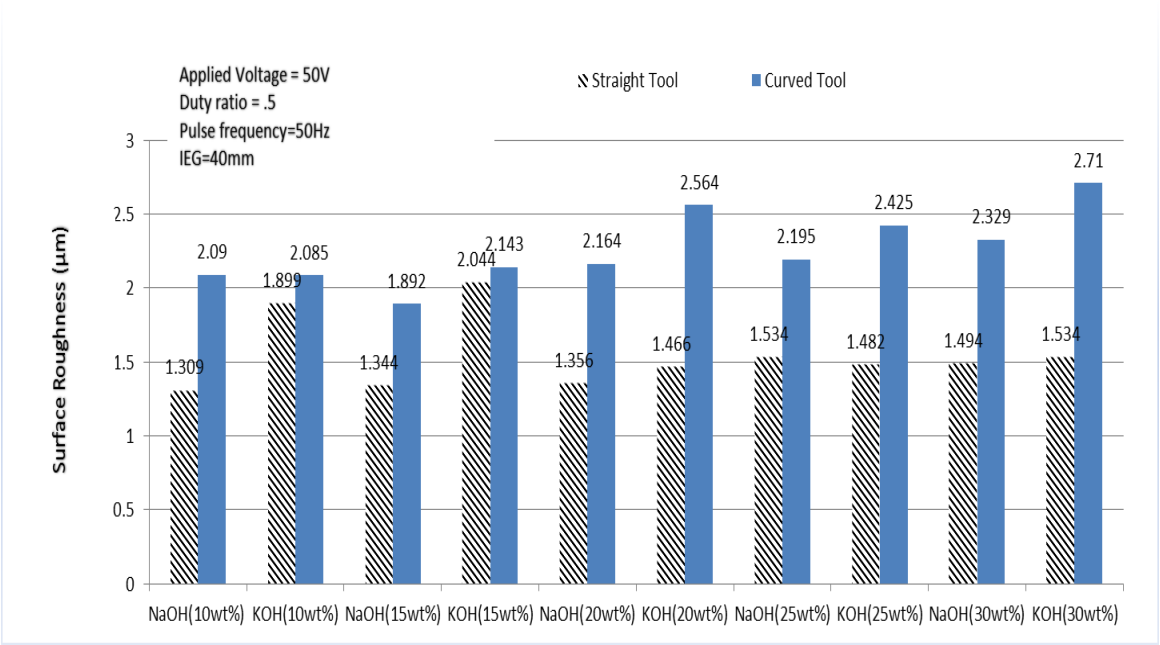

Fig. 4.12 Effects of different tool shapes on Surface Roughness (R_a) using NaOH & KOH at different electrolyte concentrations

4.2.5.5 Images of Micro-Channels at Different Experimental Conditions

Fig. 4.13 shows the optical and SEM images of curved and straight micro-channels obtained at different experimental conditions by using different electrolytes. Fig.4.14 shows the optical images of cross-sections of micro-channels cut by (i) curved tool at 50V/25wt% KOH electrolyte and (ii) straight tool at 65V/10wt% NaOH electrolyte and SEM images of bottom surfaces of micro-channel. This figure indicates that no. of voids are found more when KOH is used as electrolyte but micro-cracks are found more when NaOH is used as electrolyte. Most interesting is that the surface is comparatively smooth for NaOH electrolyte and the width of cut of micro-channels are uniform throughout its depth where as it becomes narrower and looks like taper as curved tool is used.

Type of tool	Using NaOH electrolyte	Using KOH electrolyte
Curve tool	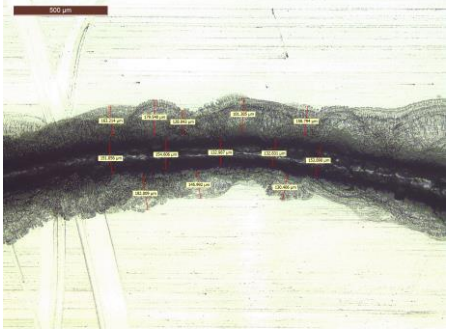 at 50V/15 wt%	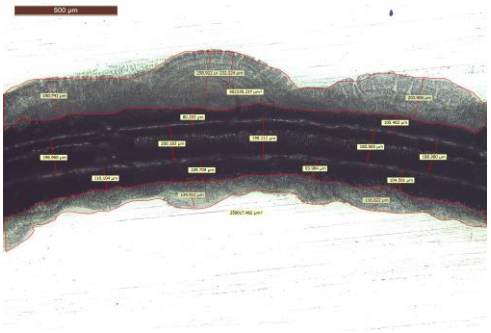 at 50V/15 wt%
	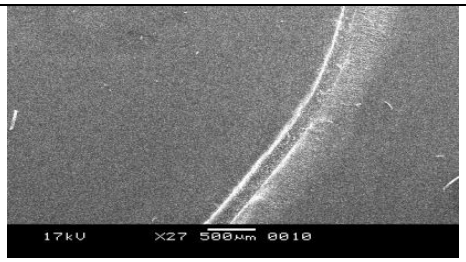 at 60V/30 wt%	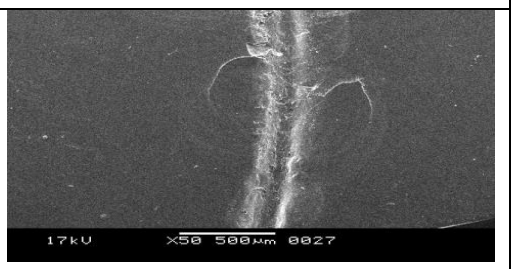 at 65V/30 wt%
Straight tool	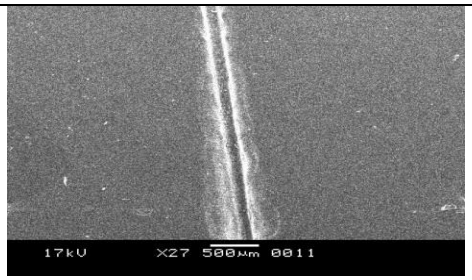 at 55V/20wt%	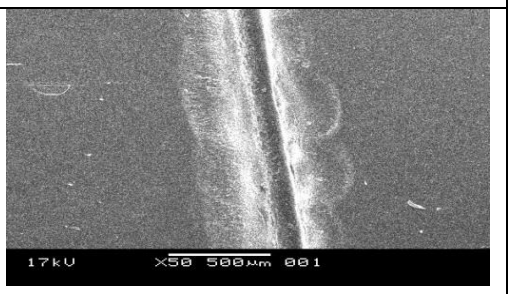 at 50V/20wt%
	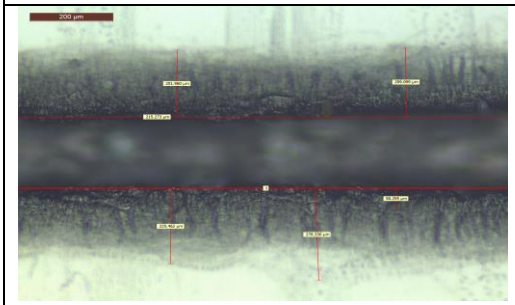 at 55V/15 wt%	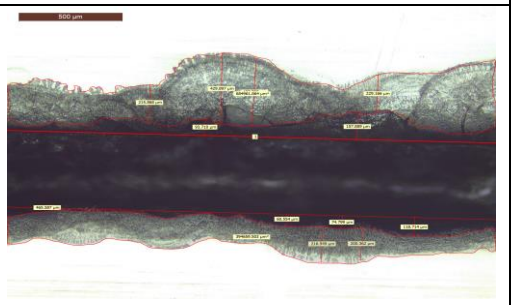 at 55V/15wt%

Fig. 4.13 Micro-channels cut by different tool shapes and electrolyte.

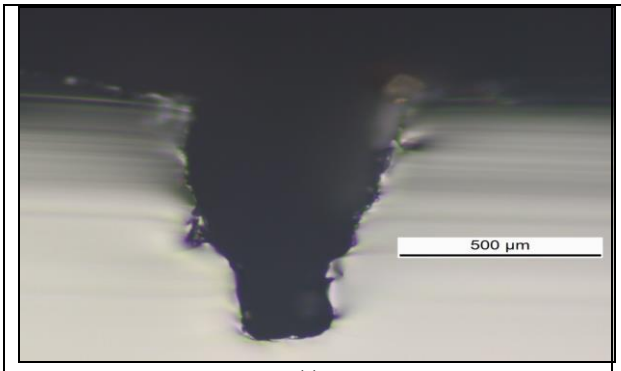

(i)

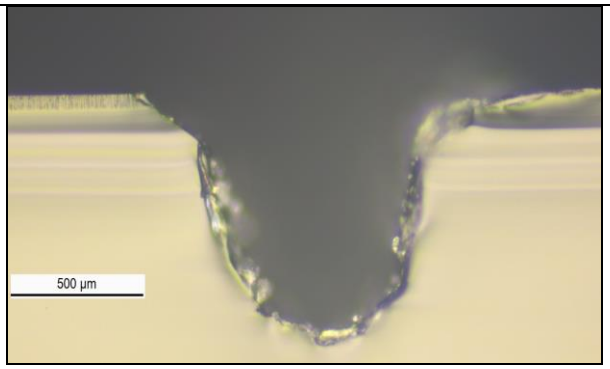

(ii)

(a) Optical images of cross-sections of micro-channel cut by (i) curved tool at 50V/25wt% KOH electrolyte and (ii) straight tool at 65V/10wt% NaOH electrolyte

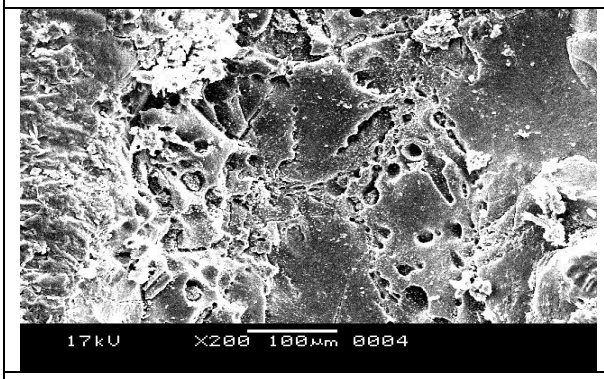

(i) at 60V/30wt%/KOH/Curved tool

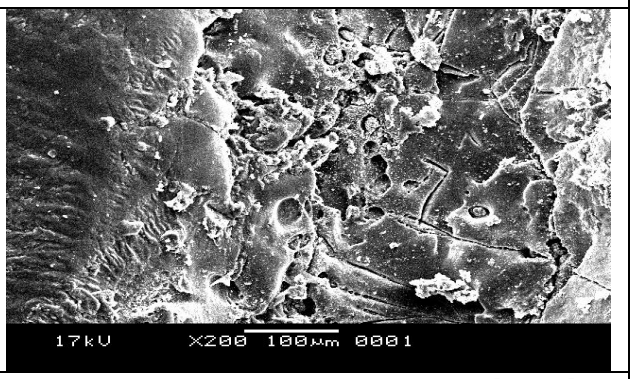

(ii) at 55V/20wt%/NaOH/straight tool

(b) SEM image of bottom surfaces of micro-channel

Fig.4.14 (a) Optical images of cross-sections of micro-channel and (b) SEM image of bottom surfaces of micro-channels.

4.2.6 Outcomes of Present Research Work

The electrochemical discharge machining micro-machining (µ-ECDM) process may be applied successfully for micro-channel cutting on electrically non-conducting material like glass irrespective of its chemical and mechanical properties and also the tool geometry. As observed the µ-ECDM process reveals a tremendous prospective for micro-channel cutting on glass. MRR and OC enhance with the rise of applied voltage for fixed electrolyte concentration. Also, MRR and OC vary with the shape of tool. 30wt% of NaOH with curved tool provides maximum MRR at 65 V but KOH of 30wt% with straight tool attains higher MRR. MRR is found to be more by using KOH than NaOH electrolyte since KOH electrolyte has higher specific conductance than that of NaOH electrolyte at the 10-25wt% of electrolyte concentration but at 30wt% of electrolyte concentration of NaOH provides higher machining rate at higher voltage than KOH. The least OC is observed at applied voltage of 50 V with 15

wt% KOH electrolyte concentration using straight tool but NaOH of 30wt% with curved tool at 65V creates higher OC. The lowest HAZ area is observed at 50 V and KOH 10 wt% electrolyte concentration with curved tool but higher HAZ area is found when KOH of 30wt% with curved tool is used at 65V. Surface roughness (R_a) is found to be lower at applied voltage of 60V for both electrolytes and tools at 10-15wt% and becomes higher at high voltage with curved tool for both electrolytes. In case of NaOH electrolyte the suitable parametric combination for micro-channelling is found out as applied voltage 55V, 20 wt% NaOH electrolyte concentrations and using KOH as electrolyte the favourable condition is selected as applied voltage 50V, 20 wt% KOH electrolyte concentration. The straight tool shape is more suitable for micro-channel cutting on glass by the developed µ-ECDM system. Although surface roughness is found to be higher while using KOH electrolyte with higher thermal effect, while using NaOH electrolyte better surface quality can be achieved.

During this investigation, it has been observed that machining of micro-channels, proper optimal parametric combination chosen is a very difficult task and for utilized the knowledge of this fundamental investigations in industry field, modelling and optimization is needed during micro-channel cutting on glass by µ-ECDM process.

4.3. INVESTIGATIONS INTO MACHINING CRITERIA THROUGH RESPONSE SURFACE METHODOLOGY (RSM) AND GENETIC ALGORITHAM (GA) BASED APPROACH

4.3.1 SCHEME FOR EXPERIMENTATION

In the current research work three process parameters were considered such as voltage, electrolyte concentration and inter-electrode gap (IEG). In ECDM the inter-electrode gap is referred as the gap between two electrodes i.e. tool-electrode (cathode) and auxiliary electrode (anode) since here the job specimen material is an electrically non-conducting whereas machining gap is considered as the gap between tool-electrode and job specimen material. The machining gap is very short in the range of several microns as compared to the inter-electrode gap, which are several millimetres in this process. The inter-electrode gap plays a vital role in ECDM process. The current flow in the inter-electrode gap changes with the variation of gap resistance, which in turn depends on the length of inter-electrode gap. So the machining rate in ECDM process varies with the change in inter-electrode gap. The inter-electrode gap was set at 30mm, 35mm, and 40mm. The selection of electrolyte is one of the important parameters for this kind of machining process because the concentration of electrolyte influences the chemical reactions. NaOH solution was used as electrolyte for this experiment. The electrolyte concentrations were varied at 15, 22.5 and 30wt%. The flow of electrolyte was not considered because it removed the gas bubbles generated during machining operation, resulting in weak sparking and low material removal.

The other important task was to select the nature of power supply and the voltage range. Here, pulsed DC power supply was selected and experiments were carried out at three different voltage levels *viz* 50 V, 55 V and 60 V. By applying the pulsed DC voltage instead of continuous DC voltage the changes in the electrolyte composition and the temperature rise and also the change of electrical resistivity can be avoided. Again the current efficiency is much more depended on the current density when pulsed voltage is used than the use of continuous voltage. With the continuous DC voltage the efficiency decreases gradually when the current density is reduced whereas with the pulsed voltage the decrease in efficiency is much more rapid. A steep fall in efficiency with decreasing current density depends upon the pulse duration and to somewhat lesser extent on the interval. By using pulsating current extremely high instantaneous current density can be applied in the inter-electrode gap without the need for an elaborated electrolyte pumping system and rigid machine frame. This is

followed by a relaxation time of zero current, which allows for removal of reaction products and heat from the inter-electrode gap. Pulsed DC power supply consists of constant DC and variable components. By suitable choice of the variable component of pulsating current the electrolyte conductivity can be changed and the high instantaneous mass transportation can be attained even at low electrolyte flow rate. Also, MRR with low HAZ was found to be greater for pulsed DC than smooth DC and the tool life also increased in pulse DC. The experiments were conducted by using smooth DC power supply. The ranges of above three process parameters were chosen by the trial and error method.

Rectangular shaped thin sheet with flat faces of length 8mm and thickness 100 μm was used as micro-tool. The length of the μ-channel cut by this tool electrode was almost equal to the length of the tool and the tool length was chosen based on the experimental observations. If the length of tool is more than the present tool length the glass job specimen breaks due to high thermal spalling. Stainless steel was the material for the micro-tool electrode because it has high corrosion resistance and high melting point.

Metal Removal Rate, Overcut, Heat Affected Zone area and machining depth were considered as performance criteria during micro-channel cutting on glass. All the machining criteria have been measured by previous method. Other experimental conditions and the ranges of parameters are exhibited in the Table 4.4.

Table 4.4 Ranges and levels of different machining parameters

	Machining parameters	Ranges/Level
Variable parameters	Applied voltage Electrolyte concentration Inter electrode gap (IEG)	50-60 V/ 50(-1), 55(0), 60(+1) 15-30 wt%/ 15(-1), 22.5(0), 30(+1) 30-40 mm/ 30(-1), 35(0), 40(+1)
Fixed Parameters	Electrolyte Pulse Frequency Duty ratio Feed mechanism	NaOH solution 50 Hz 0.5 Gravity feed

4.3.2 EXPERIMENTAL DESIGN AND RESPONSE SURFACE METHODOLOGY BASED ANALYSIS

Experimentation was conducted based on rotatable face centred design (FCD) of response surface methodology (RSM) using a developed µ-ECDM set-up. In this experimental investigation for micro-machining with ECDM, the upper level of each variable was coded as +1 and the lower level as – 1 for every process parameters in order to design the experiments in an optimized way. Table 4.5 represents the experimental conditions designed based on response surface methodology. The general second order polynomial equation based on response surface method, which correlates various process parameters with different machining criteria, is described as follows:

$$Y_u = b_o + \sum_{i=1}^{n} b_i X_{iu} + \sum_{i=1}^{n} b_{ii} X_{iu}^{\ 2} + \sum_{i \le j} b_{ij} X_{iu} X_{ju} + \in \qquad \text{.....Eq.(4.2)}$$

Where,

where, Y_u = the corresponding response, e.g. MRR, OC, HAZ, R_a

X_{iu} = the coded values of the ith machining parameters for u^{th} experiment, b_o=constant,

ϵ= the error, n = number of machining parameters and b_i, b_{ii}, b_{ij} = second order regression coefficients.

Table 4.5 Experimental parametric combinations

Expt. No.	Process Parameters		
	Applied voltage (V)	Electrolyte con. (wt %)	Inter electrode gap (mm)
1	50	15.0	30
2	60	15.0	30
3	50	30.0	30
4	60	30.0	30
5	50	15.0	40
6	60	15.0	40
7	50	30.0	40
8	60	30.0	40
9	50	22.5	35
10	60	22.5	35
11	55	15.0	35
12	55	30.0	35
13	55	22.5	30
14	55	22.5	40
15	55	22.5	35
16	55	22.5	35
17	55	22.5	35
18	55	22.5	35
19	55	22.5	35
20	55	22.5	35

4.3.3 EXPERIMENTAL RESULTS AND DISCUSSION

Based on the experimental results the second order non-linear models have been established and the influences of various process parameters such as applied voltage (X_1), electrolyte concentration (X_2) and inter-electrode gap (X_3) on different machining criteria *i.e*. material removal rate (MRR), overcut (OC) heat affected zone (HAZ) area and machining depth (MD) have been studied. Design of experiment (DOE) features of MINITAB software was utilized to obtain the second order rotatable face centred design (FCD). Three set of experiments have

been conducted at each parametric combination and the average value of results as shown in Table 4.6 were considered for analyses.

Table 4.6 Experimental results at different parametric combinations

Expt. No.	Experimental Results			
	MRR (mg/hr)	OC (µm)	HAZ (mm^2)	MD (µm)
1	24.46	337.590	0.76125	270.105
2	25.64	275.030	1.10227	299.423
3	24.51	276.916	1.59475	213.346
4	25.41	249.107	2.16547	302.984
5	11.89	109.413	0.76125	274.250
6	22.02	189.611	0.97227	310.324
7	14.62	136.960	1.59475	218.276
8	21.92	295.508	1.96547	307.210
9	20.59	239.736	0.83475	213.130
10	24.34	255.930	1.27251	282.102
11	18.10	187.402	0.83538	337.860
12	19.58	210.014	1.95645	315.120
13	25.03	325.266	1.41353	318.282
14	19.27	244.378	1.13251	322.162
15	22.23	266.180	1.18566	312.211
16	22.23	250.198	0.89153	308.670
17	21.23	256.198	0.93859	310.231
18	22.32	250.190	1.27452	312.243
19	21.23	246.198	1.13400	314.350
20	22.23	256.178	1.13251	312.987

4.3.3.1 Development of Empirical Models Based on RSM

A model has been developed to correlate the interaction and higher-order effects of the previously mentioned µ-ECDM process parameters, utilizing the relevant experimental data as observed during micro-channel cutting operation. The empirical model for MRR of µ-ECDM has been established and expressed as below:

$$Y_u\,(MRR) = -321.4 - 7.07X_1 + 2.246X_2 - 7.52X_3 + 0.0461X_1^2 - 0.04351X_2^2 + 0.0341X_3^2 - 0.01014X_1X_2 + 0.0768X_1X_3 + 0.00919X_2X_3 \quad \text{.....Eq. (4.3)}$$

Also, the mathematical models for OC, HAZ and machining depth of micro-ECDM have been established and expressed in Eqs. (4.4-4.6) respectively.

$$Y_u\,(OC) = 5539 - 52.1X_1 - 4.23X_2 - 213.5X_3 - 0.097X_1^2 - 0.917X_2^2 + 1.382X_3^2 + 0.3770X_1X_2 + 1.646X_1X_3 + 0.7335X_2X_3 \quad \text{.....Eq. (4.4)}$$

$$Y_u\,(HAZ) = -8.18047 + 0.515163X_1 - 0.191005X_2 - 0.245419X_3 - 0.00407266X_1^2 + 0.00427499X_2^2 + 0.00470284X_3^2 + 0.00129800X_1X_2 - 0.00165000X_1X_3 - 0.000233333X_2X_3 \quad \text{…. Eq. (4.5)}$$

$$Y_u\,(MD) = -6478 + 273.08X_1 - 34.71X_2 - 28.09X_3 - 2.5124X_1^2 + 0.2856X_2^2 + 0.3918X_3^2 + 0.3773X_1X_2 + 0.0303X_1X_3 - 0.0196X_2X_3 \quad \text{....Eq. (4.6)}$$

These above mathematical models were used to analyze the effects of various process parameters on different machining criteria and to search out the suitable parametric conditions for the best performances.

4.3.3.2 Adequacy Test for Developed Models

The total corrected sum of squares (SS) in analysis of variance (ANOVA) is used as a measure of overall variability in data. Intuitively, this is reasonable because the sample variance of the Y's, which is a standard measure of variability, could be obtained if 'SS' is divided by appropriate number of degree of freedom (DOF). The total variability in the data as measured by the total corrected sum of squares (SS) is partitioned into the sum of squares due to factors or parameters (SS_{Factor}) (i.e. between factors) and sum of squares due to error (SS_E) (i.e. within factors). Therefore, the analysis of variance provides us with two estimates

of σ^2 – one based on the inherent variability within factors and one based on the variability between factors. If there are no differences in the factor means, these two estimates should be very similar otherwise it is suspected that the observed difference must be caused by differences in the factor means. Then a test of the hypothesis of no difference in factor means can be performed by comparing mean sum of squares (MSS) due to factors or parameters and due to error. The mean sum of squares (MSS) due to factors and due to error are calculated by dividing the sum of squares due to factors and sum of squares due to error by the number of their respective degree of freedom (DOF). Heuristically, mean sum of squares due to error (MSS_E) is an unbiased estimator of σ^2 and also mean sum of squares due to factors (MSS_{Factor}) is an unbiased estimator of σ^2 if there are no differences in the factor means i.e. under the null hypothesis. But if factor means do differ, the expected value of the factor mean squares is greater than σ^2.

In the ANOVA of RSM, the mean sum of the squares of the first order, terms, second order terms, lack of fit and experimental error evaluated by dividing their sum of square with their respective degree of freedom. For the value of F ratio, the mean sum of the squares of lack fit (MSS_L) is divided by the mean sum of squares of experimental error (MSS_E). The calculated F ratio is compared with standard value of F ratio. If the calculated F ratio is less than the corresponding standard value of F ratio for a particular confidence level, then the test will justify the adequacy of the developed mathematical second order model at that confidence level for the chosen parametric consideration and other involved assumptions. Alternatively, the P-value approach is used for decision making.

Therefore, an ANOVA test for P value and F ratio were performed to justify the goodness of fit of the developed mathematical models. Since the calculated values of F ratio for the lack of fit is found to be less than the standard F ratio values (4.06) for (5, 5) DOF for MRR, OC, HAZ and machining depth, it can be ascertained that the second order regression models are adequate and significant at 95% confidence level with 5, 5 degrees of freedom (DOF) to represent the relationship between MRR, OC, HAZ and machining depth with various machining parameters of the micro-ECDM process. Estimated regression coefficients and analysis of variance for MRR, OC, HAZ and machining depth suggest that these models adequately fit the data. The values of R^2 for MRR, OC, HAZ and machining depth are 97.73%, 98.39%, 95.32% and 98.72% respectively indicating the goodness of the models. Also, the values of adj-R^2 for MRR, OC, HAZ and machining depth are very close to R^2 indicating the goodness of the models. Hence, the developed mathematical models, which

link the various machining parameters with MRR, OC, HAZ and machining depth can adequately be represented through the response surface methodology. The analysis of Variance (ANOVA) tests for MRR, OC, HAZ and machining depth are shown in Table 4.7-4.10 respectively.

Table 4.7 Analysis of Variance (ANOVA) test results for MRR

Source	**DOF**	**SS**	**MSS**	**F**	**P**
Regression	9	0.000229	0.000025	47.74	0.000
Linear	3	0.000180	0.000060	112.88	0.000
Square	3	0.000017	0.000006	10.55	0.002
Interaction	3	0.000032	0.000011	19.77	0.000
Lack-of-Fit	5	0.000004	0.000001	2.81	0.041
Pure Error	5	0.000001	0.000000		
Total	19		R^2 for MRR = 98.39%		

Table 4.8 Analysis of Variance (ANOVA) test results for OC

Source	**DOF**	**SS**	**MSS**	**F**	**P**
Regression	9	57050.7	6339.0	67.95	0.000
Linear	3	27009.0	9003.0	96.51	0.000
Square	3	8850.8	2950.3	31.63	0.000
Interaction	3	21190.8	7063.6	75.72	0.000
Lack-of-Fit	5	685.3	137.1	2.77	0.0144
Pure Error	5	247.6	49.5		
Total	19		R^2 for OC = 97.73%,		

Table 4.9 Analysis of Variance (ANOVA) test results for HAZ

Source	**DOF**	**SS**	**MSS**	**F**	**P**
Regression	9	3.15135	0.35015	22.64	0.000
Linear	3	2.75719	0.91906	59.42	0.000
Square	3	0.36098	0.12033	7.78	0.006
Interaction	3	0.03318	0.01106	0.72	0.565
Lack-of-Fit	5	0.04546	0.00909	0.42	0.0501
Pure Error	5	0.10921	0.02184		
Total	19		R^2 for HAZ = 95.32%		

Table 4.10 Analysis of Variance for (ANOVA) test results Machining Depth

Source	**DOF**	**SS**	**MSS**	**F**	**P**
Regression	9	26000.2	2888.9	399.68	0.000
Linear	3	11695.0	3898.3	539.34	0.000
Square	3	12695.1	4231.7	585.46	0.000
Interaction	3	1610.1	536.7	74.25	0.000
Lack-of-Fit	5	51.7	10.3	2.52	0.0167
Pure Error	5	20.5	4.1		
Total	19		R^2 for MD = 98.72%		

4.3.3.3 Analysis of the Parametric Influences Based on Developed Models

The effects of applied voltage, electrolyte concentration and inter-electrode gap on MRR, OC, HAZ and machining depth during micro-channel cutting on glass are shown in Figs. 4.15 -4.19 respectively. These figures were prepared based on the empirical models represented in Eqs. (4.3), (4.4), (4.5) and (4.6). The smooth lines in the figures have been drawn on the basis of above Eqs. Whereas each dotted line represents the experimental results. From the Figs. 4.15 -4.19 it is clear that the trends of dotted lines and smooth lines are almost similar. Therefore, it can be said that experimental results corroborate the developed empirical models outside the ranges already used to develop the models.

From the Fig. 4.15, it is observed that MRR increases as electrolyte concentration and applied voltage are increased keeping the inter-electrode gap fixed at 35mm. Sparking rate is increased if applied voltage is increased because the current density becomes high under higher voltages. The conductivity of electrolyte increases with increase of electrolyte concentration, causing a higher rate of bubbles generation and high intensity of sparking. Energy released due to electrochemical discharges under higher voltages and higher electrolyte concentrations is much more and it causes higher material removal. It is also clear from the Figs. 4.15 (i) and (ii) that MRR increases as electrolyte concentration increases upto 22.5wt%, after that MRR decreases. If electrolyte concentration increases then the solubility of electrolyte decreases and causes lower machining rate in micro-machining operation. Also, the conductivity of NaOH electrolyte solution attains the maximum value near about 22wt% concentration. Fig. 4.15 (ii) reveals that MRR decreases with increase of inter-electrode gap. The inter-electrode gap resistance increases with increment of gap distance between tool and auxiliary electrode. As a result rate of sparking decreases since the current flows at low rate and it reduces the number of nucleation site of bubble generation.

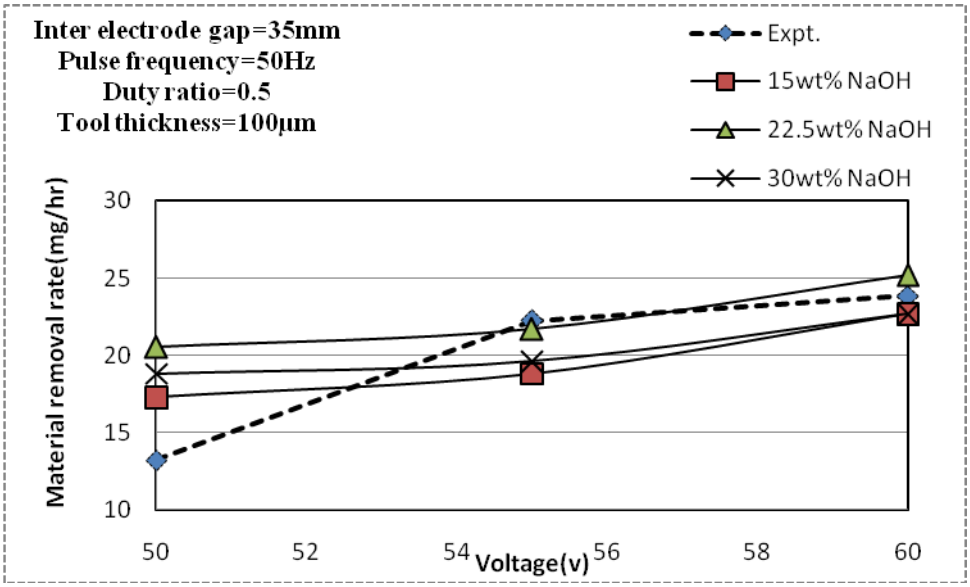

(i) Effect of applied voltage on MRR

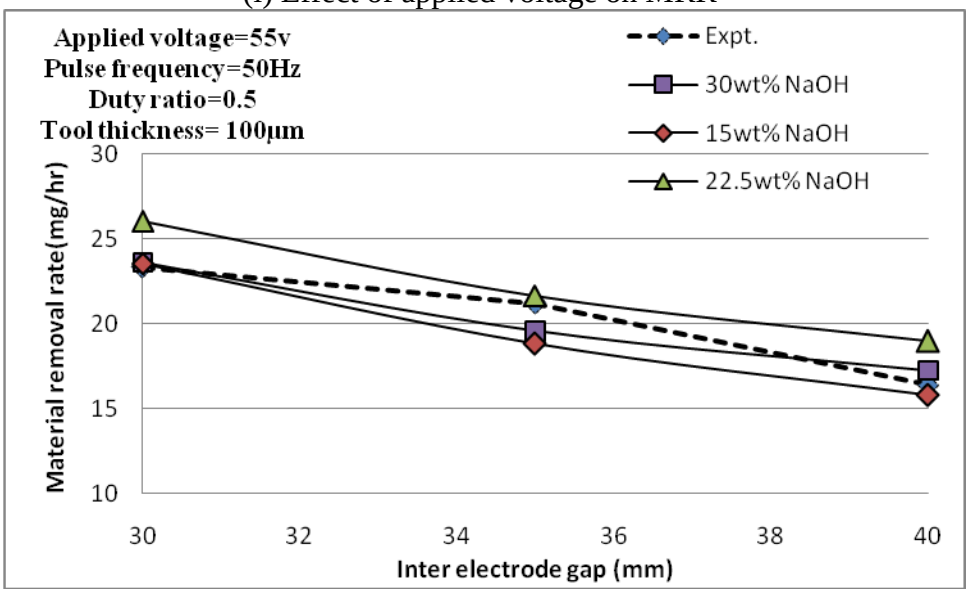

(ii) Effect of inter electrode gap(IEG) on MRR

Fig.4.15 Effects of (i) applied voltage, electrolyte concentration and (ii) IEG on MRR.

The influences of the applied voltage, inter electrode gap and electrolyte concentration on OC during micro-channel cutting operation are observed and exhibited in Fig.4.16. The nature of variation of overcut with varying applied voltage and electrolyte concentration is comparable with that of MRR with varying applied voltage and electrolyte concentration. Fig.4.16 (i) reveals that the overcut during micro-channel cutting operation increases with increase of applied voltage. This is because of the fact that under high applied voltage more number of gas bubbles is generated at the sidewall of tool on account of joule heating of electrolyte due to constriction effect. It may increase the possibility of stray sparking as well as energy released, which causes larger OC due to higher material removal from the sidewall of micro-

channels. From the Figs. 4.16 (i) and (ii), it is also observed that overcut is maximum at 22.5wt% but thereafter if electrolyte concentration is increased further OC is found to be decreased. Therefore, it implies that the micro-channels become wider up to 22.5wt% of electrolyte concentration on account of higher material removal from the sidewall of micro-channels. Up to 22.5wt% concentration the electrolyte conductivity enhances the electrochemical reactions, which are responsible for gas bubble generation. Overcut decreases with the increase of inter-electrode gap since the electrical resistance in the inter-electrode gap changes with the length of gap. So, the rate of sparking is reduced not only at the bottom surface of tool but also at the sidewall of tool.

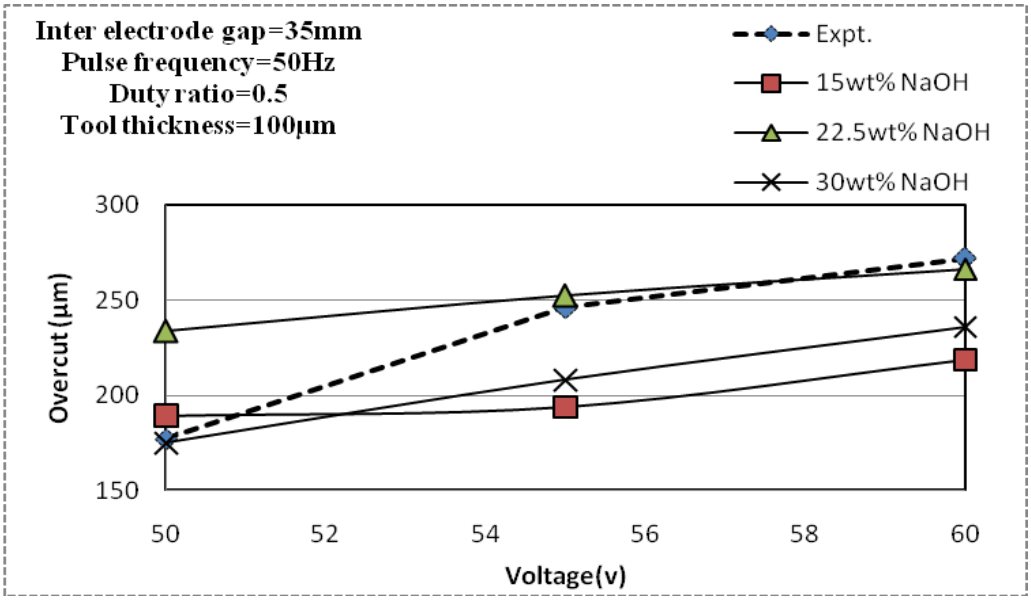

(i) Effect of applied voltage on OC

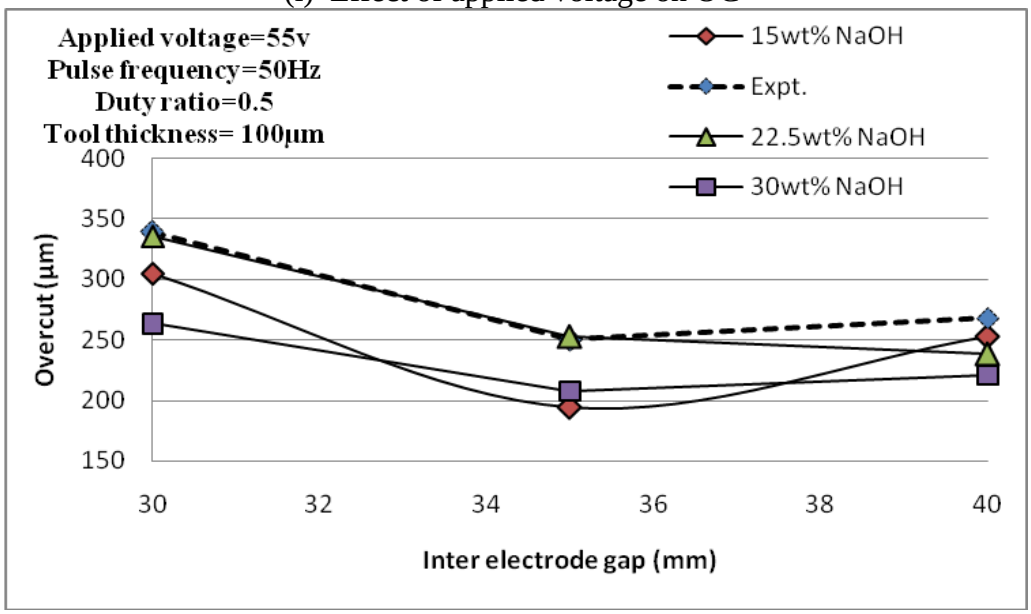

(ii) Effect of inter electrode gap (IEG) on OC

Fig.4.16 Effects of (i) applied voltage, electrolyte concentration and (ii) IEG on OC.

The heat affected zone (HAZ), which is formed around the outer edge of machining zone due to lack of melting of job material and non-removal of molten material is considered as undesirable result because cracks are formed in the zone and degrade the quality of products. The variation of HAZ area with varying applied voltage, electrolyte concentration and inter-electrode gap has been observed and depicted in Fig. 4.17, which shows that HAZ area increases with increase of applied voltage and electrolyte concentration and decrease of inter-electrode gap. Due to increase of applied voltage and electrolyte concentration and decrease of inter-electrode gap high thermal energy is released by electro-spark discharge phenomenon and conducted to the glass job specimen. But this heat is not sufficient to melt or vapourise completely the material up to which heat is conducted. So, the amount of unmolten material is increased and that causes bigger heat affected zone (HAZ) area.

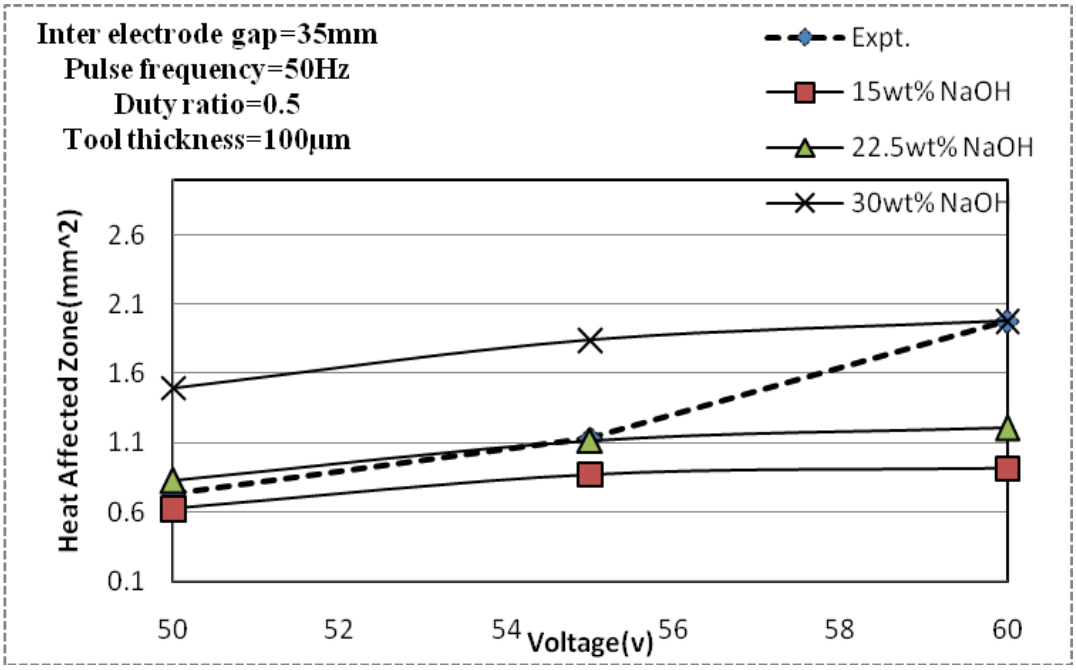

(i) Effect of applied voltage on HAZ

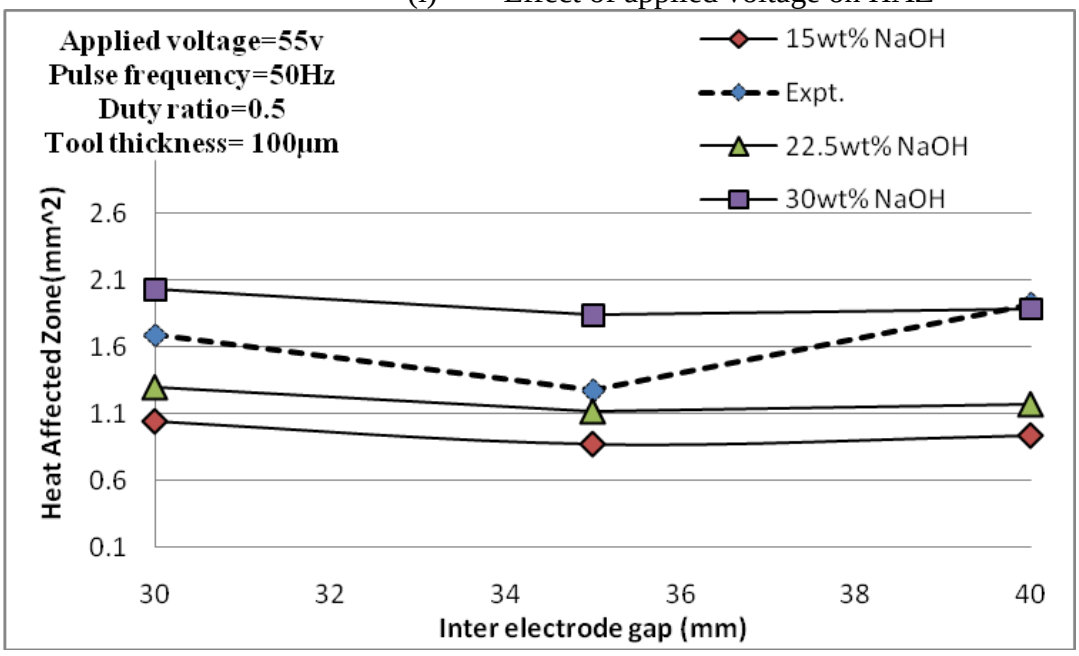

(ii) Effect of inter electrode gap (IEG) on HAZ

Fig.4.17 Effects of (i) applied voltage, electrolyte concentration and (ii) IEG on HAZ.

Fig. 4.18 (i) shows that the machining depth is increased initially with applied voltage up to 55V then decreases with its increment. Figs. 4.18 (i) and (ii) refer that the machining depth is found to decrease with increase of electrolyte concentration. Therefore, it can be said that the machining depth depends upon the amount of electrolyte available at the machining zone during micro-channel cutting operation. The number of hydrogen bubbles and vapour bubbles are found to be more with rise of applied voltage and electrolyte concentration as well but these bubbles restrict the flow of electrolyte at the bottom of tool due to buoyancy force. So,

there is a delay in the formation of insulating gas film layer at tool surroundings and it reduces the rate of sparking and also the spark energy. Hence, material removal rate as well feeding rate are found to be slower and thereby causing a decrease in machining depth with the increase of applied voltage and electrolyte concentration. From the Fig. 4.18 (ii) it is evident that the inter-electrode gap has less effect on machining depth during micro-channel cutting operation on glass. Almost no variation is found in machining depth with change of the inter-electrode gap.

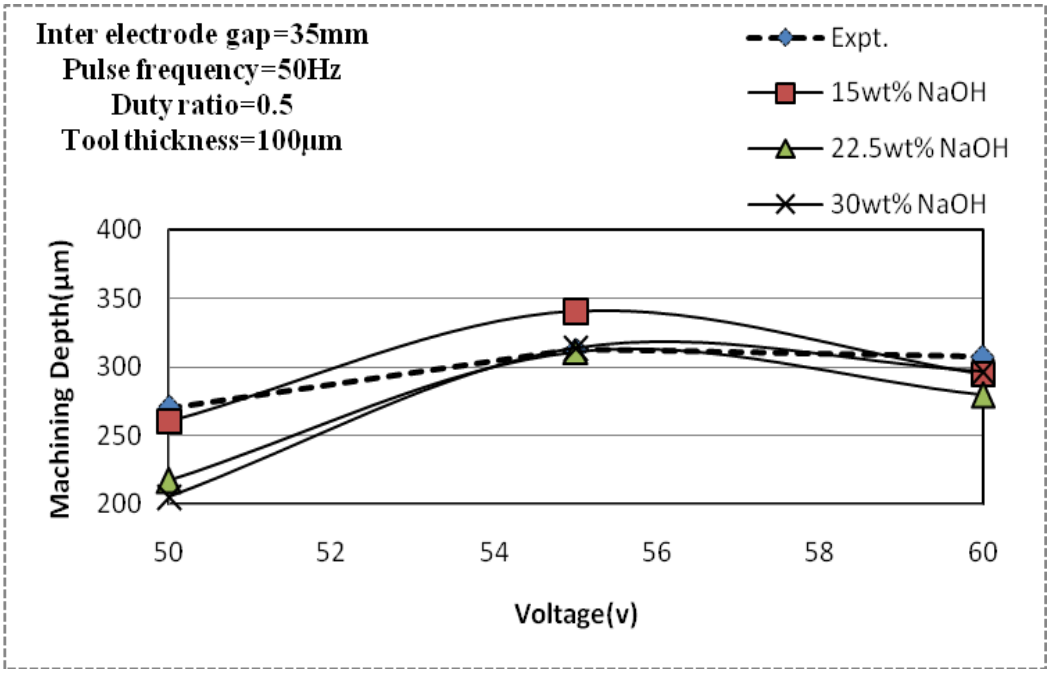

(i) Effect of applied voltage on machining depth (MD)

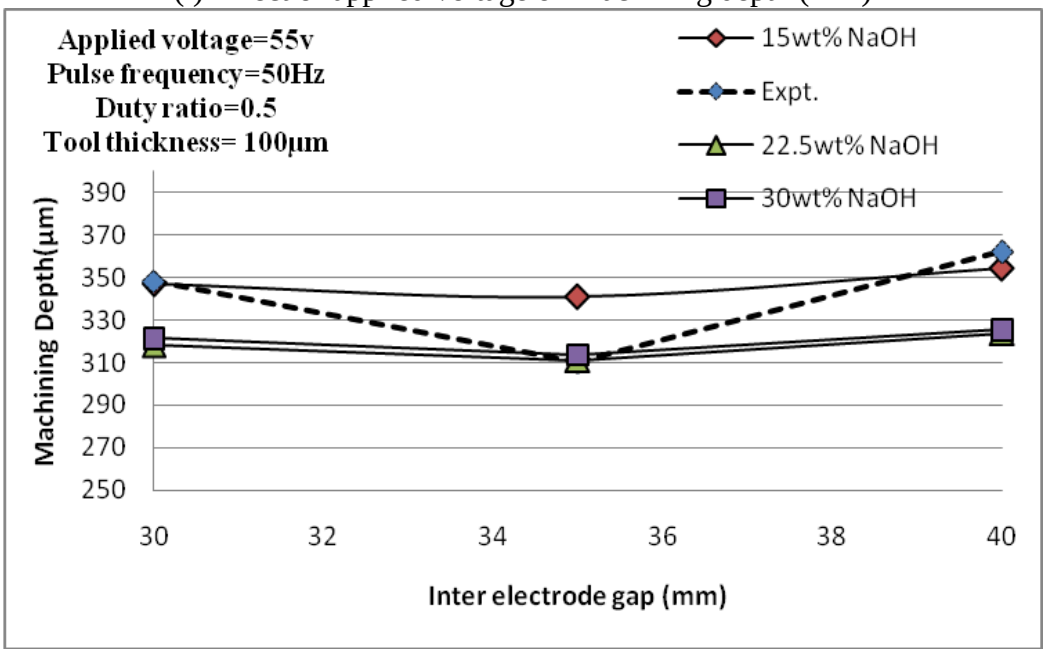

(ii) Effect of inter electrode gap (IEG) on machining depth(MD)

Fig.4.18 Effects of (i) applied voltage, electrolyte concentration and (ii) IEG on machining depth.

4.3.3.4 Determination of Optimal Parametric Condition

In this present investigation the desired objectives are to get maximum MRR & machining depth and minimum OC and HAZ for good micro-channel cutting on glass.

4.3.3.4 1 Single Objective Optimization for Maximum MRR, Minimum OC, Maximum MD and Minimum HAZ

Figs. 4.19 (a) - (d) represent the graphical views of single objective optimization conditions based on desirability function analysis for maximum MRR & machining depth and minimum OC & HAZ. It is found that maximum MRR is found as 27.60 mg/hr at the parametric combination of 60V/21.9697wt%/30mm using RSM. Fig. 4.19 (b) represents the graphical view of single objective optimization condition based on desirability function analysis for minimum OC and the figure reveals that minimum OC is achieved as 106.464 μm at 50V/15wt%/40mm. Fig. 4.19 (c) and (d) inform that the minimum HAZ area of 0.625 mm^2 and maximum machining depth of 355.415 μm are obtained at the parametric combination of 50V/15.7576wt%/35.2525mm and at 55.7576V/15wt%/40mm respectively according to single-objective optimization based on desirability function analysis.

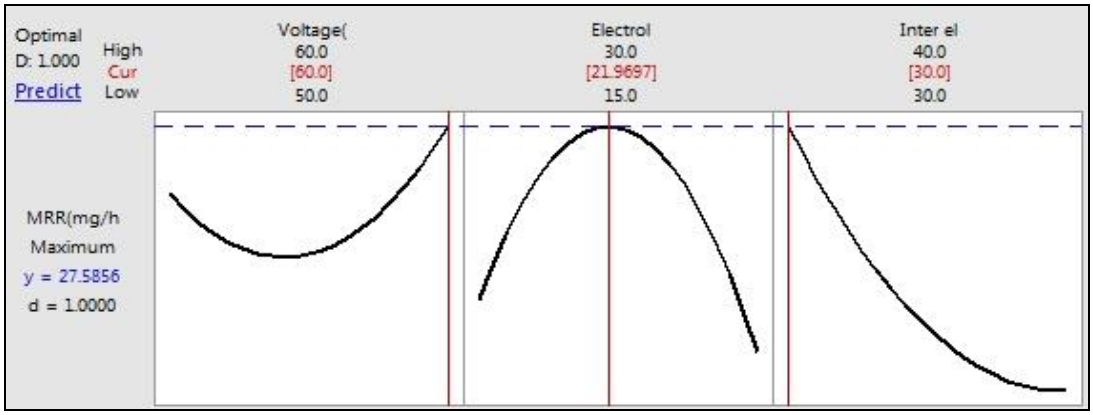

(a) For Maximize MRR

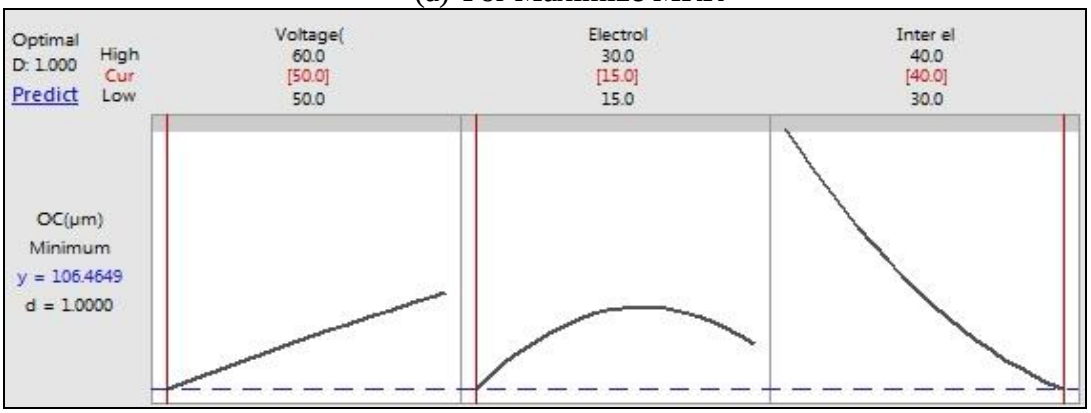

(b) For Minimize OC

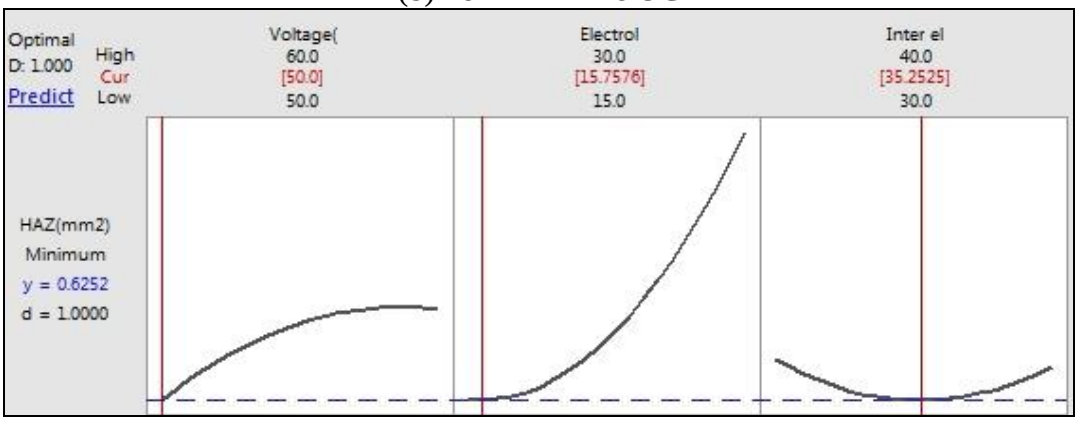

(c) For Minimize HAZ

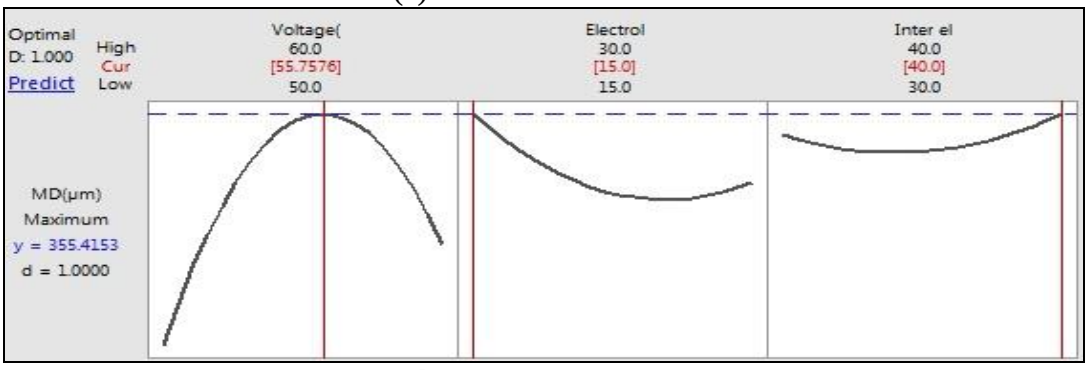

(d) For Maximize MD

Fig.4.19 Single-objective optimizations based on desirability function analysis for maximum (a) MRR & (d) machining depth and (b) minimum OC & (c) HAZ.

According to single-objective optimisation, it is found that maximum MRR is obtained as 27.523 mg/hr at the parametric combination of 60V/22wt%/30mm based on genetic algorithm (GA). The minimum overcut and HAZ area are found as 293.468 µm and 0.625mm^2 at 50V/15wt%/40mm and 50V/15wt%/35mm respectively based on GA. It is found that maximum machining depth is achieved as 355.733 µm at 55V/15wt%/40mm. The single-objective optimisations based on GA are shown in the Fig. 4.20.

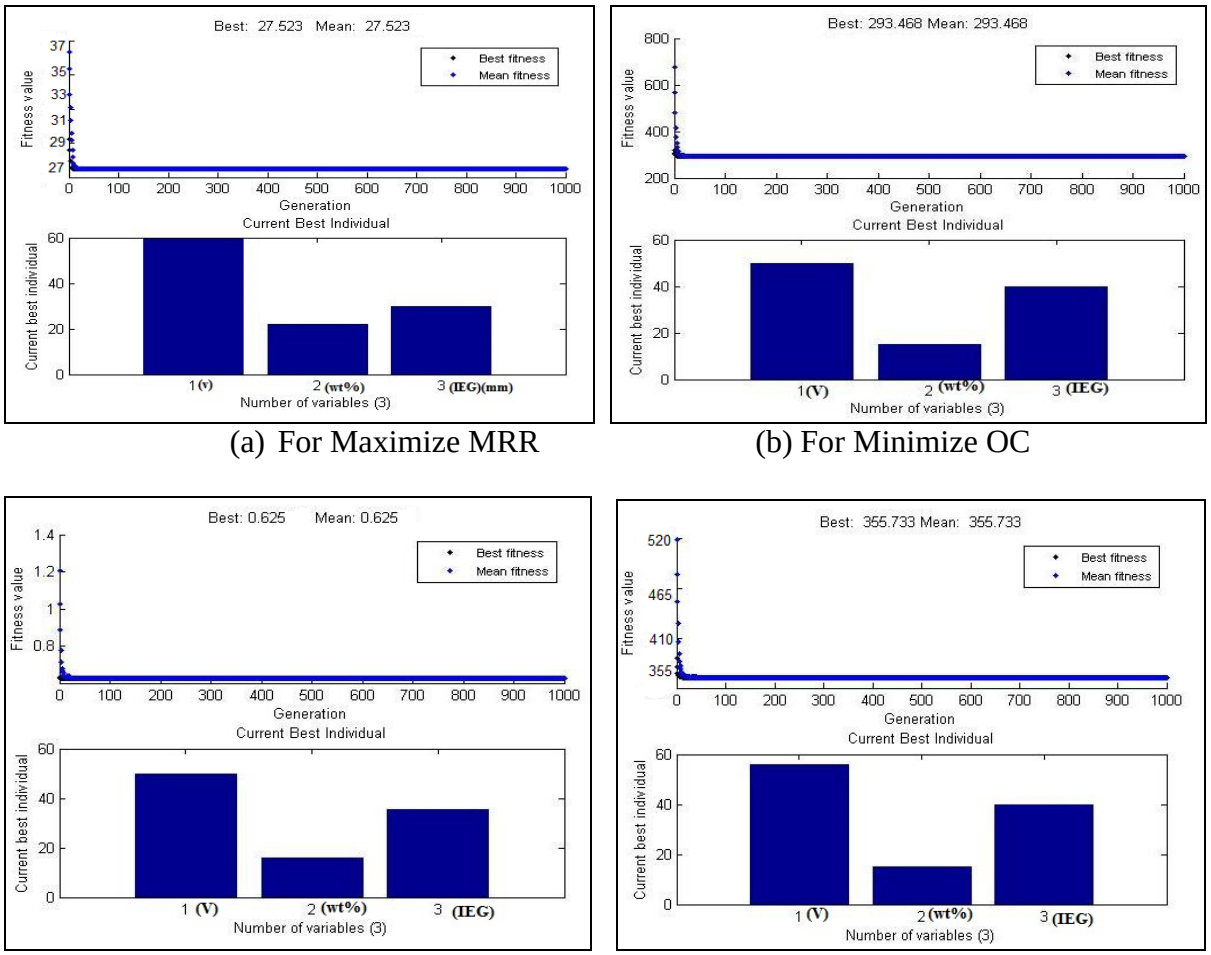

(a) For Maximize MRR (b) For Minimize OC

(c) For Minimize HAZ (d) For Maximize machining depth

Fig.4.20 Single-objective optimizations based on GA for (a) & (d) maximum MRR & machining depth and (c) & (d) minimum OC & HAZ.

4.3.3.4.2 Multi-Objective Optimization for Maximum MRR, Minimum OC, Maximum MD and Minimum HAZ

Fig. 4.21shows the graphical view of multi-objective optimization for maximum MRR & machining depth and minimum OC & HAZ obtained simultaneously at the parametric combination of 57.9798V/15wt%/36.7677mm using desirability function analysis. The graphical view represents that MRR, OC, HAZ and machining depth may be attained as 19.965 mg/hr, 180.640 μm, 0.911mm^2 and 331.352 μm respectively at the above condition.

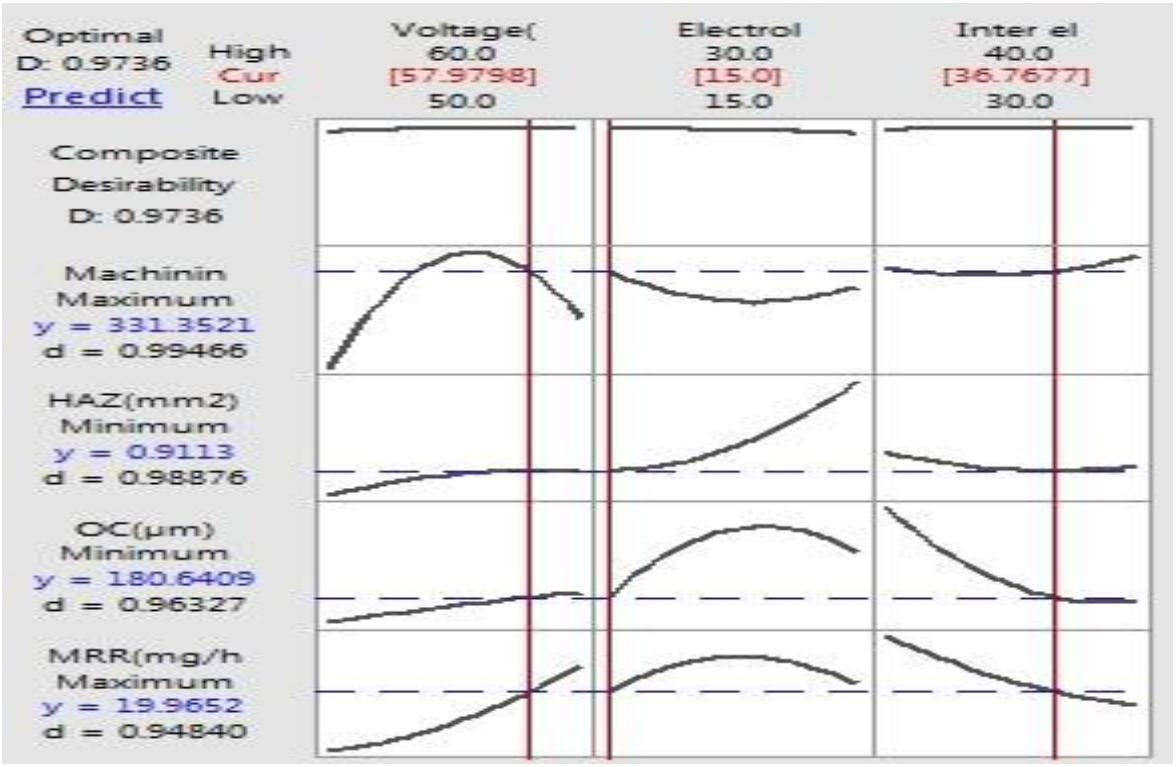

Fig. 4.21 Multi objective optimization based on desirability function analysis for maximum MRR & machining depth and minimum OC & HAZ.

The parametric conditions are obtained using RSM, cannot be set by any instrument due to fractional value of parameter levels. Therefore, there is an urgent need to use an advanced optimised method, which can nullify the above problem. Also, for better accuracy, the evolutionary optimization method has been searched out for better optimized results. There are various evolutionary optimization methods available today for finding out the optimal results of machining criteria. Genetic Algorithms (GAs) has the capability to solve the engineering optimization problems as a form of complex non-linear problem. GA optimizes the responses by more and more iterations until the function comes to stop condition. As a

result better optimized value can be found out and the result represents experimentally validated. So, again optimization was done based on GA for searching out better optimized value. 80 chromosomes were generated randomly for better crossover generation and these were the population of involved regeneration crossover. The iteration was continued till the stop condition for n = 1000 generation was reached during both single-objective optimisation and multi-objective optimization for MRR, OC, HAZ and machining depth. The probability of crossover and the probability of mutation were taken as 0.8 and 0.05 respectively. Eq. (4.7) represents the minimized function of MRR, OC, HAZ and machining depth based on GA.

So, minimize $F(X_1, X_2, X_3) = 1/MRR+1/MD + OC +HAZ$ … Eq. (4.7)

Where, $50 \leq X_1 \leq 60$, $15 \leq X_2 \leq 30$, $30 \leq X_3 \leq 40$, and X_1 = Voltage, X_2= Electrolyte concentration and X_3= Inter electrode gap.

The Fig. 4.22 exhibits the graphical view of multi objective optimization of Pareto front-function for maximum MRR & machining depth and minimum OC and HAZ with parametric combination and machining range. The multi-objective responses are found as MRR of 27.523 mg/hr, OC of 293.485 μm, HAZ area of 0.625 mm^2 and also machining depth of 355.732μm at the parametric combination of 55V/15wt%/40mm using GA and these are experimentally validated. The average overcut, HAZ area and machining depth are measured as 185.585 μm, 0.925 mm^2 and 317.125 μm respectively for micro-channels cut at 55V/15wt%/37mm and 205.565 μm, 0.805 mm^2 and 310.125 μm respectively for micro-channels cut at 55V/15wt%/40mm. Material removal rate is obtained as 19.13 mg/hr and 18.32 mg/hr for above two machining conditions respectively.

After studying both single and multi-optimised predicted results obtained by using response surface methodology (RSM) and genetic algorithm (GA) it is very clear that genetic algorithm would be preferable attaining the maximum material removal rate whereas response surface methodology would give the better result for minimum overcut in μ-ECDM during micro-channelling. But both the techniques will show the same prediction for minimum HAZ area and maximum machining depth. Yet it can be said that genetic algorithm would be the better option for searching out the suitable parametric combination since that levels of parameters for different combinations can be set in the electrochemical discharge micro-machining setup for conducting experiments effortlessly and it will be helpful to the researchers as well as shop floor engineers. Fig. 4.23 (a) & (b) show the optical and scanning electron microscope (SEM) images of μ-channels machined by μ-ECDM on glass at the

parametric conditions of 58V/15wt%/37mm (close to the parametric combinations 57.9799V/15wt%/36.7216mm) and 55V/15wt%/40mm respectively.

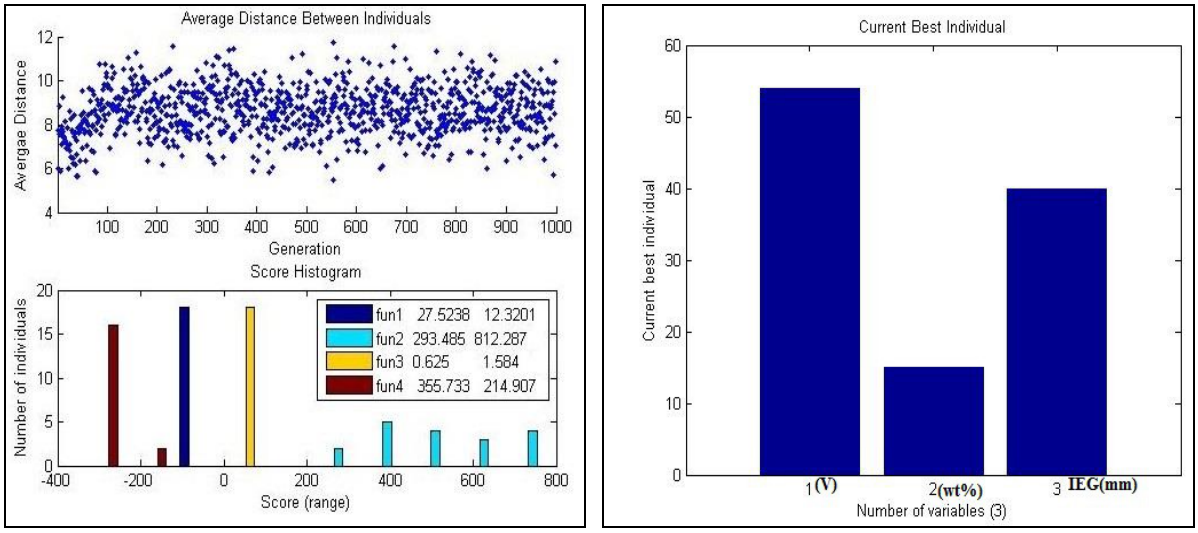

(a) (b)

Fig. 4.22 Multi objective optimization based on GA for maximum MRR & machining depth and minimum OC & HAZ.

Optical image	**SEM image**
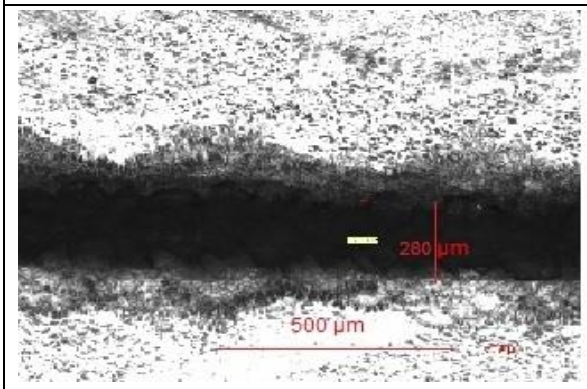	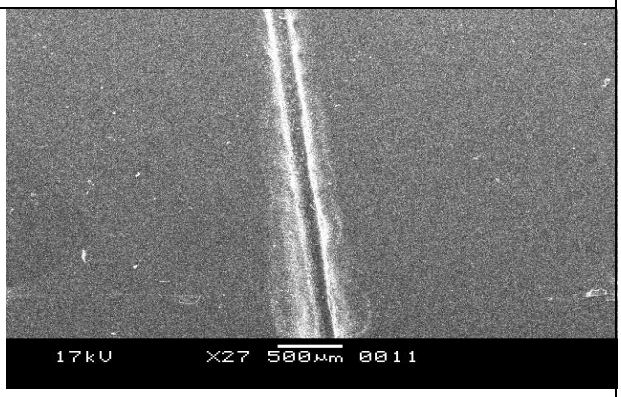
(a) at 58V/15wt%/37mm	

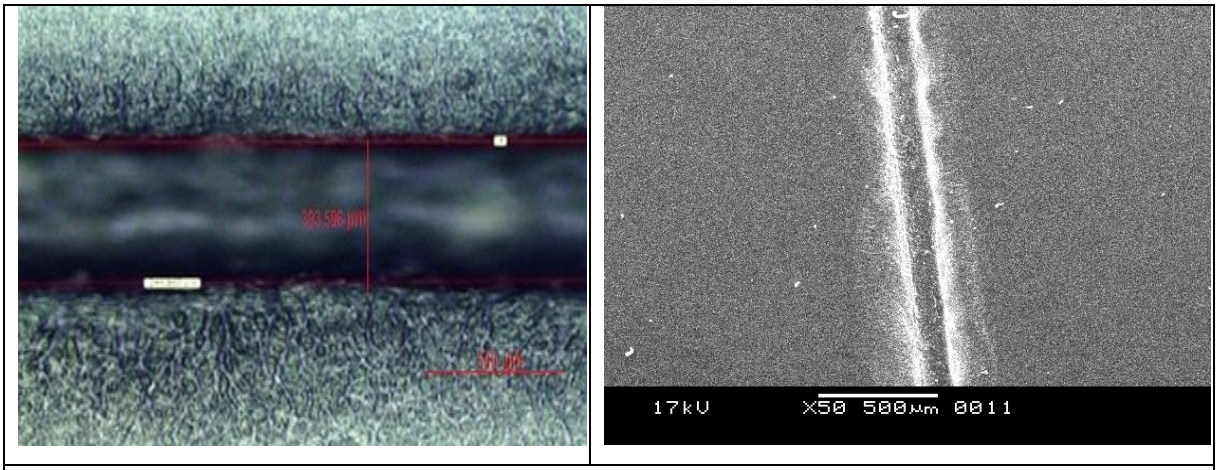

(b) at 55V/15wt%/40mm

Fig. 4.23 Optical and SEM Images of µ-channels on glass (a) at 58V/15wt%/37mm and (b) at 55V/15wt%/40mm.

4.3.3.5 Outcomes of the Present Research Work

From the present experimental investigation it can be concluded that micro-channel can be generated on brittle electrically non-conducting glass successfully in µ-ECDM process by using thin metal sheet as a tool. MRR increases with the increase of applied voltage and electrolyte concentration when NaOH electrolyte is used for micro-channel cutting on glass by ECDM process. Overcut always increases with increase of applied voltage but it increases with increase of concentration up to 22.5wt%. HAZ area increases with increase of applied voltage and electrolyte concentration. It is also clear, applied voltage is the predominant process parameters to influence the formation of HAZ. Machining Depth depends on the availability of electrolyte in the machining zone. Machining depth increases with applied voltage up to 55V and decrease of electrolyte concentration. Inter-electrode gap has comparatively the low effect on machining depth. From the SEM images of micro-channel, which is cutting on glass in micron range at above two machining conditions, it is clear that the heat affected zone formed in machining zone is free of micro-cracks. The optimal parametric combination for multi-objective optimisation for maximum MRR & machining depth and minimum OC & HAZ is searched out as applied voltage of 55V, electrolyte concentration of 15 wt% and inter-electrode gap of 40 mm by using Genetic Algorithms during micro-channel generation on glass.

During this investigation, it has been observed that increasing of machining depth is trouble sometimes and hard to generate the micro-tool, according to the desired shape of micro-channels. Further the length of micro-channel is limited to 8mm, which is undesirable. The generation of complex shape of µ-channels found difficult with straight tool. Therefore there is a need of fabrication a µ-ECDM set up, which can be used to cut the micro-channel with different micro-profiles as per desired shapes and sizes. At the same time fundamental investigation should be carried out in order to analyse the machining performances during cutting micro-channels of different shapes and sizes using cylindrical tool and mixed electrolyte by indigenously designed and developed µ-ECDM set up with template guided spring feed.

CHAPTER-V

5. INVESTIGATIONS INTO µ-ECDM PROCESS FOR MICRO-CHANNEL CUTTING ON GLASS USING TEMPLATE GUIDED CYLINDRICAL TOOL WITH MOTION AND SPRING FEED MECHANISM

Machining of micro-channels of different shapes and increasing of machining depth is a challenging task. Also the effects of process parameters like applied voltage, electrolyte concentration, duty ratio, pulse frequency etc are needed to analyses during basic experimentation of micro-channel cutting on glass by developed µ-ECDM system. Therefore, there is a need of fabricate a µ-ECDM set up, which can be used to cut the micro-channel as well as micro-profile as per desired shapes and sizes with higher machining depth. In this section fundamental investigation has been carried out to analyse the machining performances during cutting of micro-channels of different shapes and sizes using a developed µ-ECDM set up**.**

5.1 EXPERIMENTAL PLANNING

To investigate the influences of process variables like applied voltage, electrolyte concentration, duty ratio, pulse frequency etc on different machining criteria such as material removal rate (MRR), overcut (OC), heat affected zone (HAZ), machining depth (MD) and surface roughness (SR) (R_a) with the help of spring feed mechanism by using a cylindrical shaped stainless steel tool with flat end of diameter 250µm were used for each experiment and the experiments were conducted in a mixture solution of NaOH and KOH at the ratio of 1:0, 0:1, ,1:1, 3:1 and 1:3 ratio. The process parameters *i.e.* voltage, electrolyte concentration, pulse frequency and duty ratio have been varied as 35-55 V; 10-30wt%; 200-1000 Hz and 45-65% respectively. Other parameters such as inter-electrode gap and length of tool have been kept fixed as 40mm and 10mm respectively. Silica glass was chosen as job specimen material to cut µ-channels. During experimentations one parameter has been varied while other process parameters were fixed at low levels and a new identical micro-tool was always used for each experiment. The machining conditions for cutting micro-channel on glass have been shown in Table 5.1.

Experimental procedures for performing the experiments are done as per the procedure of experiments discus in chapter-4. In this research work the feed motion is applied to the job specimen by means of spring feeding mechanism with template guided system in which the

job specimen holding unit is placed on four springs in upward direction so that the job specimen can be in touch with the micro-tool and the voltage and other parameters such as pulse frequency, duty ratio are applied with the help of a digital oscilloscope. The readings of these parameters were recorded. For direct polarity tool is connected to negative terminal and auxiliary electrode is connected to positive terminal of the DC power supply system and for reverse polarity this connection was reversed. MRR is measured as per the Eq.(4.1) and **Overcut=**Width of Cut of channel – Diameter of the Tool used to cut the channel. For measurement of overcut, surface roughness, machining depth and heat affected zone, same procedure is maintain which is discussed in previous chapter.

Tool electrode wear rate (TEWR) = {(Wt.of tool before machining – Wt. of tool after machining)/Machining time} …….Eq.(5.1).

Table 5.1 Machining conditions during micro-channel cutting on glass

Expt. No	Voltage (V)	Elect Conc. (wt %)	Pulse Freq. (Hz)	Duty Ratio (%)
1	35	10	200	45
2	35	10	200	50
3	35	10	200	55
4	35	10	200	60
5	35	10	200	65
6	35	10	400	45
7	35	10	600	45
8	35	10	800	45
9	35	10	1000	45
10	40	10	200	45
11	45	10	200	45
12	50	10	200	45
13	55	10	200	45
14	35	15	200	45
15	35	20	200	45
16	35	25	200	45
17	35	30	200	45

5.2 EXPERIMENTAL RESULTS AND DISCUSSION

The process parameters were applied voltage, electrolyte concentration, pulse frequency and duty ratio and machining characteristics were material removal rate, overcut, heat affected zone, surface roughness and machining depth. Each experiment was conducted three times at every machining parametric combination. The average values of the experimental results thus obtained were used and plotted in graphs to analyse the influences of the various process parameters on various machining characteristics. Table 5.2 shows the average values of material removal rate during the experimentations using different mixed electrolytes. Other machining characteristics like OC, HAZ, surface roughness and MD are shown in Tables 5.3-5.6. Table 5.7 and 5.8 show the machining criteria obtained during micro-channel cutting by using different proportion of mixed electrolytes at direct as well as reverse polarities respectively at same parametric conditions.

Table 5.2 Material removal rate (MRR) (mg/hr) obtained during micro-channel cutting on glass using different electrolytes

Expt. No	**(MRR) (mg/hr)** (NaOH:KOH :: 1:0)	**(MRR) (mg/hr)** (NaOH:KOH ::3:1)	**(MRR) (mg/hr)** (NaOH:KOH ::1:1)	**(MRR) (mg/hr)** (NaOH:KOH ::1:3)	**(MRR) (mg/hr)** (NaOH:KOH ::0:1)
1	13.27	16.30	12.820	18.31	15.35
2	15.46	28.40	14.360	30.41	13.67
3	20.26	30.47	21.870	36.37	22.36
4	20.87	34.32	22.285	38.30	24.30
5	24.07	37.21	25.090	40.21	26.31
6	12.36	13.20	10.850	12.42	9.25
7	11.57	12.87	10.564	12.86	8.36
8	9.02	12.30	10.75	12.89	9.12
9	8.46	13.42	9.72	13.41	8.62
10	27.16	33.12	29.2	29.32	31.24
11	30.87	38.70	31.855	33.86	32.30
12	32.27	40.41	32.30	38.87	32.31
13	54.35	62.12	55.70	64.21	56.87
14	36.97	39.10	36.10	39.10	35.10
15	72.70	78.10	71.94	79.21	73.20
16	76.51	82.50	76.20	88.32	75.87
17	108.67	126.25	113.260	127.20	118.57

Table 5.3 Overcut (OC) (μm) obtained during micro-channel cutting on glass using different electrolytes

Expt. No	**(OC) (μm)**	**(OC) (μm)**	**(OC) (μm)**	**(OC) (μm)**	**(OC) (μm)**

	(NaOH:KOH :: 1:0)	(NaOH:KOH ::3:1)	(NaOH:KOH ::1:1)	(NaOH:KOH ::1:3)	(NaOH:KOH ::0:1)
1	198.826	132.10	182.21	142.10	164.681
2	245.842	190.21	298.1	196.12	248.8
3	286.356	178.1	290.12	198.1	296.21
4	274.878	210.25	291.02	232.1	294.22
5	348.826	132.1	182.21	142.1	164.681
6	152.78	108.1	143.35	120.1	134.23
7	105.241	76.25	85.1	95.34	99.25
8	100.299	88.1	97.2	109.1	118.3
9	106.617	132.1	119.2	137.25	148.71
10	165.009	162.10	172.10	181.21	169.12
11	259.524	251.21	262.10	267.25	268.20
12	264.494	258.30	267.20	270.10	269.70
13	457.347	422.12	471.20	471.25	472.38
14	199.431	198.21	190.21	212.10	206.243
15	309.583	288.30	282.30	228.15	219.38
16	342.867	347.10	345.21	310.10	198.536
17	373.210	361.10	368.10	369.25	341.515

Table 5.4 Heat affected zone (HAZ)$(\mu m)^2 x10^3$ measured during micro-channel cutting on glass using different electrolytes

Expt. No	**(HAZ) $(\mu m)^2 x10^3$**	**(HAZ) $(\mu m)^2 x10^3$**	**(HAZ) $(\mu m)^2 x10^3$**	**(HAZ) $(\mu m)^2 x10^3$**	**(HAZ) $(\mu m)^2 x10^3$**

	(NaOH:KOH :: 1:0)	(NaOH:KOH ::3:1)	(NaOH:KOH ::1:1)	(NaOH:KOH ::1:3)	(NaOH:KOH ::0:1)
1	307.323	317.1	310.28	325.1	288.734
2	320.461	368.21	310.17	358.25	348.42
3	282.1	274.15	262.1	240.16	272.1
4	284.316	290.21	300.21	251.12	321.1
5	297.323	317.1	310.28	325.1	288.734
6	315.679	332.18	348.1	337.1	327.25
7	254.657	262.21	278.21	238.21	258.1
8	218.508	285.1	279.1	258.1	285.21
9	234.514	350.25	340.25	308.12	389.32
10	322.858	307.1	370.1	437.2	468.342
11	452.955	402.21	425.25	533.212	571.1
12	714.806	620.1	705.1	728.12	798.25
13	1027.323	317.1	310.28	325.1	288.734
14	410.221	462.1	450.25	482.21	390.68
15	308.92	441.32	402.1	413.21	411.79
16	406.739	410.21	412.1	418.24	460.81
17	694.771	732.25	867.2	900.25	952.512

Table 5.5 Surface Roughness (R_a) (µm) measured during micro-channel cutting on glass using different electrolytes

Expt. No	**Surface Roughness**	**Surface Roughness**	**Surface Roughness**	**Surface Roughness**	**Surface Roughness**

	(R_a) (µm) (NaOH:KOH :: 1:0)	**(R_a)** (µm) (NaOH:KOH ::3:1)	**(R_a)** (µm) (NaOH:KOH ::1:1)	**(R_a)** (µm) (NaOH:KOH: :1:3)	**(R_a)** (µm) (NaOH:KOH ::0:1)
1	1.098	0.074	1.02	1.95	1.52
2	1.313	1.08	1.342	1.97	1.656
3	1.72	1.68	1.37	2.05	1.86
4	2.125	2.14	1.95	2.33	2.024
5	3.013	2.88	3.14	3.26	3.167
6	1.067	0.079	1.016	2.12	1.506
7	1.038	0.082	1.018	2.129	1.49
8	1.865	1.032	1.98	2.189	2.24
9	1.994	1.452	2.67	2.709	2.67
10	2.313	1.23	2.12	1.98	2.456
11	2.82	1.89	2.37	2.69	2.76
12	2.465	1.42	1.95	2.129	2.044
13	3.194	2.12	3.04	2.89	3.367
14	1.534	1.45	1.494	1.99	1.578
15	1.882	1.75	1.864	2.023	1.879
16	1.494	1.52	1.565	1.74	1.484
17	2.465	2.57	2.62	2.64	2.887

Table 5.6 Machining Depth (µm) measured during micro-channel cutting on glass using different electrolytes

Expt. No	**Machining Depth**	**Machining Depth**	**Machining Depth**	**Machining Depth**	**Machining Depth**

	(µm) (NaOH:KOH :: 1:0)	**(µm)** (NaOH:KOH ::3:1)	**(µm)** (NaOH:KOH ::1:1)	**(µm)** (NaOH:KOH ::1:3)	**(µm)** (NaOH:KOH ::0:1)
1	296.010	318.002	288.010	298.043	310.132
2	382.054	370.143	377.021	420.001	382.098
3	507.005	496.003	520.014	499.121	507.112
4	580.110	538.001	605.210	588.003	580.007
5	535.004	518.121	575.034	598.164	535.002
6	278.190	280.324	267.056	276.087	292.231
7	289.021	270.009	254.113	268.017	272.111
8	253.007	265.032	246.00	254.006	258.089
9	216.012	242.004	208.027	221.002	232.032
10	378.00	420.006	356.129	387.034	390.345
11	432.026	489.211	379.165	422.012	443.123
12	590.008	598.054	495.003	567.098	588.025
13	572.021	578.068	521.165	553.068	565.231
14	377.008	365.002	307.116	377.320	372.008
15	432.006	410.012	402.176	428.004	422.097
16	573.123	528.003	528.213	567.267	568.010
17	598.0032	575.005	548.009	597.005	582.031

Table 5.7 Machining characteristics of direct polarity during micro-channel cutting on glass using different electrolyte

Type of	**Experimental Results**

electrolyte mixture	Machining Performances with direct polarity					
	MRR (mg/hr)	**OC (µm)**	**HAZ $(\mu m)^2 x10^3$**	**MD (µm)**	**R_a (µm)**	**TEWR (mg/min)**
NaOH:KOH::1:0	13.27	198.826	327.323	296.001	1.098	0.0098
NaOH:KOH::3:1	16.3	132.1	307.1	318.121	0.074	0.0083
NaOH:KOH::1:1	12.82	182.21	310.28	288.026	1.02	0.00682
NaOH:KOH::1:3	18.31	142.1	300.1	298.190	1.95	0.00536
NaOH:KOH::0:1	15.35	164.681	388.734	310.043	1.52	0.00991

Table 5.8 Machining characteristics of reversed polarity during micro-channel cutting on glass using different electrolyte

Type of electrolyte mixture	Experimental Results					
	Machining Performances with reversed polarity					
	MRR (mg/hr)	**OC (μm)**	**HAZ $(\mu m)^2 x10^3$**	**MD (μm)**	**R_a (μm)**	**TEWR (mg/min)**
NaOH:KOH::1:0	13.27	198.826	327.323	296.21	1.098	0.0098
NaOH:KOH::3:1	16.3	132.1	307.1	318.091	0.074	0.0083
NaOH:KOH::1:1	12.82	182.21	310.28	288.154	1.02	0.00682
NaOH:KOH::1:3	18.31	142.1	300.1	298.102	1.95	0.00536
NaOH:KOH::0:1	15.35	164.681	388.734	310.009	1.52	0.00991

5.2.1 Influences of Process Parameters on Material Removal Rate (MRR)

The influences of applied voltage, electrolyte concentration, pulse frequency and duty ratio on material removal rate for fixed inter-electrode gap (40mm) when micro-channel is cut on glass using NaOH electrolyte are shown in Figs. 5.1 (a) - (d) respectively. These figures show

that material removal rate increases with the increase of applied voltage, NaOH electrolyte concentration and duty ratio but decreases with increase of pulse frequency. Figs. 5.1 (a) and (b) reveal that MRR is high for 55 V and 30 wt% electrolyte concentration. Due to electrolysis the major ions like Na^+, OH^- are generated and these increase the dipole moment into the electrolysis cell and cause the formation of higher rate of hydrogen bubbles with increase of electrolyte concentration. Also MRR increases with increase of duration of ON-time, which increases with duty factor. As the discharge duration increases, the removal rate increases since the temperature of glass channel rises. MRR falls down with increase of pulse frequency because the duration of the discharge increases as the frequency decreases, even though the total time that voltage is applied stays the same. Fig. 5.1 (d) shows that material removal rate is almost same for the pulse frequency of 800 and 1000 Hz. At 200 Hz frequency and 65% duty ratio MRR is found higher as shown in Figs. 5.1 (c) and (d) respectively. The current intensity is proportional to pulse on-time and duty ratio of applied voltage, but pulse frequency is reciprocal of duty ratio, so as due to increase of pulse frequency rate of discharge decreases, MRR is decreased.

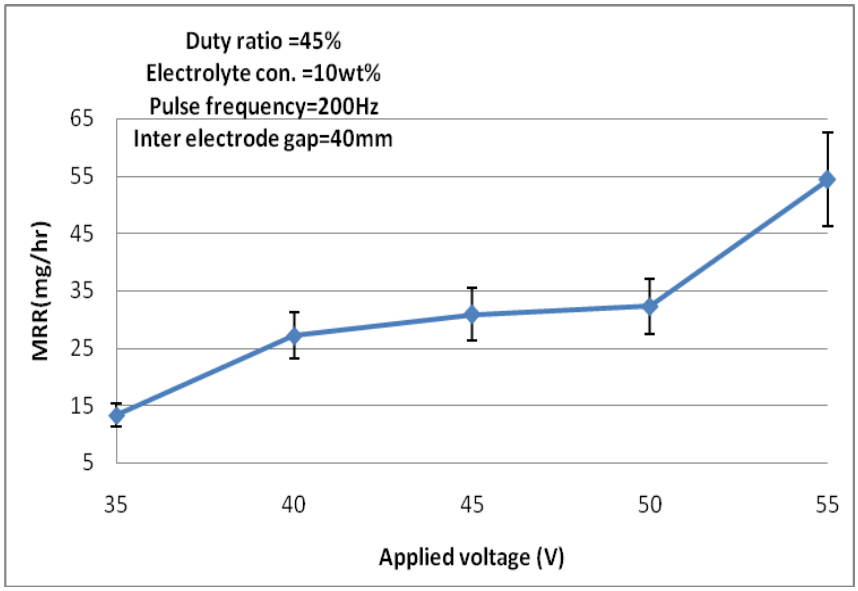

(a) Effect of applied voltage on MRR

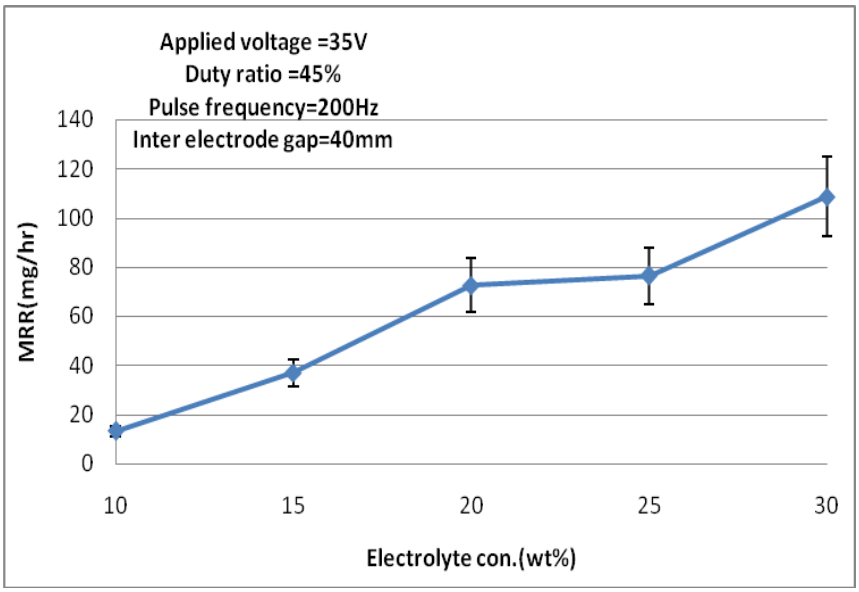

(b) Effect of electrolyte concentration on MRR

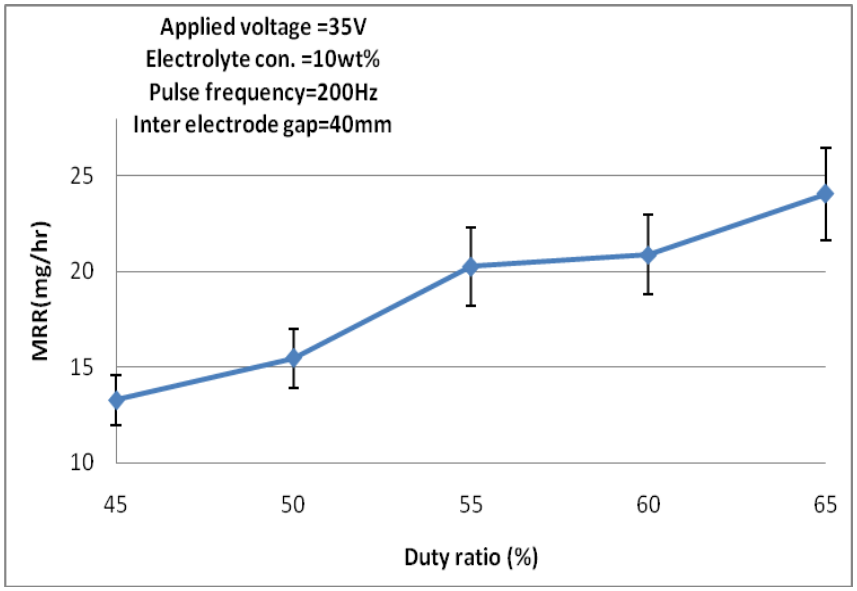

(c) Effect of duty ratio on MRR

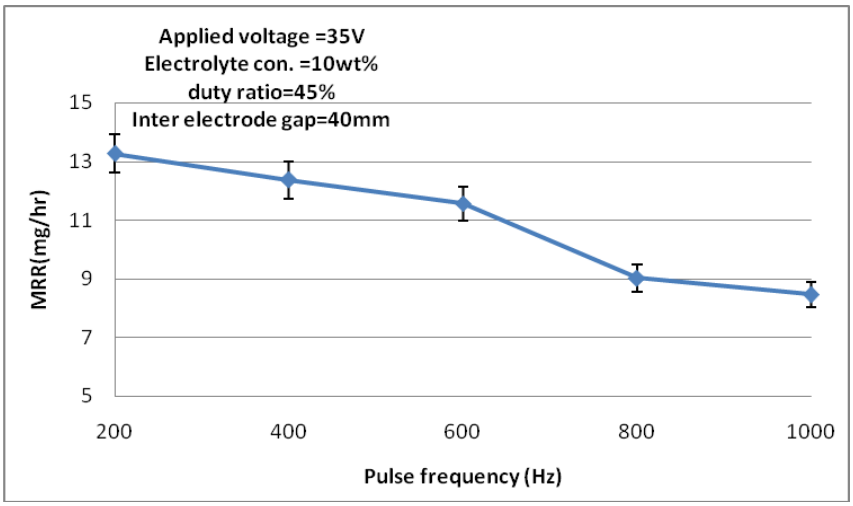

(d) Effect of pulse frequency on MRR

Figs. 5.1 (a) - (d) Effects of (a) applied voltage, (b) electrolyte concentration, (c) duty ratio and (d) pulse frequency on MRR

5.2.2 Influences of Process Parameters on Overcut (OC)

Overcut is an undesirable characteristic in case of micro-machining operations. In every machining operation, the desirable condition is the least overcut or zero overcut if possible. In the present work, overcut has also been observed with varying the input process parameters. Figs. 5.2 (a) and (b) exhibit the influences of applied voltage and electrolyte concentration respectively on overcut using only NaOH as electrolyte. Generally, rate of sparking increases with the increase of both applied voltage and electrolyte concentration and consequently it increases not only MRR but also width of cut (WOC) due to side wall sparking from the tool

electrode and thereby increases overcut. Figs. 5.2 (c) and (d) represent the variation of overcut with pulse frequency and duty ratio respectively using NaOH as electrolyte. Overcut increases with increase of duty ratio and decreases with increase of pulse frequency. One possible reason is that the discharge gets more powerful because the current density increases with increase of duty ratio and causes violent sparking.

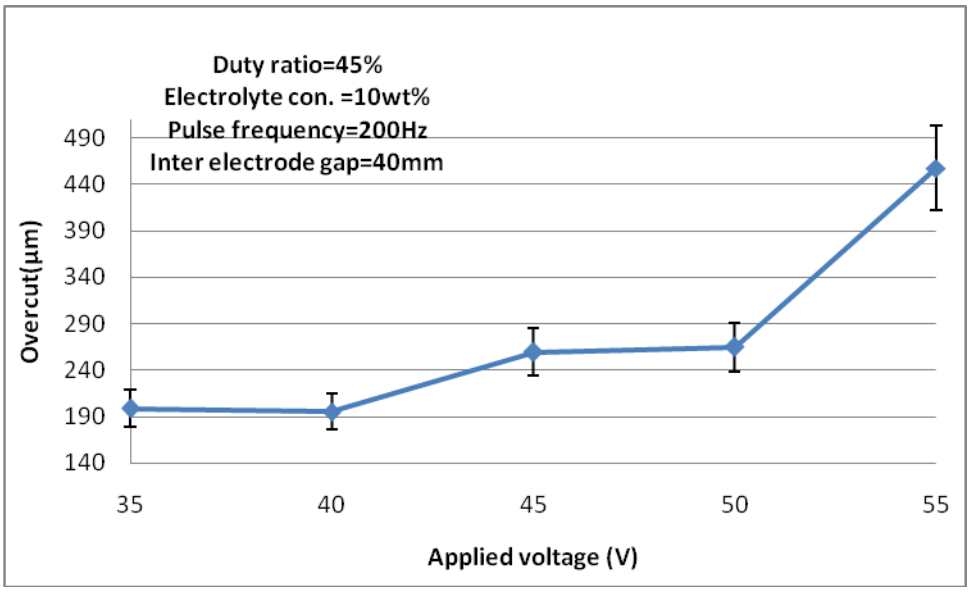

(a) Effect of applied voltage on OC

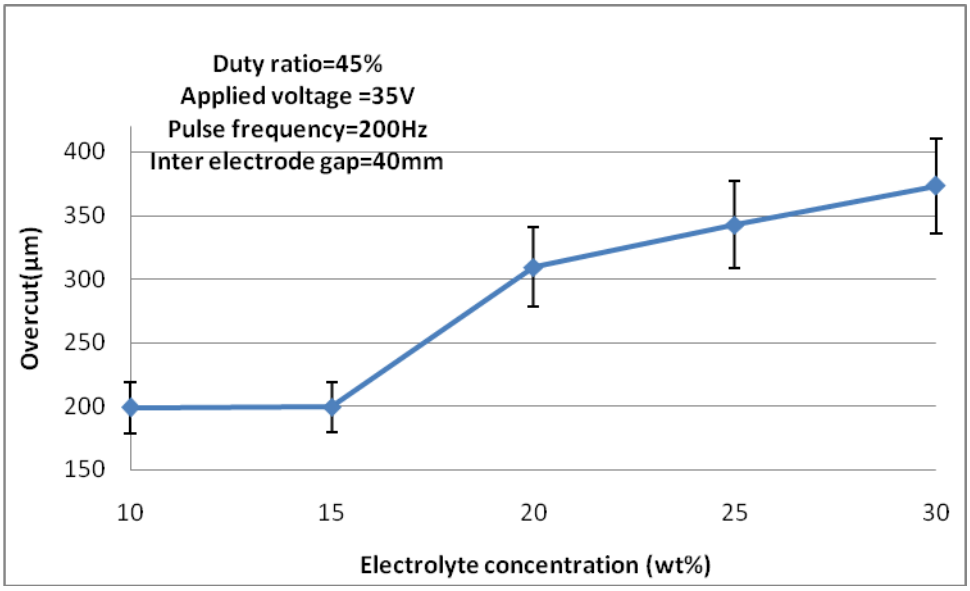

(b) Effect of electrolyte concentration on OC

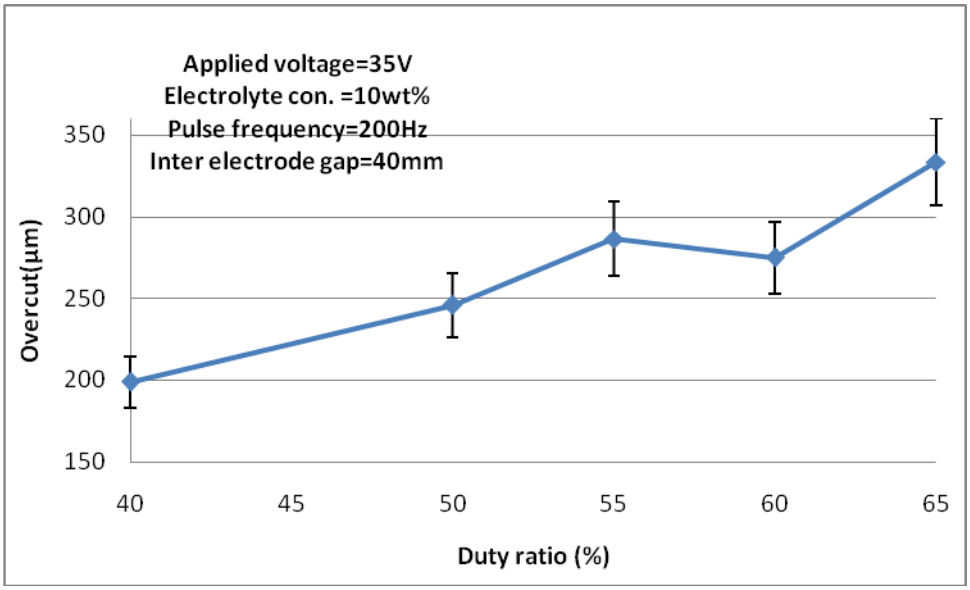

(c) Effect of duty ratio on OC

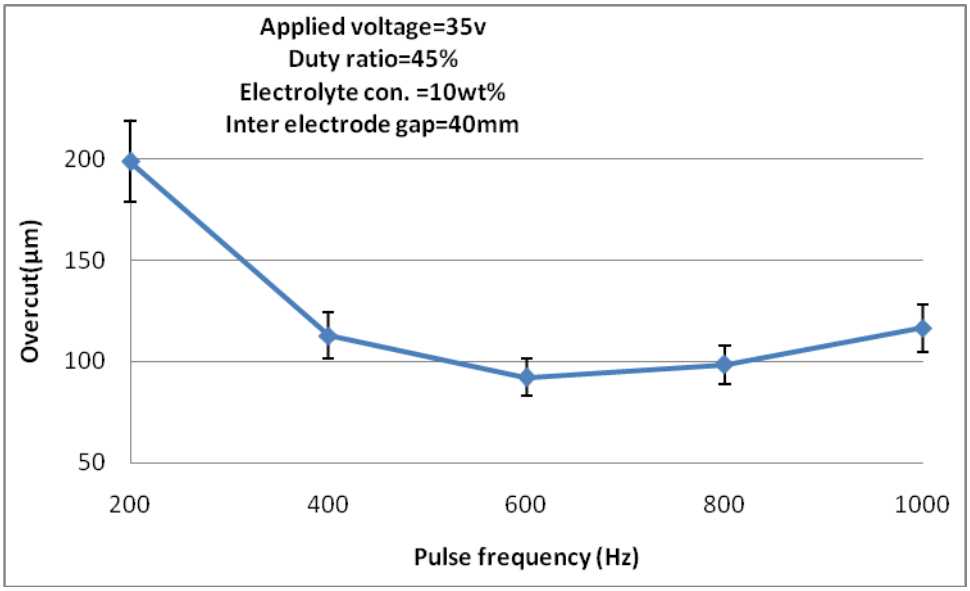

(d) Effect of pulse frequency on OC

Figs. 5.2 (a) - (d) Effects of (a) applied voltage, (b) electrolyte concentration, (c) duty ratio and (d) pulse frequency on OC

5.2.3 Influences of Process Parameters on Heat Affected Zone (HAZ) Area

Figs. 5.3 (a) and (b) depict the influences of applied voltage and electrolyte concentration on heat affected zone (HAZ) area. In ECDM process huge heat is generated during the machining of a glass material. A portion of this heat is conducted to the job specimen and is responsible for the development of HAZ around the machined profile on the job specimen. It is observed from Figs. 5.3 (a) and (b) that HAZ area almost gradually increases with increase of applied voltage and electrolyte concentration and it becomes higher at 55 V and 30 wt%

electrolyte concentration. Accordingly Joule's law $H=I^2Rt/J$, where; H=amount of heat, I=current, R=internal resistance, t=time, J=Joule constant, so as it is propounded that during cutting operation by ECDM process, applied voltage is proportional to current flow, which is participated to Joule's law and produced large number of vapour bubbles. So the vigorous sparking is discharged from the tool surface and this causes the increase of heat affected zone.

Variations of HAZ area with pulse frequency and duty ratio are shown in Figs. 5.3 (c) and (d) respectively. It is obvious from the figures that initially HAZ area increases and then it decreases with frequency whereas it increases with duty ratio after 55% of duty ratio. As a result HAZ grows larger. The experimental results reveal that HAZ area can be reduced by decreasing the duty ratio and increasing the pulse frequency of the applied voltage, although the amount of time required to cut micro-channel will increase because MRR decreases. Fig. 5.4 shows HAZ area with width of cut of micro-channels cutting on glass at different machining conditions.

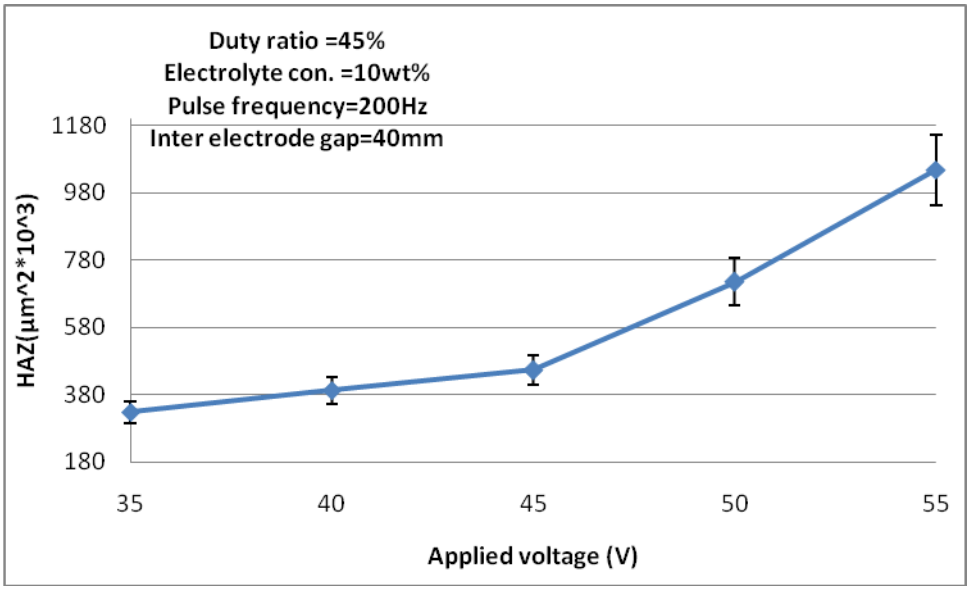

(a) Effect of applied voltage on HAZ

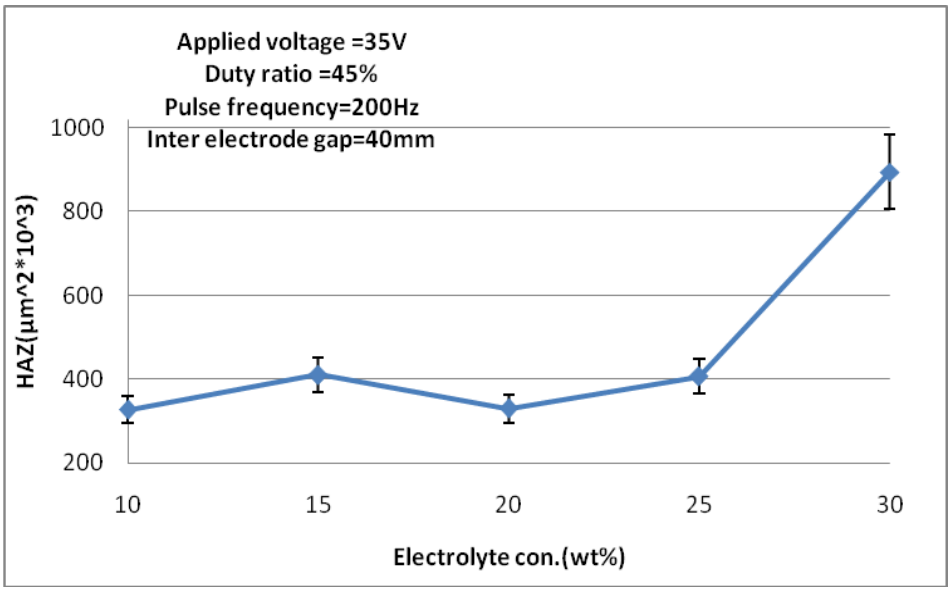

(b) Effect of electrolyte concentration on HAZ

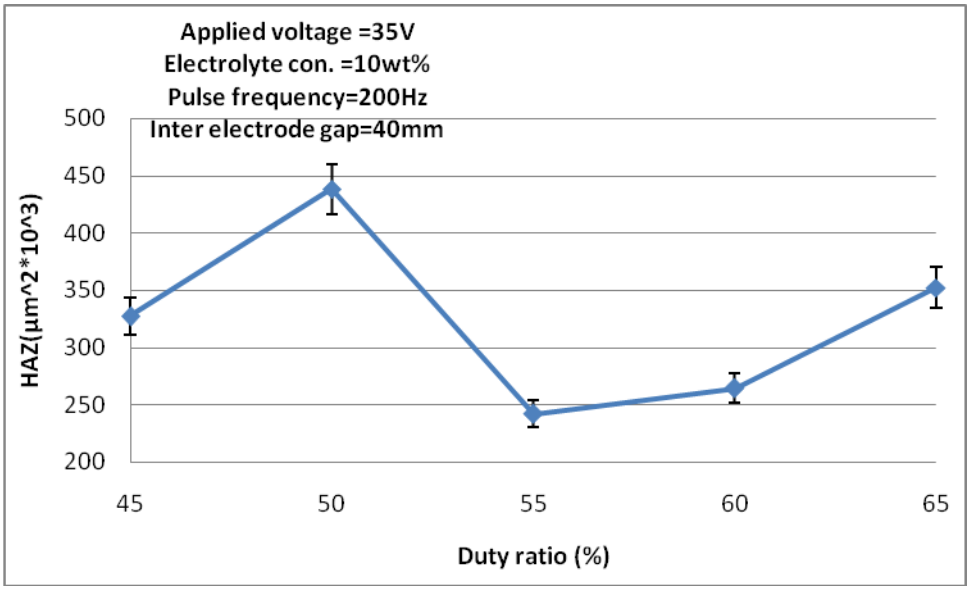

(c) Effect of duty ratio on HAZ

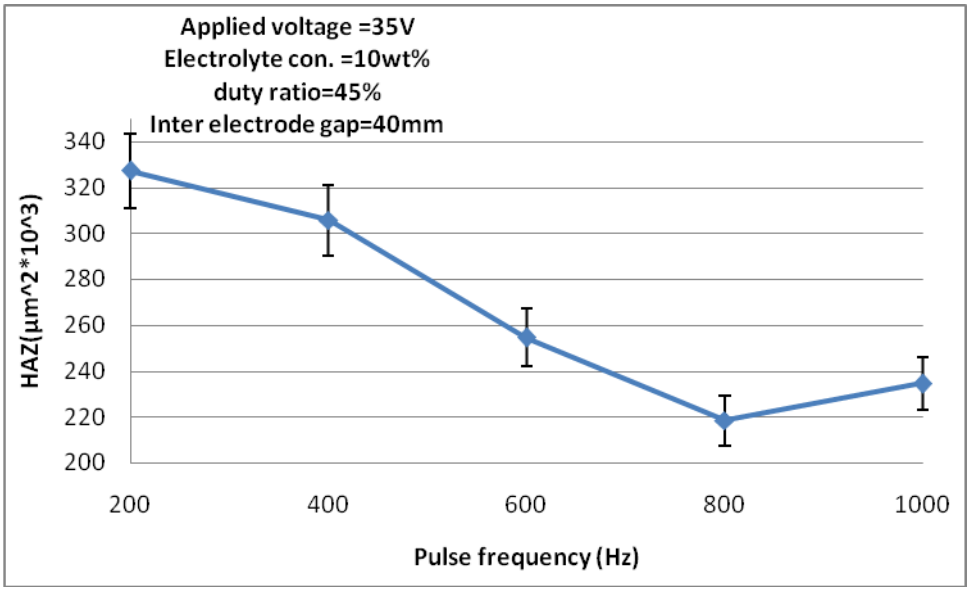

(d) Effect of pulse frequency on HAZ

Figs.5.3 (a) - (d) Effect of (a) applied voltage, (b) electrolyte concentration, (c) duty ratio and (d) pulse frequency on HAZ

Machining Condition	Optical Microscopic Images
35V/10w% NaOH/200 Hz/45%	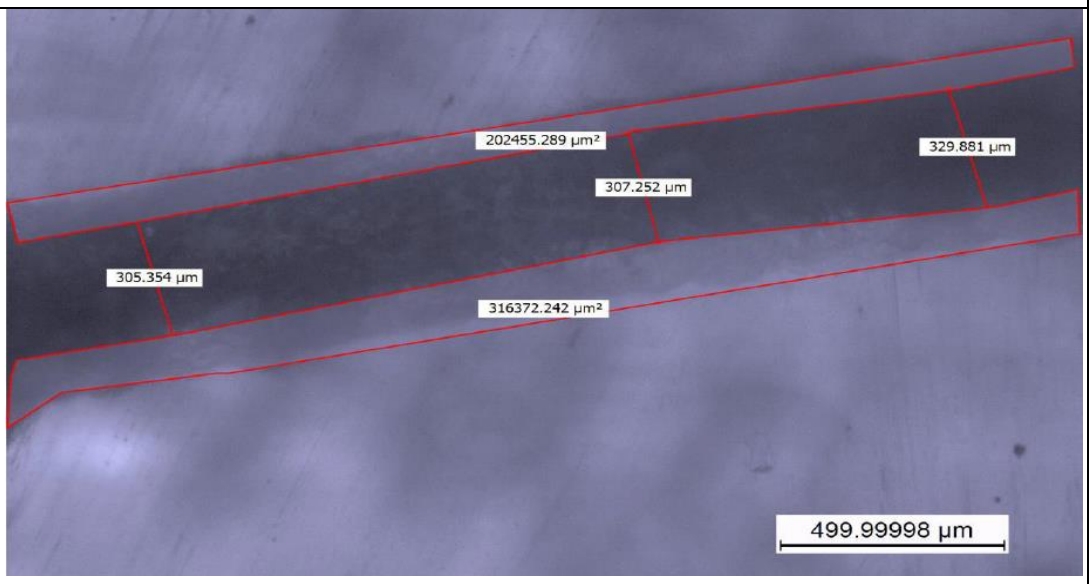
35V/25wt% NaOH/200 Hz/45%	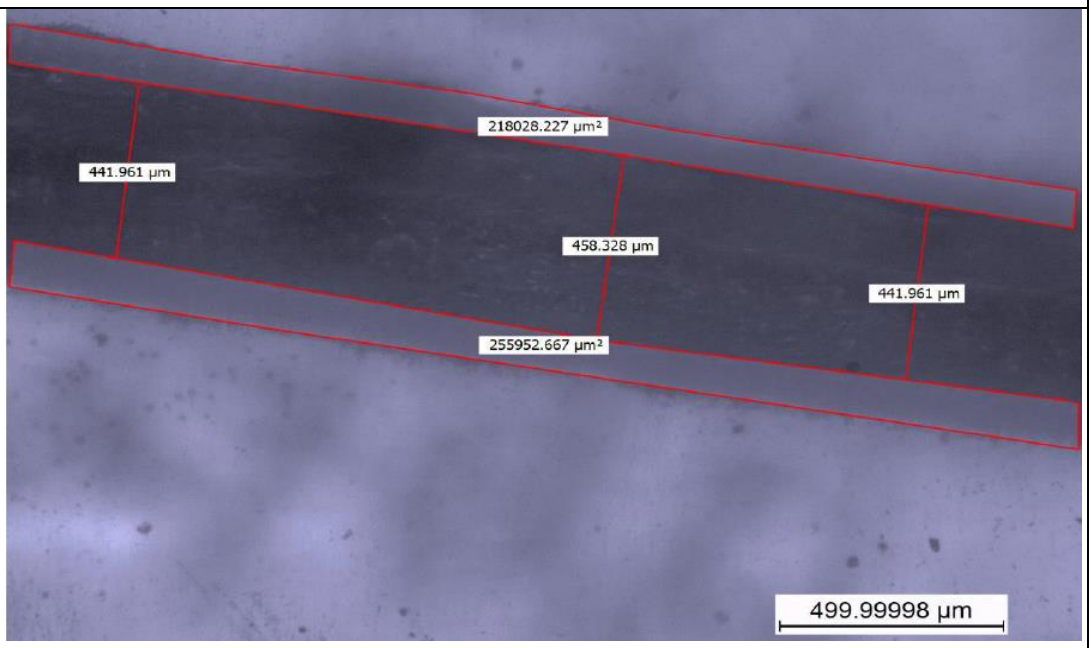

50V/10wt% NaOH/200 Hz/45%	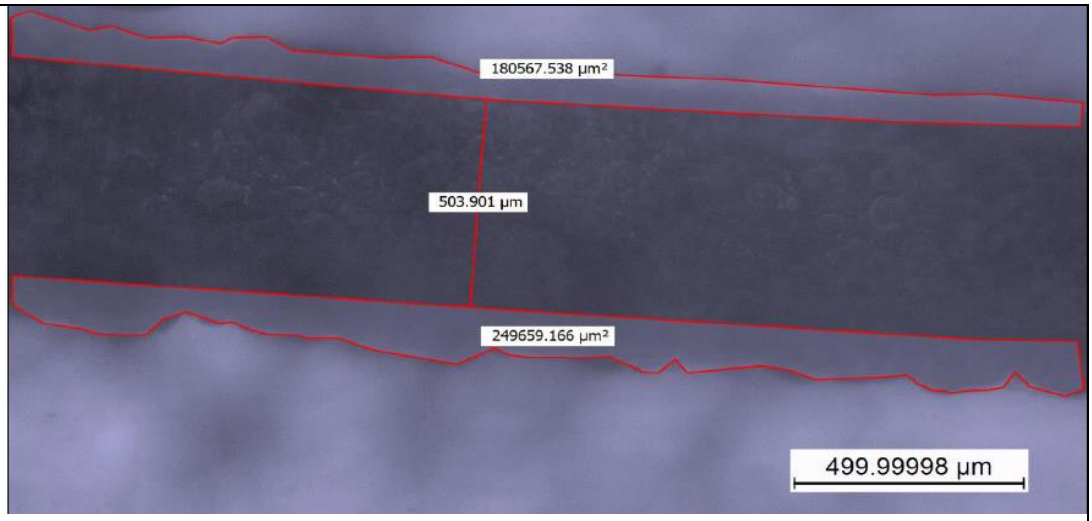

Fig.5.4 Optical microscopic images of micro-channel with HAZ area at different conditions

5.2.4 Influences of Process Parameters on Machining Depth (MD)

The influences of applied voltage, electrolyte concentration, and duty ratio and pulse frequency on machining depth using NaOH as electrolyte have been shown Figs. 5.5 (a) - (d). From these figures it is found that with the increase of applied voltage, duty ratio and electrolyte concentration the machining depth (MD) increases up to 50 V, 60% duty ratio and 30 wt% of electrolyte concentration respectively but after that machining depth decreases. One possible reason is that the current density on the tool's side surface rises and the lack of electrolyte at the tip of tool is found and also side sparking happens due to gathering of hydrogen bubble at the side wall of the micro tool. But it is also observed that at higher voltage and higher duty ratio i.e. 55V, 65% MD is comparatively higher than that at lower voltage and lower duty ratio i.e. 35V, 45%. MD decreases with the increase of pulse frequency. The possible reason is that the pulse on-time deceases with the increase of pulse frequency for the fixed duty ratio and it decreases the sparking rate at the machining zone.

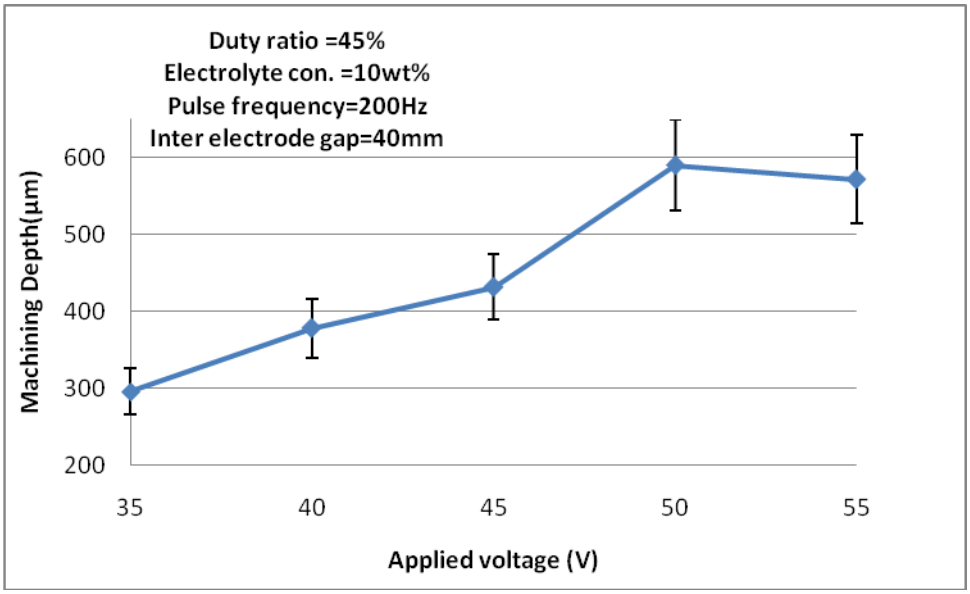

(a) Effect of applied voltage on Machining Depth

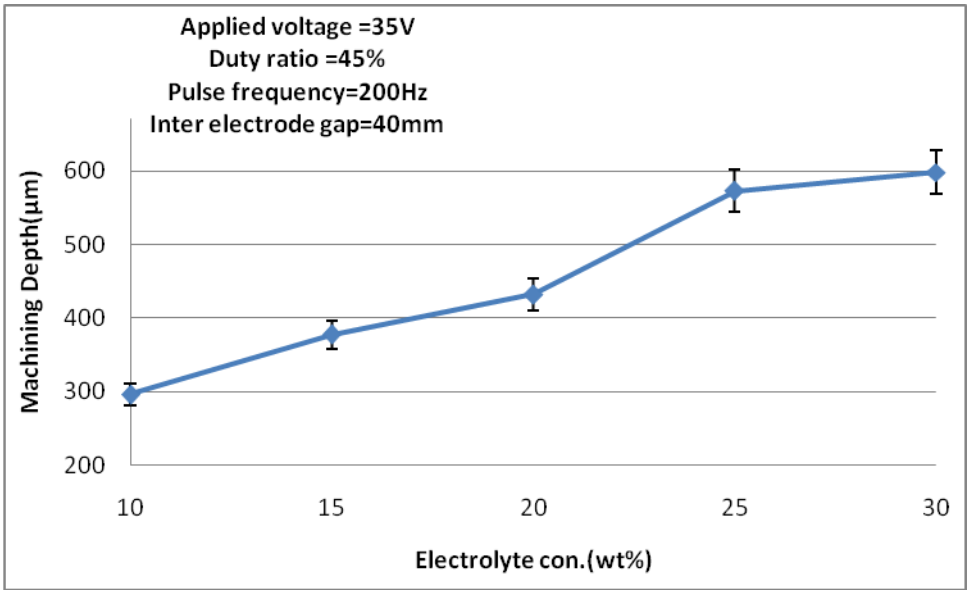

(b) Effect of electrolyte concentration on Machining Depth

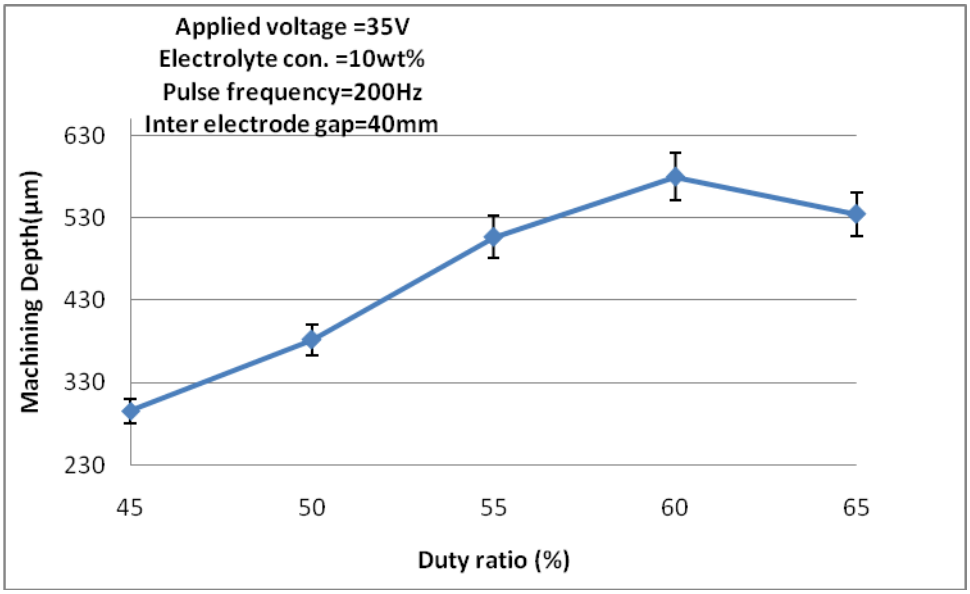

(c) Effect of duty ratio on Machining Depth

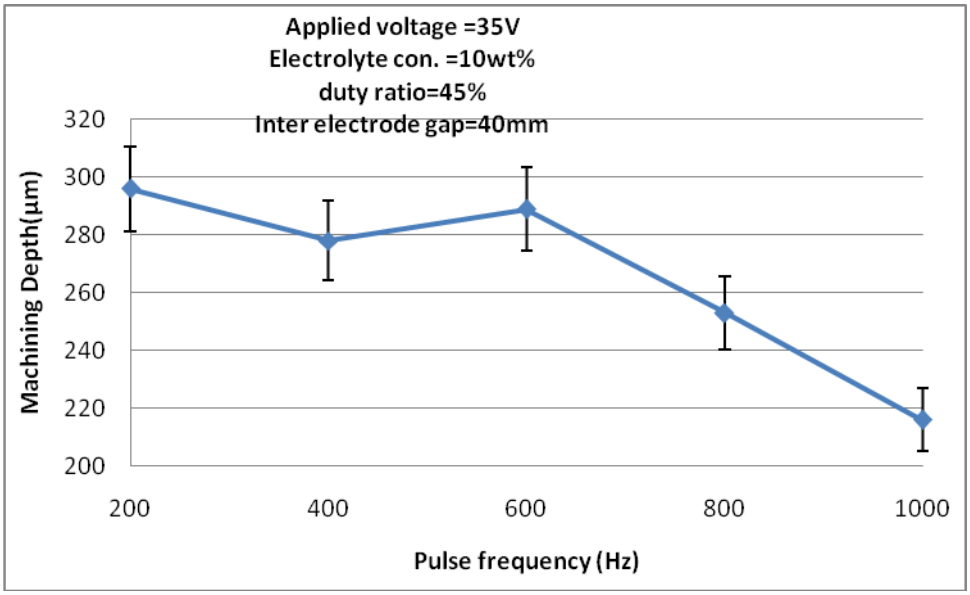

(d) Effect of pulse frequency on Machining Depth

Figs. 5.5 (a) - (d) Effects of (a) applied voltage, (b) electrolyte concentration, (c) duty ratio and (d) pulse frequency on machining depth

5.2.5 Influences of Process Parameters on Surface Roughness (R_a)

The influences of applied voltage, electrolyte concentration, and duty ratio and pulse frequency on average surface roughness for fixed inter-electrode gap are shown in Figs. 5.6 (a) - (d) respectively when micro-channel is cut on glass using NaOH as electrolyte. From the Figs. 5.6 (a), (b) and (c) it is clear that surface roughness increases as voltage, electrolyte concentration and duty ratio are increased due to increase in sparking rate but it decreases only at 50 V and 25% electrolyte concentration. Large amount of heat is produced into the

machined channel during sparking and as a result, HAZ area increases and produces irregularities on the surface of the job specimen that increases surface roughness of the micro-channels. If the rate of sparking is continuous and stray sparking is less, better surface finish could be obtained. From the Fig. 5.6 (d) it is observed that if pulse frequency is increased, initially surface roughness is slightly decreased because pulse on-time is decreased since the rate of sparking and stray sparking are reduced but 200 Hz to 600Hz pulse frequency, surface roughness is moderately same. But at higher pulse frequency, it is very difficult to control the continuous sparking that causes irregularities on the machining surface. So, after that surface roughness is increased.

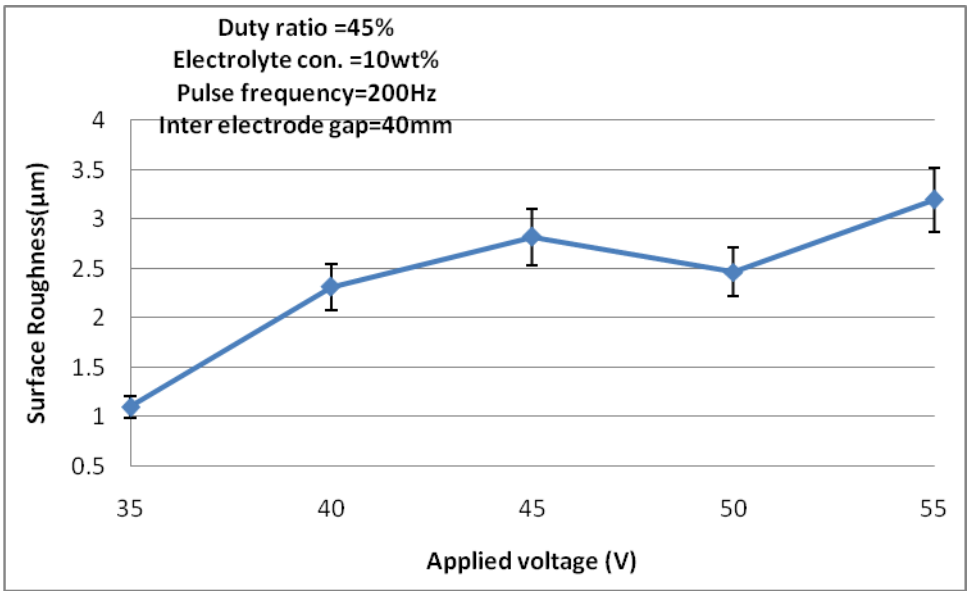

(a) Effect of applied voltage on Surface Roughness (R_a)

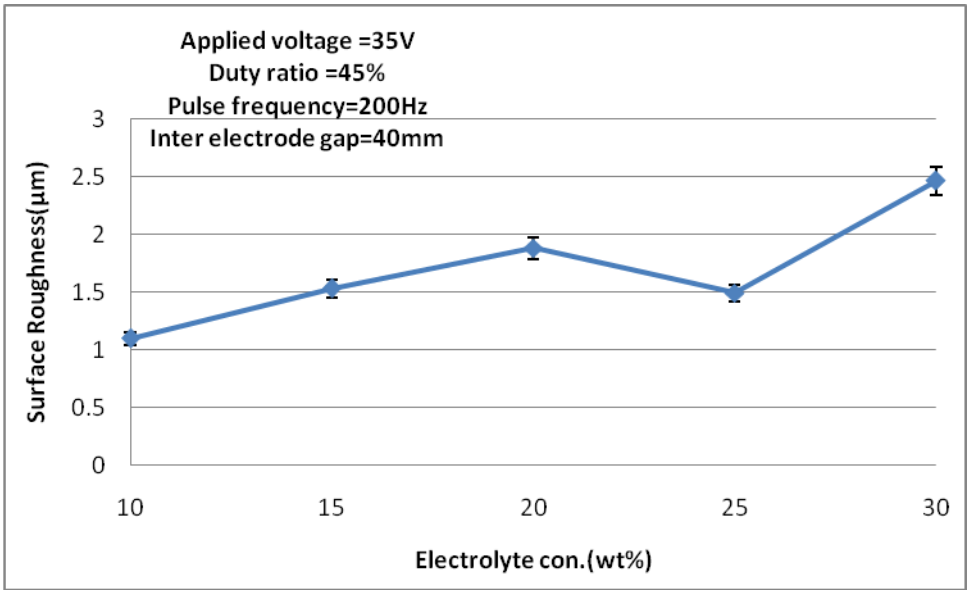

(b) Effect of electrolyte concentration on Surface Roughness (R_a)

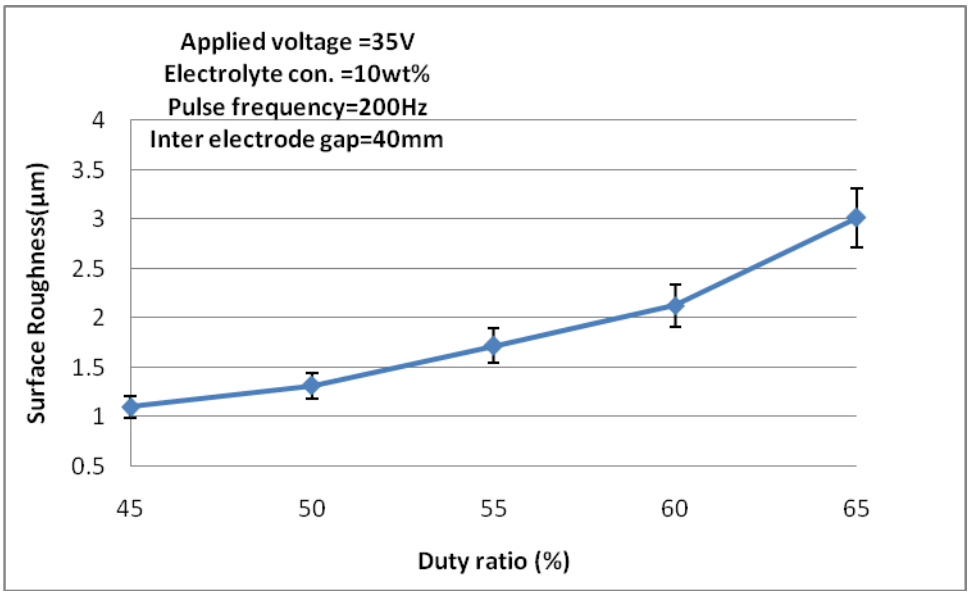

(c) Effect of duty ratio on Surface Roughness (R_a)

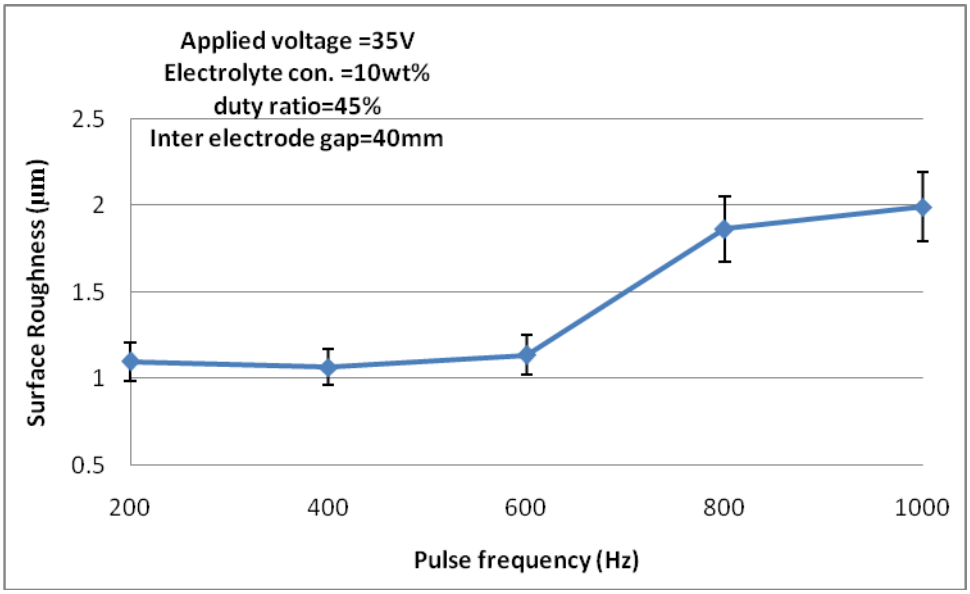

(d) Effect of pulse frequency on Surface Roughness (R_a)

Figs. 5.6 (a) - (d) Effects of (a) applied voltage, (b) electrolyte concentration, (c) duty ratio and (d) pulse frequency on Surface Roughness (R_a)

5.2.6 Comparative Studies of Various Machining Performances Using Different Mixed Electrolyte

Mixed electrolyte of NaOH and KOH with different proportion have different range of conductivity as well as different chemical and physical nature, so they play vital role during machining by µ-ECDM process and also different polarities have different nature to provide

discharge current beyond the critical voltage.

5.2.6.1 Comparative Study on Material Removal Rate (MRR)

The comparative study on the material removal rate (MRR) by using five different mixtures of electrolyte NaOH and KOH at the weight ratio of 1:0, 3:1, 1:1, 1:3 and 0:1 with their varying concentration and voltage, duty ratio and pulse frequency has been shown in Figs. 5.7 (a) - (d). It is obvious from the Fig. 5.7 (a) that initially MRR is higher at 35 V for the ratio of 1:3 compared to other mixtures and at 40 V MRR is high for the ratio of 3:1. But after that by increasing applied voltage MRR becomes higher for the ratio of 0:1 up to 50 V and MRR attains the highest value for the ratio of 1:3 at the applied voltage of 55 V. From the Fig. 5.7 (a), it is cleared that the average MRR increases with increase of percentage of KOH in the mixture and 1:1 ratio of NaOH and KOH mixture is found preferable within the voltage range of 35-55 V. But enrichment of KOH in this mixture is not always useful since MRR is more only for the change of voltage from 40 to 50 V. Kalium ('K') is at the higher level compared to Natrium ('Na') in electro valence periodic table of elements and it has more cationic nature than 'Na. Therefore, generation of H_2 bubbles in the electrolyte gets boost up due to enrichment of KOH in the mixture and it accelerates the development of thermal energy; thereby increases MRR. Almost similar phenomena are observed with variations of duty ratio, electrolyte concentration and pulse frequency. From the Figs. 5.7 (b) to (d) the ratio of 1:3 electrolyte mixtures is preferable for improvement MRR. 100% of KOH in mixture may not be highly acceptable due to contamination of removed melted material with the electrolyte solution and redepositing of it in the machining zone.

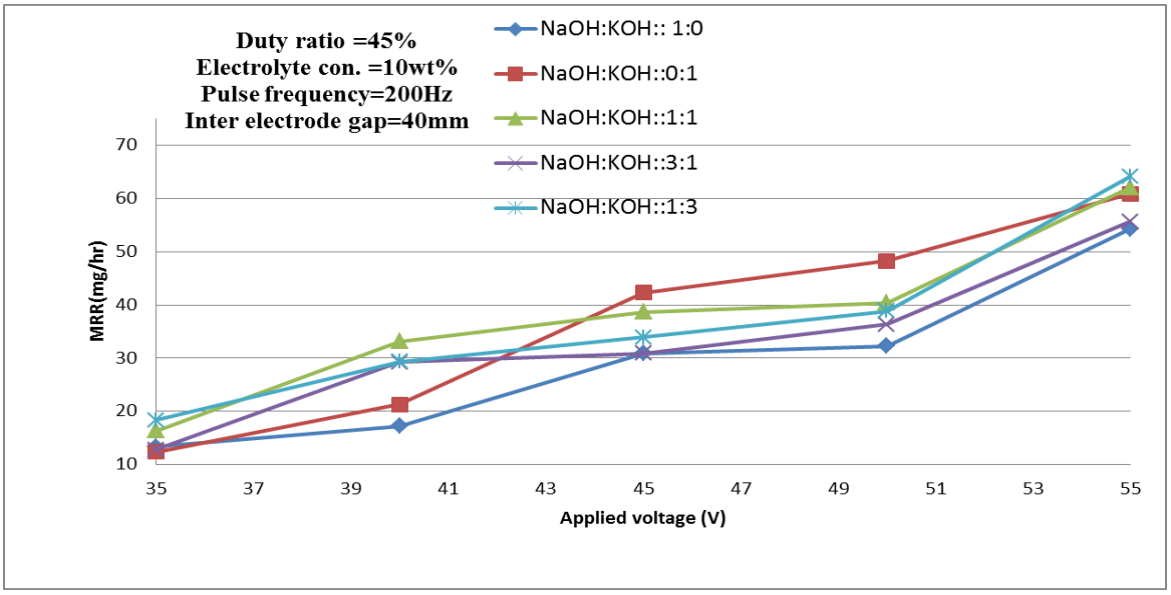

(a)Effect of applied voltage on MRR

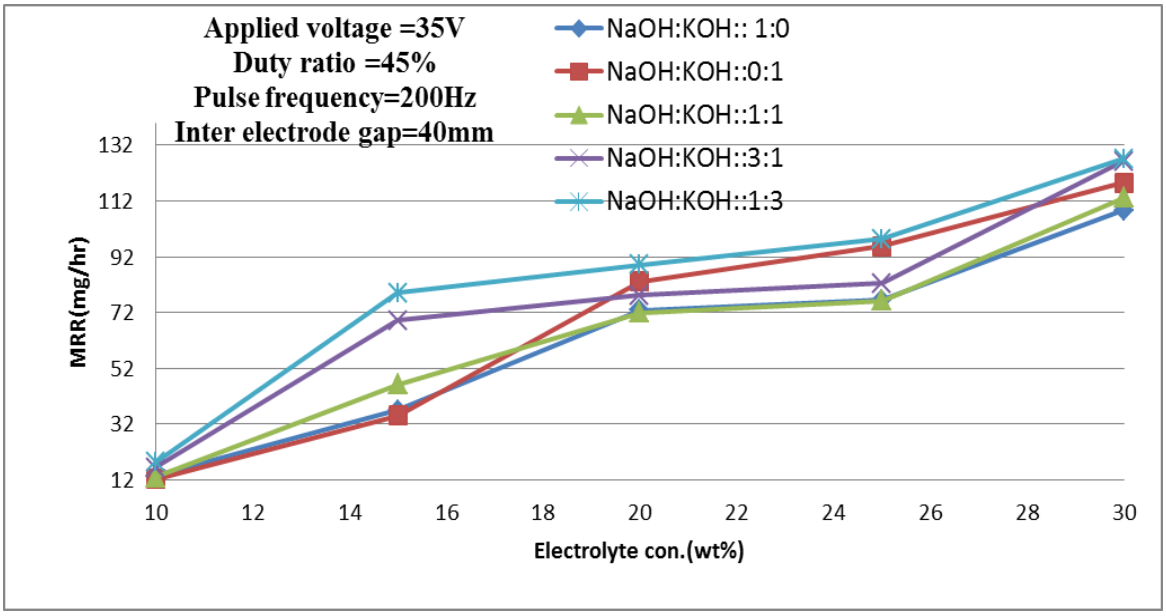

(b) Effect of concentration on MRR

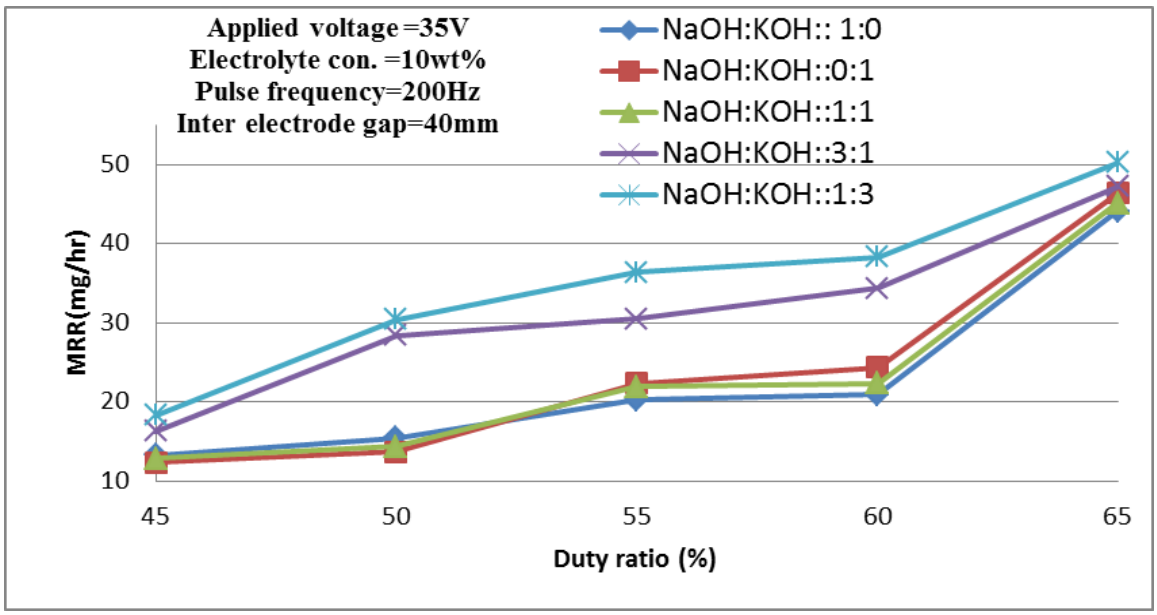

(c) Effect of duty ratio on MRR

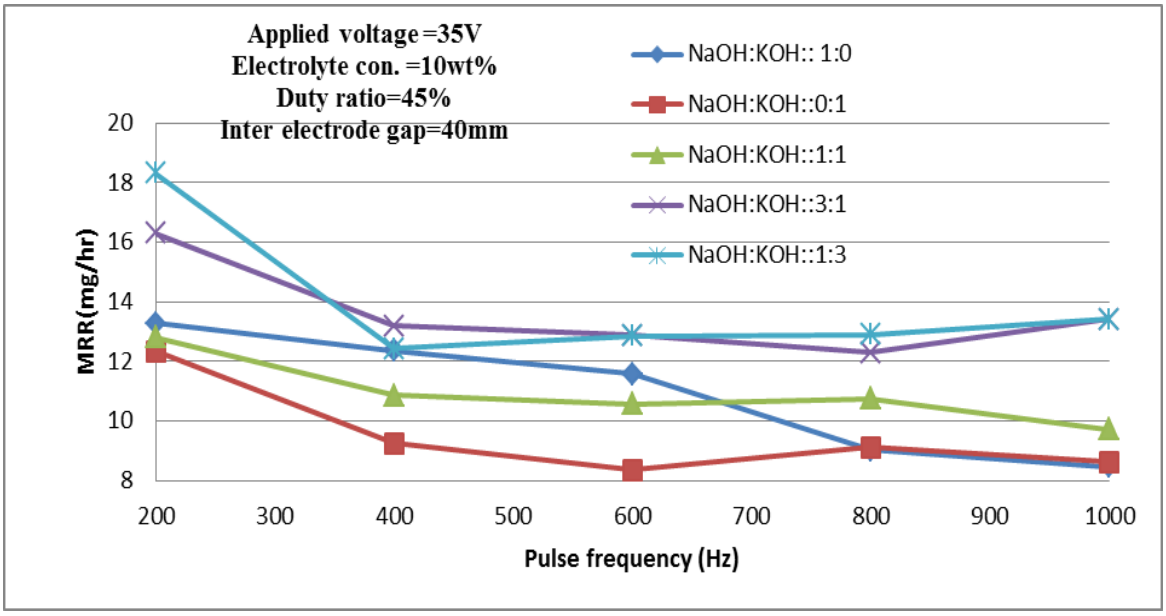

(d) Effect of pulse frequency on MRR

Figs. 5.7 (a) - (d) Effect of electrolyte mixtures on MRR with variation of (a) applied voltage, (b) electrolyte concentration, (c) duty ratio and (d) pulse frequency

5.2.6.2 Comparative Study on Overcut (OC)

Figs. 5.8 (a) - (d) reflect overcut (OC) using five different mixtures of electrolyte NaOH and KOH at the ratio of 1:0, 3:1, 1:1, 1:3 and 0:1 with their varying concentration and voltage, duty ratio and pulse frequency. From the Fig. 5.8 (a) it is clear that the overcut is higher while NaOH and KOH mixture is used at the ratio of 1:0 and lower for the ratio of 3:1 solution. The overcut is found increasing with increase of applied voltage for all ratios of mixture of electrolyte. From the Fig. 5.8 (b) it is rendered that at 15wt%/35V/40%/IEG 40mm, overcut is lower when NaOH and KOH are mixed as the ratio 1:3 during micro-channel cutting on glass. As shown in Fig. 5.8 (c) the ratio of 3:1 provides better micro-range profile as well as channel when duty ratio is increased, kept other parameter fixed at initial level and the ratio 0:1 and 1:3 gives higher width of cut at 65% duty ratio. From the Fig. 5.8 (d) it is obviously that when NaOH and KOH is used as the ratio of 3:1 in the mixture lower overcut is achieved during micro channel cutting on glass. If pulse frequency is increased, overcut decreases because the intensity of sparking rate decreases and pulse-on-time decreases. It is said that up

to 600Hz overcut decreases but after that increases, provably cause of that rate of side sparking increase.

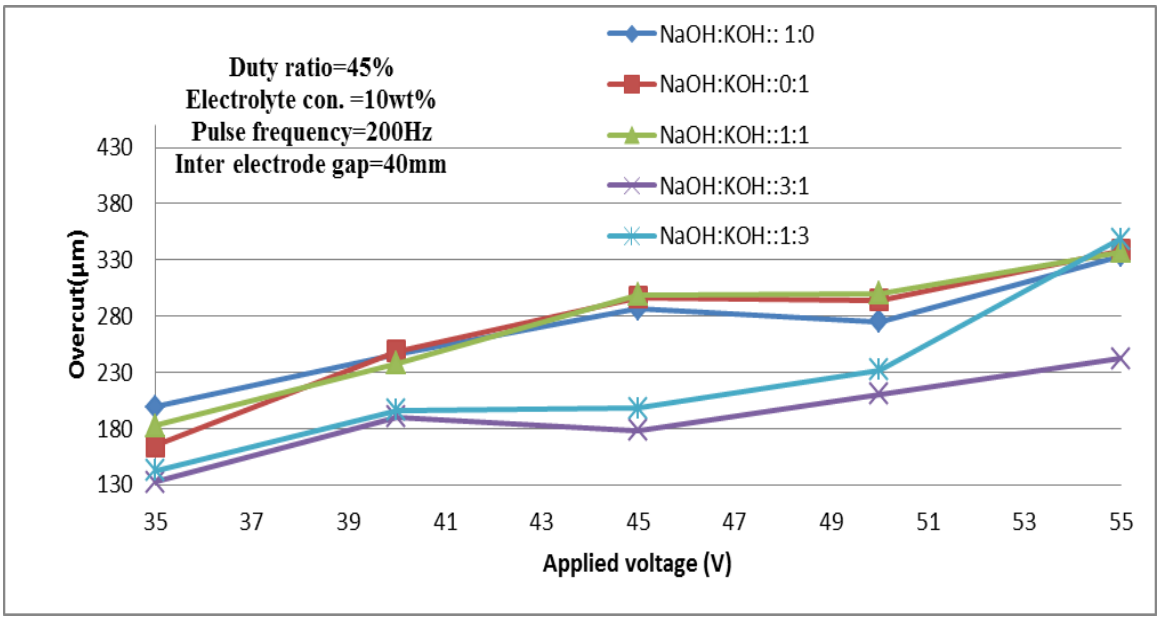

(a) Effect of applied voltage on OC

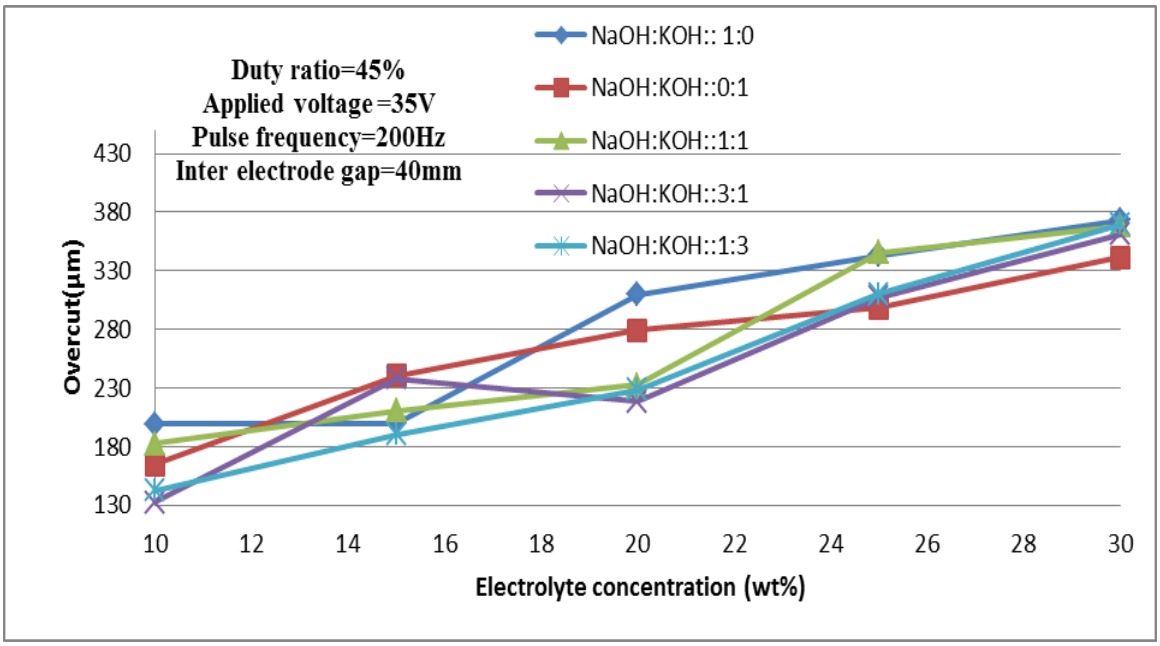

(b) Effect of concentration on OC

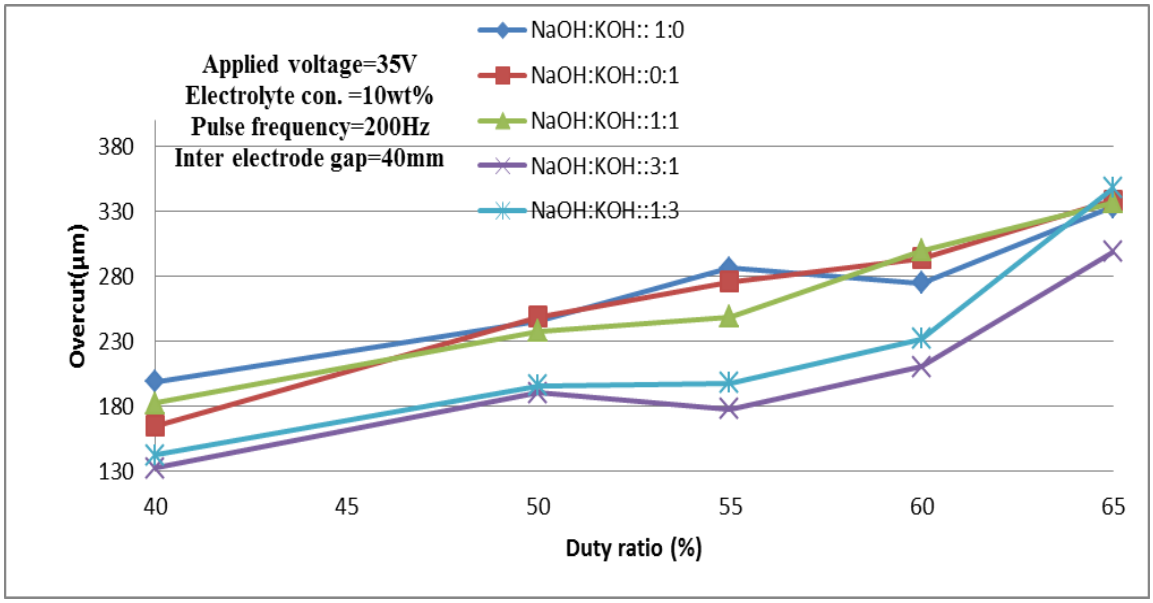

(c) Effect of duty ratio on OC

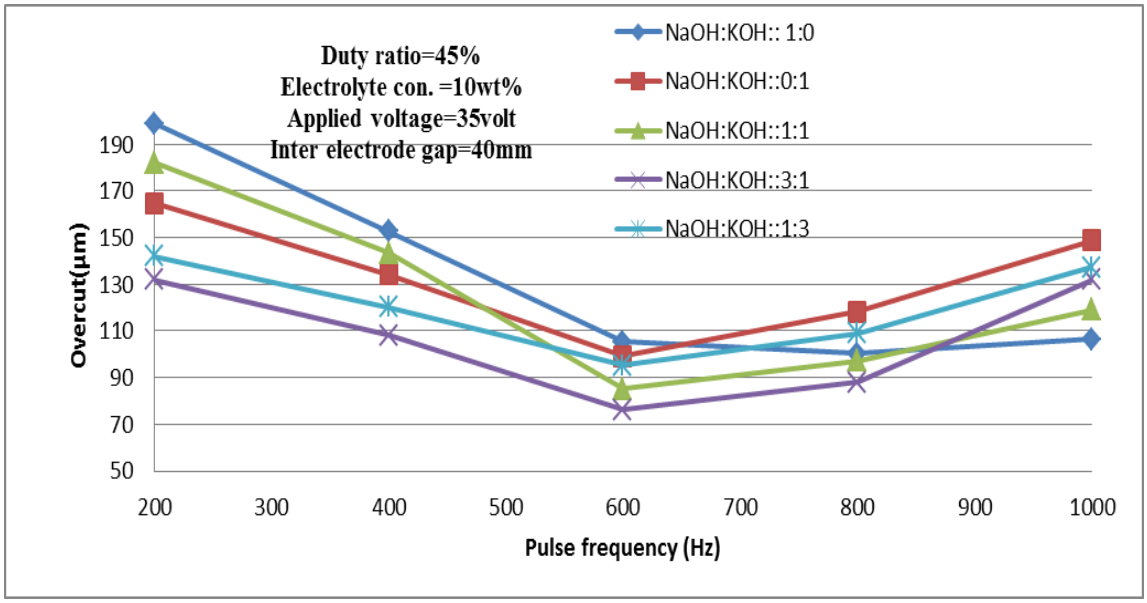

(d) Effect of pulse frequency on OC

Figs. 5.8 (a) - (d) Effects of electrolyte mixtures on OC with variation of (a) applied voltage, (b) electrolyte concentration, (c) duty ratio and (d) pulse frequency

5.2.6.3 Comparative Study on Heat Affected Zone (HAZ) Area

The comparison of the Heat Affected Zone (HAZ) using five different mixtures of electrolyte NaOH and KOH at the ratio of 1:0, 3:1, 1:1, 1:3 and 0:1 with their varying concentration and voltage, duty ratio and pulse frequency has been shown in Figs. 5.9 (a)-(d). In Fig. 5.9 (a) HAZ area is found very larger for the ratio of 0:1 of NaOH and KOH in the

mixture than that of four types of ratio and lower at the ratio of 3:1 for 10wt% of electrolyte concentration, pulse frequency of 200 Hz and duty ratio of 45 %. It is clear from the figure that HAZ area is the least for the ratio of 1:1 at 10 wt% electrolyte concentration, applied voltage of 35 V, pulse frequency of 200 Hz and duty ratio of 45 %. From Fig. 5.9 (b) changing electrolyte concentration and other parameter constant at 35V/200Hz/45% duty ratio/IEG 40mm, HAZ area is lower at 10wt% of the ratio of 0:1 but at higher electrolyte concentration HAZ area is larger. From Fig. 5.9 (c) HAZ become smaller when the duty ratio is varied using NaOH and KOH at the ratio of 1:3 in the mixture. From Fig. 5.9 (d) HAZ area becomes larger at 200Hz for all types of electrolyte and the least at 600Hz when NaOH and KOH is used as the ratio of 1:3 during micro-channel cutting on glass.

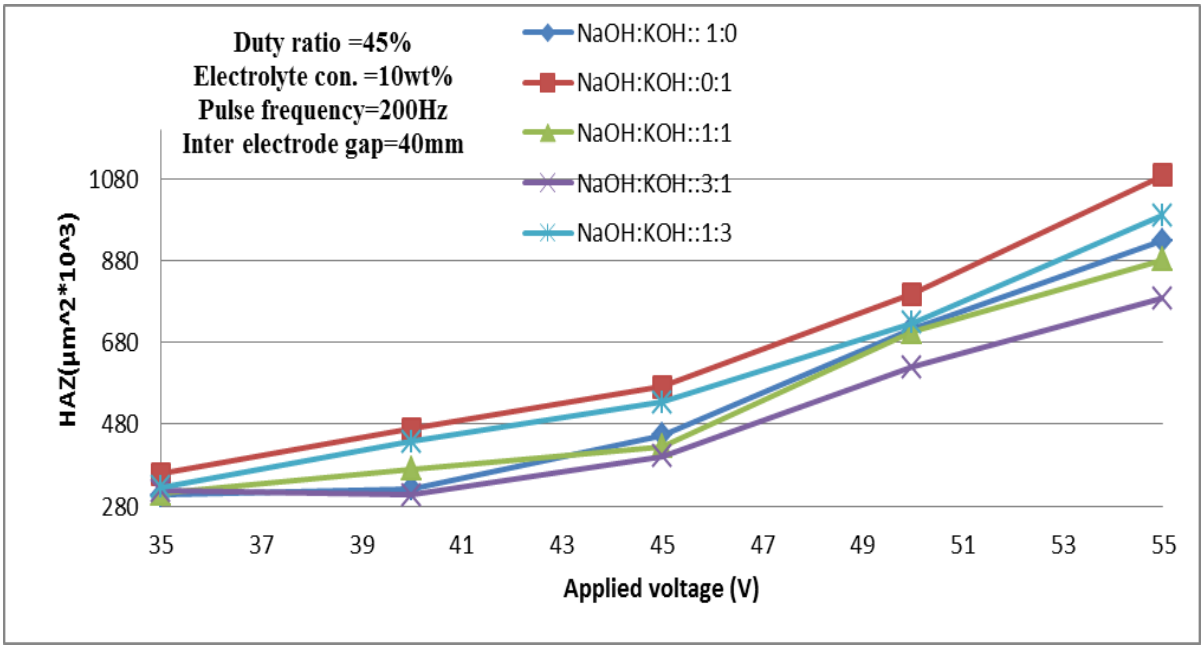

(a) Effect of applied voltage on HAZ

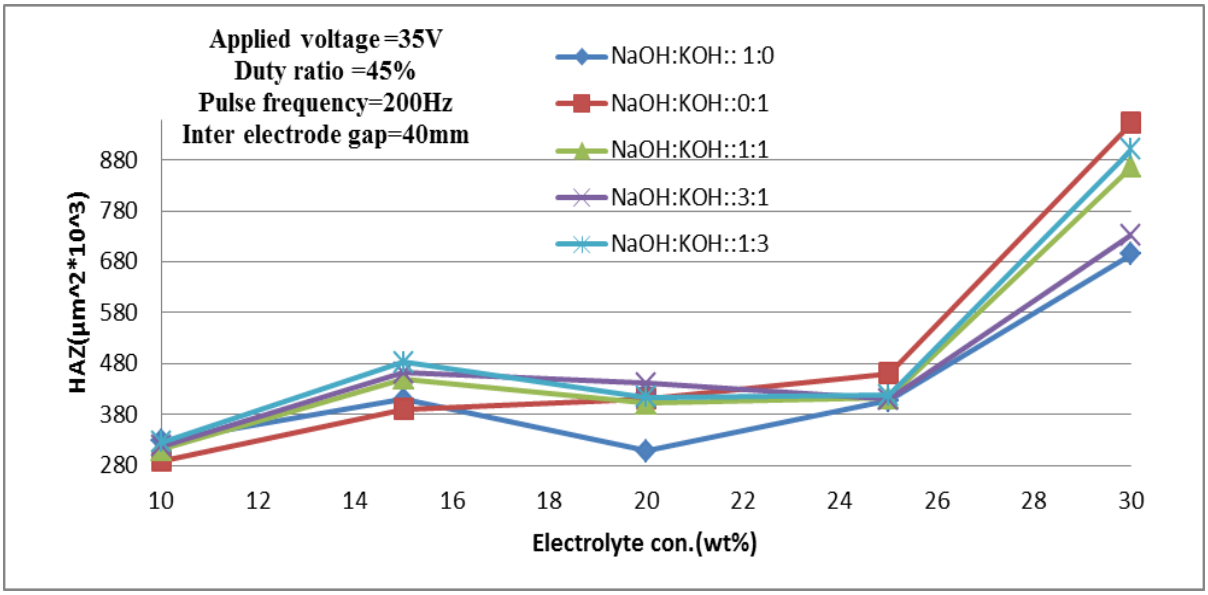

(b) Effect of concentration on HAZ

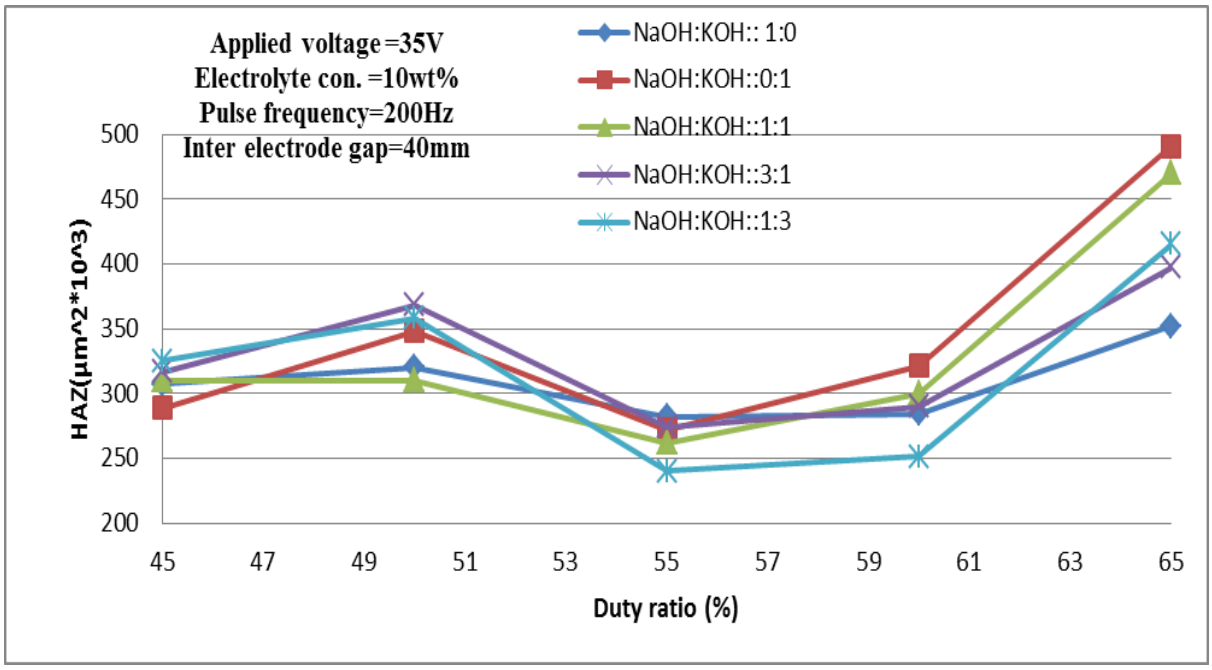

(c) Effect of duty ratio on HAZ

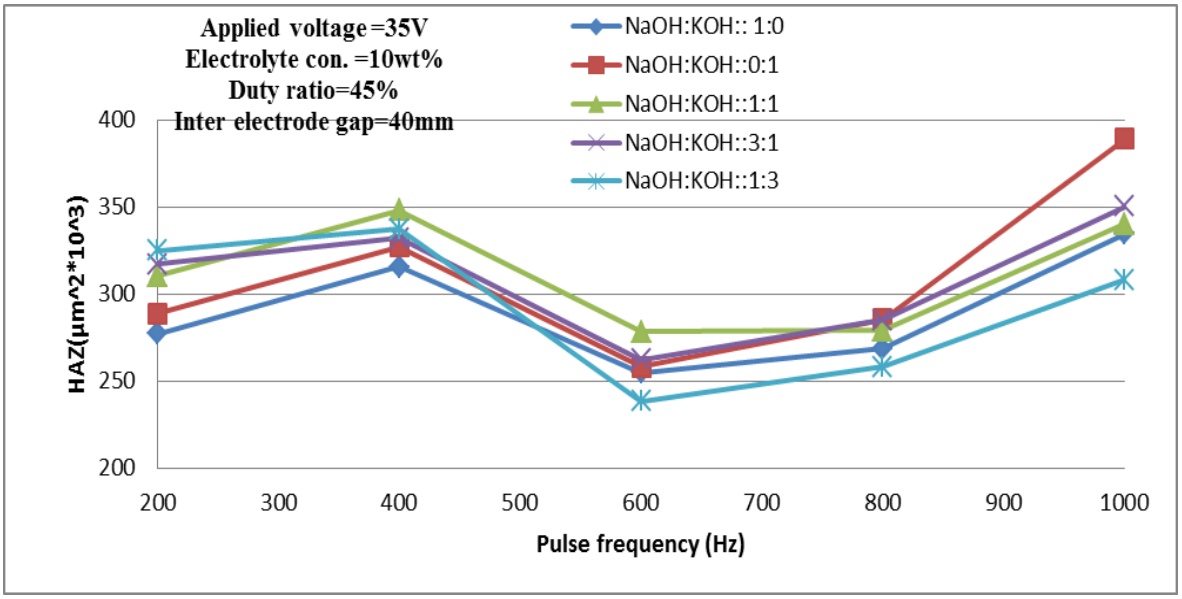

(d) Effect of pulse frequency on HAZ

Figs. 5.9 (a) - (d) Effects of electrolyte mixtures on HAZ with variation of (a) applied voltage, (b) electrolyte concentration, (c) duty ratio and (d) pulse frequency

5.2.6.4 Comparative Study on Machining Depth (MD)

The comparative study on the Machining Depth (MD) using different mixtures of electrolyte NaOH and KOH at the ratio of 1:0, 3:1, 1:1, 1:3 and 0:1 with different concentration, voltage, duty ratio and pulse frequency has been represents in Figs. 5.10 (a)-(d). The Fig. 5.10 (a) shows the ratio of 3:1 provides larger machining depth at 50V and the ratio of 1:1 attains smaller machining depth. From the Fig. 5.10 (b) it is imaged that machining depth is lower at the lower concentration of the ratio of 1:1 and highest at higher electrolyte concentration of NaOH and KOH at the ratio 1:3. Fig. 5.10 (c) shows that machining depth is larger at 60% of duty ratio. Fig. 5.10 (d) illustrates that machining depth becomes higher at lower pulse frequency by using NaOH and KOH at the ratio of 3:1 and lower at the ratio of 1:1.

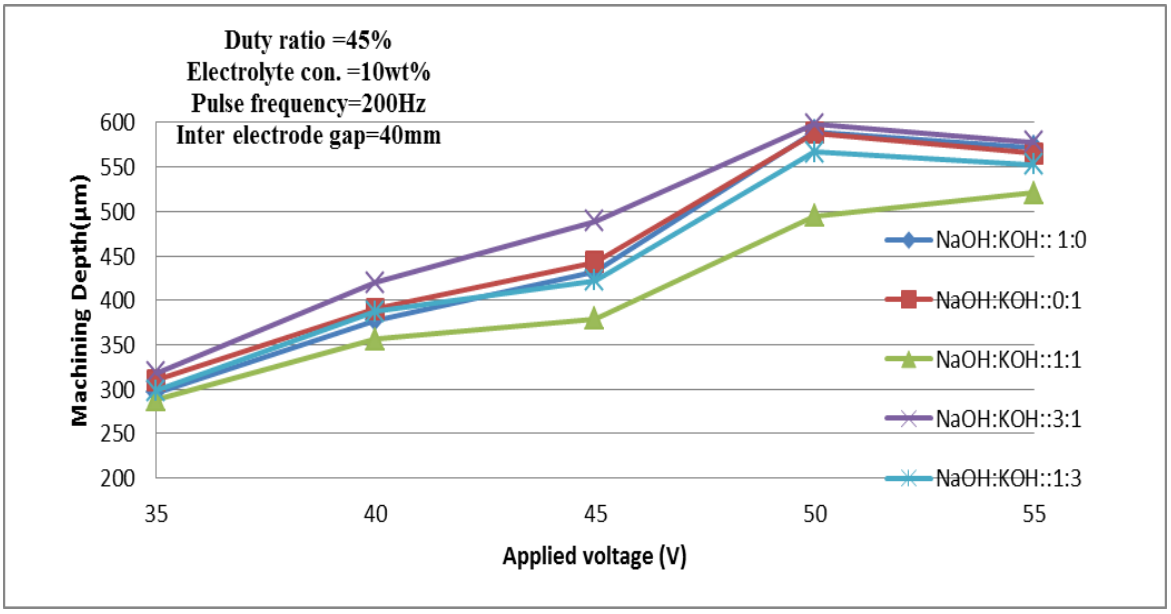

(a) Effect of applied voltage on MD

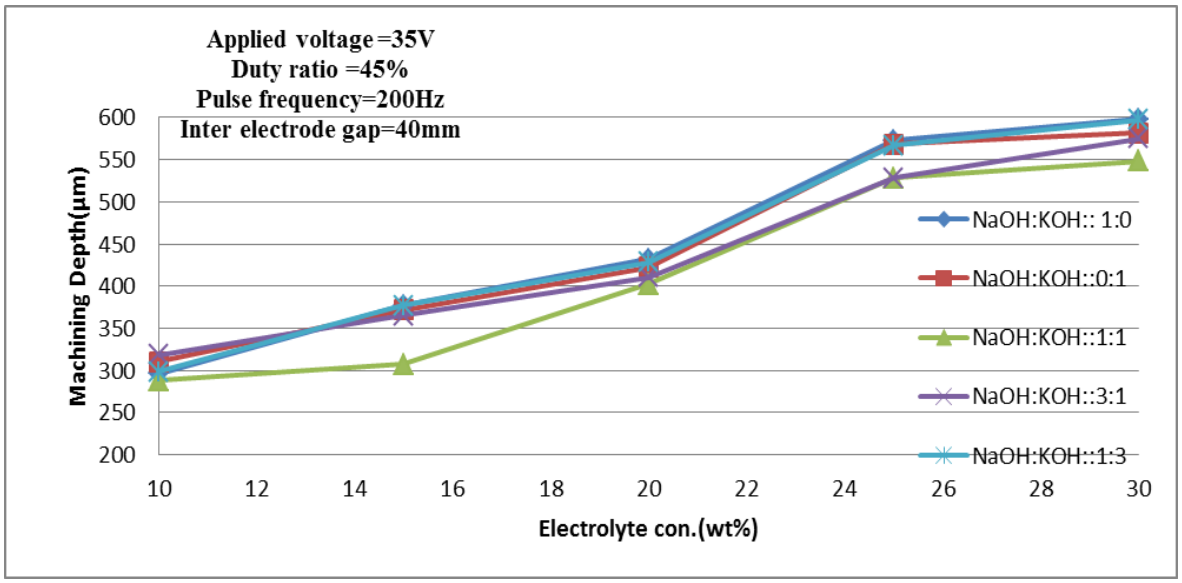

(b) Effect of concentration on MD

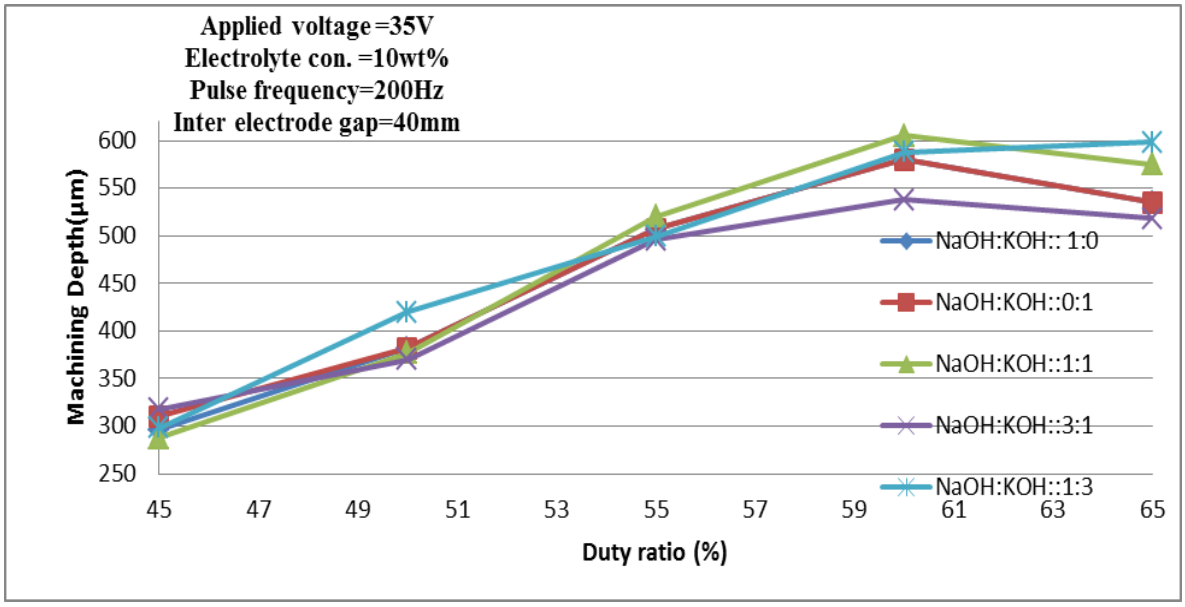

(c) Effect of duty ratio on MD

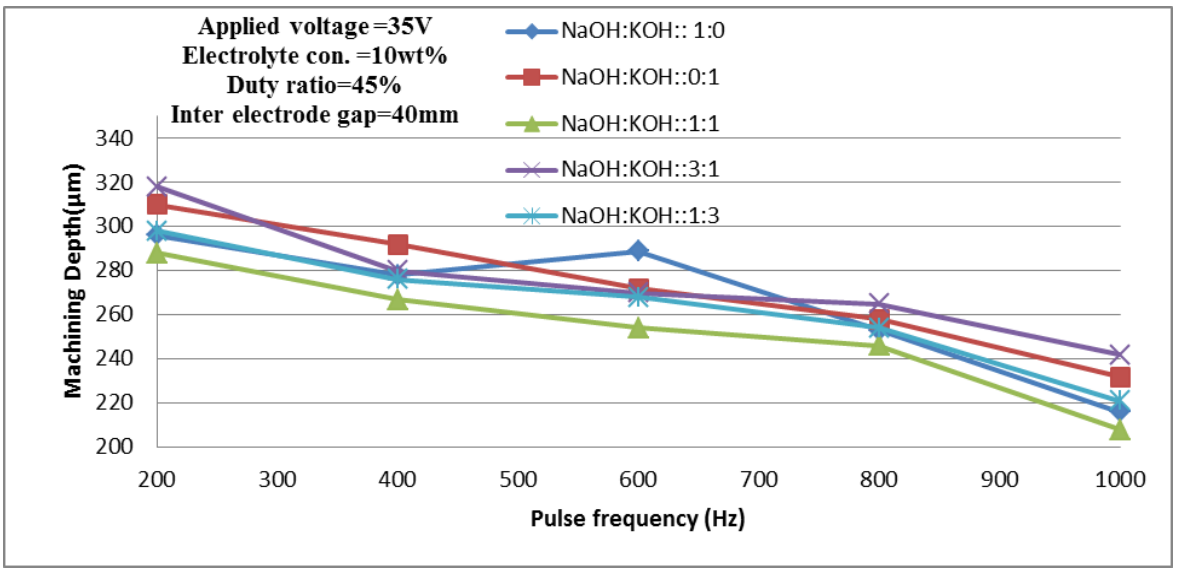

(d) Effect of pulse frequency on MD

Figs. 5.10 (a) - (d) Effects of electrolyte mixtures on machining depth with variation of (a) applied voltage, (b) electrolyte concentration, (c) duty ratio and (d) pulse frequency

5.2.6.5 Comparative Study on Surface Roughness (R_a)

Figs. 5.11 (a)-(d) represent the comparative study on the Surface Roughness (R_a) by using five different types of electrolyte, NaOH and KOH at the ratio of 1:0, 3:1, 1:1, 1:3 and 0:1 with different concentrations, voltage, duty ratio and pulse frequency. Fig. 5.11 (a) represents the lower surface roughness at 3:1 ratio of NaOH and KOH. Surface roughness is higher at

35 V when NaOH and KOH are used at the ratio of 1:3 and surface roughness becomes lower at the ratio of 3:1. Fig. 5.11 (b) shows that NaOH and KOH at the ratio of 3:1 provides lower surface roughness and the ratio 1:3 gives uniform surface finish and increases upto 25 wt% and surface roughness becomes larger when NaOH and KOH is mixed at the ratio of 0:1 at the level of 30wt% concentration. From the Fig. 5.11 (c) it is obvious that surface roughness is increased when duty ratio is increased, due to higher sparking, thermal damage occurred and irregularities in to the micro-channel increases at 55% duty ratio and at 45% duty ratio surface roughness is lower for the ratio of 3:1 and also becomes larger at 65% duty ratio. From the Fig. 5.11 (d) it is observed that surface roughness is uniform upto 600Hz and at 200Hz surface roughness is lower at 3:1 ratio and higher at 1 KHz in case of 0:1ratio. Fig. 5.12 represents the surface textures of micro-channel on glass machined at direct polarity 50V/25wt% NaOH:KOH:: 1:0/55%/600Hz. Fig. 5.13 shows the surface textures of micro-channel at direct polarity 35V/15wt% NaOH:KOH::3:1/50%/600Hz. Fig. 5.14 exhibits the surface textures of micro-channel on glass, machined at direct polarity 50V/15wt% NaOH:KOH::1:3/ 50%/400Hz.

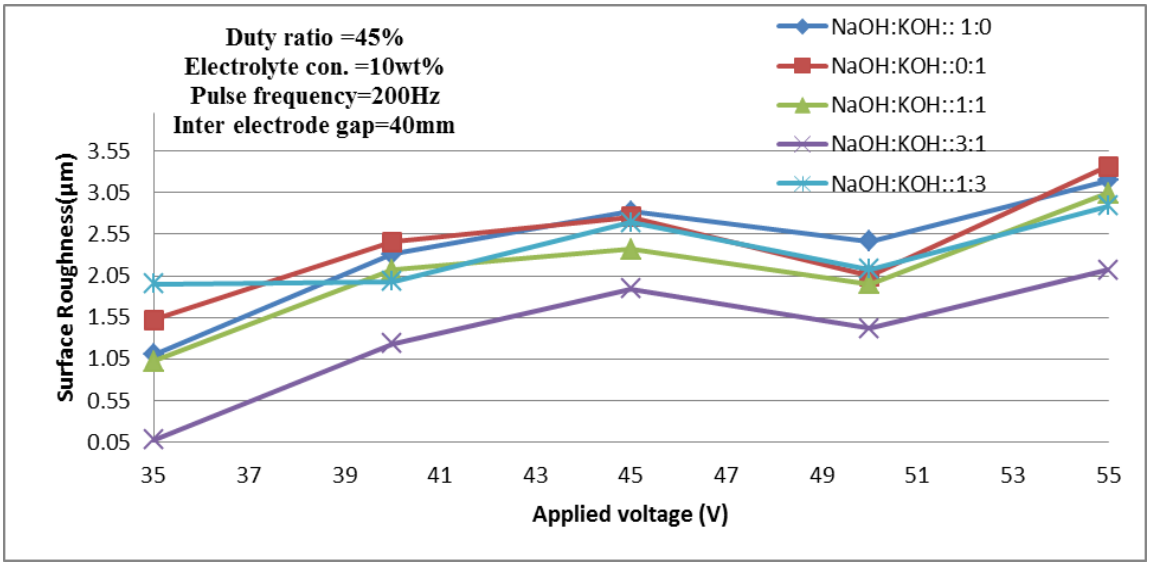

(a) Effect of applied voltage on surface roughness

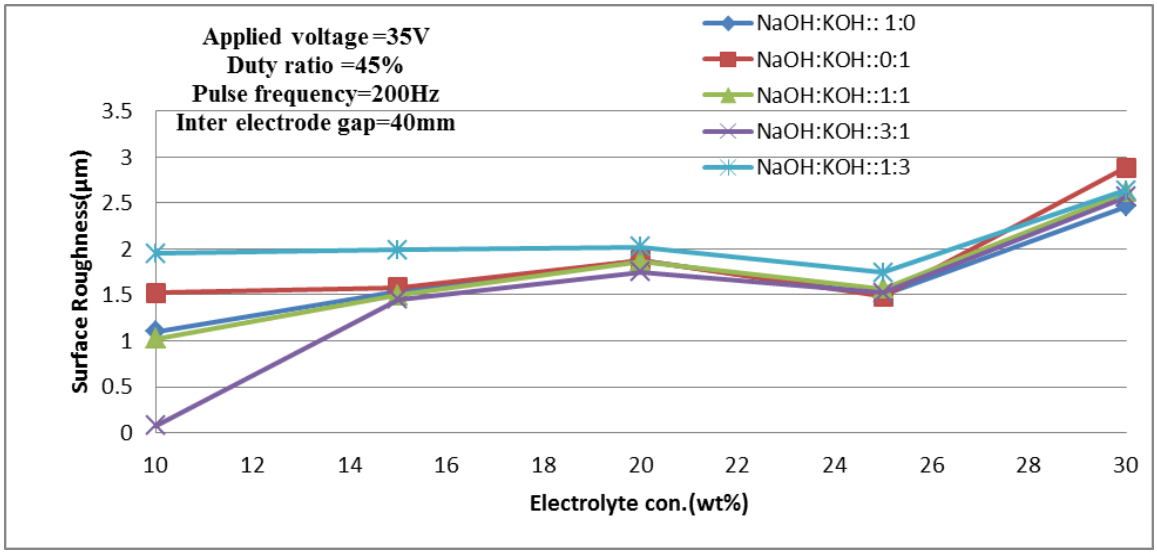

(b) Effect of concentration on surface roughness

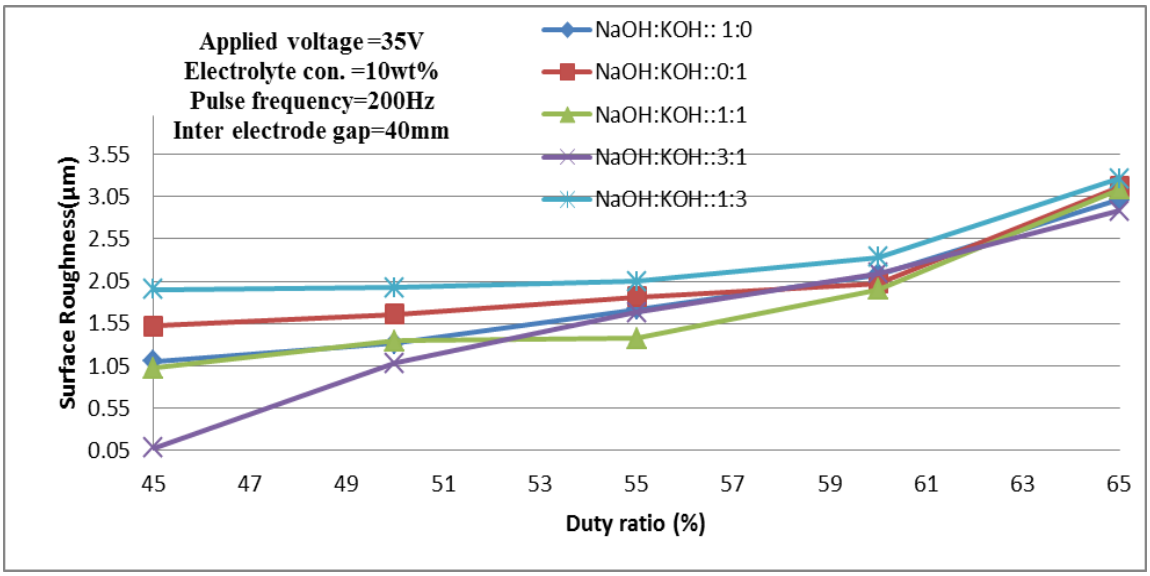

(c) Effect of duty ratio on surface roughness

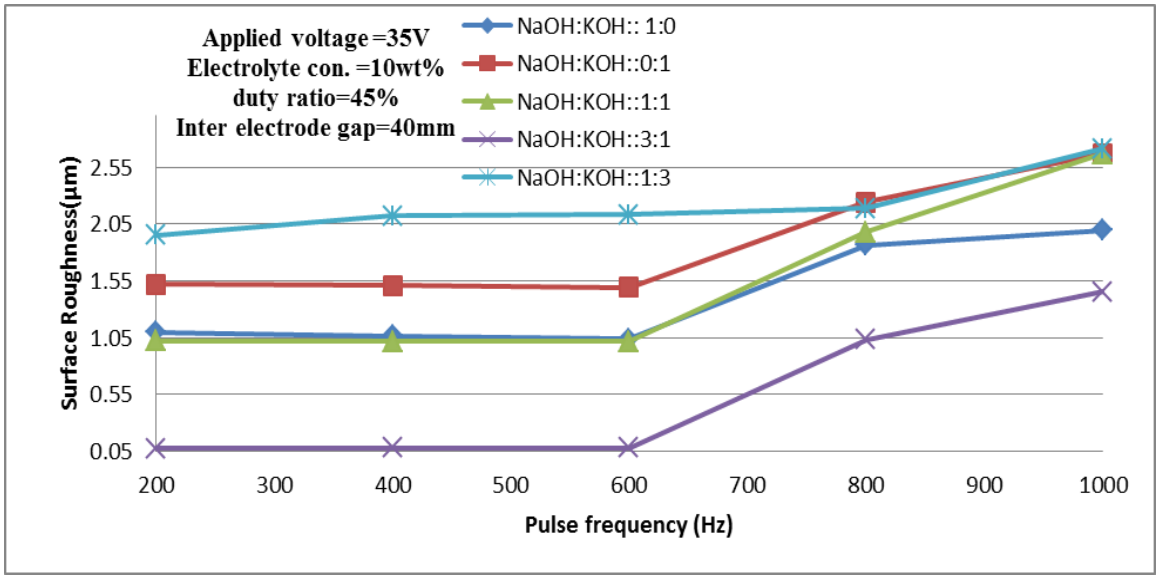

(d) Effect of pulse frequency on surface roughness

Figs. 5.11 (a) - (d) Effects of electrolyte mixtures on surface roughness with variation of (a) applied voltage, (b) electrolyte concentration, (c) duty ratio and (d) pulse frequency

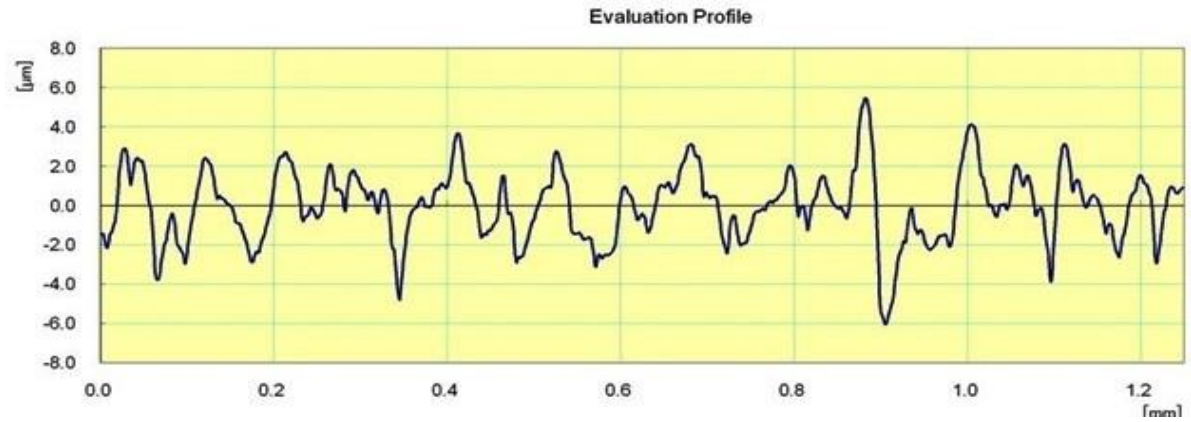

Fig. 5.12 Surface texture of micro-channel at 50V/25wt% NaOH:KOH:: 1:0/55%/600Hz

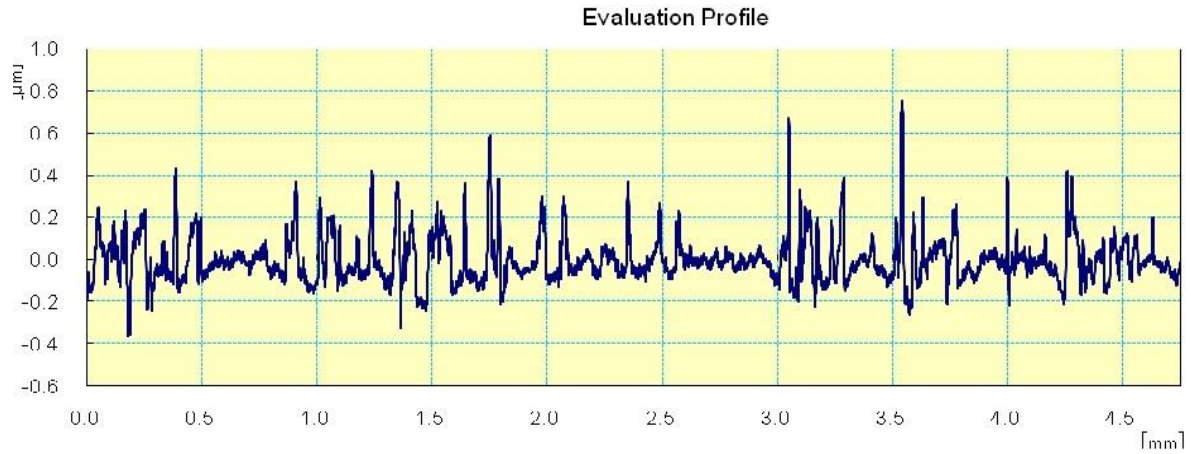

Fig. 5.13 Surface texture of micro-channel at 35V/15wt% NaOH:KOH::3:1 /50%/600Hz

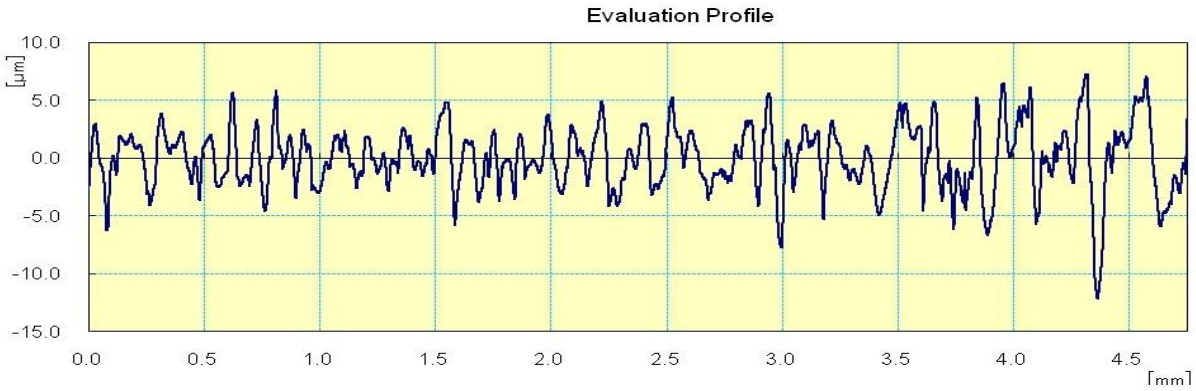

Fig. 5.14 Surface texture of micro-channel at 50V/15wt% NaOH:KOH::1:3 /50%/400Hz

5.2.7 Comparative Studies of Various Machining Performances Using Different Polarities

Total fifteen experiments have been conducted with different polarities for five different electrolytes mixtures *i.e.*, NaOH and KOH are mixed at the ratio of 1:0, 3:1, 1:1, 1:3 and 0:1, by fixing the electrolyte concentration at 10 wt% and other process parameters viz. applied voltage, type of electrolyte; pulse frequency, inter-electrode gap and duty ratio. Figs. 5.15 (a) and (b) show the arrangement of direct polarity and reverse polarity of micro-tool in micro-ECDM process.

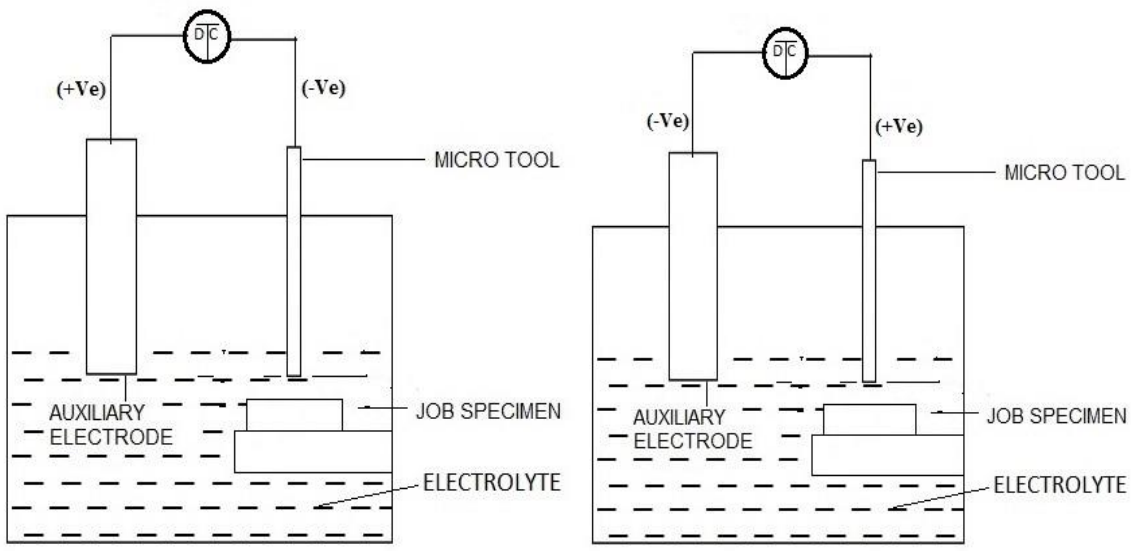

(a) Direct polarity (b) Reverse polarity

Fig. 5.15 Schematic diagrams of (a) direct polarity and (b) reverse polarity of µ-tool of µ-ECDM.

5.2.7.1 Effect of Polarity on Material Removal Rate (MRR)

A comparative study for material removal rate has been carried out between direct polarity and reverse polarity with varying five different types of electrolyte mixtures i.e., NaOH and KOH are mixed at the ratio of 1:0, 3:1, 1:1, 1:3 and 0:1 for fixed electrolyte concentration of 10 wt%, applied voltage of 35 V, pulse frequency of 200 Hz and duty ratio of 45 %. It is clear from Fig. 5.16 that material removal rate is very high in direct polarity than that in reverse polarity. In direct polarity generation of bubbles due to chemical reactions at the negatively charged electrodes is more as the hydrogen and oxygen bubbles are produced at the ratio of 2:1 of volume due to dissociation of electrolyte at cathode and anode. So, the formation of insulating bubble layer becomes faster. Therefore the intensity of spark is very low for reverse polarity and thereby material removal rate is low. Fig. 5.16 exhibits that MRR is found higher for the ratio of 1:3 and lower for the ratio of 1:1 when the direct polarity is used. In case of reverse polarity, the opposite phenomena is observed and MRR is obtained lower for the ratio of 1:3 and higher for the ratio of 1:1.

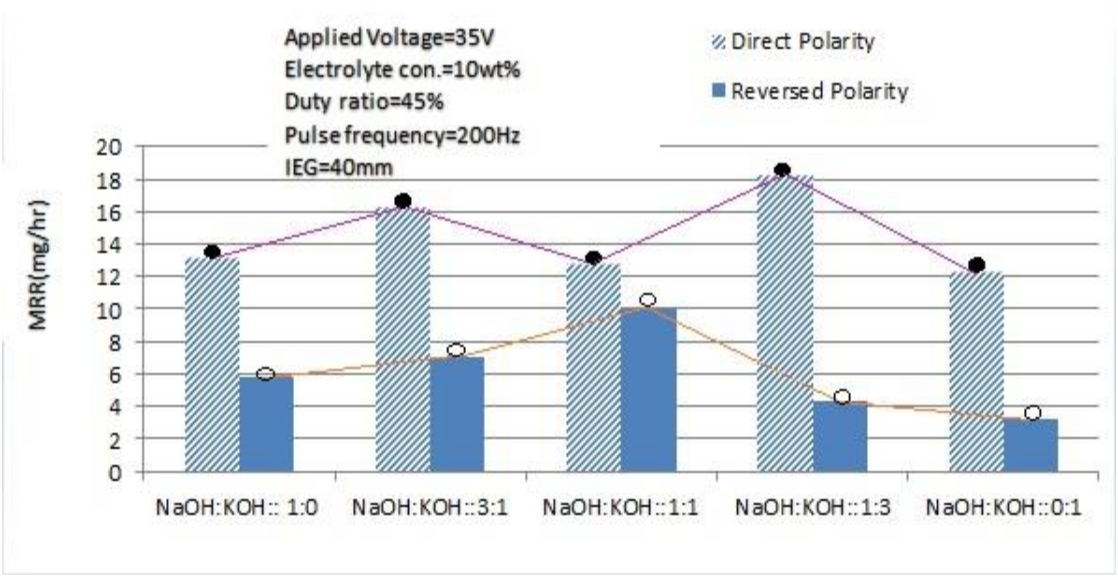

Fig. 5.16 Effect of polarities on MRR

5.2.7.2 Effect of Polarity on Overcut (OC)

In the present work, overcut has been compared for both polarities *i.e.* direct and reverse and a comparative study for overcut has been carried out between direct polarity and reverse polarity with varying five different types of electrolyte mixtures i.e., NaOH and KOH are mixed at the ratio of 1:0, 3:1, 1:1, 1:3 and 0:1. Fig. 5.17 shows the comparison of overcut between direct polarity and reverse polarity with five different mixtures of electrolyte. In the Fig. 5.17 it can be observed that overcut is small for the ratio of 3:1 in direct polarity and for the ratio of 0:1 for reversed polarity. While only NaOH electrolyte is used with direct polarity of power supply it provides higher overcut at 35V/200Hz/10wt%/40% duty ratio/IEG 40mm and at reverse polarity the mixture of 1:1 ratio provides higher overcut during micro-channel cutting on glass. In direct polarity number of side sparking is more due to faster bubble layer formation.

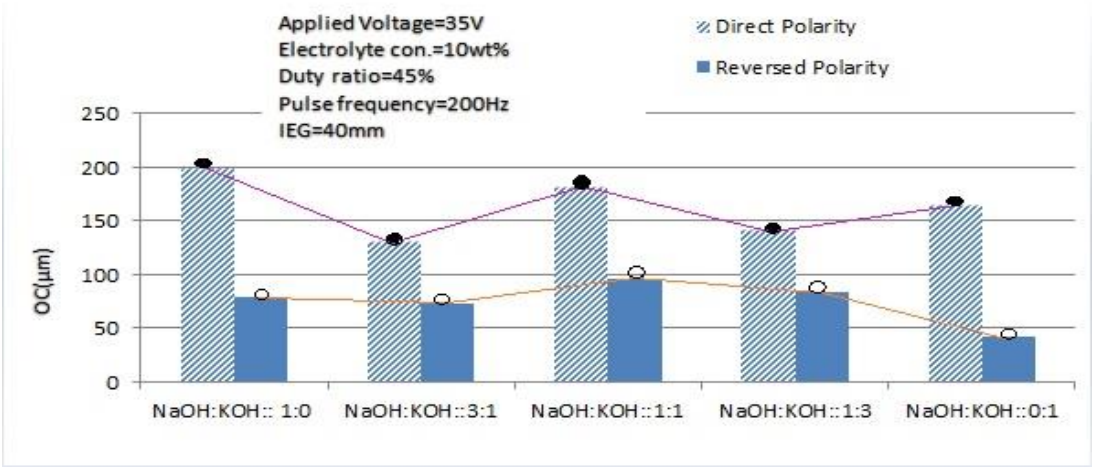

Fig. 5.17 Effect of polarities on OC

5.2.7.3 Effect of Polarity on Heat Affected Zone (HAZ) Area

The variation of heat affected zone has been compared for both polarities *i.e.* direct and reverse with varying five different types of electrolyte mixtures which are prepared by mixing NaOH and KOH at the ratio of 1:0, 3:1, 1:1, 1:3 and 0:1 and shown in Fig. 5.18. It is known that excessive heat can affect the micro structural properties of material. So in case of machining by µ-ECDM process HAZ can be produced, one should try to minimize HAZ for the sake of materials dimensions, physical properties and micro-structural properties. In comparative study of HAZ areas, it has been found that HAZ area is measured lower for the ratio of NaOH and KOH as 1:3 in the mixture at direct as well as revered polarity. From Fig. 5.18 it is assured that using only KOH electrolyte it provides higher HAZ at direct and reversed polarity. Further, HAZ area decreases with increase in the percentage of KOH in the

electrolyte mixture for both polarities and gets the lowest value for 1:3 weight ratio of NaOH and KOH electrolytes. The Fig. 5.19 shows the photographs of micro-tool after machining with direct polarity and reverse polarities. From these photographs it is clear more tool wear has occurred for direct polarity compared to that at reverse polarity.

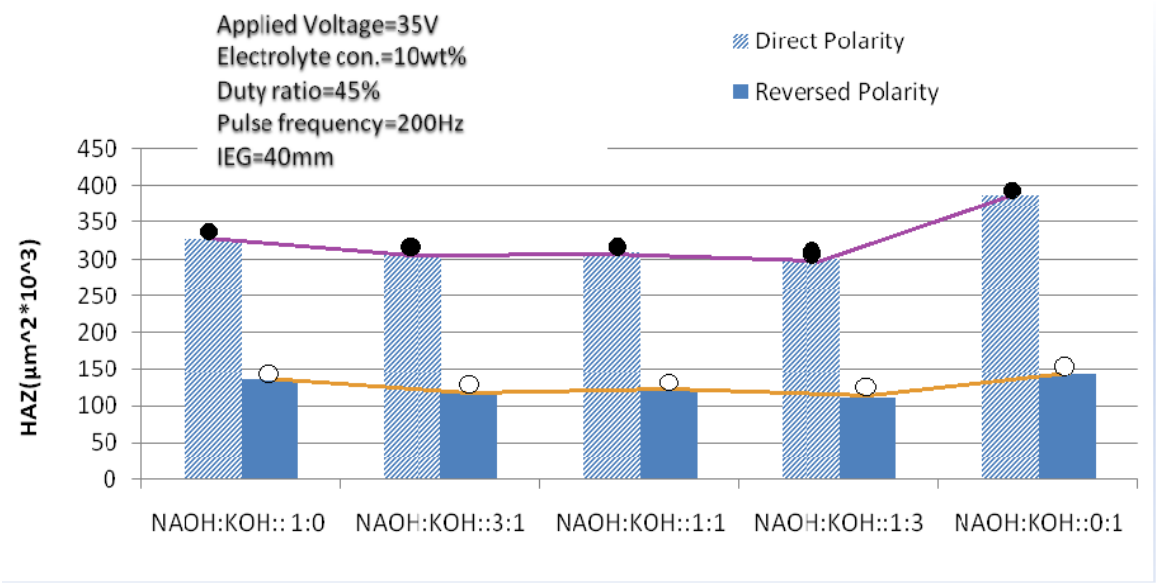

Fig. 5.18 Effect of polarities on HAZ

Conditions	Stainless steel Micro-tool
(a) After Machining with direct Polarity at 55V/45% duty ratio/20wt%/3:1 NaOH & KOH	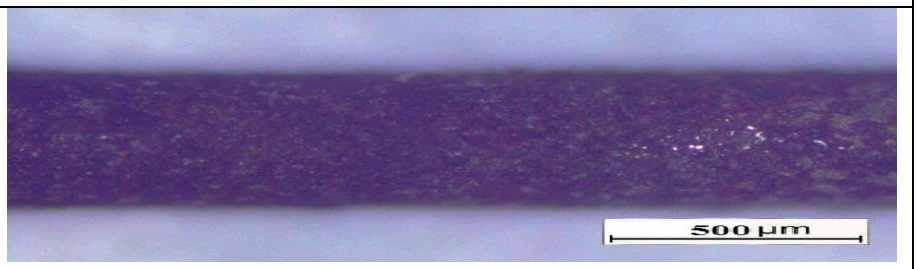
(b) After Machining with reverse Polarity at 50V/45% duty ratio/25wt%/1:13 NaOH & KOH	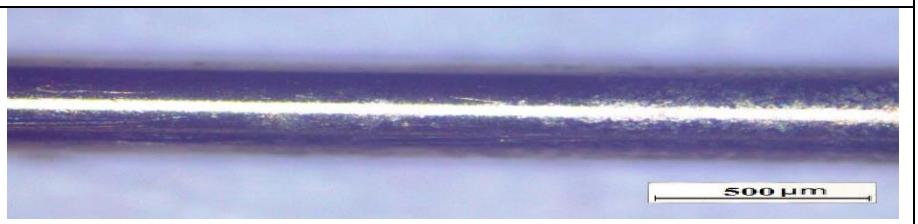

Fig. 5.19 Optical images of micro-tools using (a) direct and (b) reverse polarity before and after machining

5.2.7.4 Effect of Polarity on Machining Depth (MD)

In the present work, the machining depth has been compared for both polarities *i.e.* direct and reverse in five different mixtures of electrolyte solutions and exhibits in Fig. 5.20. The Fig. 5.20 clearly indicates that in case of reversed polarity the machining depth is obtained low because machining rate is low due to low sparking rate. It is found that for reversed polarity as well as direct polarity the 50-50% mixture of electrolytes provides lower machining depth whereas 3:1 ratio of NaOH and KOH electrolyte mixtures provides higher machining depth during micro-channel cutting on glass. The variation of machining depth is found similar for both polarities in five different mixtures.

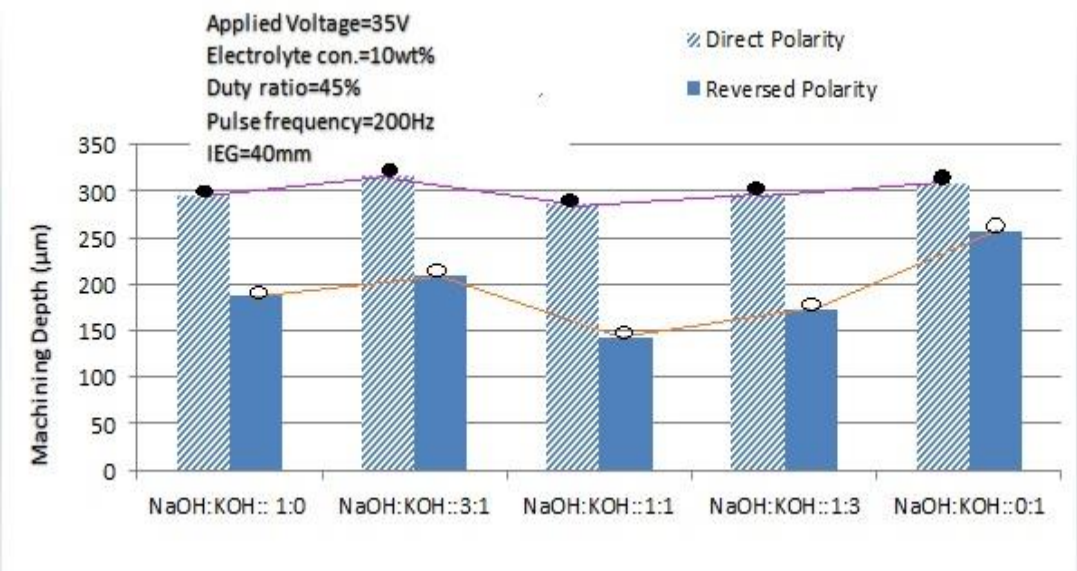

Fig.5.20 Effect of polarities on Machining Depth

5.2.7.5 Effect of Polarity on Surface Roughness (R_a)

Fig. 5.21 exhibits the effects of polarities of D.C. power supply on surface roughness for different mixtures of electrolyte. It can also be notice from the Fig. 5.21 that good surface finish can be achieved by using direct polarity rather than reverse polarity. In direct polarity uniform sparking rate is high whereas in revered polarity uniform sparking rate is comparatively low. There is a tendency to stray around the cutting zone; as a result

irregularities are formed on the machining zone and the value of surface roughness becomes higher. From this observation it can be predicted that direct polarity is better than reverse polarity in case of surface texture of machined zone of the job specimen. From the Fig. 5.21 it is found that at 10wt% of electrolyte mixture at the ratio 0:1 solution gives more irregular surface and causes higher surface roughness at reversed polarity whereas the ratio of 3:1 provides lower surface roughness in case of reverse polarity. For direct polarity the ratio of 1:3 of NaOH and KOH provides higher surface roughness comparatively to other types and lower for the ratio of 3:1.

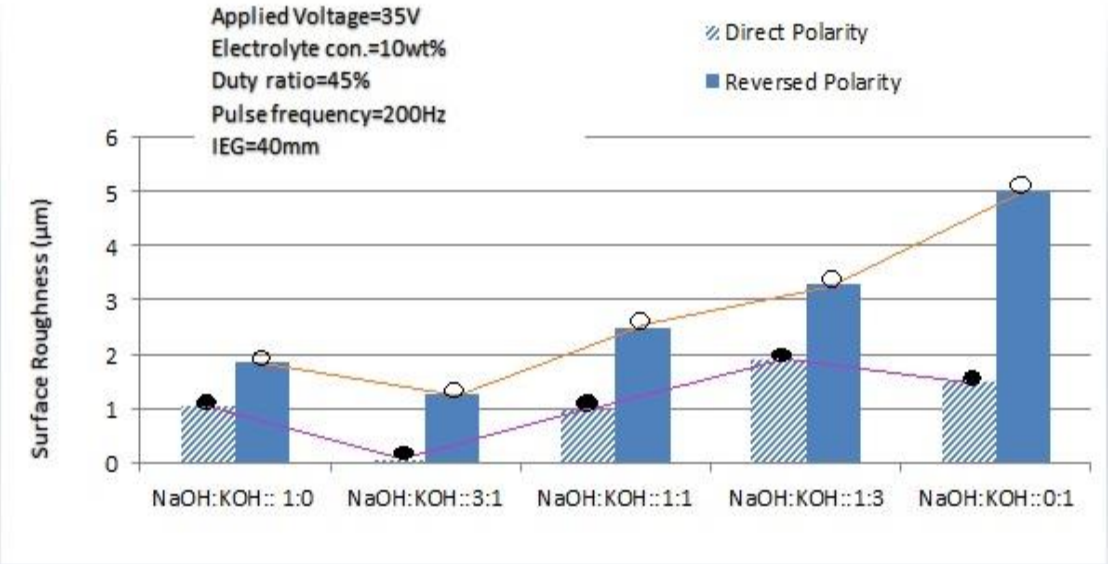

Fig.5.21 Effect of polarities on Surface Roughness

5.2.7.6 Effect of Polarity on Tool Electrode Wear Rate (TEWR)

Tool electrode wear rate has been compared for both polarities *i.e.* direct and reverse in five different types of electrolyte mixture i.e., NaOH and KOH are mixed at the ratio of 1:0, 3:1, 1:1, 1:3 and 0:1 and are shown in Fig. 5.22. It is observed from Fig. 5.22 that more tool electrode wear rate is occurred in case of direct polarity compared to the reverse polarity. In direct polarity sparking rate is high compared to that in revered polarity and higher temperature raises in the cutting zone, as a results more tool wear is occurred in case of direct or straight polarity. From the Fig. 5.22 it is found that more tool wear rate is occurred due to higher rate of sparking at direct polarity with 10wt% of 0:1 ratio of NaOH and KOH electrolyte mixture and 1:3 ratio provides lower tool wear rate for both direct and reverse polarity. The tool wear rate initially starts at 45 V for stainless steel micro-tool for direct as

well as reverse polarity during micro-machining by ECDM process. Tool wear rate is found low in case of mixed electrolyte compared to NaOH and KOH electrolyte. But increasing of material removal rate is the main target, so direct polarity is the best polarity for the micro-channel cutting on glass by µ-ECDM process. When micro-tool acts as cathode (-ve), H_2 bubble generates and accumulate on tool surface and O_2 accumulates at anode, but when reverse polarity is used, reverse phenomenon is occurred. Sparking takes place from tool electrode. SEM images of micro-channel cutting on glass are exhibited in Fig. 5.23 using various electrolyte solutions and at different machining conditions.

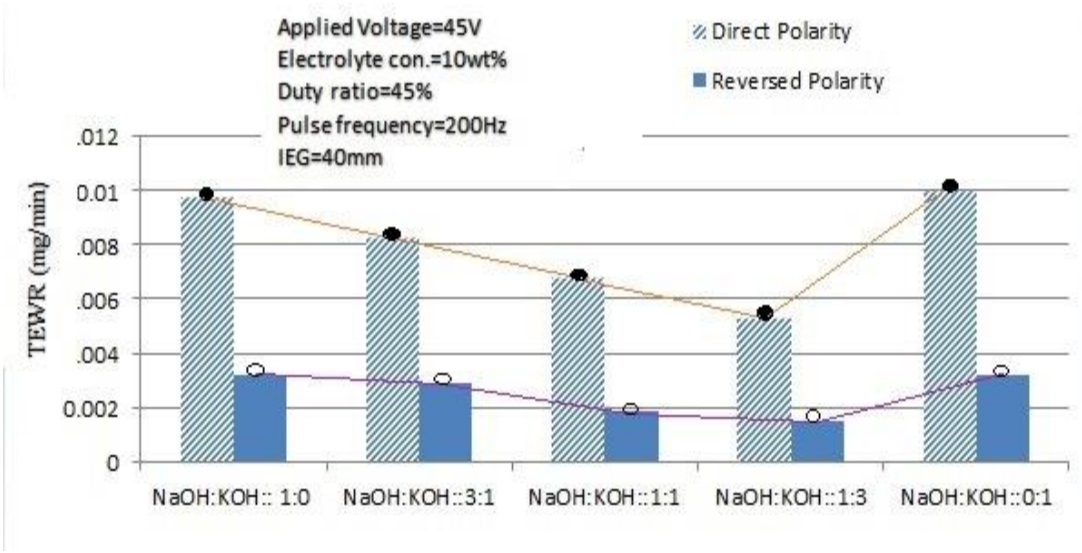

Fig.5.22 Effect of polarities on Tool Electrode Wear Rate (TEWR)

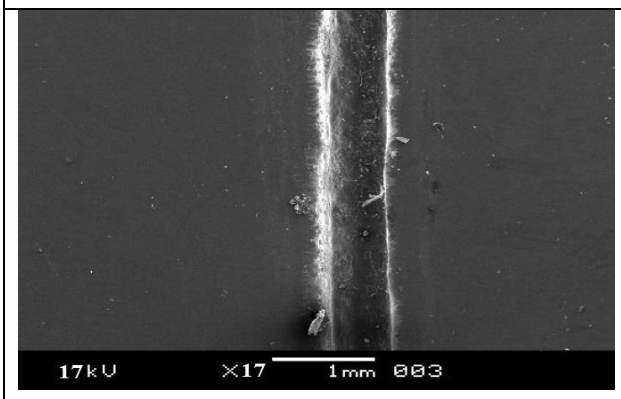

(a) at direct polarity 35V/10wt% NaOH:KOH::3:1 200Hz/45%

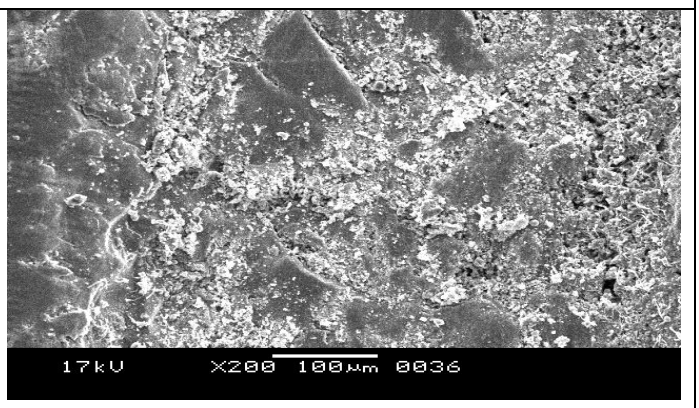

(b) at reverse polarity 35V/10wt%/ NaOH:KOH::0:1/200Hz/45%

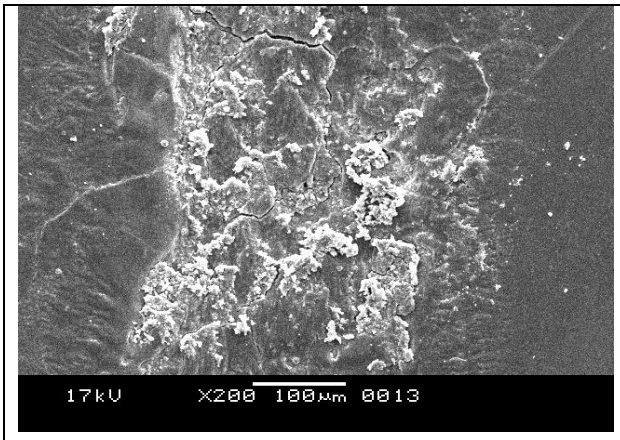

(c) at reverse polarity 35V/10wt% NaOH:KOH::3:1 /200Hz/45%

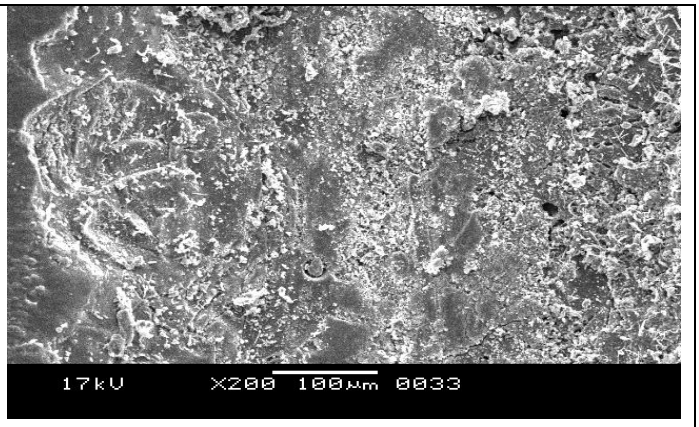

(d) at reverse polarity 35V/10wt% NaOH:KOH::1:3 /200Hz/45%

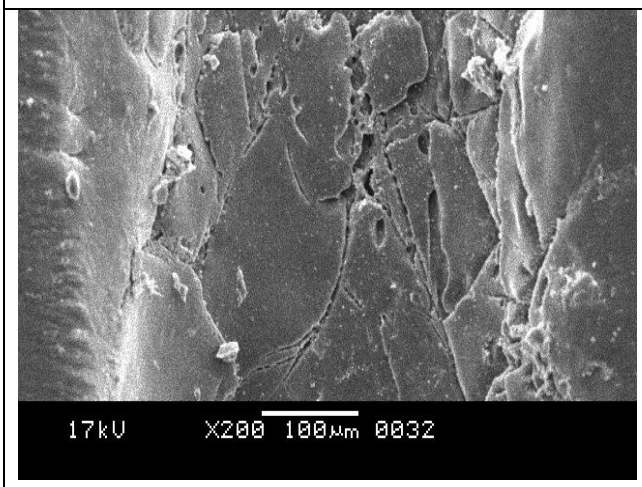

(e) at direct polarity,50V/20wt% NaOH:KOH::3:1 /200H/45%

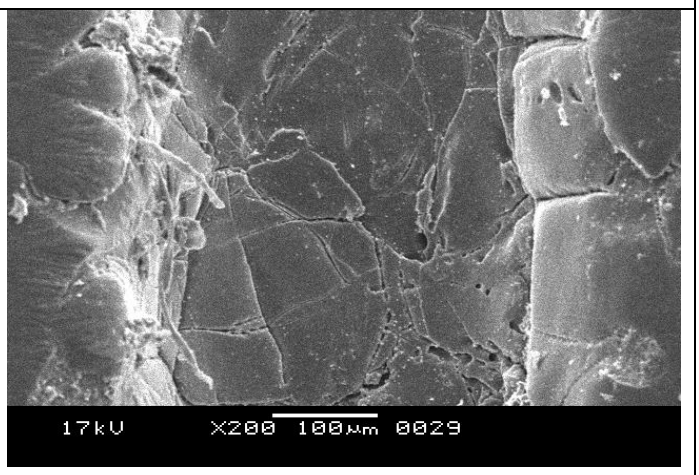

(f) at direct polarity, 50V/15wt% NaOH:KOH::3:1 /200H/45%

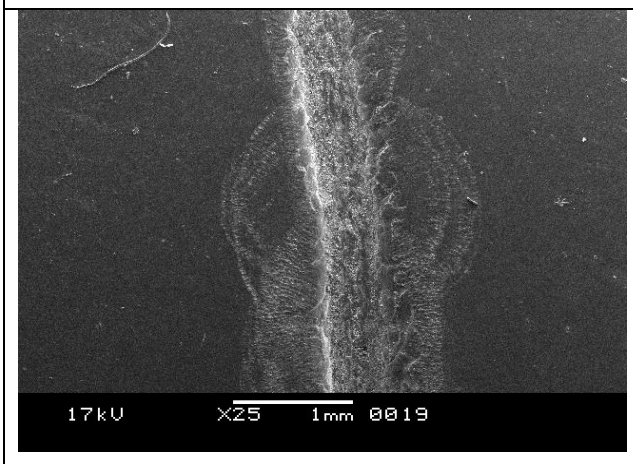

(g) at direct 50V/10wt% NaOH:KOH::1:3 /200Hz/45%

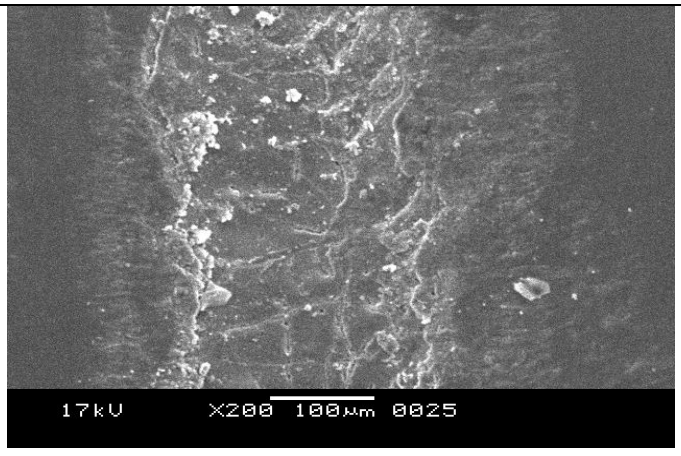

(h) at reverse polarity, 35V/10wt% NaOH:KOH::1:3/200Hz/45%

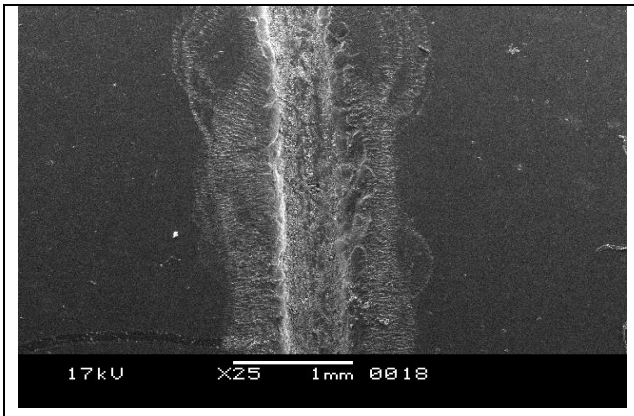

(i) at direct 35V/10wt% NaOH:KOH::1:3 /200Hz/45%

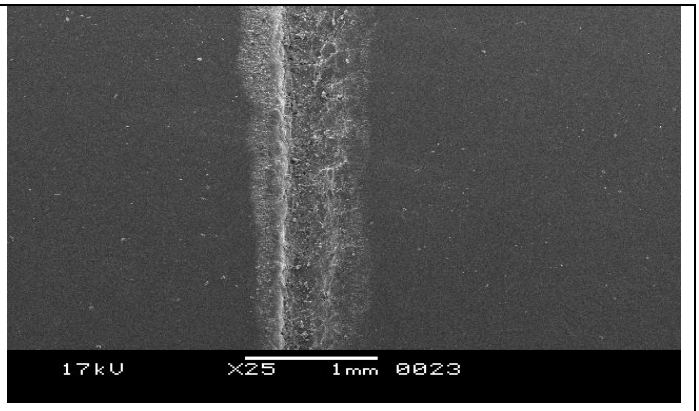

(j) at direct 35V/10wt% NaOH:KOH::3:1 /200Hz/45%

Fig. 5.23 SEM images of micro-channel cutting at different conditions

5.2.8 Outcomes of the Present Research Work

In the present research work the parametric analysis as well as comparative study has been carried out successfully using different electrolytes and tool polarities in the developed µ-ECDM set up. From the present research work it has been observed that MRR increases with the increase of applied voltage, electrolyte concentration, duty ratio but decrease with pulse frequency when any type of electrolyte is used for micro-channel cutting on glass with µ-ECDM process. Overcut always increases with increase of applied voltage and it has predominant effects on OC for any type of electrolyte. But it increases with increase of concentration and with duty ratio. Also it decreases with increase of pulse frequency up to 600Hz but after that OC increases. HAZ area increase with increase of applied voltage and HAZ is lower at 20wt% and 55% duty ratio. Initially HAZ area decreases with increasing pulse frequency and after 800Hz it increase. Machining depth increases when applied voltage and electrolyte concentration increases but after 55 V, MD decreases. Increasing of duty ratio, MD increases. Surface roughness is increased when applied voltage, duty ratio and electrolyte concentration are increased but pulse frequency has least effect on surface roughness. It is observed that the material removal rate (MRR) becomes higher for NaOH:KOH::1:3/55 V, pulse frequency of 200 Hz/IEG 40mm and duty ratio of 45 % at direct polarity. The overcut becomes smaller for NaOH:KOH::3:1 solution at 35 V. HAZ area is found lower at NaOH:KOH::3:1 at 10wt%, pulse frequency of 200 Hz and duty ratio of 45% and using NaOH:KOH::3:1 electrolyte solution, µ-ECDM provides the highest

machining depth (MD) at direct polarity. Using the mixture of electrolyte in the ratio NaOH:KOH::3:1, it provides lower surface roughness for reverse polarity and NaOH:KOH::1:3 gives better surface finish when electrolyte concentration is increased up to 25 wt%. Using direct polarity and NaOH:KOH::1:3 electrolyte mixture, it provides higher surface roughness. It is observed from Scanning Electron Microscopy (SEM) images that surface texture of μ-channel on glass varies with different process parameters and micro-cracks are observed for both direct as well as reverse polarity. From SEM analysis of micro-channel little debris are found and thermal effect is clearly observed.

The present investigation is not sufficient for predicting the responses of μ-ECDM process during μ-channel cutting operation. Also this does not give any clear idea about the optimised results as well as optimal parametric setting, which is very much needed in industries. Also, the interactive effects of different process parameters need to investigate so that the exact behaviour of the process can be identified at the intermediate levels as well as outside the range of process parameters. Further, from this investigation, it is clear that the machining performances are affected by energy distribution, which is generated during spark discharges and there is an urgent need to control this energy distribution during sparking so that the optimal performances can be obtained during μ-channelling operation. Therefore, next set of investigation will be carried out on modelling and optimisation of process parameters during μ-channel cutting on glass by ECDM process.

5.3 INVESTIGATIONS INTO MACHINING CRITERIA THROUGH RESPONSE SURFACE METHODOLOGY (RSM) AND GENETIC ALGORITHAM (GA) BASED APPROACH

5.3.1 EXPERIMENTAL PLANNING

For analysing the effects of applied voltage, electrolyte concentration, duty ratio and pulse frequency on different machining criteria such as Material Removal Rate (MRR), Overcut (OC), Heat Affected Zone (HAZ) and Surface Roughness (R_a) with the machining condition during micro-channel cutting on glass have been shown in Table 5.9 and 5.10 respectively.

Other parameters such as inter-electrode gap and length of stainless steel tool have been kept fixed as 40mm and 10mm respectively. The micro-tool just touches the job specimen during experimentation and controlled by spring feed mechanism. Silica glass slide was chosen as work piece material to cut micro-channel. During experimentations one parameter has been varied while other process parameters were fixed at low levels within their respective ranges in order to expect minimum effects of these parameters. As high heat is formed during ECDM process a new identical micro-tool was always used for each experiment as tool wear rate (TWR) may be occurred.

In this experimental investigation for machining by µ-ECDM, each variable was coded and the upper level was taken as +1 and the lower level as – 1 of every process parameters in order to design the experiments (DOE) in an optimized way by choosing face centred design (FCD) of response surface methodology. Flat end cylindrical stainless steel tool of 250µm diameter was used for each experiment and the experiments were conducted in a NaOH solution with varying the electrolyte concentration. The process parameters *i.e*. voltage, electrolyte concentration, duty ratio and pulse frequency have been varied as 35-55 V; 20-30wt%; 40-60%, and 200-1000 Hz respectively.

Table 5.9 Different parametric combinations

SL. NO	Voltage (V)	Electrolyte con. (wt%)	Duty ratio (%)	Pulse frequency (Hz)
1	35	20	40	200
2	55	20	40	200
3	35	30	40	200
4	55	30	40	200
5	35	20	60	200
6	55	20	60	200
7	35	30	60	200
8	55	30	60	200
9	35	20	40	1000
10	55	20	40	1000
11	35	30	40	1000
12	55	30	40	1000
13	35	20	60	1000
14	55	20	60	1000
15	35	30	60	1000
16	55	30	60	1000
17	35	25	50	600
18	55	25	50	600
19	45	20	50	600
20	45	30	50	600
21	45	25	40	600
22	45	25	60	600

23	45	25	50	200
24	45	25	50	1000
25	45	25	50	600
26	45	25	50	600
27	45	25	50	600
28	45	25	50	600
29	45	25	50	600
30	45	25	50	600
31	45	25	50	600

5.3.2 EXPERIMENTAL RESULTS AND DISCUSSION

Three set of experiments have been conducted at each parametric combination according to Table 5.9 and the average value of results as shown in Table 5.10 were considered for analyses. The experimental results were calculated based on equation 4.1 and using Leica microscope and tally surf instruments.

Table 5.10 Experimental Results at different parametric combinations

SL. NO	MRR (mg/hr)	OC (µm)	HAZ (µm^2)x10^3	Surface Roughness R_a(µm)
1	72.93	212.856	264.12	1.2387
2	88.65	265.234	384.23	1.7980
3	102.48	186.430	336.80	1.4873
4	122.42	288.240	580.24	2.3881
5	77.56	254.650	271.34	1.2700
6	86.87	294.432	296.70	1.3200
7	102.56	155.240	323.22	1.4077
8	112.24	309.447	532.20	1.7560
9	35.55	108.365	259.78	1.3100
10	46.31	202.234	392.24	2.0413
11	68.45	106.356	279.11	1.2540
12	76.56	299.586	528.43	2.2890
13	64.34	104.856	271.23	1.3978
14	68.22	264.494	333.80	1.6948
15	88.38	104.874	265.11	1.2050
16	102.24	309.584	412.30	1.6952
17	77.47	132.299	218.90	1.2060
18	84.54	302.867	369.30	1.8460
19	48.42	273.223	288.66	1.6114
20	72.36	264.494	380.12	1.7240
21	56.44	210.265	248.00	1.6003
22	72.64	208.000	201.60	1.3931
23	87.32	278.376	342.24	1.9686

24	60.24	243.243	334.00	2.0830
25	66.18	254.212	267.34	1.6850
26	66.12	257.278	268.12	1.7045
27	65.82	252.278	269.15	1.7070
28	66.15	258.320	267.12	1.7023
29	62.24	256.342	264.98	1.7120
30	64.24	256.876	265.71	1.6980
31	64.26	258.387	266.98	1.7021

5.3.2.1 Development of Empirical Models Based on RSM

Mathematical model has been developed to correlate the µ-ECDM process parameters and the co-efficient of those parameters during micro-channel cutting on glass. Design of experiment (DOE) features of MINITAB software was utilized to obtain the second order rotatable face centred design (FCD). The empirical model using co-efficient of those parameters on MRR, OC, HAZ and R_a of µ-ECDM has been established and expressed as Eq.(5.2)., Eq.(5.3) ,Eq.(5.4) and Eq.(5.5) respectively.

$$Y_u\,(MRR) = 65.318 + 5.463X_1 + 14.380X_2 + 5.848X_3 - 13.486X_4 + 15.32X_1^2 - 5.30X_2^2 - 1.15X_3^2 + 8.09X_4^2 + 0.745X_1X_2 - 1.113X_1X_3 - 1.128X_1X_4 - 1.128X_2X_3 + 0.470X_2X_4 + 6.473X_3X_4 \quad \text{Eq. (5.2)}$$

$$Y_u\,(OC) = 252.53 + 65.01X_1 + 2.443X_2 + 7.00X_3 - 27.85X_4 - 30.61X_1^2 + 20.67X_2^2 - 39.06X_3^2 + 12.62X_4^2 + 19.27X_1X_2 + 7.32X_1X_3 + 18.95X_1X_4 - 8.20X_2X_3 + 14.27X_2X_4 + 0.39X_3X_4 \quad \text{Eq. (5.3)}$$

$$Y_u\,(HAZ) = 271.16 + 74.44X_1 + 48.64X_2 - 20.30X_3 - 14.17X_4 + 18.15X_1^2 + 58.44X_2^2 - 51.15X_3^2 + 62.17X_4^2 + 31.78X_1X_2 - 18.83X_1X_3 - 0.40X_1X_4 - 4.03X_2X_3 - 20.51X_2X_4 - 2.20X_3X_4 \quad \text{Eq. (5.4)}$$

$$Y_u\,(Ra) = 1.70341 + 0.28066X_1 + 0.08468X_2 - 0.12595X_3 - 0.01865X_4 - 0.1796X_1^2 -$$

$$0.0379X_2^2 - 0.2089X_3^2 + 0.3202X_4^2 + 0.07104X_1X_2 - 0.12756X_1X_3 + 0.04344X_1X_4 - 0.04057X_2X_3 - 0.08832X_2X_4 + 0.01606X_3X_4 \quad \text{Eq. (5.5)}$$

Here, X_1 = Voltage, X_2= Electrolyte concentration, X_3= duty ratio and X_4= pulse frequency.

5.3.2.2 Adequacy Test for Developed Models

Response surface regression analysis on MRR, OC, HAZ and R_a considering different influencing parameters as independent variables has been made using coded units. From the analysis it can be concluded that applied voltage, electrolyte concentration, pulse frequency and duty ratio, square and interaction effects of these parameters are significantly influencing for controlling MRR, OC, HAZ and R_a as the p-value of each term are less than 0.05. To test the developed model whether the data is fitted well in the model or not, the calculated S values of the regression analysis for MRR, OC, HAZ and R_a are obtained as 2.362, 13.144, 12.814 and 0.030 respectively. The values of R^2 and adj-R^2 for MRR, OC, HAZ and R_a are 99.21% & 98.51%, 97.77% & 95.82%, 98.94% & 98.01% and 99.48% & 99.02% respectively reveal the presence of significant terms in those mathematical models. Hence, the data for each response are well fitted in the developed models.

In the ANOVA test, P value and F-ratio test were used for justification of adequacy of the developed mathematical models. Tables 5.11-5.14 show the analysis of variance (ANOVA) test results for MRR, OC, HAZ and Ra respectively. The calculated values of F-ratio for the lack-of-fit are found to be less than the standard F-ratio values (2.32260) for 10 DOF or 4.6 for 5 DOF or P value 0.05 for MRR, OC, HAZ and surface roughness. Therefore, it can be assured that the second order regression models are adequate at 95% confidence level with 10 degrees of freedom (DOF) or 5 DOF to present the relationship between the micro-machining performances and machining parameters of µ-ECDM process. Estimated regression coefficients and analysis of variance for those machining criteria suggest that these models adequately fit the experimental data. Figs. 5.24 (a) –(d) show the individual standardized effects of parametric dominancy on MRR, OC, HAZ and R_a.

Table 5.11 Analysis of Variance (ANOVA) test results for MRR

Source	DOF	SS	MSS	F	P
Regression	14	11146.9	796.21	142.69	0.000
Linear	4	8148.3	2037.07	365.06	0.000
Square	4	2255.4	563.86	101.05	0.000
Interaction	6	743.2	123.86	22.20	0.000
Lack-of-Fit	10	75.9	7.59	2.35	0.074
Pure Error	6	13.4	2.23		
Total	30		R^2 for MRR = 99.21%	Adj-R^2 for MRR=98.94%	

Table 5.12 Analysis of Variance (ANOVA) test results for OC

Source	DOF	SS	MSS	F	P
Regression	14	121351	8667.9	50.17	0.000
Linear	4	91026	22756.5	131.72	0.00
Square	4	13445	3361.2	19.46	0.000
Interaction	6	16880	2813.3	16.28	0.000
Lack-of-Fit	10	2734	273.4	2.25	0.000
Pure Error	6	30	5		
Total	30		R^2 for OC = 98.51%	Adj-R^2 for OC=98.01%	

Table 5.13 Analysis of Variance (ANOVA) test results for HAZ

Source	DOF	SS	MSS	F	P

Regression	14	245284	17520.3	106.69	0.000
Linear	4	153341	38335.4	233.45	0.000
Square	4	63045	15761.2	95.98	0.000
Interaction	6	28898	4816.3	29.33	0.000
Lack-of-Fit	10	2616	261.6	2.18	0.000
Pure Error	6	12	2		
Total	30		R^2 for HAZ = 97.77%	Adj-R^2 for HAZ=99.48%	

Table 5.14 Analysis of Variance (ANOVA) test results for Surface Roughness (R_a)

Source	**DOF**	**SS**	**MSS**	**F**	**P**
Regression	14	2.78745	0.19910	218.05	0.000
Linear	4	1.83876	0.45969	503.44	0.000
Square	4	0.42215	0.10554	115.58	0.000
Interaction	6	0.52654	0.08776	96.11	0.000
Lack-of-Fit	10	0.01417	0.00142	1.55	0.001
Pure Error	6	0.00043	0.00007		
Total	30		R^2 for R_a = 95.82%	Adj-R^2 for R_a = 99.02%	

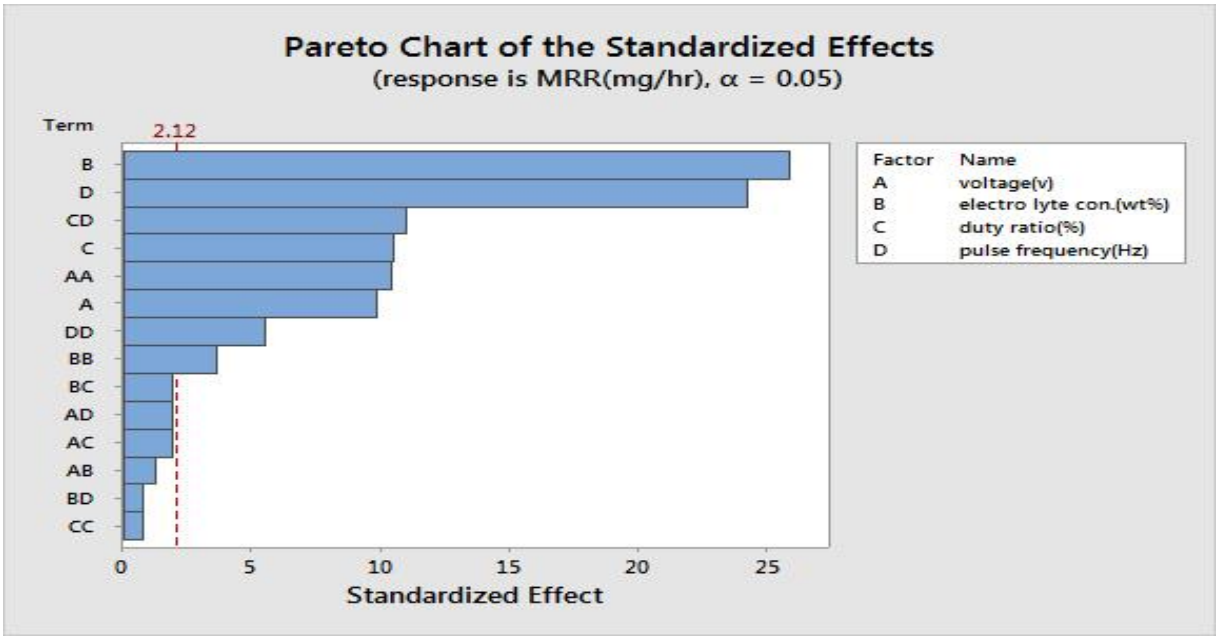

(a) Pareto chart of the effect of individual parameter on MRR

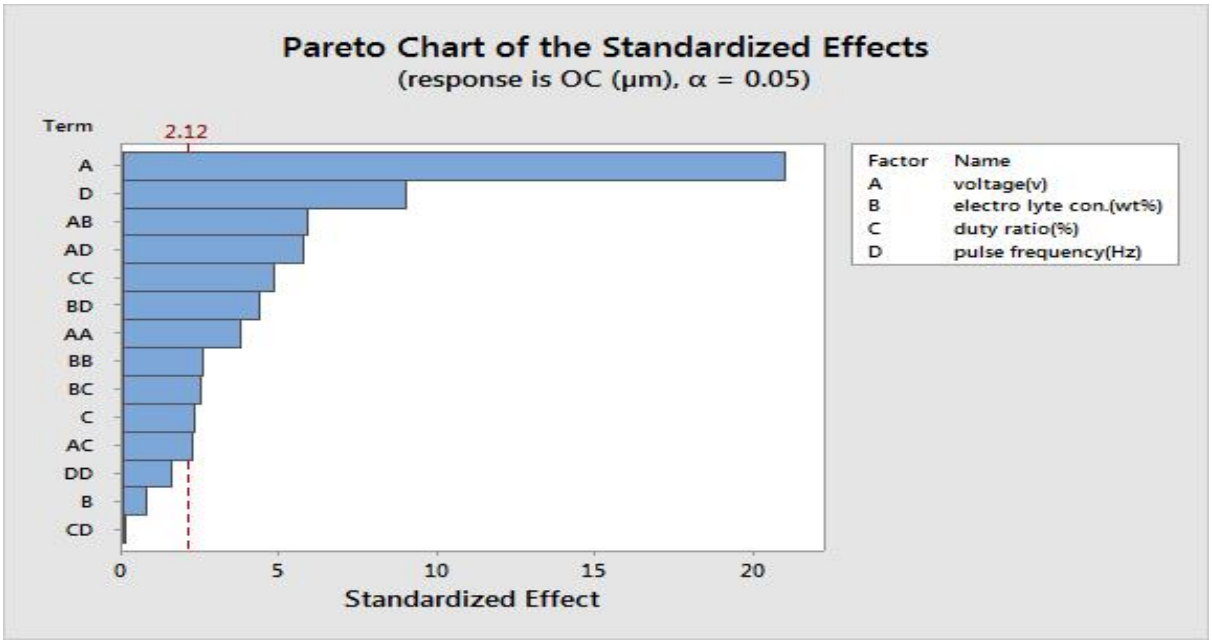

(b) Pareto chart of the effect of individual parameters on OC

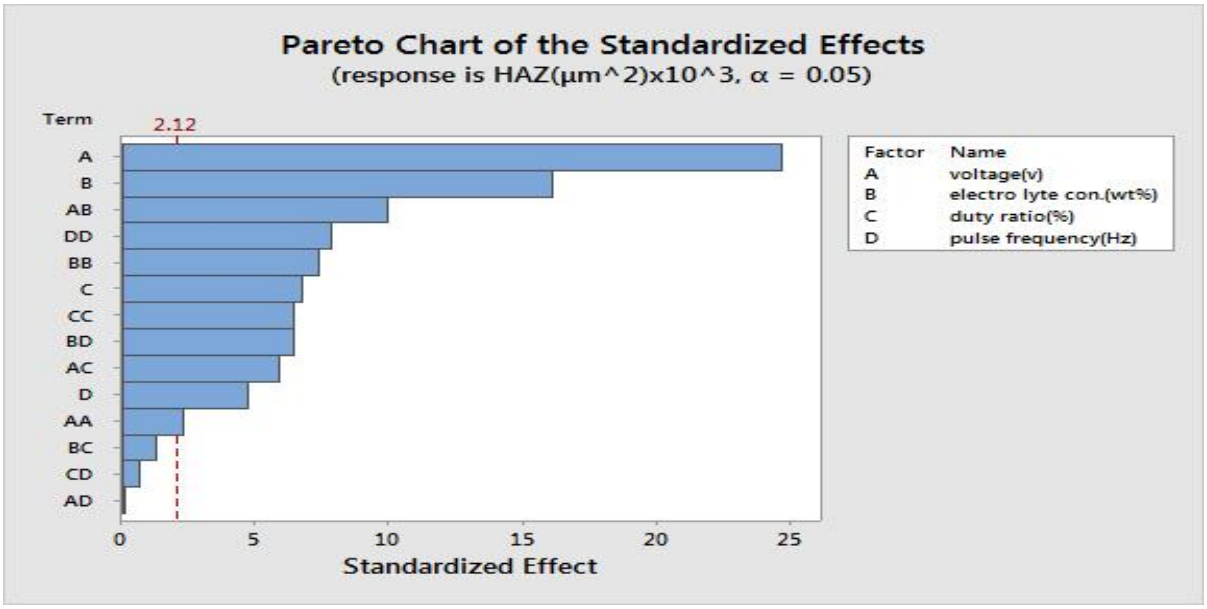

(c) Pareto chart of the effect of individual parameters on HAZ

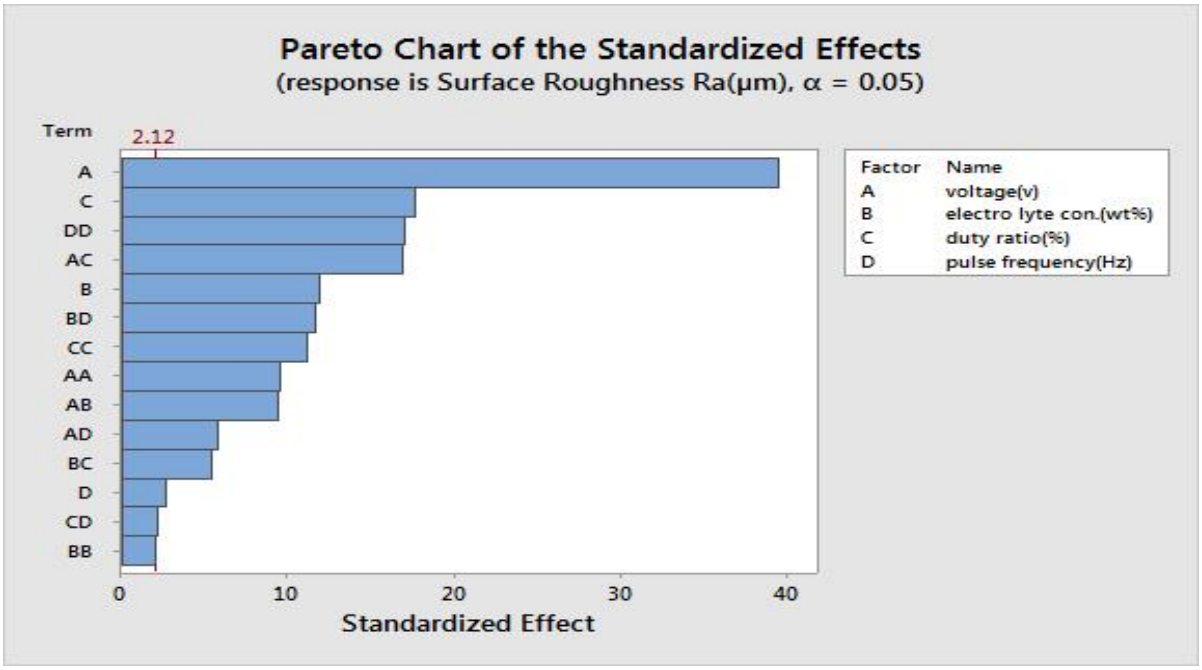

(d) Pareto chart of the effect of individual parameters on Surface Roughness

Figs. 5.24 (a) – (d) Standardized effects of parametric dominancy on (a) MRR, (b) OC,(c) HAZ and (d) surface roughness (Ra)

5.3.2.3 Analysis of the Parametric Influences Based on Developed Models

The average values of the three set of experimental results thus obtained, were used and plotted in graph to analysis the influences of the various process parameters on various machining characteristics. The influences of applied voltage, electrolyte concentration, duty ratio and pulse frequency on average material removal rate for fixed inter-electrode gap (40mm) when micro- channel is cut on glass using NaOH electrolyte are shown in Figs. 5.25 (a) -(c) respectively. From the Fig 5.25 (a) it is observed that MRR is increased when voltage is increased because the sparking rate becomes higher as increasing voltage but at 45 V MRR is comparatively low and become higher at 30wt% of electrolyte and lower at 20 wt% when the voltage is 55 V, is found from respective mathematical model analysis. Experimental results are shown as dotted line that also revealed the mathematical models. It is propounded that at 55V/25 wt%/600Hz/50%/IEG 40mm machining rate is better to achieve maximum material removal for micro-channel cutting on glass. From the Fig. 5.25 (b) MRR increases with the increasing of duty ratio and electrolyte concentration based on mathematical modeling as well as experimental results. MRR increased due to increase of duty ratio because pulse on time is increased, so rate of discharge increased. From the Fig. 5.25 (c) it is clear that MRR decreases as pulse frequency is increases, keeping other parameters constant and it is obvious that at 200Hz, MRR is higher and at 1000Hz is lower.

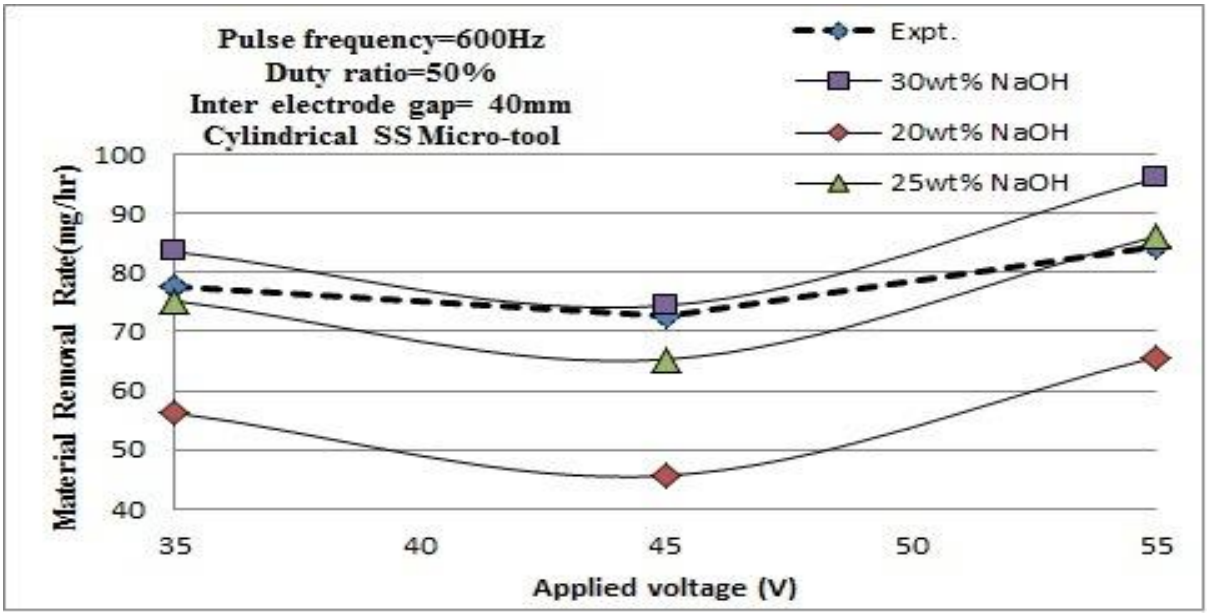

(a) Effect of applied voltage on MRR

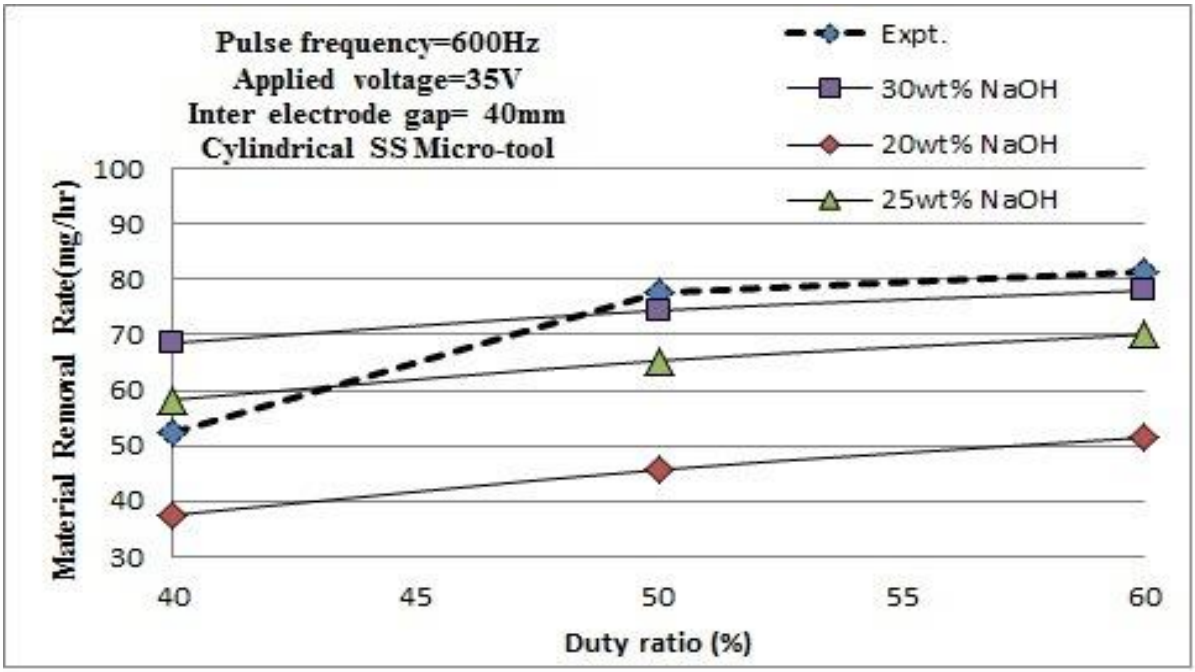

(b) Effect of duty ratio on MRR

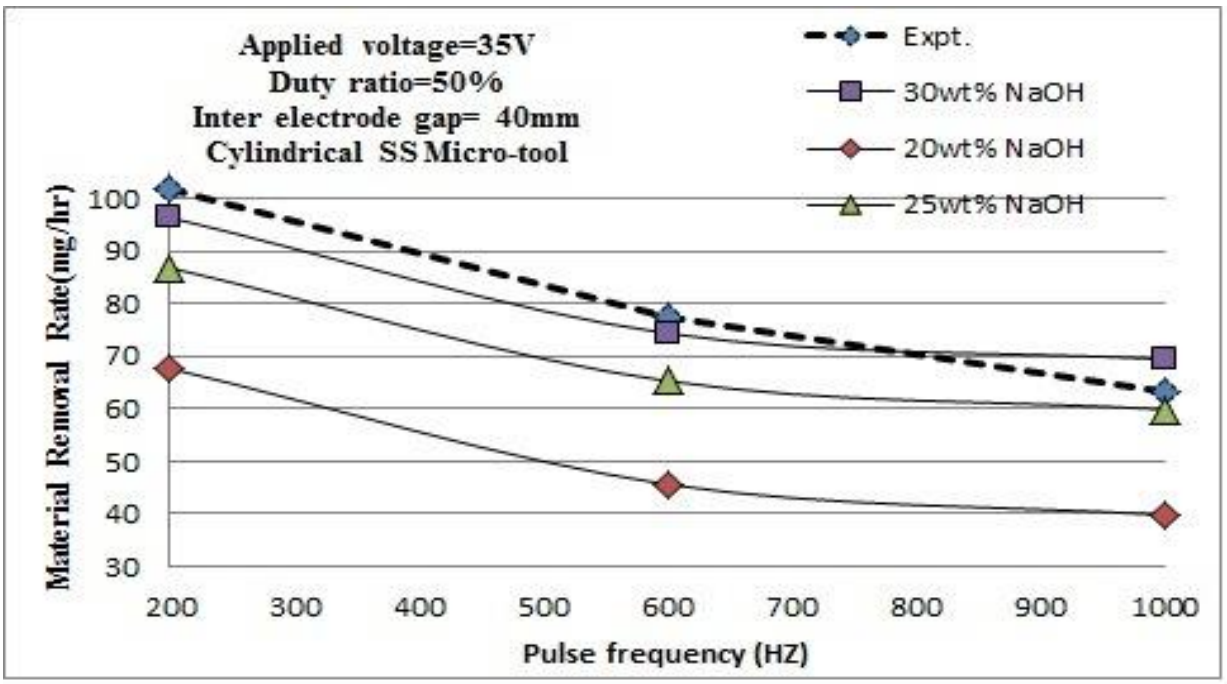

(c) Effect of pulse frequency on MRR

Figs. 5.25 (a) - (c) Effect of (a) applied voltage, (b) duty ratio and (c) pulse frequency on MRR

Figs. 5.26 (a) - (c) exhibits the influences of applied voltage, electrolyte concentration, duty ratio and pulse frequency respectively on average overcut using NaOH as electrolyte. Generally, rate of sparking increases with the increase of both applied voltage and electrolyte concentration and consequently increases not only MRR but also width of cut due to side wall sparking from the tool electrode and thereby increases overcut. From the Figs. 5.26 (a)-(c) it is clear that overcut increases with increase of voltage, duty ratio and decreases with increase of pulse frequency. From the Figs. 5.26 (a)-(b) it is found that overcut increases to increase applied voltage due to increasing discharge rate with violent spark and hydrogen bubble assemble in the side wall of the tool, so side sparking also happened and increasing duty ratio up to 50% OC increases and at 60% of duty ratio OC decreases, if other process parameters are kept constant. From Fig. 5.26 (c) it is observed that OC is decreased when pulse frequency increases because intensity of discharge become low and it is found that at 200Hz OC is higher.

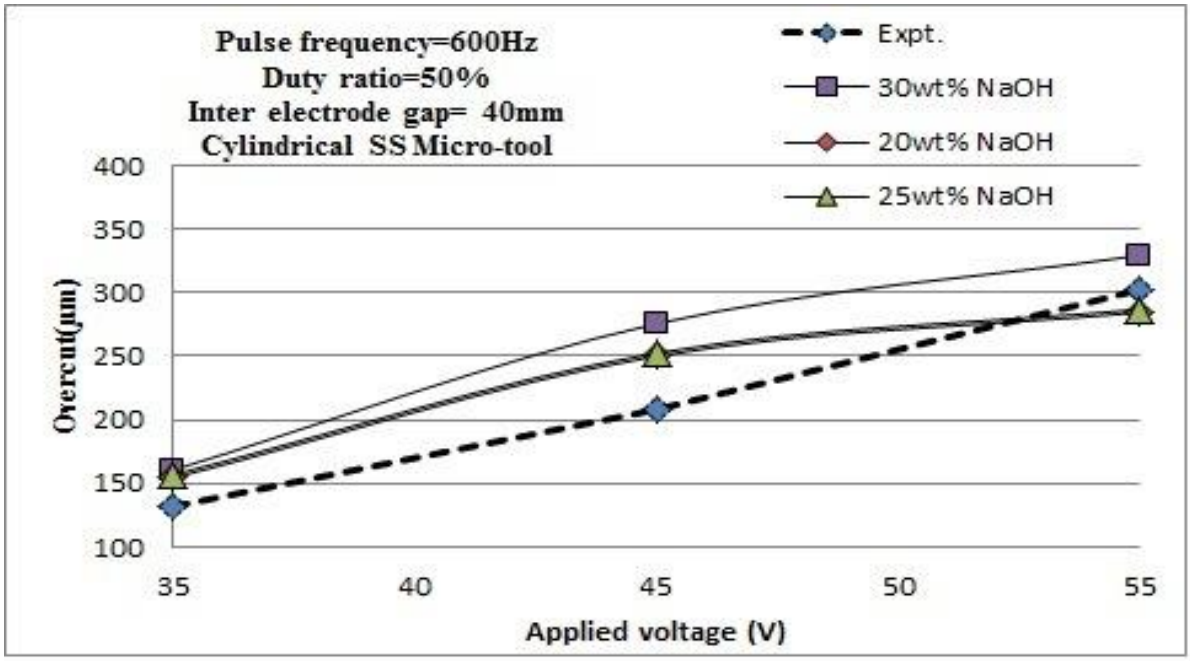

(a) Effect of applied voltage on OC

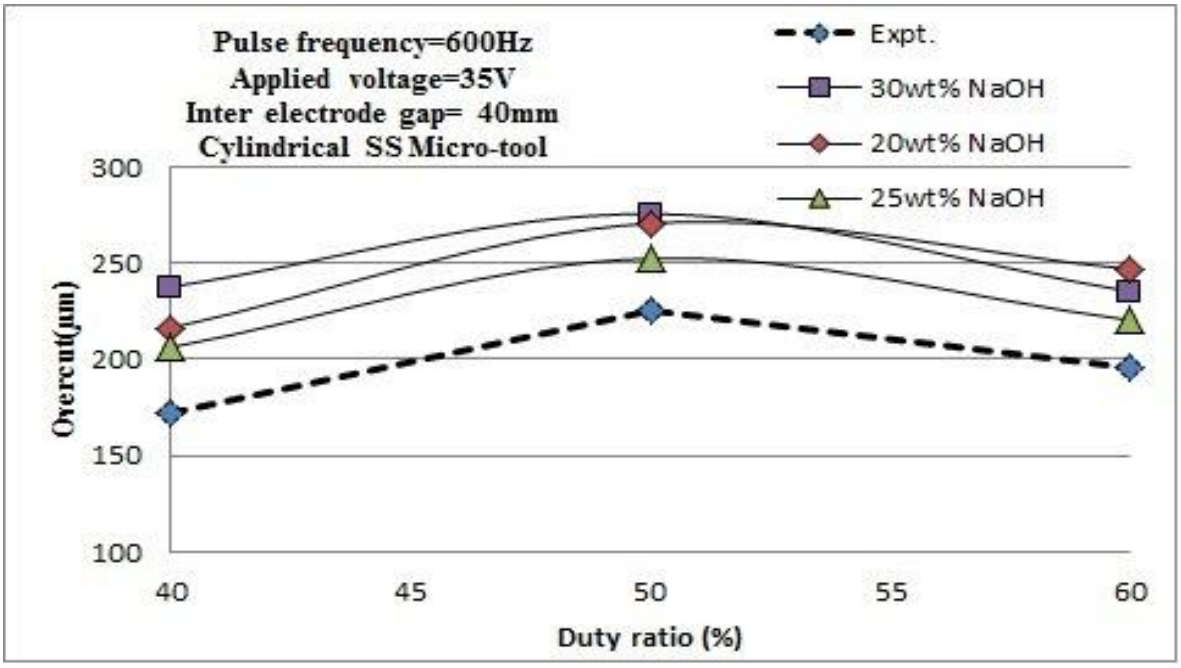

(b) Effect of duty ratio on OC

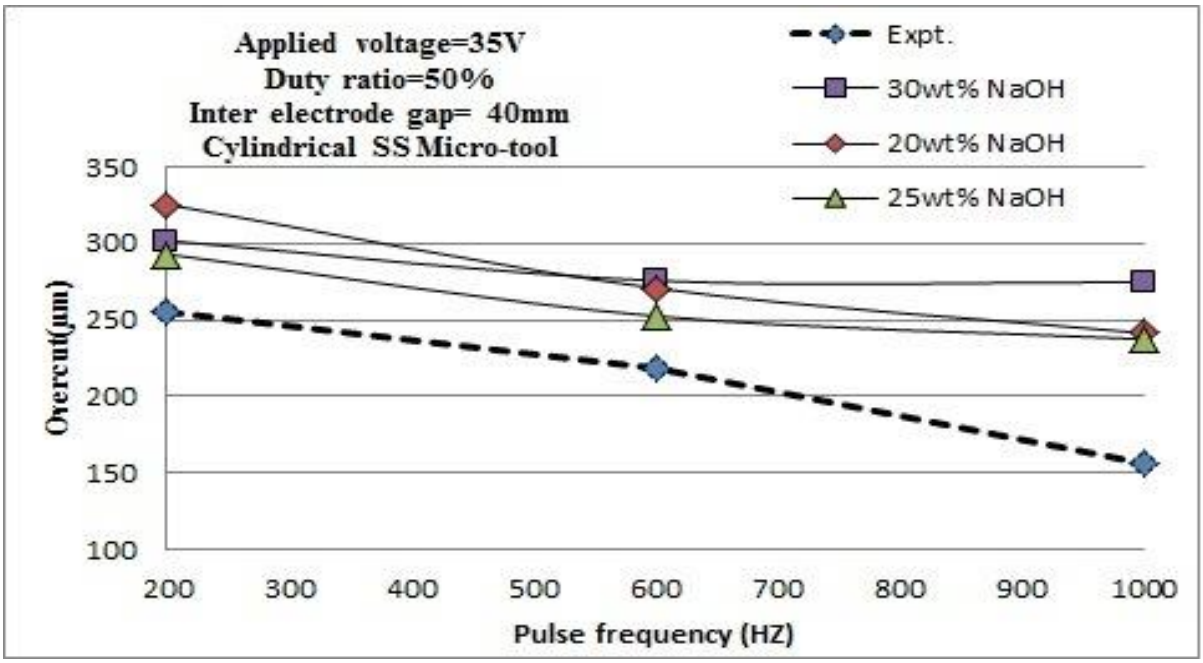

(c) Effect of pulse frequency on OC

Figs. 5.26 (a) - (c) Effect of (a) applied voltage, (b) duty ratio and (c) pulse frequency on Overcut.

Figs. 5.27 (a) - (c) show the influences of applied voltage, electrolyte concentration, duty ratio and pulse frequency on average heat affected zone (HAZ) area. In ECDM process a large amount of heat is generated during the micro-machining on glass. A little portion of this heat is radiated, some is absorbed to the electrolyte by convection and remainder is conducted

to the job specimen. The main cause of the HAZ formation around the machining zone is due to the heat energy conducted to the job specimen. It is observed from Fig. 5.27 that HAZ area almost gradually increases with increase of applied voltage, electrolyte concentration and duty ratio and it becomes higher at 55v/30 wt%. From the Fig. 5.27 (a) it can be highlighted that voltage has a predominant effect on HAZ and higher electrolyte concentration has the highest effectiveness on it. From the Fig. 5.27 (b) it is tendered that HAZ is comparatively lower at 40% duty ratio, keeping other parameters constant. The experimental results reveal that HAZ area can be reduced by decreasing the duty ratio after 50 % and increasing the pulse frequency of the applied voltage up to 600 Hz. From the Fig. 5.27 (c) it is observed that at lower pulse frequency, sparking rate become higher that causes higher heat affected zone and it is found at 600Hz lower HAZ formed and at 200Hz higher when varying pulse frequency, keeping other parameter constant.

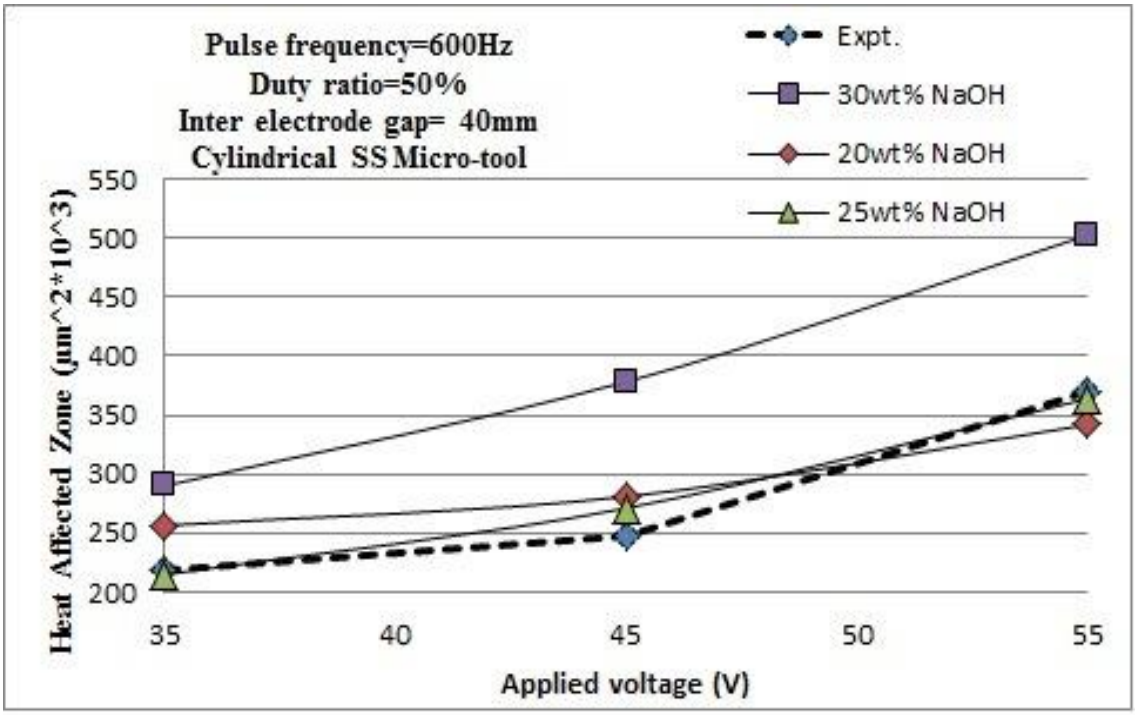

(a) Effect of applied voltage on HAZ

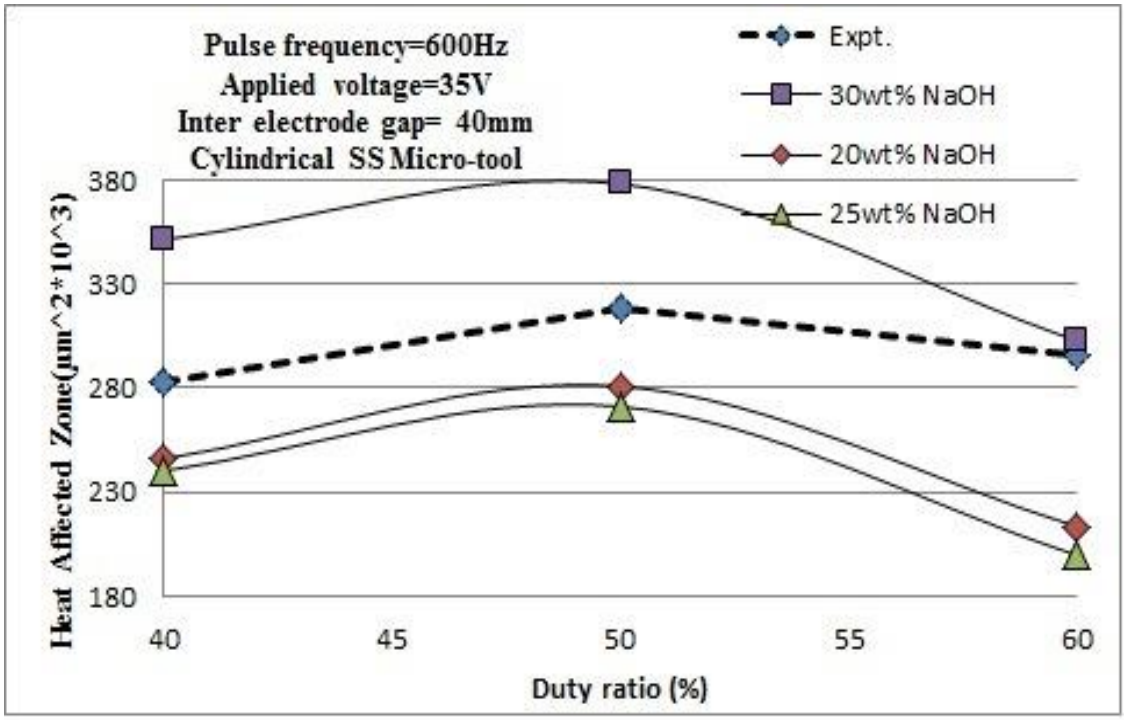

(b) Effect of duty ratio on HAZ

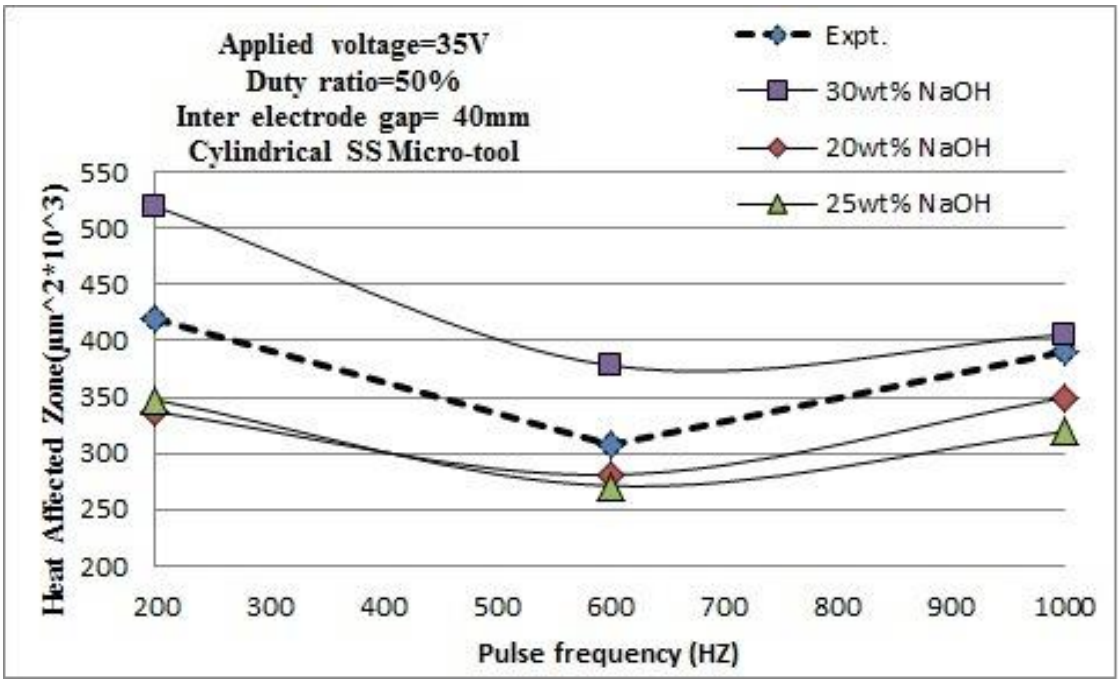

(c) Effect of pulse frequency on HAZ

Figs. 5.27 (a) - (c) Effect of (a) applied voltage, (b) duty ratio and (c) pulse frequency on Heat Affected Zone

The influences of applied voltage, electrolyte concentration, duty ratio and pulse frequency on surface roughness when micro-channel is cut on glass using NaOH as

electrolyte are shown in Figs. 5.28 (a) - (c) respectively. From the Figs. 5.28 (a)-(b) it is clear that surface roughness increases as voltage and duty ratio is increased due to increase in sparking rate but it decreases only at 50 V, 25% electrolyte concentration and 55% duty ratio. The surface texture of micro-channel becomes more irregular at higher voltage due to high thermal shock. Large amount of heat is produced into the machined channel during sparking and as a result, HAZ area increases and makes irregularities on the surface of the job specimen that increased surface roughness of the micro-channel. If the rate of sparking is continuous and stray sparking is less, side wall sparking reduced then better surface finish may be found. From the Fig. 5.28 (c) it is observed that if pulse frequency is increased, initially surface roughness is decreased because pulse on-time is decreased since the rate of sparking and stray sparking are reduced. But at higher pulse frequency, it is very difficult to control the continuous sparking that causes irregularities on the machining surface. So, after that surface roughness is increased.

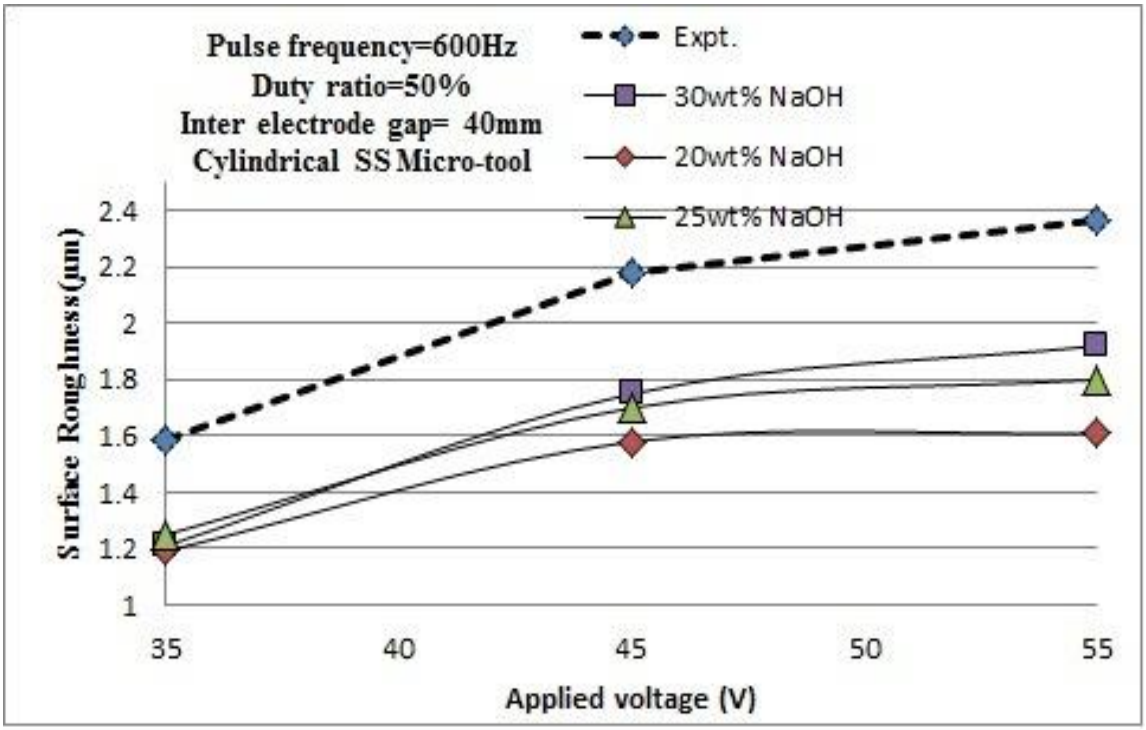

(a) Effect of applied voltage on surface roughness

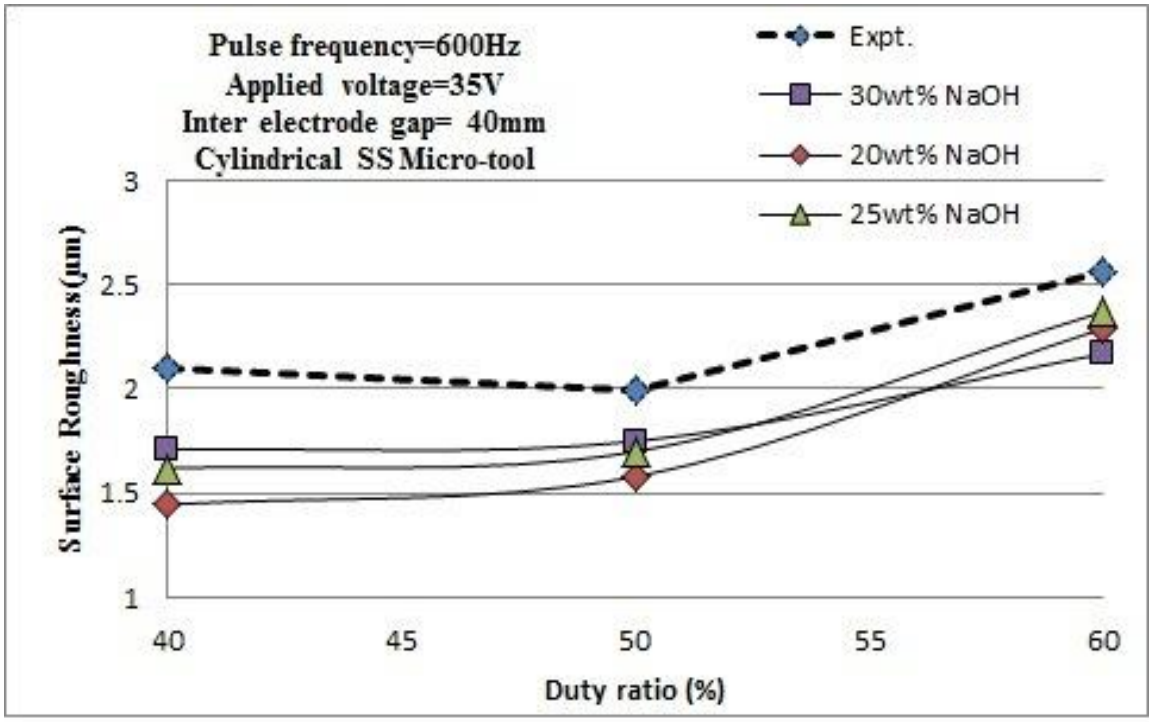

(b) Effect of duty ratio on surface roughness

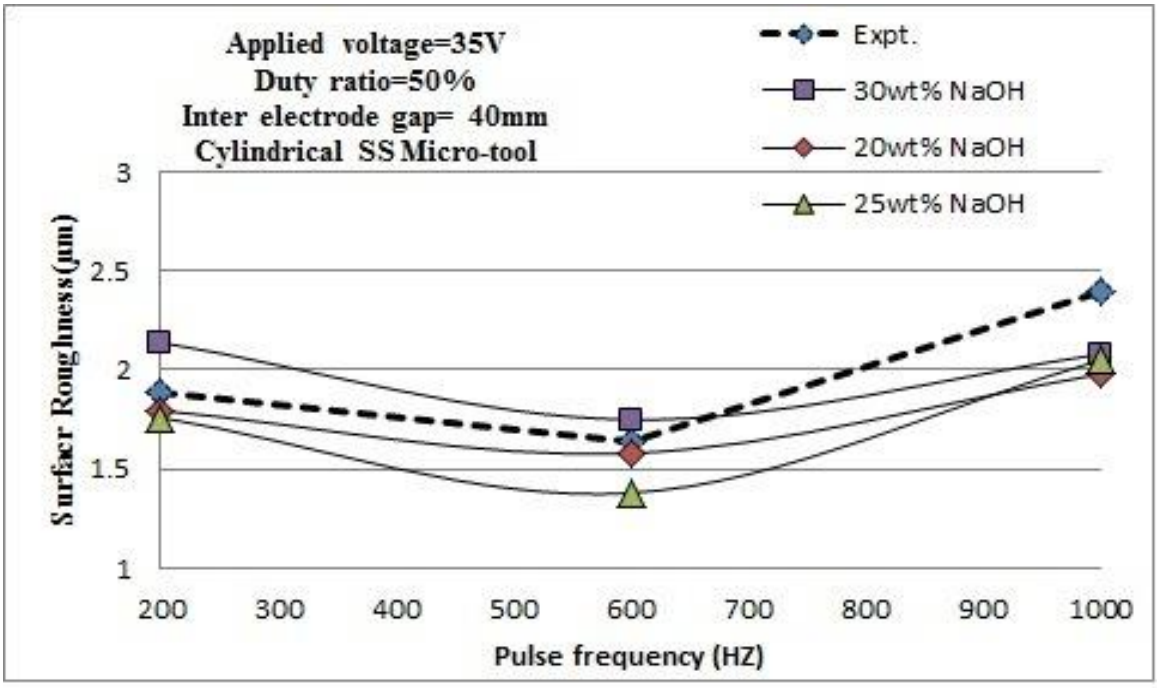

(c) Effect of pulse frequency on surface roughness

Figs. 5.28 (a) - (c) Effect of (a) applied voltage, (b) duty ratio and (c) pulse frequency on Surface roughness (R_a)

5.3.2.4 Determination of Optimal Parametric Conditions

To select the optimal parametric combinations in trial and error method is an exhaustive task and it consumed longer time and cost on account of large number of experimentations. So this is undesirable in industry. Hence an optimized technique is highly needed to overcome this problem so that the optimized conditions can be attained at a shorter time with least cost and will be helpful to industry. In this investigations single as well as multi objective optimization was done by using desirable function analysis and genetic algorithms. The following sections include the discussion on determination of single as well as multi objective optimization conditions.

5.3.2.4.1 Single Objective Optimization for Maximum MRR, Minimum OC, Minimum HAZ and Surface Roughness (R_a)

Fig. 5.29 shows the graphical view of single optimization for MRR, OC, HAZ and R_a and it is found that optimized MRR is 119.8768mg/hr at the parametric combination 55V/30wt%NaOH/40%/200Hz. It is found that minimum OC (82.33μm) in 35V/26wt%NaOH/60%/1000Hz and minimum HAZ (160.76 X 10^3 μm^2) at 55V/25wt%NaOH/60%/644Hz and also the minimum surface roughness (0.963μm) is achieved at 35V/30wt%NaOH/60%/660Hz using desirability function analysis. Fig. 5.30 show the graphical view of single optimization for MRR, OC, HAZ and R_a based on GA and it is found that maximum MRR is 119.963mg/hr at the parametric combination 55V/30wt%NaOH/40%/200Hz. It is found that minimized OC (81.8577μm) in 35V/26wt%NaOH/60%/1000Hz and minimized HAZ (159.632 X 10^3 μm^2) at 35V/24.553wt%NaOH/60%/645Hz and also the minimum surface roughness (0.94642μm) are achieved at 35V/20wt%NaOH/40%/525Hz based on GA.

Single objective optimization using RSM	Graphical view and Optimized condition
For Maximized MRR	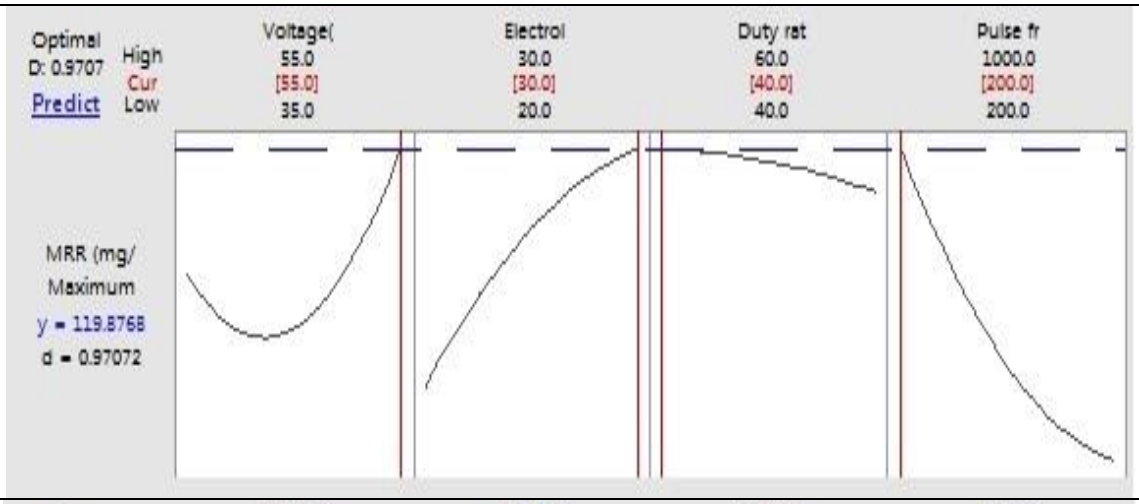
For Minimized OC	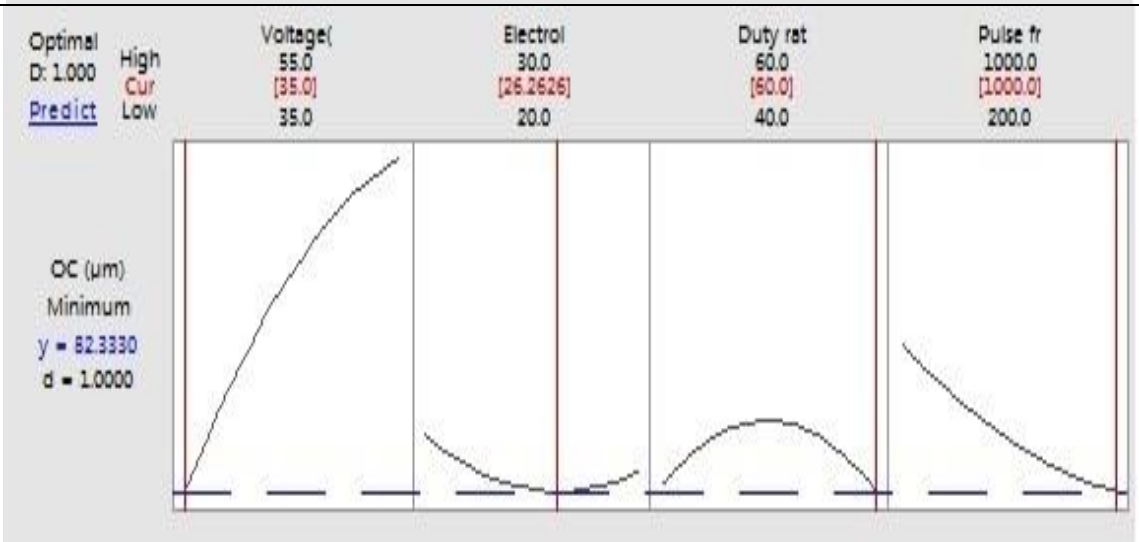
For Minimized HAZ	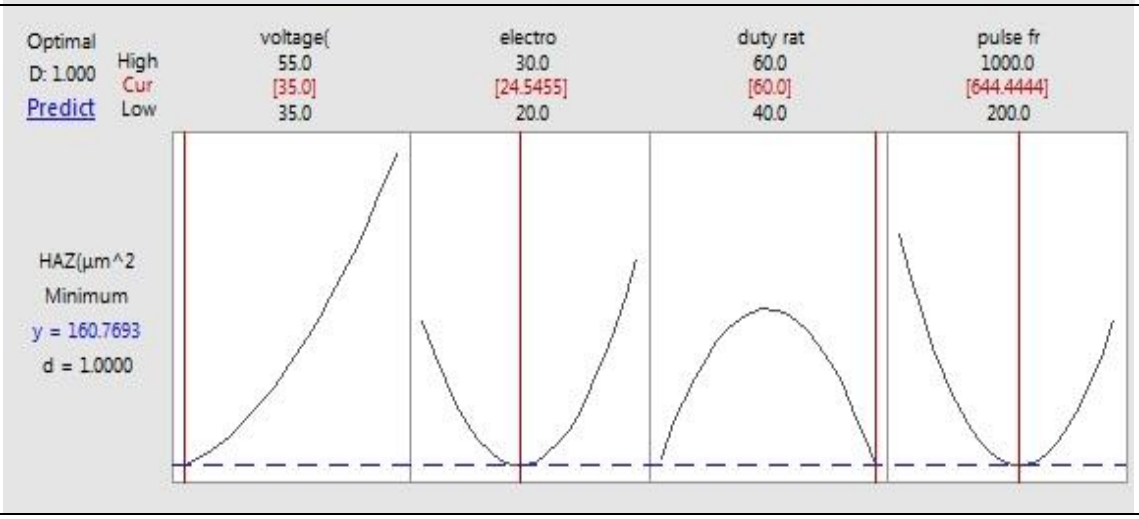

For Minimized Surface Roughness	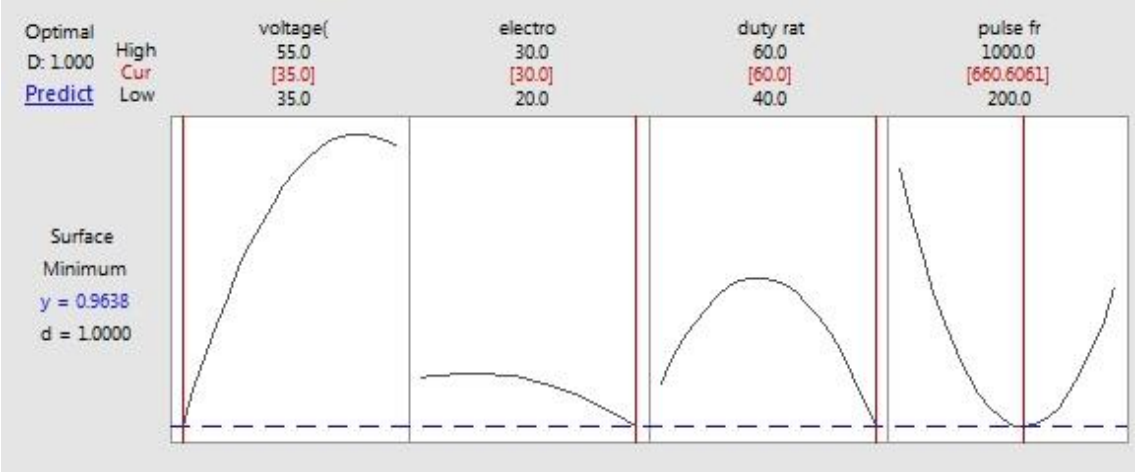

Fig. 5.29 Graphical view of single optimization of MRR, OC, HAZ and surface roughness based on desirability function analysis

Single objective optimization Based on GA	**Graphical view of Best Fitness and Optimized condition**
For Maximized MRR	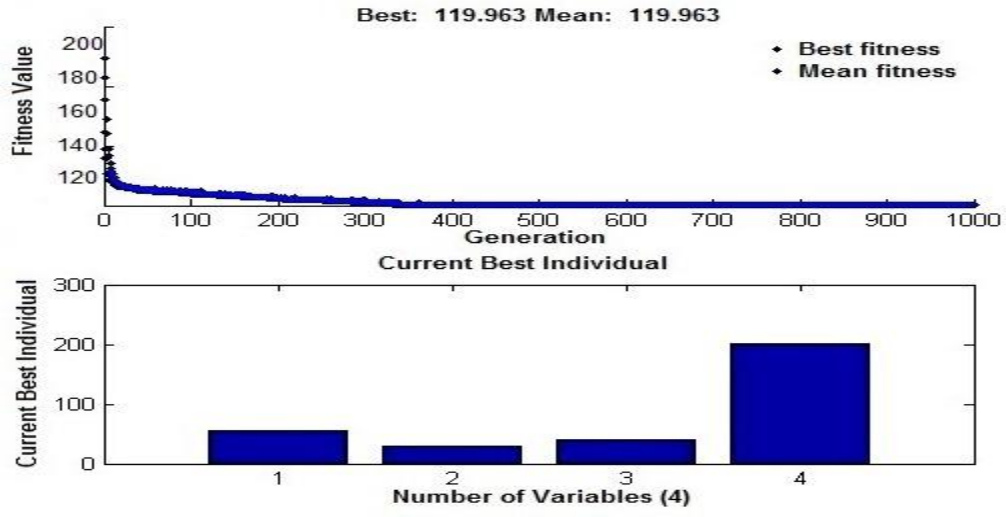

For Minimized OC	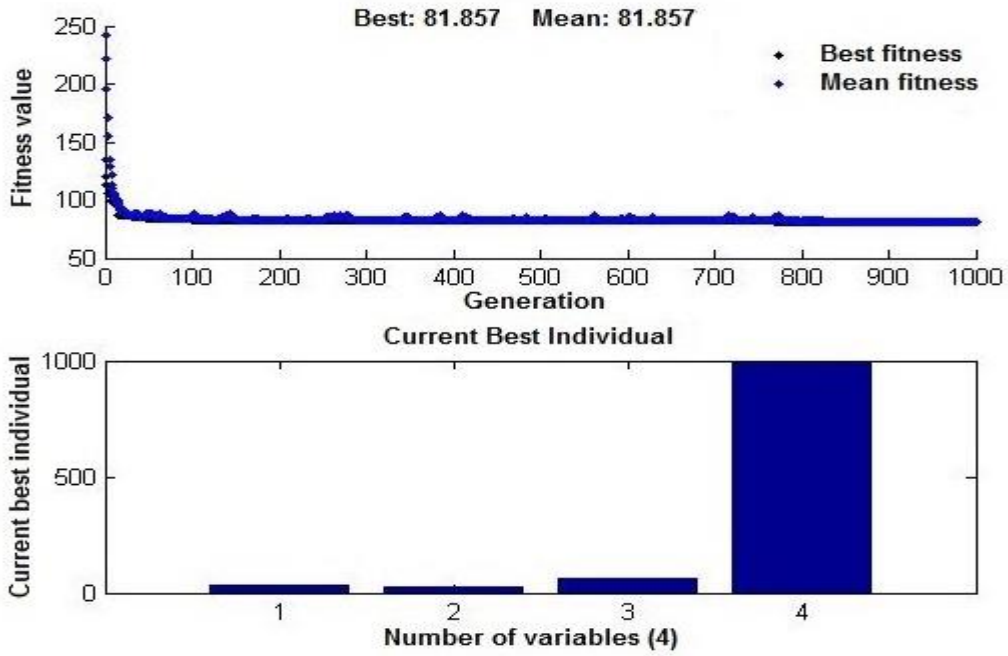
For Minimized HAZ	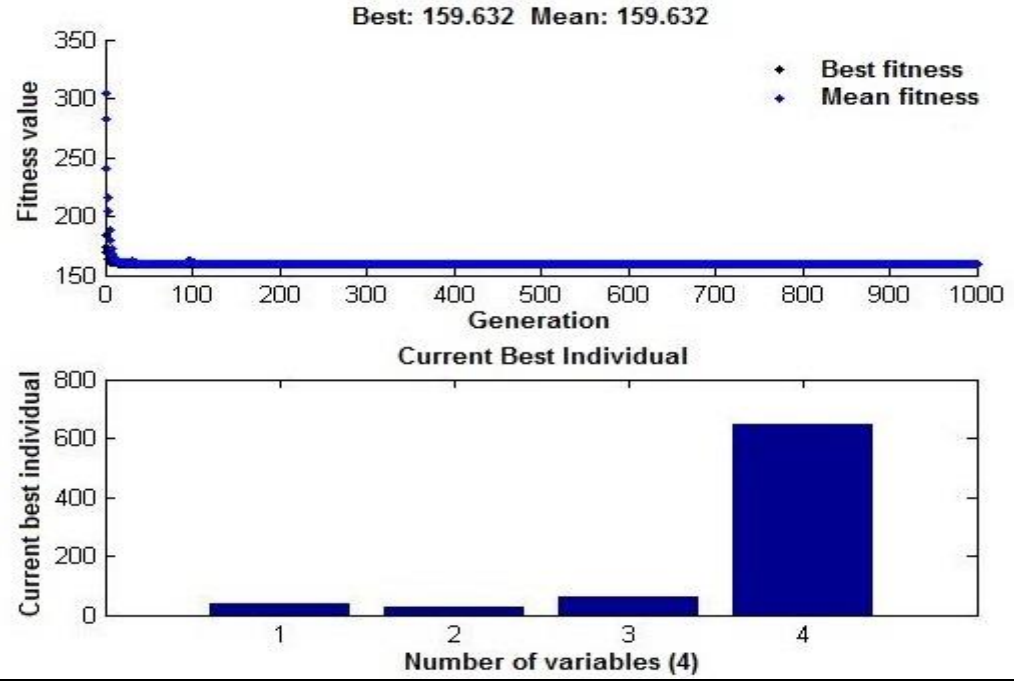

For Minimized Surface Roughness (R_a)	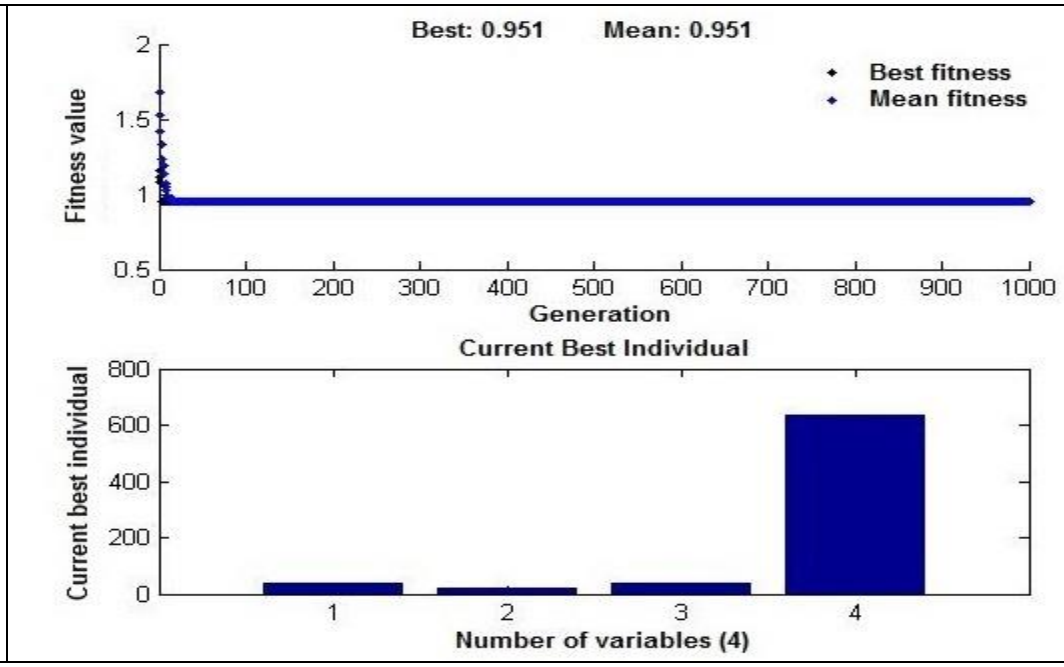

Fig 5.30 Graphical view of single optimization of MRR, OC, HAZ and surface roughness based on GA

5.3.2.4.2 Multi-Objective Optimization for Maximum MRR, Minimum OC, Minimum HAZ and Surface Roughness

Multi response optimization analysis for micro-channeling on glass has been performed utilizing MINITAB software and optimization results for MRR, OC, HAZ and Ra are exhibited in Fig.5.31 based on RSM. MRR, OC, HAZ and Ra have been optimized all together in one setting and represented in Fig. 5.32 based on GA. Each column of the graph corresponds to a process parameter whereas each row of the graph corresponds to a response variable. Each cell of the graph shows how one of the response variables changes as a function of one of the parameters, while all other parameters remain fixed. The numbers displayed at the top of a column show the current, the high and low parameter level settings in the experimental design. At the left of each row, the goal for response (optimum), predicted response, 'y' at current parametric settings and individual desirability score are given. The current parametric settings are as applied voltage of 35V, electrolyte concentration of 28.7879wt%, duty ratio 60% and pulse frequency of 668.6869 Hz for achieving predicted optimum value of MRR (y_{MRR}) of 86.7086 mg/hr, OC (y_{OC}) of 104.68 µm, HAZ area (y_{HAZ}) of 201.93 x $10^3 \mu m^2$ and R_a (y_{Ra}) of 0.9902µm. The composite desirability, D is displayed at the upper left corner of the graph and its value is 0.9868, which is very close to 1. The composite desirability label refers to the current setting and changes for moving the process

parametric settings interactively. When the optimization plot is developed, the label is optimal. The current parametric settings are represented by vertical lines inside the graph and the current response values by the horizontal dotted lines.

Many-objective optimization has attractive attention and gradually developed into the field of micro-machining research work. GA is faster; more efficient as compared to the other optimization methods, provides a list of good solutions that's can be used as per requirement but not give a single solution like RSM. Genetic algorithm can be used to solve the engineering optimization problems as a form of complex non-linear problems. In genetic algorithm, five phases are observed which initial population, fitness function, selection, and cross over and finally mutation. 80 chromosomes were generated randomly and they are involved to regenerate crossover and iterated until the stop condition of n = 1000 generation is reached for MRR, OC, HAZ and R_a for single as well as multi objective optimization of those machining criteria and the probability of crossover .80 and probability of mutation is chosen .05. Equation (5.6) represents the minimized function of the output parameters of MRR, OC, HAZ and R_a.

So minimize the multi objective function

$$Y(MRR, OC, HAZ, R_a) = w1Y(1/MRR) + w2\,Y(OC) + w3Y(HAZ) + w4Y(Ra) \quad \text{Eq. (5.6)}$$

w1=w2=w3=w4=weightage for output parameter=1

Fig. 5.33 shows the overlaid contour plot and white area, which reflects the feasible region. The feasible region is the area formed by two significant process parameter i.e., applied voltage, electrolyte concentration keeping other design variables i.e., duty ratio and pulse frequency constant, such that the acceptable values for each response are lays between their respective contours. The feasible region selected for MRR is 85 mg/hr as lower value and 110 mg/hr as upper value respectively. For OC, HAZ area and R_a the upper and lower values are selected as 82 μm & 125 μm, 225 **x** $10^3\mu m^2$ & 250 **x** $10^3\mu m^2$ and 0.9 μm & 1.4 μm respectively. The other two parameters, duty ratio and pulse frequency are set fixed at 60% and 1000 Hz respectively.

The evaluation profile of surface roughness as graphical representation is shown in Fig. 5.34, which is found during the measurement of R_a of micro-channel cut at 35V/28wt%/60%/668Hz and 55V/30wt%NaOH/40%/200Hz on glass. According to GA, maximised MRR=119.846.70mg/hr and minimised OC=291.646 μm, minimized HAZ area

588.26 X $10^3 \mu m^2$ and minimized surface roughness (2.37µm) at 55V/30wt%NaOH/40%/200Hz. Fig. 5.35 and 5.36 show the optical microscopic and SEM images of micro-channel as well as micro-channel cut at 35V/28wt%/60%/668Hz and 55V/30wt%NaOH/40%/200Hz respectively and debris, micro-crater, thermal effect have been observed and shown in Fig. 5.35 and 5.36. Fig. 5.37 and 5.38 represents the XRD pattern of micro-channels on glass cut at 35V/28wt%/60%/668Hz/40IEG and55V/30wt%/40%/200Hz/40IEG respectively. The XRD pattern of glass does not show any peak because it is amorphous. After micro-channel cutting on glass, the intensity (CPC) has slightly been decreased but the property of glass after machining is found unchanged as the chemical reactions take place in NaOH electrolyte solution where major element is sodium, which is also present in glass but at higher voltage the intensity will be higher.

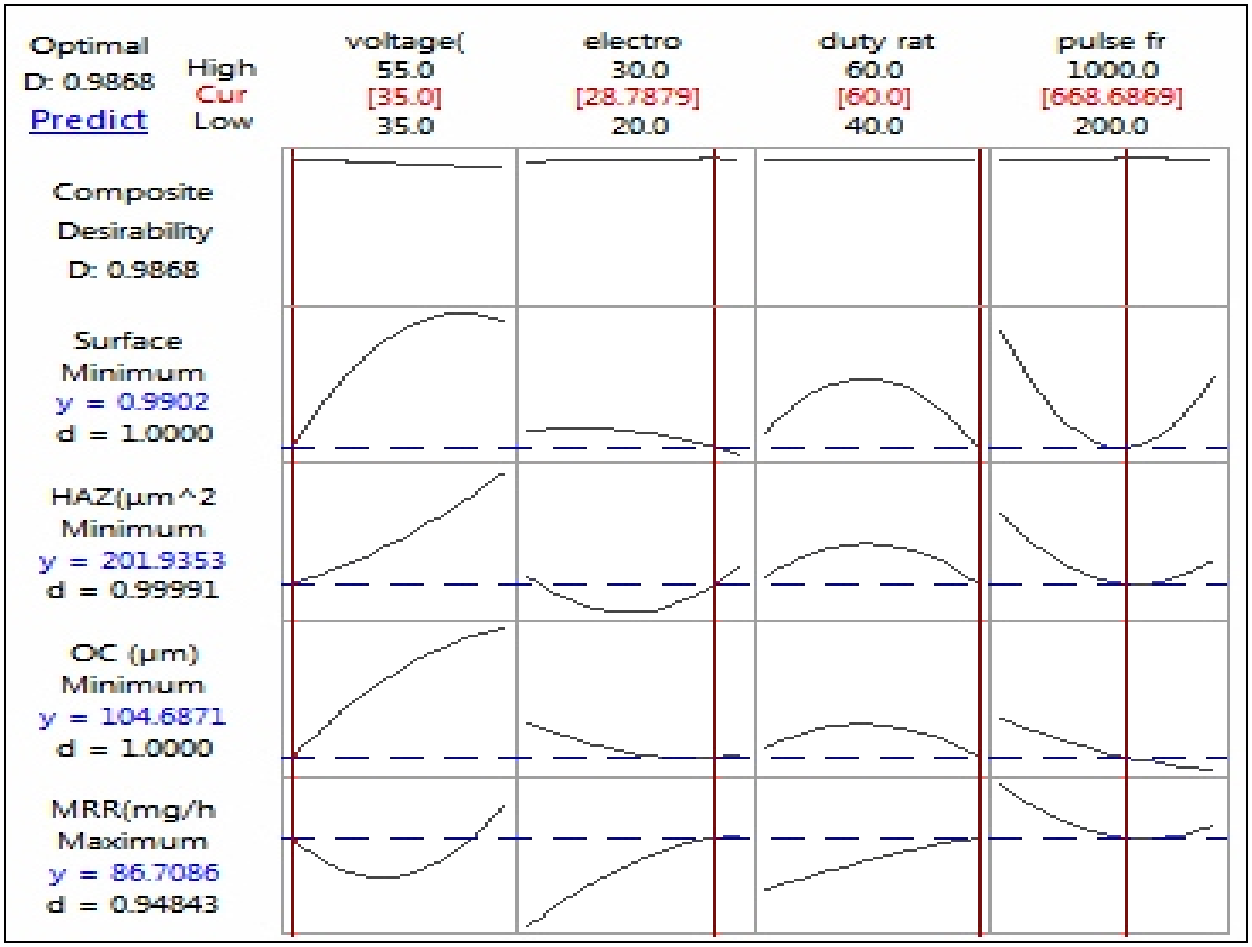

Fig. 5.31 Multi-objective optimization of process parameters based on desirability function analysis

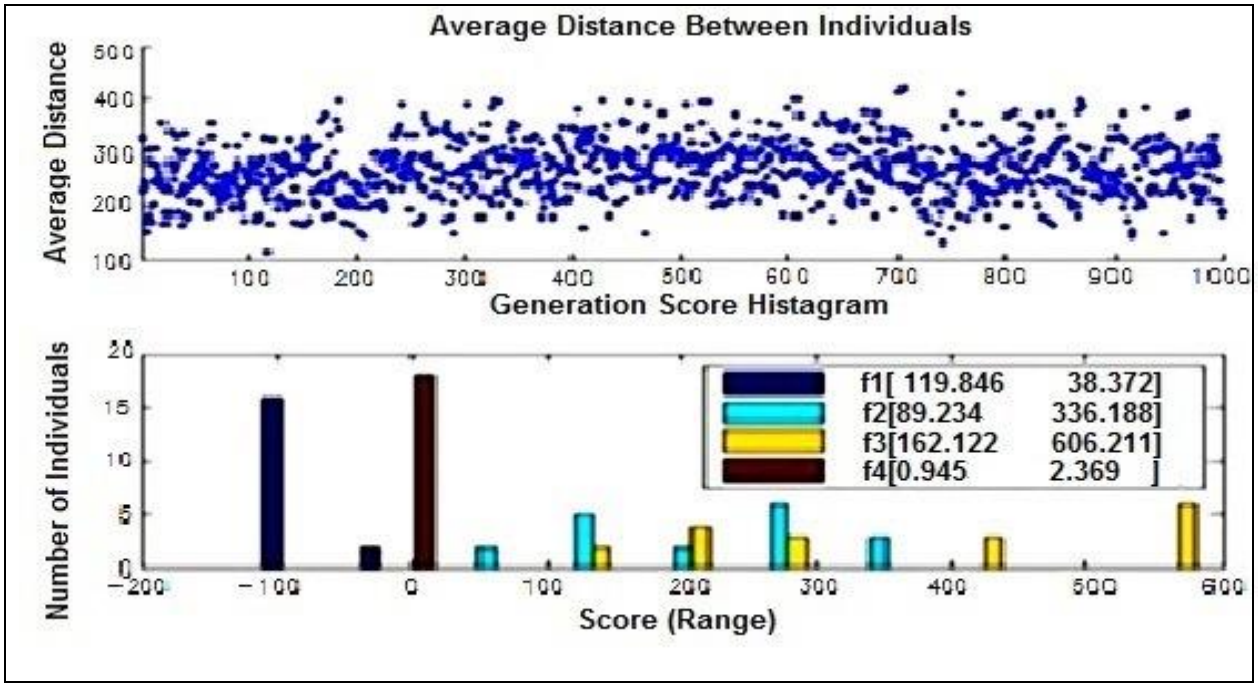

Fig. 5.32 Multi-objective optimization results based on GA with pareto-front

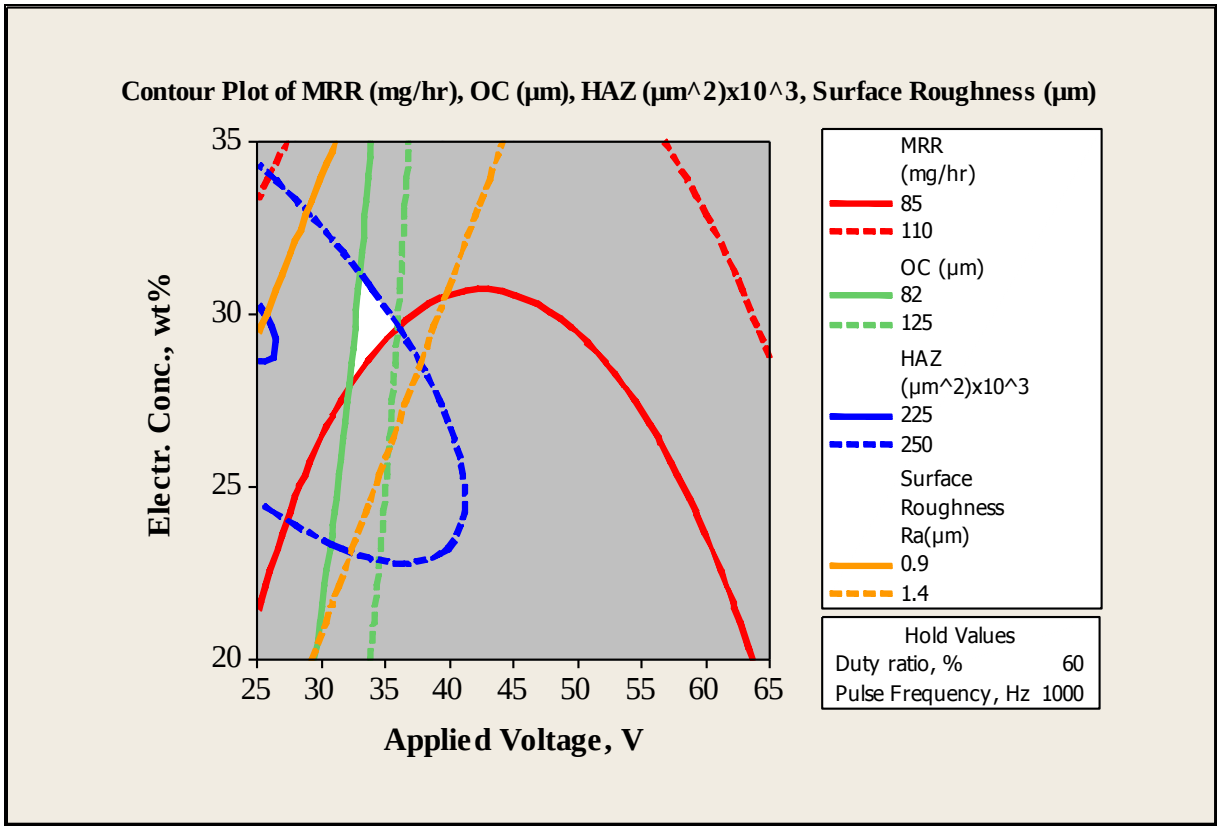

Fig. 5.33 Overlaid contour plot for MRR, OC, HAZ area and R_a based on RSM

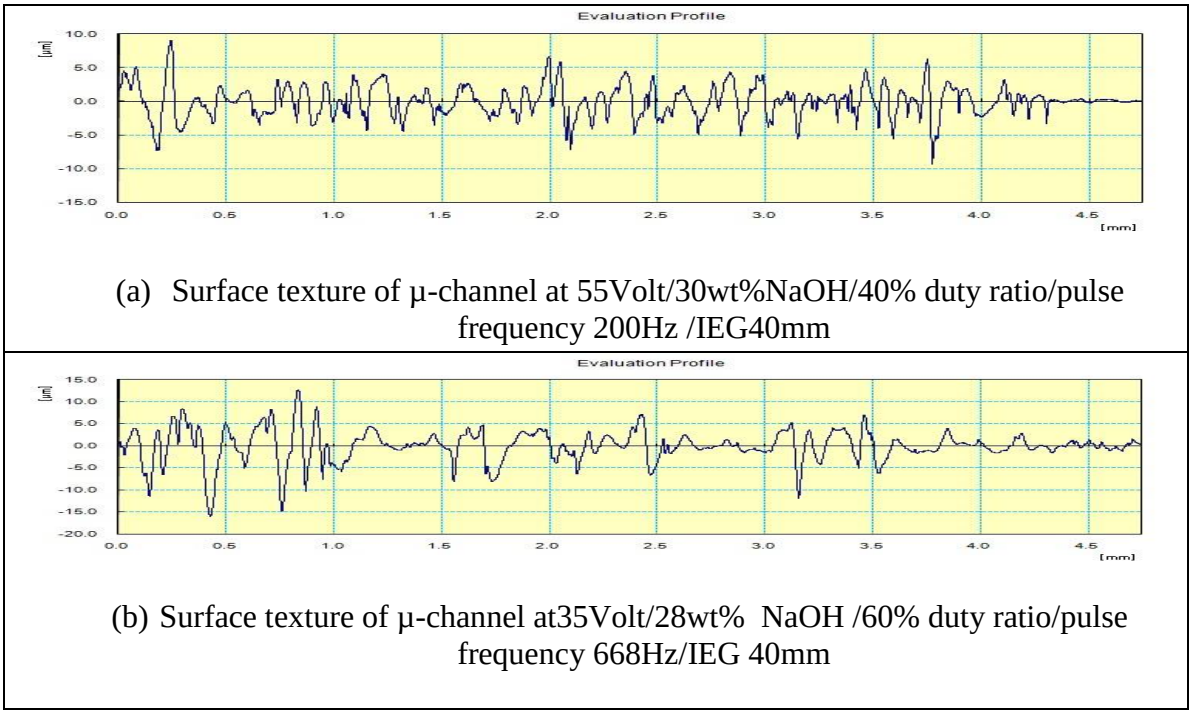

(a) Surface texture of µ-channel at 55Volt/30wt%NaOH/40% duty ratio/pulse frequency 200Hz /IEG40mm

(b) Surface texture of µ-channel at35Volt/28wt% NaOH /60% duty ratio/pulse frequency 668Hz/IEG 40mm

Fig. 5.34 Surface texture of µ-channels at 55V/30wt%/40%/200Hz and 35V/28wt%/60%/668Hz

Optical image	SEM Image

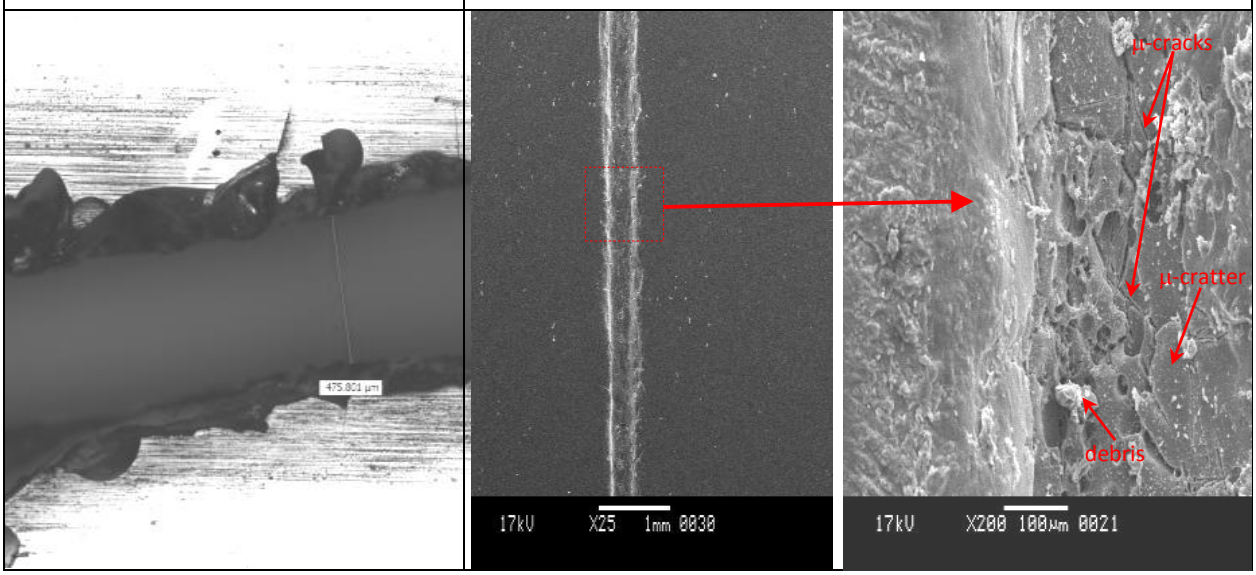

Fig. 5.35 Micro-channel at 35V/28wt%/60%/668Hz

Optical image	SEM Image

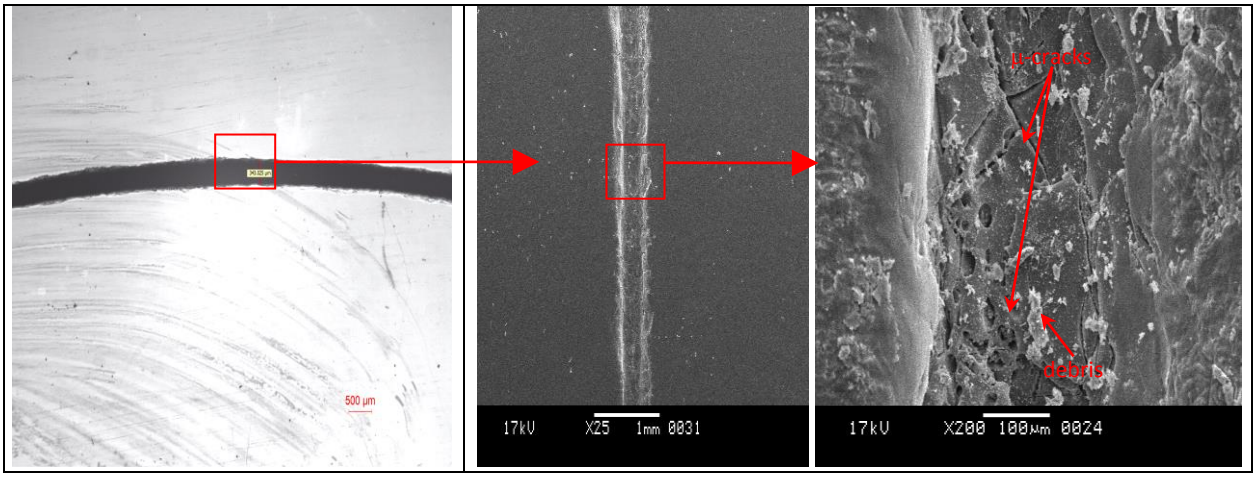

Fig. 5.36 Optical and SEM image of micro-channel cutting at 55V/30wt%/40%/200Hz/ IEG 40mm

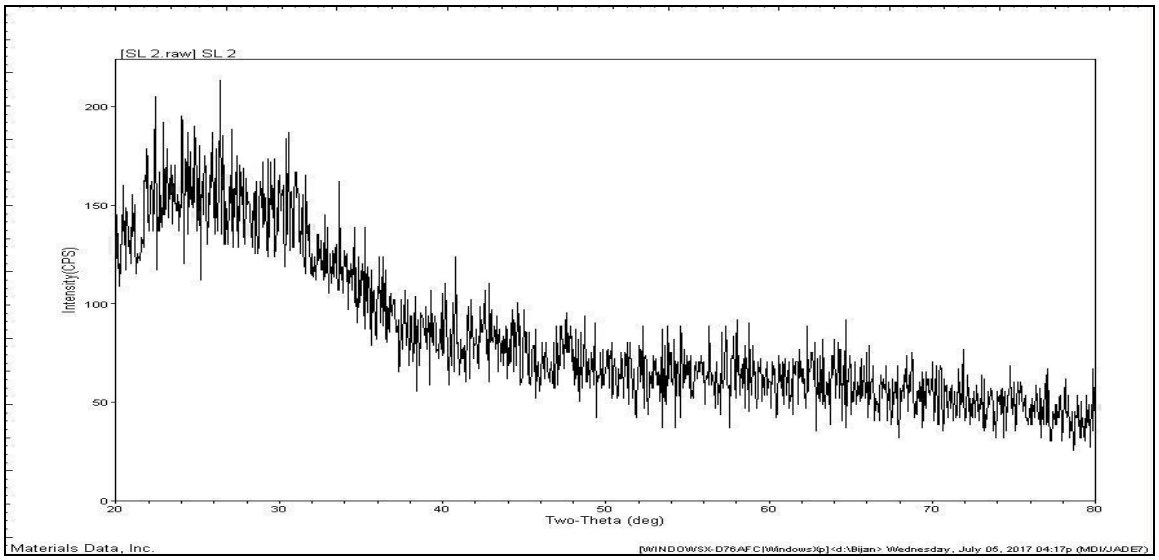

Fig. 5.37 XRD pattern of micro-channel on glass at 35V/28wt%/60%/668Hz/40IEG

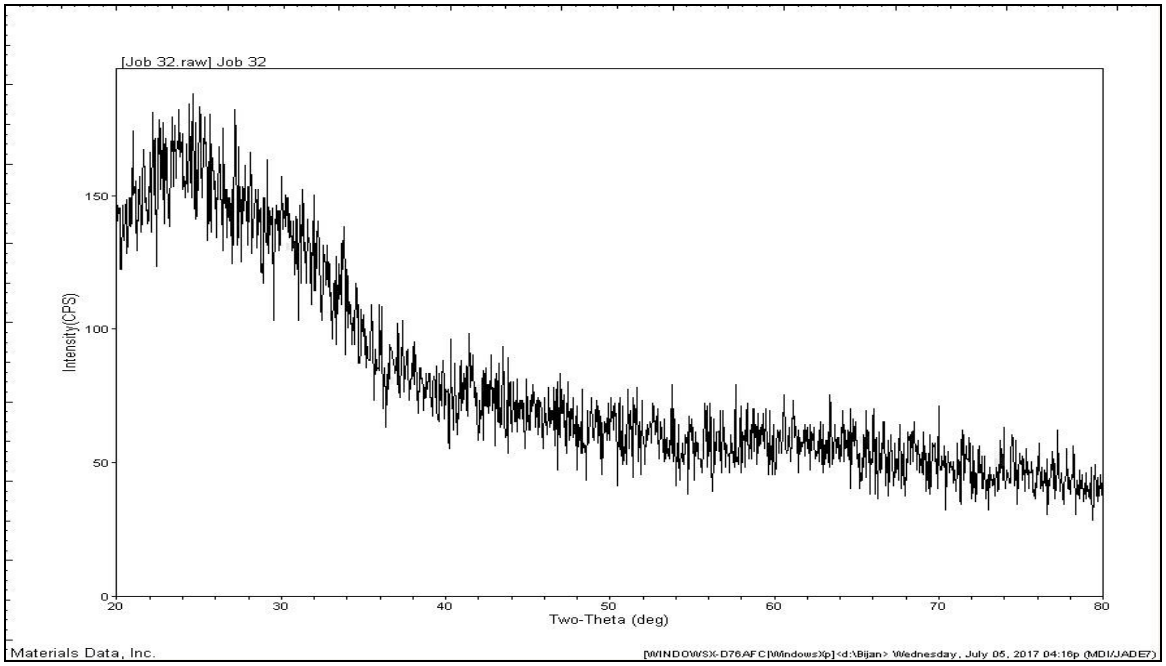

Fig. 5.38 XRD pattern of micro-channel on glass at 55V/30wt%/40%/200Hz/40IEG

From the table 5.15 it is clear that MRR and machining depth is increased up to 4 times and also surface roughness is improved 2.5 times and OC is reduced 3.5 times, HAZ area decreased up to 4 times using template guided spring feed mechanism than that of gravity feed.

Table 5.15 Machining Performances at Optimal Conditions of Different feeding

Feeding Type	Single Machining Performances at Optimal Conditions				
Gravity feed	MRR=27.523mg/hr	OC=293.468µm	HAZ=0.625 mm^2	MD=355.733 µm	R_a=2.564µm
Automated spring feed	MRR=119.877mg/hr	OC=82.33µm	HAZ=160.76 x 10^3 μm^2	MD=1350 µm	R_a=0.964 µm

5.4. GENERATION OF DIFFERENT µ-CHANNELS

Various types of micro-channel, micro-profile, micro-slot and different shapes of micro-fluidic channel has been generated for the purpose of micro-fluidic or lab-on-chip applications.

5.4.1MICRO- CHANNELS AND PROFILES GENERATION ON GLASS

Micro-channels as well as micro-profiles are cut at the optimal parametric conditions which have been achieved from the analysis of process parameters using response surface methodology and genetic algorithm and test results have been validated. Fig. 5.39 shows the optical and SEM images of micro-channels cutting at 55V/30wt%/40%/200Hz and 35V/28wt%/60%/668Hz that is experimentally validated.Fig. 5.40 exhibit the optical view of curved micro-channel which is cutting at 50V/600Hz/ 25wt%/55%duty ratio. Fig. 5.41 and 5.42 represents the SEM images of micro-channels cut at 35V/25wt%KOH/200Hz/45% and at 35V/10wt%NaOH/200Hz/45% respectively. Table 5.15 shows the machining performances at optimal conditions of different feeding arrangement used in µ-ECDM process.

Machining Condition	Optical Microscopic Images	SEM Images
55V/30wt% NaOH /40% / 200Hz / 40mm	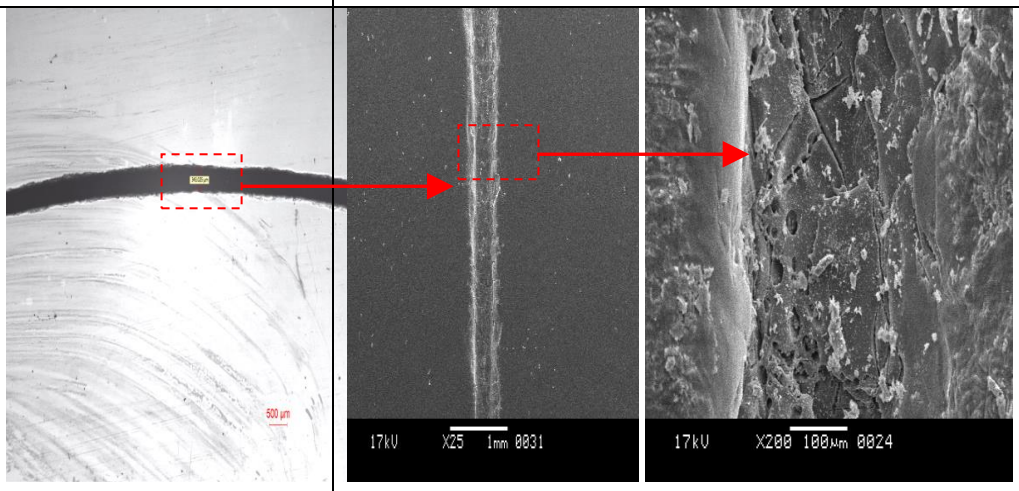	
35V/28wt% NaOH /60% /668Hz / 40mm	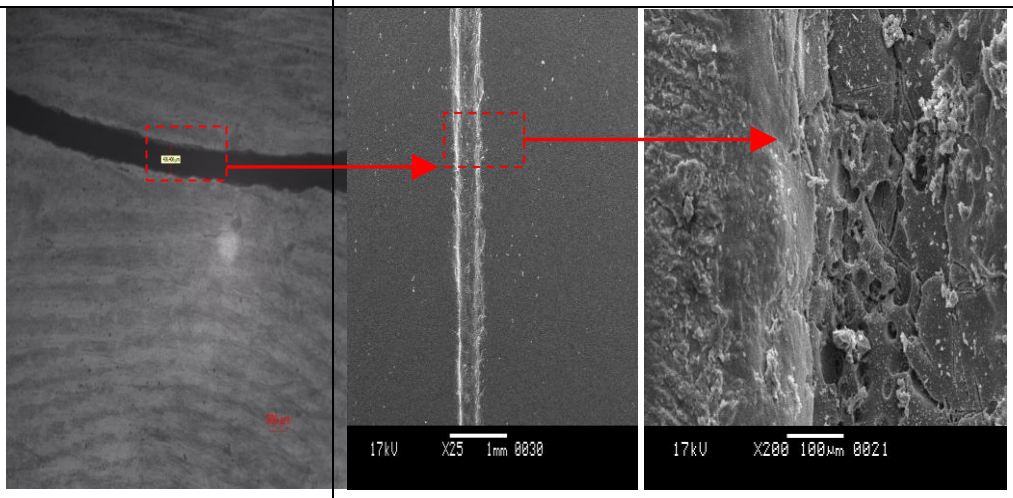	

Fig. 5.39 Micro-channels cut at 55V/30wt%/40%/200Hz and 35V/28wt%/60%/668Hz

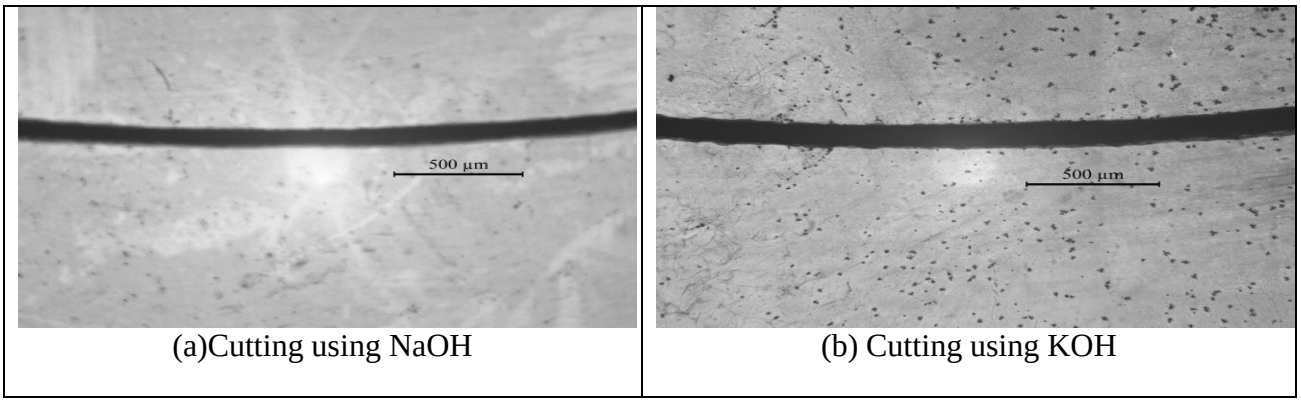

(a)Cutting using NaOH (b) Cutting using KOH

Fig. 5.40 Curved micro-channels (a) cut using NaOH and (b) cut using KOH at 50V/600Hz/ 25wt%/55%.

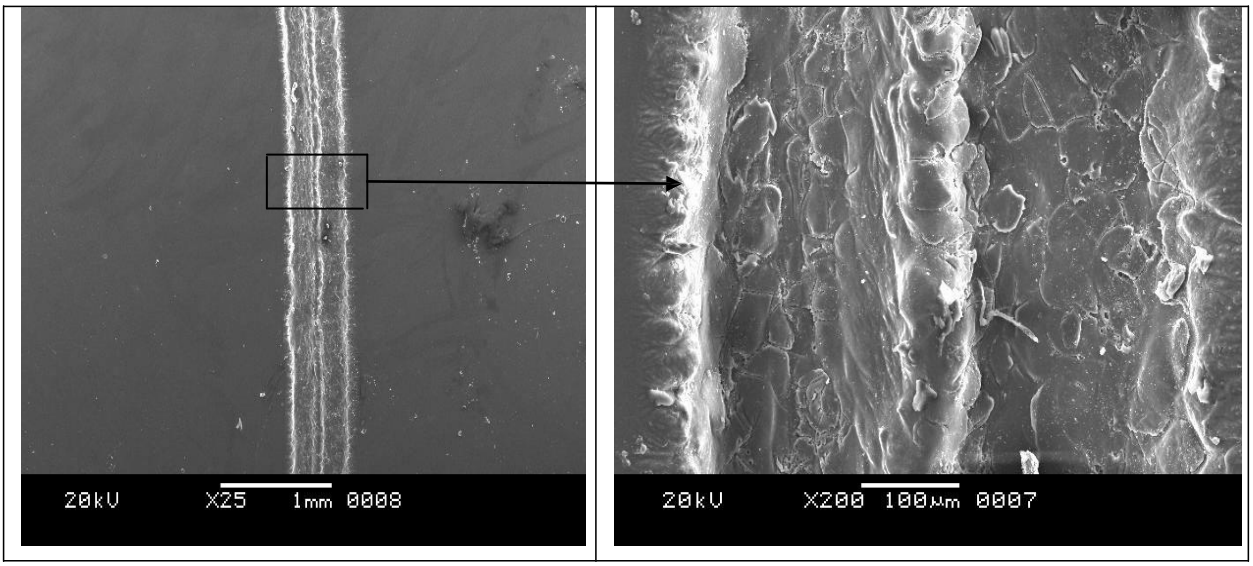

Fig. 5.41 SEM image of µ-channel cut at 35V/25wt%KOH/200Hz/45% on glass by µ-ECDM process

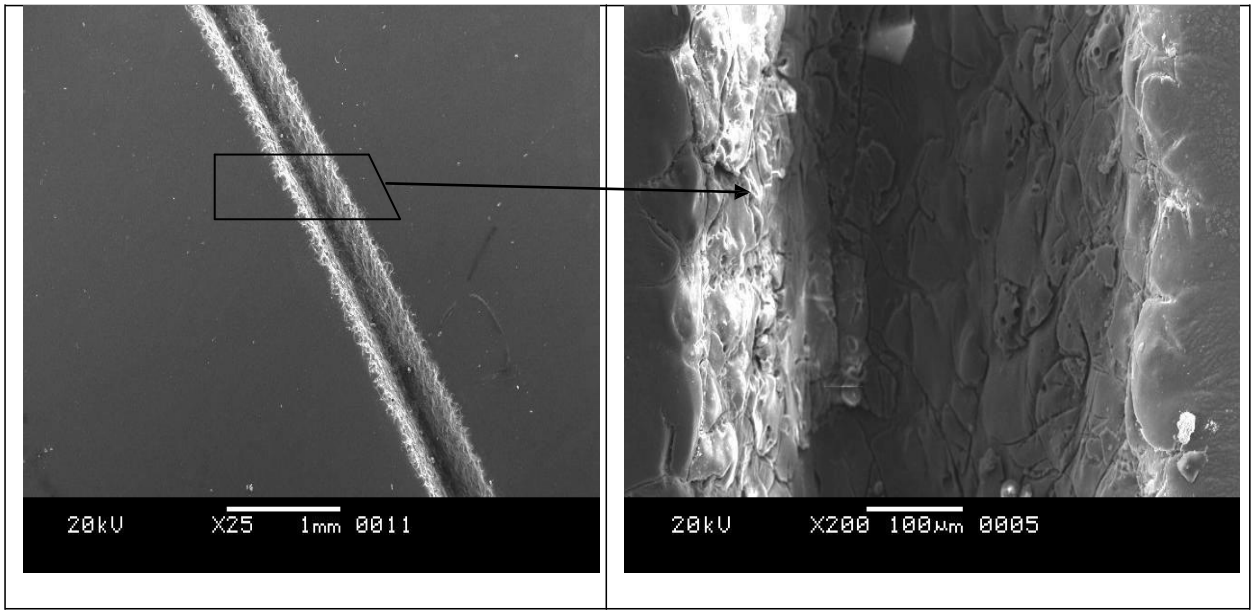

Fig. 5.42 SEM image of µ-channel cut at 35V/10wt%NaOH/200Hz/45% on glass by µ-ECDM process

5.4.1.1 Different Complex Shapes Channels Cutting on Glass

Different shapes of micro-channels are used in the field of micro-fluidic operations and flow of fluid can go any direction, so different shapes of channels generation on glass are become highly necessary. Fig. 5.43 shows the (a) 'Zig-Zag' micro-channel cut on glass at 50V/10wt% NaOH:KOH::3:1 /200Hz/45% and (b)'Y' Shaped micro-channel cut at 50V/10wt% NaOH:KOH::3:1/200Hz/45% on glass using µ-ECDM process.

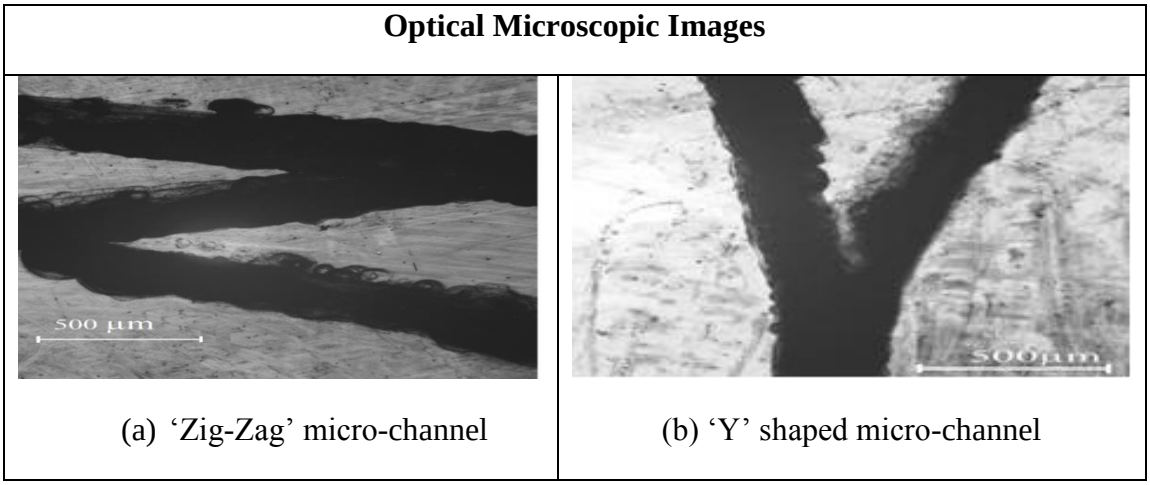

Fig. 5.43 (a)'Zig-Zag' micro-channel cut on glass at 50V/10wt% NaOH:KOH::3:1 /200Hz/45% and (b)'Y' Shaped micro-channel cutting at 50V/10wt% NaOH:KOH::3:1/200Hz/45%

5.4.1.2 Micro-Slot on Glass

Micro-slots are cut using stainless steel cylindrical micro-tool which diameter was 250µm. Micro-slots are cut by rotating the tool holding unit by handle with the help of CAM flower mechanism using template guided spring feed.

Micro-slots are cut at the optimal parametric condition on glass job specimen which thickness was 1.5mm. Fig. 5.44 and 5.45 shows the optical microscopic view of micro-slot cutting at parametric combination of 35V/10wt% NaOH:KOH::3:1 200Hz/45% and 55V/200Hz/ NaOH30wt%/40%/40mm IEG with machining depth of 1.35mm on glass by µ-ECDM process respectively.

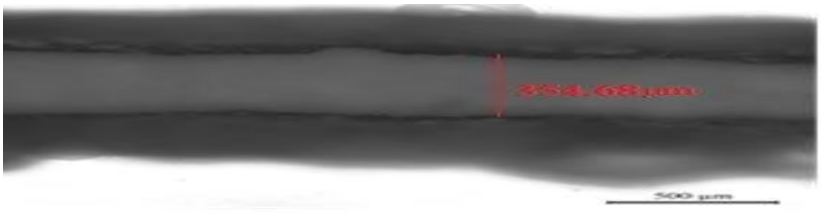

Fig. 5.44 Cross section of 'Micro-slot' cut at 35V/10wt% NaOH:KOH::3:1 200Hz/45% with machining depth of 1.35mm

Fig. 5.45 Cross section of micro-slot of 1.35mm machining depth cut at 55V/200Hz/ NaOH30wt%/40%/40mm IEG

5.5 Outcomes of Present Investigations

After this investigation it can be concluded that the developed µECDM system can be used successfully for micro-channel cutting applications using template guided spring feed mechanism on glass and the process parameters can be optimally controlled for achieving maximum MRR and minimum OC, HAZ area and surface roughness. During micro-channeling on glass by µ-ECDM applied voltage has strong significant effect on the responses, i.e., MRR, OC, HAZ area and R_a and predominant to other controlling parameters. MRR is increased with the increase of applied voltage, electrolyte concentration, duty ratio but decreased with pulse frequency using NaOH as electrolyte during micro-channel cutting on glass. Width-of-cut of micro-channel always increases with increase of applied voltage, electrolyte concentration, so OC increases but it decreases with increase of pulse frequency

upto 600Hz after that it increases. HAZ area almost gradually increases with increase of applied voltage, electrolyte concentration and duty ratio and it becomes higher at 55 V and 30 wt% electrolyte concentration. But the heat affected zone area is decreased after 50% of duty ratio and with the increase of pulse frequency beyond 600 Hz. If pulse frequency is increased, initially the surface roughness is decreased but at higher pulse frequency, it is very difficult to control the stray and secondary sparking that cause irregularities on the machining surface and make the surface rougher. MRR is found maximum at 55V/30wt%NaOH/40%/200Hz and better surface quality of micro-channel can be achieved with higher machining depth at 35V/30wt%NaOH/60%/660Hz and maximised MRR=119.846.70mg/hr and minimised OC=291.646 µm, minimized HAZ area 588.26 X $10^3 \mu m^2$ and minimized surface roughness (2.37µm) at 55V/30wt%NaOH/40%/200Hz based on GA. The present set of developed mathematical models and optimal analyses will be very much effective and useful for achieving high quality precision micro-channeling on glass by µ-ECDM process. Different types and complex shapes of µ-channels such as ZIG-ZAG, Y-shapes, and curved µ-channels and profiles can be cut by indigenously developed µ-ECDM set up successfully.

The outcomes of present investigation on µ-ECDM process for µ-channel cutting operation may be accepted and used successfully in modern manufacturing industries for generation of different complex shapes of µ-channels which are utilized for fabrication of micro-fluidic devices.

CHAPTER-VI

6. GENERAL CONCLUSIONS AND FUTURE SCOPE OF RESEARCH

6.1 GENERAL CONCLUSIONS

Within the limitation of the present research work, based on the detailed experimental observations and analysis on the performance characteristics of µ–ECDM process during generation of micro-channel, micro-profile and micro-slots on glass in the present research, the following conclusions may be drawn:

The indigenously designed and developed µ-ECDM set up can be used satisfactorily and successfully for cutting of micro-channel as well as micro-profile of different shapes on electrically non-conducting hard and brittle materials like glass.

a) Investigations on electrochemical discharge micro-machining using form tool and gravity feed mechanism

(i) Material removal rate, overcut, heat affected zone and surface roughness have been enhanced with the increased of applied voltage and electrolyte concentration but decreased with the increase of inter electrode gap of µ-ECDM.

(ii) MRR is found to be more by using KOH than NaOH electrolyte since KOH electrolyte has higher specific conductance than that of NaOH electrolyte for the range 10-25wt% of electrolyte concentration but 30wt% of electrolyte concentration of NaOH provides higher machining rate at higher voltage than that of KOH electrolyte solution.

(iii) It is concluded that the overcut can be reduced to the lower value by using NaOH electrolyte for straight tool at the parametric setting of 50 V and 20 wt% concentration. But OC is found to be lower value when µ-channelling is performed with straight tool by using 15wt% of KOH electrolyte at 50V.

(iv) The width of cut (WOC) becomes more than 500µm during machining at high voltage of 65V and higher concentration of both NaOH & KOH electrolytes

using both straight and curved tools. The lower HAZ area is found at 50V while 10wt% of KOH is used with curved tool.

(v) Surface roughness (R_a) is found to be lower at applied voltage of 55V for NaOH electrolytes of 20wt% concentration and R_a becomes higher at high applied voltage with curved tool for both electrolytes.

(vi) The values of R^2 for models on MRR, OC, HAZ and machining depth are 97.73%, 98.39%, 95.32% and 98.72% respectively indicating the goodness of the fit of models. Also, the values of adj-R^2 for MRR, OC, HAZ and machining depth are very close to R^2 indicating the goodness of fit of the models. F values and P values for lack-of-fit of models on MRR, OC, HAZ and machining depth are (2.81 & 0.041), (2.77 & 0.0144), (0.42 & 0.0501) and (2.52 & 0.0167) respectively, indicates the goodness of fit of models.

(vii) It is found that maximum MRR is obtained as 27.60 mg/hr at the parametric combination of 60V of applied voltage,21.9697wt% of NaOH electrolyte,30mm of IEG minimum OC is 106.464 μm at 50V of applied voltage,15wt% of NaOH electrolyte,40mm of IEG, and minimum HAZ area is 0.625 mm^2 at 50V of applied voltage,15.7576wt% of NaOH electrolyte, 35.252mm of IEG and maximum machining depth 355.415 μm is obtained at the parametric combination of 55V of applied voltage,15wt% of NaOH electrolyte, 40 mm of IEG according to single-objective optimization based on desirability function analysis.

(viii) Maximum MRR is obtained as 27.523 mg/hr at the parametric combination of 60V/22wt%/30mm, minimum overcut and HAZ area are found as 293.468 μm and 0.625 mm^2 at 50V of applied voltage,15wt% of NaOH electrolyte, 40mm of IEG and 50V of applied voltage, 15wt% of NaOH electrolyte, 35mm of IEG respectively and maximized machining depth is achieved 355.733 μm at 55V/15wt%/40mm based on genetic algorithm (GA).

(ix) Based on multi-objective optimization MRR of 27.523 mg/hr, OC of 293.485 μm, HAZ area of 0.625 mm^2 and also machining depth of 355.732μm are obtained at the parametric combination of 55V of applied voltage, 15wt% of NaOH electrolyte, 40mm of IEG using GA based approach. Based on multi-

0bjective optimization using desirability function analysis MRR, OC, HAZ and machining depth have been attained as 19.9652 mg/hr, 180.640 μm, 0.911 mm^2 and 331.352 μm respectively at optimal parametric setting of 58V of applied voltage, 15wt% of NaOH electrolyte, 37mm of IEG.

b) Investigations on electrochemical discharge micro-machining using cylindrical tool and template guided spring feed

(i) Material removal rate, overcut, heat affected zone, machining depth, tool wear rate and surface roughness increases with the increase of applied voltage, duty ratio and electrolyte concentration but decrease with the increase of pulse frequency.

(ii) It is observed that the material removal rate (MRR) becomes higher at applied voltage 55V, pulse frequency of 200 Hz, IEG of 40mm and duty ratio 45 % in the mixture of 1:3 ratio of NaOH and KOH electrolyte. The overcut and HAZ are found as smaller at ratio of 3:1 of NaOH and KOH mixture at 10wt%, pulse frequency of 200 Hz and duty ratio of 45%.

(iii) The mixture of NaOH and KOH electrolytes of ratio 3:1 provides the highest machining depth (MD) and lower surface roughness R_a value whereas 1:3 ratio of mixture reduces lower tool wear rate. But considering overall parametric influences on different machining criteria, the optimal parametric condition is found as applied voltage of 35V with direct polarity, 10wt% with 3:1 ratio of NaOH &KOH, pulse frequency 200Hz and duty ratio 45% during μ-channel cutting using cylindrical stainless steel tool and spring feed mechanism.

(iv) The values of R^2 and adj-R^2 for models on MRR, OC, HAZ and R_a are (99.21% & 98.51%), (97.77% & 95.82%), (98.94% & 98.01%) and (99.48% & 99.02%) respectively which reveal the presence of significant terms in those mathematical models. The F-ratio for the lack-of-fit is found less than the standard F-ratio values (2.32260) for 10 DOF, indicates the adequacy of fit of models.

(v) The single objective optimization gives maximum MRR as 119.877 mg/hr at the parametric combination of 55V/30wt%NaOH/40%/200Hz during micro-channel

cutting on glass. The minimum OC (82.33μm) and minimum HAZ (160.76 X $10^3\mu m^2$) and also the minimum average surface roughness (R_a) value (0.964μm) are achieved at parametric combination of 35V/26wt%NaOH/60%/1000Hz, 55V/25wt%NaOH/60%/644Hz and 35V/30wt%NaOH/60%/660Hz respectively based on desirability function analysis.

(vi) The maximum MRR is obtained as 119.963mg/hr at the parametric combination of 55V/30wt%NaOH/40%/200Hz. Minimum OC (81.857μm) and minimum HAZ (159.632 X $10^3\mu m^2$) and minimum surface roughness (0.94642μm) are found at parametric combination of 35V of applied voltage, 26wt% of NaOH,60% and 1000 Hz pulse frequency & 35V of applied voltage, 24.553wt% of NaOH,60% and 645Hz pulse frequency and 35V of applied voltage, 20wt% of NaOH,40% and 525Hz pulse frequency respectively based on GA during μ-channel cutting on glass using die sinking ECDM with cylindrical tool shapes.

(vii) Multi-objective optimization provides the maximum MRR of 86.70mg/hr and minimum OC of 104.68 μm, minimum HAZ area of 201.93X$10^3\mu m^2$ and minimum surface roughness of 0.990μm as optimal process parametric setting at 35V of applied voltage, 28wt% of NaOH,60% and 668Hz pulse frequency using desirability function analysis. But using GA, maximum MRR of 119.846 mg/hr and minimum OC of 291.646 μm, minimum HAZ area of 588.26 X $10^3\mu m^2$ and minimum surface roughness of 2.37μm are found at parametric combination of 55V of applied voltage, 30wt% of NaOH,40% and 200 Hz pulse frequency.

(viii) It is observed from Scanning Electron Microscopy (SEM) images that surface texture of μ-channel on glass varies with different process parameters such as applied voltage and electrolyte concentrations etc. Direct polarity is found suitable for obtaining higher machining performances e.g. high MRR with good surface texture.

(ix) Material removal rate and machining depth has been increased up to 4 times using mixed NaOH and KOH electrolytes at 3:1 ratio, overcut and heat affected zone has been reduced up to 3.5 times and 4 times respectively with better

quality of surface finish using template guided spring feed mechanism compared with gravity feed mechanism

(x) Different types of micro-channels and complex shapes of µ-channels such as ZIG-ZAG, Y-shapes, and curved µ-channels and profiles cut by indigenously developed µ-ECDM set up successfully for utilization in fabrication of micro-fluidic devices. Micro-slots have been cut successfully with 1.35mm machining depth on silica glass by developed µ-ECDM set up.

Micro-channels, micro-complex profile, micro-holes, round, square or taper marking, contour machining, micro-structure of glass wafers preparation and micro-reactor applications are highly needed in micro-products of MEMS and micro-fluidic devices or lab-on chips, which can be generated by developed µ-ECDM process on silica glass. The present research work on electrochemical discharge micro-machining on hard and brittle non-conducting material has wide scope of applications in the field of bio-medical, electronics and mechanical engineering.

6.2 FUTURE SCOPE OF RESEARCH

After fulfill the desired objectives of the present research work, author thinks that further investigation and development of µ-ECDM is highly required for utilizing the process in modern industrial field and to generate different complex shapes on other advanced ceramic materials as well as on quartz. So, further scopes of research are needed to include:

(i) To control and adjust the proper depth of cut during micro-machining;
(ii) To utilized µ-ECDM process for turning and milling operations;
(iii) To perform blanking and piercing operation on hard brittle materials by µ-ECDM process;
(iv) To develop CNC based µ-ECDM process for various micro-machining operations.

The developed µ-ECDM set up can be utilized for carrying out further research on non-conducting materials for utilized in modern industrial field. The findings of experimental results will provide fruitful technical knowledge to the students, researchers, scientists and manufacturing engineers who are doing research in the field of µ-ECDM process.

BIBLIOGRAPHY

[1] A.Ghosh & A.Mallik, "Manufacturing science",2nd edition, *East west press*, ISBN: 9788176710633, 8176710636, 2010.

[2] B. R. Sarkar, B. Doloi, B. Bhattacharyya, "Non-traditional Micromachining Processes Fundamentals and Applications"-10.Electrochemical Discharge Micro-machining of Engineering Materials, *Springer International Publishing*, and ISBN: 978-3-319-52008-7, 2017.

[3] S. Tandon, V. K. Jain, P. Kumar and K. P. Rajurkar, Investigations into machining of composites, *International Journal of Precision Engineering*, 227-238, 1990.

[4] V. Raghuram, T. Pramila, Y. G. Srinivasa and K. Narayanasamy.Effect of the circuit parameters on the electrolytes in the electrochemical discharge phenomenon, *Journal of Materials Processing Technology*, 52, 301-318, 1995.

[5] I. Basak, A. Ghosh. Mechanism of spark generation during electrochemical-discharge machining- A theoretical model and experimental verification. *Journal of Materials Processing Technology*.62, 46-53, 1996.

[6] I. Basak, A. Ghosh. Mechanism of material removal in electrochemical discharge machining: a theoretical model and experimental verification. *Journal of Materials Processing Technology*.71, 350-359, 1997.

[7] L. Xiaowel, J. Zhixin, Z. Jiaqi and L. Jinchun, A combined machining process for the production of a flexure hinge, *Journal of Material Processing Technology*, 71, 373-376, 1997.

[8] B. Bhattacharyya, B. N. Doloi, S. K. Sorkhel. Experimental investigations into electro-chemical discharge machining (ECDM) of non-conductive ceramic materials. *Journal of Materials Processing Technology*, 95, 145-154, 1999.

[9] J. Kozak and K. E. Oczos. Selected problems of abrasive hybrid machining.*Journal of materials processing technology*, 109, 360-366, 2001.

[10] V. K. Jain , S. K. Choudhury and K. M. Ramesh. On the machining of alumina and glass, *International Journal of Machine Tools & Manufacture*, 42, 1269–1276, 2002.

[11] A. Kulkarni, R. Sharan, G. K. Lal. An experimental study of discharge mechanism in electro-chemical discharge machining. *International Journal of Machine Tools & Manufacture*.42, 1121–1127, 2002.

[12] T. K. K. R. Mediliyegedara, A. K. M. De Silva, D. K. Harrison, J. A. McGeough. An intelligent pulse classification system for electro-chemical discharge machining (ECDM)—a preliminary study. *Journal of Materials Processing Technology*.149, 499–503, 2004.

[13] G. Skrabalak, M. Z. Skrabalak and A. Ruszaj.Building of rules base for fuzzy-logic control of the ECDM process, *Journal of Materials Processing Technology*, 149, 530-535, 2004.

[14] W.Y. Peng, Y.S. Liao. Study of electrochemical discharge machining technology for slicing non-conductive brittle material, *Journal of material processing technology*, 149, 343-369, 2004.

[15] R. Wüthrich, V. Fascio. Machining of non-conducting materials using electro-chemical discharge phenomenon—an overview. *International Journal of Machine Tools & Manufacture*. 45, 1095–1108, 2005.

[16] D. J. Kim, Y. Ahn, S. H. Lee, Y. K. Kim. Voltage pulse frequency and duty ratio effects in an electro-chemical discharge micro-drilling process of Pyrex glass. *International Journal of Machine Tools & Manufacture*.46, 1064–1067, 2006.

[17] C. T. Yang, S. L. Song, B. H. Yan, F. Y. Huang. Improving machining performance of wire electro-chemical discharge machining by adding SiC abrasive to electrolyte. *International Journal of Machine Tools & Manufacture*.46, 2044–2050, 2006.

[18] B. R. Sarkar. B. N. Doloi, B. Bhattachryya. Parametric analysis on electrochemical discharge machining of silicon nitride ceramics.*International Journal of Advanced Manufacturing Technology*.28, 827-881, 2006.

[19] K. L. Bhondwe, V. Yadava, G. Kathiresan. Finite element prediction of material removal rate due to electro-chemical spark machining. *International Journal of Machine Tools & Manufacture*.46, 1699–1706, 2006.

[20] M. S. Han, B. K. Min, S. J. Lee. Improvement of surface integrity of electro-chemical discharge machining process using powder-mixed electrolyte. *Journal of Materials Processing Technology*.191, 224–227, 2007.

[21] S. K. Chak, P. V. Rao. Trepanning of Al2O3 by electro-chemical discharge machining (ECDM) process using abrasive electrode with pulsed DC supply.*International Journal of Machine Tools & Manufacture*.47, 2061–2070, 2007.

[22] K. Furutani and H. Maeda.Machining a glass rod with a lathe-type electro-chemical discharge machine.*Journal of micro mechanics and micro engineering*, 18, 065006 (8pp), 2008.

[23] V.K. Jain, S. Adhikary. On the mechanism of material removal in electrochemical spark machining of quartz under different polarity conditions.*Journal of material processing technology*, 200, 460-470, 2008.

[24] R. Wuthrich, V. Fascio, H. Langen. Machining of non-conducting materials using electro-chemical discharge phenomena- an overview, *International Journal of Machine Tools & Manufacture*, 45, 1095–1108, 2005.

[25] J. W. Liu, T. M. Yue and Z. N. Guo. Wire Electrochemical Discharge Machining of Al_2O_3 Particle Reinforced Aluminum Alloy 6061. *Materials and manufacturing process*, 24, 446-453, 2009.

[26] X. D. Cao, B. H. Kim, C. N. Chu. Micro-structuring of glass with features less than 100 μ m by electrochemical discharge machining. *Precision Engineering*.33, 459–465, 2009.

[27] J. W. Liu, T. M Yue, Z. N. Guo. An analysis of the discharge mechanism in electro-chemical discharge machining of particulate reinforced metal matrix composites. *International Journal of Machine Tools & Manufacture*.50, 86–96, 2010.

[28] C. K. Yang, C. P. Cheng, C. C. Mai, A. C. Wang, J. C. Hung, B. H. Yan. Effect of surface roughness of tool electrode materials in ECDM performance. *International Journal of Machine Tools & Manufacture*.50, 1088–1096, 2010.

[29] K. Khas, A. Manna. A study on MECD-machining during drilling of electrically non-conductive ceramic.*National Conference on Advancements and Futuristic Trends in Mechanical and Materials Engineering*. February 19-20, 2010.

[30] C. P. Cheng, K. L. Wu, C. C. Mai, C. K. Yang, Y. S. Hsu, B. H. Yan. Study of gas film quality in electro-chemical discharge machining.*International Journal of Machine Tools & Manufacture*.50, 689–697, 2010.

[31] C. Wei, D. Hu, K. Xu , J. Ni. Electro-chemical discharge dressing of metal bond micro-grinding tools.*International Journal of Machine Tools & Manufacture*.51, 165–168, 2011.

[32] C. K. Yang, K. L. Wu, J. C. Hung, S. M. Lee, J. C. Lin, B. H. Yan. Enhancement of ECDM efficiency and accuracy by spherical tool electrode. *International Journal of Machine Tools & Manufacture*.51, 528–535, 2011.

[33] Y. MOCHIMARU, M. OTA and K. YAMAGUCHI,Micro Hole Processing Using Electro-Chemical Discharge Machining, *Journal of advanced mechanical design, systems and manufacturing*.Vol. 6, No. 6, 949-957, 2012.

[34] C. S. Jawalkar, A. K. Sharma and P. Kumar, Micromachining with ECDM: Research Potentials and Experimental Investigations, *World Academy of Science, Engineering and Technology*, 61, 340-345, 2012.

[35] D. Jana. A. Ziki, T. F. Didar, R. Wuthrich, Micro-texturing channel surfaces on glass with spark assisted chemical engraving. *International Journal of Machine Tools & Manufacture*, 57, 66–72, 2012.

[36] C.S. Jawalkar, P. Kumar and A. K. Sharma, On Mechanism of Material Removal and Parametric Influence While Machining Sodalime Glass using Electro-Chemical Discharge Machining (ECDM), *All India Manufacturing Technology, Design and Research Conference*, Vol. 1, 440-446, 2012.

[37] P. Lijo, S. Somashekhar, H. Ranganayakulu and J. Ranganayakulu, Experimental Investigation and Response Surface Modelling of Metal Removal Rate in Electrochemical Discharge Machining, *All India Manufacturing Technology, Design and Research Conference*, Vol. 1, 499-504, 2012.

[38] S. K. Chak and P. V. Rao, Machining of SiC by ECDM Process using Different Electrode Configurations under the Effect of Pulsed DC, *All India Manufacturing Technology, Design and Research Conference*, Vol. 1, 513-519, 2012.

[39] A. Kulkarni, V. K. Jain and K.A. Misra, Performance of Micro Machining using ECSMM with Square Pulsating Power Source, *All India Manufacturing Technology, Design and Research Conference*, Vol. 2, 995-1000, 2012.

[40] S. Biswas, B. R. Sarkar, B. Doloi and B. Bhattacharyya, Parametric Optimization of μ-ECDMing of Silicon Nitride Ceramics, *All India Manufacturing Technology, Design and Research Conference*, Vol. 2, 1079-1084, 2012.

[41] Liu, J. W., Yue, T. M. and Guo, Z. N., Grinding-aided electrochemical discharge machining of particulate reinforced metal matrix composites, *International Journal Advanced Manufacturing Technology*, 8, 4846, 2013.

[42] Cao, X. D., Kim, B. Y. and Chu, C. N., Hybrid Micromachining of Glass using ECDM and Micro Grinding, *International Journal of Precision Engineering and Manufacturing*, 14 (1), 5-10, 2013.

[43] Jiang, B., Lan, S., Ni, J., Zhang, Z., Experimental investigation of spark generation in electrochemical discharge machining of non-conducting materials, *Journal of Materials Processing Technology*, 214, 892– 898, 2014.

[44] Huang, S. F., Liu, Y., Li, J., Hu, H. X., Sun, L. Y., Electrochemical Discharge Machining Micro-Hole in Stainless Steel with Tool Electrode High-Speed Rotating, *Materials and Manufacturing Processes*, 29, 634–637, 2014.

[45] Sanjay K. Chak , P. Venkateswara Rao, "Machining of SiC by ECDM process using different electrode configurations under the effect of pulsed DC", *International Journal of Manufacturing Technology and Management*, 28(1-3),39–56., 2014.

[46] Lijo Paul Somashekhar S. Hiremath , Jinka Ranganayakulu, "Experimental investigation and parametric analysis of electro chemical discharge machining", *International Journal of Manufacturing Technology and Management* ,28(1-3), 57–79, 2014

[47] C.S. Jawalkar, Apurbba Kumar Sharma, Pradeep Kumar, Investigations on performance of ECDM process using NaOH and NaNO3 electrolytes while micro machining soda lime glass, *International Journal of Manufacturing Technology and Management*, 28(1-3), pp. 80–93, 2014

[48] Baoyang, J.; Shuhuai, L.; Kevin, W.; Jun, N, "Modeling and experimental investigation of gas film in micro-electrochemical discharge machining process", *International Journal of Machine Tools and Manufacture*, 90, 8-15, 2015.

[49] Gupta, P.K.; Dvivedi, A.; Kumar, P. "Effect of Pulse Duration on Quality Characteristics of Blind Hole Drilled in Glass by ECDM", *Materials and Manufacturing Processes*,1–9, 2016.

[50] Hajian, M.; Razfar, M.R.; Movahed, S, "An experimental study on the effect of magnetic field orientations and electrolyte concentrations on ECDM milling performance of glass", *Precision Engg*., 45,322-331, 2016.

[51] Mudimallana Goud, Apurbba Kumar Sharma, Chandrashekhar Jawalkar, "A review on material removal mechanism in electrochemical discharge machining (ECDM) and possibilities to enhance the material removal rate", *Precision Engg*., 45, 1–17, 2016.

[52] Saranya, S.; Nair, A.; Ravi Sankar, A., "Experimental investigations on the electrical and 2D-machining characteristics of an electrochemical discharge machining (ECDM) process", *Microsystem Technologies*, 22, 1-9, 2016.

[53] A. Behroozfar and M. R. Razfar, "Experimental Study of the Tool Wear During the Electrochemical Discharge Machining" *Materials and Manufacturing Processes*, 31: 574–580, 2016.

[54] Bindu Madhavi J, Somashekhar S Hiremath, "Investigation on Machining of Holes and Channels on Borosilicate and Sodalime Glass using 3-ECDM Setup", *Procedia Technology*, 25,1257 – 1264, 2016

[55] S. Elhami& M. R. Razfar., "Effect of ultrasonic vibration on the single discharge of electrochemical discharge machining" *Journal of Materials and ManufacturingProcesses*,1-8, 2017.

[56] P. K. Singh, A. K.Das, G. Hatui,G. C. Nayak., "Shape controlled green synthesis of CuO nanoparticles through ultrasonic assisted electrochemical discharge process and its application for supercapacitor", *Materials Chemistry and Physics*, 198, 16-34, 2017.

[57] S. Elhami, M.R. Razfar, "Analytical and experimental study on the integration of ultrasonically vibrated tool into the micro electro-chemical discharge drilling", *Precision Engineering*, 47, 424-433, 2016.

[58] T. Singh & A. Dvivedi., "On pressurized feeding approach for effective control on working gap in ECDM" *Materials and Manufacturing Processes*, 1-12, 2017.

[59] Jin Wang & Li Sun &ZhixinJia.,"Research on electrochemical discharge-assisted diamond wire cutting of insulating ceramics" *Int. J. Adv. Manuf. Technology*, 2017.

[60] M. Hajian& M. R. Razfar& A. H Etefagh, "Experimental study of tool bending force and feed rate in ECDM milling" , *Int. J. Adv. Manuf. Technology*, 201791:1677–1687, 2016.

[61] W.Tang, X.Kang and W. Zhao, "Enhancement of electrochemical discharge machining accuracy and surface integrity using side-insulated tool electrode with diamond coating" *Journal of Micromechanics and Microengineering*, Vol. 27, NO. 6. 2017.

[62] M. Han, K. W. Chae and B.K. Min, "Fabrication of high-aspect-ratio microgrooves using an electrochemical discharge micro milling process" *Journal of Micromechanics and Microengineering*, Vol.27, No5, 2017.

[63] Sarkar B.R.; Doloi B.; Bhattacharyya B, Experimental investigation into electrochemical discharge micro drilling on advanced ceramics, *International Journal of Material Forming and Machining Processes,* 4(2), 29 – 44, 2017.

[64] Nasim Sabahi and Mohammad Reza Razfar, "Investigating the effect of mixed alkaline electrolyte (NaOH + KOH) on the improvement of machining efficiency in 2D electrochemical discharge machining (ECDM)" *The International Journal of Advanced Manufacturing Technology,* Vol. 95, 1–4, pp 643–657, 2018

[65] Ravindra Nath Yadav, "Electro-chemical spark machining– based hybrid machining processes:Research trends and opportunities" *Proc IMech E Part B: J Engineering Manufacture,* 1–25, 2018.

[66] Ankit D. Oza, Abhishek Kumar, Vishvesh Badheka, Amit Arora, "Traveling Wire Electrochemical Discharge Machining (TW-ECDM) of Quartz Using Zinc Coated Brass Wire: Investigations on Material Removal Rate and Kerf Width Characteristics", *Silicon,* 1-12,2019.

[67] Weidong Tang, Xiaoming Kang , Wansheng Zhao," Experimental Investigation of Gas Evolution in Electrochemical Discharge Machining Process", *International Journal of electrochemical science,* 14, 970 – 984, 2019

[68] J. Bindu Madhavi, Somashekhar S. Hiremath, Machining and Characterization of Channels and Textures on Quartz Glass Using μ-ECDM Process, *S.S. Silicon,*1-13, 2019

Analysis on electrochemical discharge machining during micro-channel cutting on glass

B. Mallick, B.R. Sarkar*, B. Doloi and B. Bhattacharyya

Production Engineering Department,
Jadavpur University,
Kolkata-700032, India
Email: bijan.ju@gmail.com
Email: sarkarbiplab_s@rediffmail.com
Email: bdoloionline@rediffmail.com
Email: bb13@rediffmail.com
*Corresponding author

Abstract: Modern industrial field of micro-machining has an attractive attention to increase the machinability of electrically non-conducting materials. Electrochemical discharge micro-machining process has the ability to machine high strength non-conducting brittle materials like glass. This paper shows a development of second-order correlation between the various machining criteria and different process parameters such as applied voltage, electrolyte concentration and inter-electrode gap (IEG). The analysis of variance (ANOVA) has been performed to find out the adequacy of the developed models. The research paper includes the effects of various process parameters on material removal rate (MRR), overcut (OC), heat affected zone (HAZ) and machining depth (MD) during micro-channel generation on glass. This paper also represents the single as well as multi-objective optimised results to determine the suitable parametric combination for maximum MRR and machining depth and minimum overcut and HAZ area using response surface methodology (RSM) and genetic algorithm (GA).

Keywords: ECDM; electrochemical discharge machining; micro-channel; RSM; response surface methodology; GA; genetic algorithm; glass.

Reference to this paper should be made as follows: Mallick, B., Sarkar, B.R., Doloi, B. and Bhattacharyya, B. (2017) 'Analysis on electrochemical discharge machining during micro-channel cutting on glass', *Int. J. Precision Technology*, Vol. 7, No. 1, pp.32–50.

Biographical notes: B. Mallick is a Research Scholar of Production Engineering Department, Jadavpur University, Kolkata, India. He has more than five years of research as well as teaching experiences. He has published more than five research papers in reputed journals and presented many research works in international conferences. His research interest includes micro-machining and ECDM processes.

DOI: 10.1504/IJPTECH.2017.084554

Citation: B. Mallick; B.R. Sarkar; B. Doloi; B. Bhattacharyya, "Analysis on electrochemical discharge machining during micro-channel cutting on glass",International Journal of Precision Technology, 2017 Vol.7 No.1, pp.32 – 50

Universiti Malaysia PAHANG
Journal of MECHANICAL ENGINEERING and SCIENCES
jmes.ump.edu.my | Open access | Peer-reviewed | ISSN: 2289-4659 (Print); 2231-8380 (Online) | Frequency: Quarterly
Journal of Mechanical Engineering and Sciences
Q2 Computational Mechanics best quartile
SJR 2017 0.45 powered by scimagojr.com
SCOPUS
VOL.12,ISSUE-3,PP3942-3960,2018

Journal of Mechanical Engineering and Sciences
ISSN (Print): 2289-4659; e-ISSN: 2231-8380
Volume 12, Issue 3, pp. 3942-3960, September 2018
© Universiti Malaysia Pahang, Malaysia
DOI: https://doi.org/10.15282/jmes.12.3.2018.13.0344

Analysis on the effect of ECDM process parameters during micro-machining of glass using genetic algorithm

B. Mallick[1*], B.R. Sarkar[2], B. Doloi[2], B. Bhattacharyya[2]

[1]Research Scholar of Production Engineering Department, Jadavpur University, Kolkata-700032, INDIA
Phone: 009109432663186; Fax: 009109831993552
[2]Faculty of Production Engineering Department Jadavpur University, Kolkata-32, INDIA
*[1]Email: bijan.ju@gmail.com

ABSTRACT

Electro chemical discharge hybrid machining process involves in micro-machining to cut micro-channel, micro-profile as well as micro-slot, blind hole on hard materials like ceramic, quartz and glass. Experimentation has been performed using an indigenously developed micro-ECDM set up in which pressurized automated spring feeding mechanism and cam follower system is used to control the working gap. This paper emphasis to the influences of different process parameters like applied voltage (V), electrolyte concentrations (wt%), pulse frequency (Hz) and duty ratio (%) on different machining performance characteristics such as Material Removal Rate (MRR), Overcut (OC), Surface Roughness (R_a) and Heat Affected Zone (HAZ) during micro-channel cutting on glass. The empirical mathematical model has been validated by the analysis of variances. This research paper rendered the suitable optimal parametric condition during single as well as multi objective optimization using genetic algorithm (GA). Applied voltage and duty ratio has dominating role to increase MRR, OC, HAZ and surface roughness. Machining Depth increased using automated spring feeding with Cam-follower mechanism and achieved machining depth of 1.35mm. This research paper also presented the SEM analysis of micro-channel to find out the debris and other particles.

Keywords: Genetic algorithm; micro-ECDM; micro-slot; spring-feed; surface roughness

INTRODUCTION

Electrochemical Discharge micro-machining process plays a great roll in modern research of non-traditional machining process since 1968. The material removal took place due to the emerged effects of electrochemical (EC) reaction and electrical spark discharge (ESD) action [1-3]. The overall performance of ECDM process was increased by maintaining the electrode gap and the stability and robustness of the controller were higher when peak voltage was used in feedback signal [4]. Electrochemical discharges depended on the electrolyte concentration and the surface roughness of the work piece was affected by the electrolyte concentration as well as the applied voltage and also it was propounded that the gas film stability highly required and found clear sparking at 30volt during ECDM process [5]. Material removal rate, heat affected zone and overcut was affected by applied voltage and electrolyte concentration during micro-drilling on silicon nitride and achieved maximum machining rate at 70volt, 18wt% of electrolyte concentration and 27 mm inter electrode gap [6]. The surface roughness increased as the duty ratio increased and pulse frequency decreased during micro-drilling on glass. Increasing the drilling time, material removal rate was decreased and tool wear rate was increased when duty ratio increased [7]. The combination of flat sidewall–flat front tool and pulse voltage conspicuously increased the machining accuracy

DOI: https://doi.org/10.15282/jmes.12.3.2018.13.0344

Citation: Malick et. al / Journal of Mechanical Engineering and Sciences 12(3) 2018 3942-3960

Applied Mechanics and Materials
ISSN: 1662-7482, Vols. 592-594, pp 525-529
doi:10.4028/www.scientific.net/AMM.592-594.525

Submitted: 2014-04-24
Revised: 2014-05-19
Accepted: 2014-05-20
Online: 2014-07-15

Multi criteria optimization of Electrochemical Discharge Micro-machining process during micro-channel generation on glass

Mallick. B[*1]., Sarkar.B. R[2]., Doloi. B[3]., Bhattacharyya. B[4]

[1]Research Scholar, Production Engineering Department, Jadavpur University, Kolkata-32, India
E-mail*: bijan.ju@gmail.com
[2]Assistant Professor, Production Engineering Department, Jadavpur University, Kolkata-32, India
E-mail: sarkarbiplab_s@rediffmail.com
[3]Associate Professor, Production Engineering Department, Jadavpur University, Kolkata-32, India
E-mail: bdoloionline@rediffmail.com
[4]Professor, Production Engineering Department, Jadavpur University, Kolkata-32, India
E-mail: bb13@rediffmail.com

Keywords: μ-ECDM, MRR, OC, MD, RSM, ANOVA, Glass

Abstract: - Electrochemical Discharge micro-machining process appears better utility with greater effectiveness in the modern micro-machining industrial field. Electrochemical discharge micro-machining process is involved to generate micro-channel as well as curve profile on glass for utilization as micro-fluidic device. This paper shows second order mathematical modeling of correlation between the machining criteria such as machining rate as a form of material removal rate(MRR), overcut(OC), machining depth(MD) with various process parameters like applied voltage (V), electrolyte concentration (wt %) and inter-electrode gap (IEG) (mm). The analysis of variance (ANOVA) has been performed to find out the adequacy of the developed models.This paper also shows the multi objective optimization to achieve the optimal parametric combination for maximum MRR, MD and minimum OC using response surface methodology(RSM).

1. INTRODUCTION

The use of non-conducting materials and alloy is increased in the modern industrial field day by day. Electrochemical discharge micro-machining process is a promising technology to machine electrically non-conducting materials such as ceramics and glass. However Electrochemical Discharge micro-machining process is utilized as a future advanced hybrid micro-machining technique which is combination of electrochemical machining (ECM) and Electro discharge machining (EDM) [1] with better machining rate, precision, control, low machining cost and wide range of applications on electrically non-conducting materials like glass. In ECDM process, the material removal takes place due to the combined effects of electrochemical (EC) reaction and electrical spark discharge (ESD) action [2 - 5].

It is a reproductive shaping process in which the form of the tool electrode is mirrored on the workpiece. It uses two electrodes: one is a cathode where the tool is connected and the other is an anode or an auxiliary electrode. The workpiece is placed just below the tool and is immersed in an electrolytic solution along with the auxiliary electrode in a machining chamber. Material removal rate varies with the pulse frequency because the duration of the discharge increases as the frequency decreases, even though the total time that voltage is applied remains the same [6]. Han *et al.* [7] reported a new method for improvement of the surface integrity in electro-chemical discharge machining (ECDM) process by use of fine graphite powder mixed with electrolyte. Cao *et al.* [8] studied micro-electrochemical discharge machining (micro-ECDM) to improve the machining of 3D micro-structures on glass and to obtain good surface with minimized structures during the drilling and milling operations. The analysis of variance (ANOVA) has been performed to find out the adequacy of the developed models. Also the paper represents the multi objective optimization to achieve the optimal parametric combination for maximum MRR, MD and minimum OC etc.

DOI:https://doi.org/10.4028/www.scientific.net/AMM.592-594.525
Citation:B. Mallick et al., "Multi Criteria Optimization of Electrochemical Discharge Micro-Machining Process during Micro-Channel Generation on Glass", Applied Mechanics and Materials, Vols. 592-594, pp. 525-529, 2014